The University of Nottingham
UNITED KINGDOM · CHINA · MALAYSIA

Enhanced Dendritic cell Immunotherapy to treat Glioblastoma

By Dr Jason Adhikaree

Thesis submitted to the University of Nottingham for the degree of Doctor of Philosophy, January 2019

Abstract

Introduction: Glioblastoma (GBM) patients have a poor survival and are inevitably treatment refractory. The power of enhancing the immune system to combat the chemo-radiotherapy resistant tumour, melanoma, affirms the potential for re-directing the immune response against GBM. Furthermore, immunotherapy combines anti-cancer cytotoxicity with durable memory responses.

Dendritic cells (DC) orchestrate a central role in the adaptive immune response by antigen uptake, presentation and co-stimulation to effector T-cells. However, tumours have evolved mechanisms to evade immune recognition by DC.

Here we focussed on the myeloid $CD1c^+$ (cDC2) subset, the most abundant circulating DC, to assess the feasibility of adoptive transfer in the next generation of DC vaccines. We also study the novel use of p38 mitogen-activated protein kinase inhibitor (p38i) as an adjunct to improve DC dysfunction and combination therapy with immune checkpoint blockade (ICB).

Method: 6-colour flow cytometry of whole blood was used to enumerate and phenotype 4 circulating DC subsets in GBM patients (n=16) and healthy controls (n=16). Following magnetic bead isolation of DC, the cytokines IL-12 and IL-10 were measured post maturation from GBM patients (n=6) and modelled using healthy DC co-cultured with dexamethasone (Dex) and GBM tumour-derived lysate (TDL). A mixed lymphocyte reaction (MLR) measured T-cell stimulatory ability and phenotype. Migration was assessed using a transwell 5μM pore membrane towards a CCL21 gradient and antigen presentation measured using an autologous DC, lymphocyte and peptide co-culture expansion system. Peptide-specific responses were analysed by IFN-γ

ELISPOT. cDC2 ability to cross present gp100 peptides was analysed using transfected $gp100_{280-288}$ T-cell receptor-Jurkat cell line. The p38i, BIRB0796, was added as an adjunct prior to maturation to assess response and ICB added to determine synergy in a MLR.

Results: GBM patients had reduced cDC2 and plasmacytoid DC, with an immature phenotype, compared to controls. Likewise, cDC2 isolated from patients, showed significantly suppressed IL-12 secretion. This was modelled in healthy DC by co-culture with Dex and TDL. Treatment with p38i reversed cDC2 dysfunction with increased co-stimulation expression, IL-12 secretion and allo-stimulation. In addition, IL-10 was suppressed, migration towards CCL21 improved and cross-presentation ability maintained. Patient-derived cDC2 showed improved IL-12:IL-10 ratio, similar to healthy controls. There was a superior and synergistic Th1 proliferation when combined with ICB.

Conclusions: Circulating DC from GBM patients are dysfunctional and this represents a potential mechanism of immune evasion. Here we establish that p38i restores phenotype and function to activate a Th1 response. We have also shown favourable characteristics of a combination ICB treatment strategy. This is the first study in GBM patients to investigate the use of cDC2 in the next generation of vaccines with a p38i adjunct. We are in the process of establishing the first cDC2 vaccine trial in GBM patients.

Acknowledgements

Firstly, particular thanks to all the patients with Glioblastoma who have kindly contributed to research in the interest of helping others with their disease.

I am also indebted to the supervision and guidance from Professor Poulam Patel, Dr Andrew Jackson and informally to all members of the Host-Tumour Interaction Group, and Division of Cancer and Stem Cell department. A few noteworthy members include Poonam Bilimoria for help with isolation of DC from patients' samples and Constantinos Televantos (medical student) who jointly developed the 6-colour flow cytometry staining panel.

This opportunity has only been afforded to me because of a McPhail grant, in memory of Sam White, which supported acquisition of preliminary data during my National Institute for Health Research (NIHR) Academic Clinical Fellowship. This subsequently led to a jointly funded Medical Research Council (MRC) and Brain Tumour Charity Clinical Research Training Fellowship grant.

Finally, a noteworthy mention has to be given to my Wife, Mum, Dad and Sister for their outstanding support and patience during this period of study and, furthermore in life.

Table of Contents

ABSTRACT 3

ACKNOWLEDGEMENTS 6

INTRODUCTION 12

GLIOBLASTOMA: THE DISEASE ENTITY AND CURRENT TREATMENT LANDSCAPE 12
BRAIN TUMOUR IMMUNITY AND BARRIERS TO IMMUNOTHERAPY. 19
ANTIGEN PRESENTATION CELLS (APC) 19
LYMPHATICS 21
BLOOD BRAIN BARRIER (BBB) AND IMMUNE PRIVILEGE 25
T-CELL DYSFUNCTION 26
IMMUNOSUPPRESSIVE TUMOUR MICROENVIRONMENT 30
CORTICOSTEROIDS 31
CIRCULATING DENDRITIC CELLS 33
SUMMARY 38

MATERIALS AND METHODS 41

ETHICAL APPROVAL 41
METHODOLOGY AND RATIONALE FOR CIRCULATING DENDRITIC CELL FLOW CYTOMETRIC ANALYSIS 41
PROTOCOL FOR CIRCULATING DENDRITIC CELL SUBSET ANALYSIS 42
FLOW CYTOMETRIC GATING STRATEGY FOR IDENTIFYING CIRCULATING DENDRITIC CELL POPULATIONS 43
MULTI-COLOUR COMPENSATION 48
ISOLATION OF PERIPHERAL BLOOD MONONUCLEAR CELLS (PBMC) 49
GENERATION OF MONOCYTE DERIVED DENDRITIC CELLS (MODCS) 49
ISOLATION OF MYELOID CD1c$^+$ (CDC2) 52
PHENOTYPING ISOLATED DENDRITIC CELLS MODC OR CDC2 55
IL-12 ELISA 57
IL-10 ELISA 57
IFN-γ ELISA 58
CELL LINES 59
CO-CULTURE DC, TUMOUR LYSATE (TDL) OR DEXAMETHASONE (DEX) +/- P38 MAPK INHIBITOR 60
MIXED LYMPHOCYTE REACTION (MLR) 61
WESTERN BLOTTING OF CDC2 P38-MK2 PATHWAY 62
MIGRATION ASSAY 62
CROSS-PRESENTATION ASSAY 63
CDC2-PEPTIDE SPECIFIC CYTOTOXIC T-CELL GENERATION 64
IFN-γ ELISPOT 64
PD-1 INHIBITED CD4-TCELL CO-CULTURE WITH GBM CELL LINES 65
STATISTICAL ANALYSIS 65
TABLE 4: SUMMARY OF REAGENT. 66

RESULTS: CHAPTER 1 – CIRCULATING DENDRITIC CELLS IN GLIOBLASTOMA PATIENTS 69

INTRODUCTION **69**
RESULTS **71**
PATIENT CHARACTERISTICS FOR IMMUNOPHENOTYPING CIRCULATING DC 71
ALTERATIONS IN CIRCULATING DC NUMBERS IN PATIENTS WITH GBM 75
ASSOCIATION BETWEEN REDUCED NUMBER OF DC AND DEXAMETHASONE 80
ALTERED PHENOTYPE OF CIRCULATING DC 80
CDC2 CYTOKINE RELEASE IN GBM PATIENTS IS SUPPRESSED COMPARED TO HEALTHY CONTROLS 83
DISCUSSION **85**

RESULTS: CHAPTER 2 – DEXAMETHASONE AND TUMOUR-DERIVED FACTORS INHIBIT MODC AND CDC2 FUNCTION **93**

INTRODUCTION **93**
RESULTS **96**
DEXAMETHASONE SUPPRESSES IL-12 AND INCREASES IL-10 IN MODC 96
DEXAMETHASONE SUPPRESSES THE ALLO-STIMULATORY ACTIVITY OF MATURE MODC AND ALTERS THE PBL CYTOKINE SIGNATURE 98
DEXAMETHASONE SUPPRESSES IL-12 AND INCREASES IL-10 IN CDC2 100
DEXAMETHASONE SUPPRESSES THE ALLO-STIMULATORY ACTIVITY OF CDC2 AND ALTERS THE PBL CYTOKINE SIGNATURE 102
GBM TUMOUR-DERIVED LYSATE SUPPRESSES IL-12 AND INCREASES IL-10 IN MODC 104
GBM TUMOUR-DERIVED LYSATE SUPPRESSES THE ALLO-STIMULATORY ACTIVITY OF MATURE MODC AND ALTERS THE PBL CYTOKINE SIGNATURE 106
GBM TUMOUR-DERIVED LYSATE SUPPRESSES IL-12 AND INCREASES IL-10 IN CDC2 108
GBM TUMOUR-DERIVED LYSATE SUPPRESSES THE ALLO-STIMULATORY ACTIVITY OF CDC2 AND ALTER THE PBL CYTOKINE SIGNATURE 110
DISCUSSION **112**

RESULTS: CHAPTER 3: P38 MITOGEN-ACTIVATED PROTEIN KINASE (P38I) ENHANCES CDC2 FUNCTION IN HEALTHY INDIVIDUALS **118**

INTRODUCTION **118**
RESULTS **119**
THE P38I, BIRB 796, SUCCESSFULLY BLOCKS DOWNSTREAM MK2 SIGNALLING 119
INHIBITION OF THE P38 MAPK (P38I) PATHWAY ENHANCES THE PHENOTYPE OF CDC2 121
INHIBITION OF P38 MAPK REVERSES DEX AND TDL INDUCED CYTOKINE DYSFUNCTION IN CDC2 124
THE ALLO-STIMULATORY ACTIVITY OF CDC2 EXPOSED TO DEX AND TDL IS ENHANCED BY P38I AND THE RESULTING PBL SUPERNATANT IS IFN-γ RICH 126
THE MIGRATION OF CDC2 TOWARDS A CCL21 GRADIENT WAS SUPERIOR WITH P38I TREATMENT. THIS IS INDEPENDENT OF CCR7 EXPRESSION ON CDC2 130
MATURE AND P38I CDC2 ARE ABLE TO CROSS-PRESENT ANTIGENS 134
ENHANCED P38I CDC2 ARE CAPABLE OF INDUCING DE-NOVO PEPTIDE-SPECIFIC T-CELL RESPONSES 141
CDC2 PEPTIDE PULSING TO ACHIEVE A NAÏVE CTL RESPONSE IN HEALTHY DONORS 145
DISCUSSION **148**

RESULTS: CHAPTER 4 - ENHANCED P38 MAPK INHIBITED CDC2 IS A NOVEL IMMUNOTHERAPY STRATEGY TO RESTORE CYTOKINE DYSFUNCTION IN GBM PATIENTS **156**

INTRODUCTION **156**
RESULTS **157**
MODC AND CDC2 IN HEALTHY VOLUNTEERS PRODUCE EQUIVALENT LEVELS OF IL-12, BUT CDC2 PRODUCE LESS IL-10. OVERALL IL-12:10 FAVOURS CDC2 157
GBM PATIENTS PRODUCE LOW LEVELS OF IL-12 FROM MODC AND CDC2. CDC2 SHOWED MARKED IL-12 AND IL-10 SUPPRESSION 160
PATIENT-DERIVED P38I CDC2 SHOW INCREASED IL-12 LEVELS AND ABLATED IL-10 . THE RATIO IS SIMILAR TO HEALTHY CONTROLS' CDC2. 162
DISCUSSION **164**

RESULTS: CHAPTER 5 - THE COMBINATION OF IMMUNE CHECKPOINT BLOCKADE WITH ENHANCED P38 MAPK INHIBITED CDC2 CAN IMPROVE EITHER MONOTHERAPY IMMUNE STRATEGY **169**

INTRODUCTION **169**
RESULTS **171**
IMPROVED ACTIVATION OF A TH1 RESPONSE BY DEX EXPOSED P38I-CDC2 AND IMMUNE CHECKPOINT BLOCKADE COMBINATION 171
IMPROVED ACTIVATION OF A TH1 RESPONSE FROM TUMOUR-DERIVED LYSATE EXPOSED CDC2 BY COMBINATION P38I AND IMMUNE CHECKPOINT BLOCKADE 175
PEMBROLIZUMAB CAN PROMOTE IFN-γ SECRETION IN CD4 EXPOSED TO GBM TUMOUR CELL LINES 179
THE COMBINATION OF P38I CDC2 AND IMMUNE CHECKPOINT DOES NOT ALTER CROSS PRESENTATION 181
DISCUSSION **187**

OVERVIEW DISCUSSION **193**

DENDRITIC CELL IMMUNOTHERAPY TO TREAT GLIOBLASTOMA **193**
LIMITATIONS OF THIS STUDY **202**

CONCLUDING REMARKS **209**

REFERENCES **212**

Introduction

Glioblastoma: the disease entity and current treatment landscape

Malignant gliomas have an annual incidence of 5/100,000 worldwide of which 70% are glioblastoma (GBM) (1). In England, the overall national age standardised incidence is 4.64/100,000/year, with a median survival of 6.1 months and 5-year survival rate of 3.4% (2). Unfortunately, brain tumours are the leading cause of death from cancer in the UK in people under 40-years (3).

Gliomas are a heterogeneous group of diseases and the World Health Organisation (WHO) classifies them histologically from grade I-to grade IV. Since primary intracranial tumours do not metastasize outside the cranium, grading is used to determine prognosis and treatment and not staging (4). All GBM are grade IV by definition which includes the histological features of increased cellularity, nuclear atypia, mitotic activity and microvascular proliferation and necrosis (4).

GBM itself is a heterogenous disease both between patients and among individuals. Indeed, its heterogenous appearance macroscopically was recognized as early as the 1920s when the term glioblastoma multiforme was coined by Professor Cushing's team to describe the highly variable consisting of cysts, haemorrhagic material and necrosis (5).

It has long been appreciated that two clinically distinct subtypes, primary and secondary occur. Primary GBM occurs in older patients and has the molecular characteristics of EGFR amplifications, loss of heterozygosity of chromosome 10 and deletions of PTEN and p16. While secondary GBM occurs in younger patients as a transformation of a lower grade glioma and have a better prognosis. They are characterized by overexpression of PDGFR, mutations of p53, abnormalities in p16 and retinoblastoma pathway (1, 6, 7).

More recently GBM has been subtyped into Proneural, Neural, Classical and Mesenchymal groups by gene expression-based molecular classification (figure 1). Aberrations and gene expression of EGFR, NF1, and PDGFRA/IDH1 define this classifications system (8, 9). For example, the Proneural subtype is characterised by alterations in PDGFRA and point mutations in IDH1, which are not seen in other subtypes. This phenotype predicts a lack of response to standard treatments. Alternatively, the Classical subtype is characterised by EGFR amplification and deletions in CDKN2A (part of the retinoblastoma signalling pathway). This phenotype is chemo-radiation sensitive (8, 9). Interestingly, a group which is currently leading a phase III monocyte-derived DC vaccine (DCVax-L) trial, found in their phase I/II subgroup analysis by gene expression that the mesenchymal subtype had a significantly longer survival in the DC vaccine arm compared to the same subtype in historic controls. Furthermore, the mesenchymal gene expression signature had the highest $CD3^+$ and $CD8^+$ tumour infiltrating lymphocytes compared to other subtypes (10). It is yet to be validated whether a subtype of GBM has better immunogenic potential.

One other important clinically relevant marker is hypermethylation of the O^6-methylguanine-DNA-methyltransferase (MGMT) promoter gene which encodes a DNA repair gene and if present improves both radiation and Temozolomide responsiveness (11, 12). This translates to a survival difference of those with and without methylated MGMT of 21.7 and 12.7 months respectively (11).

The current standard of care for the treatment of GBM is referred to as the Stupp protocol, defined after the phase III trial published in 2005 showing a survival benefit with chemoradiation (13). In this trial, 573 patients were randomised, 1:1 between radiotherapy only or daily Temozolomide with radiotherapy (chemo-radiotherapy) followed by 6 months of adjuvant Temozolomide. The addition of Temozolomide provided 2.5 months overall survival benefit (14.5 vs 12.0 months) and more than a doubling in 2-year

survival rates (26.5% vs 10.4%). However, even in the context of a selective clinical trial, 5% discontinued chemo-radiotherapy and 53% discontinued adjuvant Temozolomide, mainly due to disease progression (13). Furthermore, less than half of the patients diagnosed with GBM will receive this treatment due to poor baseline fitness at presentation (14).

Furthermore, the Stupp trial excluded patients over 70 years of age, who have a worse prognosis and poorly tolerate treatment (15). Therefore, the Nordic trial compared standard radiotherapy (60Gy in 30 fractions), hypofractionated radiotherapy (34Gy in 10 fractions) and Temozolomide monotherapy in 342 patients over 60 years in a 1:1:1 phase III trial (16). They found standard radiotherapy was associated with poorer survival, particularly in the over 70s, compared to hypofractionated radiotherapy and Temozolomide, and therefore recommended the latter two options for palliating older patients (16).

Unfortunately, despite the marked advancement in our genomic understanding of Glioblastoma over the last 10 years, the hope that genomic data would lead to new molecular targets for small molecular inhibitors, which has changed the treatment landscape for many difficult to treat tumours like non-small cell lung cancer, melanoma and renal cancer has not materialized (17-21). In a systematic review of six kinase inhibitors (EGFR, mTOR, KDR, FLT1, PKCb, and PDGFR pathways), which included 2 phase III trials and 37 phase II trials, the authors concluded that these drugs were not efficacious enough to warrant their inclusion in standard treatment (22). This included routinely used first line drugs with proven efficacy for other solid organ tumours, like Sunitinib and Pazopanib (VEGF), Erlotinib and Gefitinib (EGFR) and Imatinib (PDGFR/KIT/ABL) (17, 18, 20, 21, 23).

Glioblastomas are also characterised by marked angiogenesis and overexpression of Vascular endothelial growth factor (VEGF)-A (24, 25). Bevacizumab, a humanised monoclonal antibody, neutralises all isoforms of

VEGF-A, thus reduces ligation of VEGF receptor 2 found on vascular endothelium and therefore angiogenesis (26). The US Food and Drug Administration (FDA) accelerated approval of bevacizumab for patients with recurrent GBM based on 2 phase II trials, one of which included bevacizumab monotherapy and the other in combination with irinotecan (27, 28). Response rates were between 28.2-37.8% in both trials and this led to its routine use in the US. However, 2 phase III trials (AVAgio and RTOG 8025) using Bevacizumab upfront in combination with standard first line treatment showed no overall survival benefit (29, 30). The AVAglio trial, recruited 458 patients, predominately from Europe, and although showed an improvement in progression free survival, quality of life and reduced glucocorticoid requirement, was at a cost of increased grade 3 adverse events (29). These included mucocutaneous bleeding, hypertension, proteinuria and arterial thrombotic events. Whereas the RTOG 0825 trial reported simultaneously, supported the trend towards an increase in progression free survival, however found an increase in symptom burden, a worsening in quality of life at week 46 compared to baseline and greater neurocognitive decline in the Bevacizumab group (30). Therefore, Bevacizumab is not used in the first line setting, however, remains in use in the second line setting based on phase II data in the US. It is not approved by The National Institute for Health and Care Excellence (NICE) in either the first- or second-line setting.

However, of note, Bevacizumab is currently in a number of immunotherapy combination trials, given its favourable immunomodulatory effects. These include promotion of dendritic cell maturation, T-cell cytotoxicity and migration and therefore may yet make a resurgence (31, 32).

A more recent FDA approved treatment is of a device called Optune, as an adjuvant in the first line setting. Optune delivers low-intensity, intermediate-frequency, alternating electric tumour treating fields, through electrodes placed on the scalp (33). The device needs to be worn for a minimum 18 hours, which consists of adhesive scalp pads and a battery pack carried in a rucksack. The low-intensity electric fields, disrupt mitosis and

induces apoptosis in dividing cells (34). A Phase III trial assessed adjuvant Optune in newly diagnosed patients in combination with temozolomide and had aimed to recruit 700 patients from 83 international centres. However, its success resulted in premature termination following a positive interim analysis of 315 patients. The treatment improved progression free survival (PFS) and overall survival (OS), when compared to temozolomide alone (PFS: 7.1 and OS: 20.5 months in Optune group vs 4.0 and 15.6 months in Temozolomide only group) (33). The inconvenience and cost of $20,000 per month limits its utility and there are currently no NICE recommendations for its incorporation into the UK standard of care.

An alternate NICE approved therapy includes Gliadel wafers in the first line. These are Carmustine chemotherapy wafers inserted directly into the cavity resection site if greater than 90% of tumour has been resected in newly diagnosed patients (35-37). This improves survival by 2.3 months over placebo in combination with radiotherapy (37). However, this phase III trial was performed prior to the Stupp protocol becoming standard of care and was randomised against radiotherapy. Therefore the benefit above chemoradiation with Temozolomide remains unclear (36, 37). However due to the higher rates of CSF leaks and intracranial hypertension this treatment is now not commonly used (37).

There is no standard of care second-line therapy. Patients with a good PS (PS$\leq$1) are offered combination Procarbazine, Lomustine and Vincristine (PCV) chemotherapy. This regime has been in use for four decades and has associated haematological and peripheral neuropathy toxicities. There are no phase III trials proving efficacy or survival benefits and most studies quote response rates between 3-11% (38, 39).

There are no immunotherapy treatments licenced to treat GBM (40). Immune checkpoint blockade, such as inhibition of Programme death-1 (PD-1) on T-cells, has revolutionized cancer treatment in a number of solid cancers (41). However, the phase III, randomised, multicentre trial, checkmate-143,

which compared nivolumab to Bevacizumab in 369 relapsed GBM patients, showed no overall survival advantage for the PD-1 inhibitor above Bevacizumab (42). In both treatment arms 40% of patients were on steroids at baseline including approximately 15% in both arms taking ≥4mg/day. The median overall survival (OS) was 9.8 months with nivolumab compared to 10.0 months with bevacizumab and the 12-month OS rate was 42% in both treatment arms. The progression-free survival was shorter in the nivolumab group at 1.5 month, compared to 3.5 months in Bevacizumab group. Likewise, the objective response rate was lower in the nivolumab group - 8% vs 23%, despite the majority of patients having measurable disease at baseline (83%). The duration of response was, however, longer with nivolumab - 11.1 months compared to 5.3 months and less grade 3-4 treatment related adverse events (13% vs 18%). However, on the basis of this phase III trial nivolumab could not be recommended in the relapsed setting for GBM. Ongoing adjuvant trials are yet to be reported (Checkmate-498 and -548 trials) investigating nivolumab with radical radiotherapy or chemo-radiotherapy in the 1st line setting.

Overall an urgent need for novel therapies exists and the hope for durable responses and prolonged survival with immunotherapies is at the forefront.

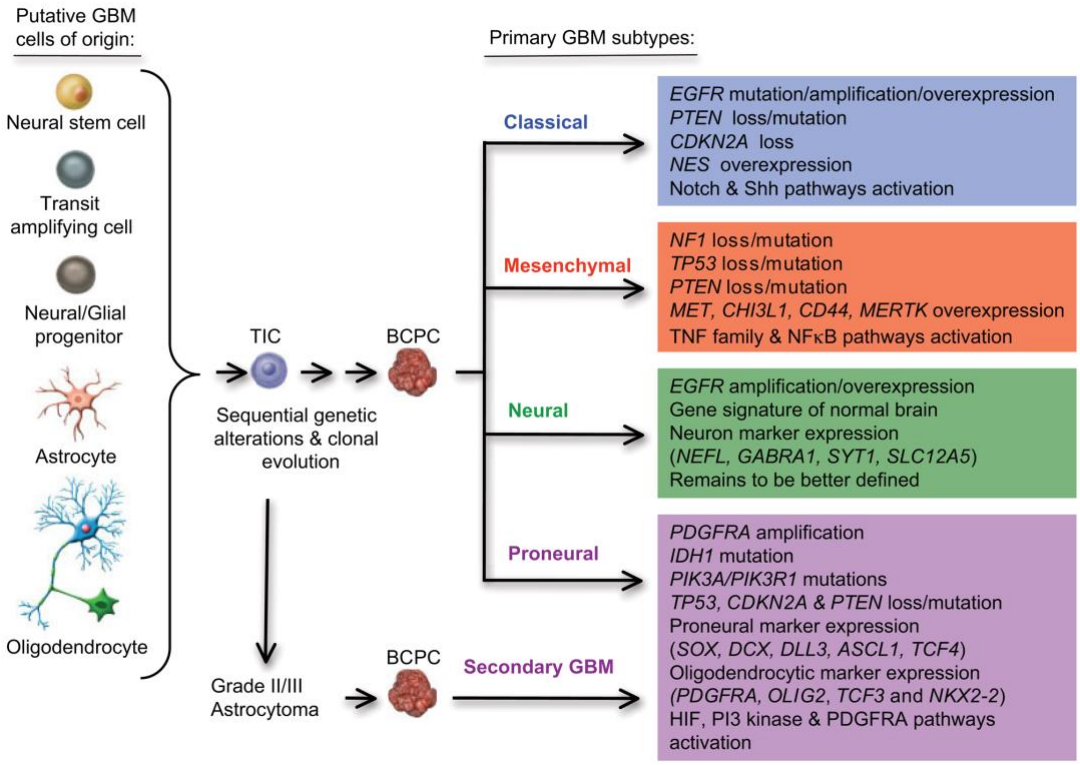


Figure 1.GBM pathogenesis and subtypes. Normal brain cells undergo genetic alterations, to create a population of tumour-initiating cells (TIC). These acquire further genetic and epigenetic alterations to become brain cancer propagating cells (BCPC). The latter cells are responsible for the development of GBM subtypes by a selection of genetic mutations. These subtypes show varied response to standard therapy and survival and may prove vital for new research avenues including immunotherapy. Image from Van Meir et al 2010 (43).

Brain tumour immunity and barriers to immunotherapy.

The brain has historically been seen as an immuno-privileged site, however it is now clear that this is highly contextual. The lack of traditional lymphatics and known antigen presenting cells have supported this theory (44). The challenge of immunotherapy to treat GBM are numerous and includes a limited understanding of basic cellular mechanisms governing anti-tumour responses in the brain, mechanical barriers such as the blood brain barrier (BBB), in addition to a suppressive tumour microenvironment (TME).

Antigen Presentation Cells (APC)

Microglia cells are tissue resident macrophages that have entered the CNS in early embryonic life. When activated, microglia express MHC class I and II molecules, as well as adhesion and co-stimulatory molecules, acquiring the ability to act as APCs (45-47). Microglia express TLR 1-9 and nucleotide-binding oligomerization domain-like receptors which contributes to their activation and recognition of a range of pathogen-associated molecular patterns (48). Macrophage and microglial cells have functional plasticity and polarise depending on the cytokine milieu and microbial environment. The M1 phenotype is activated by IFN-γ and lipopolysaccharide (LPS) to polarise a macrophage towards a pro-inflammatory IL-12 secreting cell capable of supporting a Th1 response. The M2 or alternatively activated phenotypes are induced by IL-10, glucocorticoids or IL-4 to induce a Th2 or immunoregulatory response (49). However, in the context of high-grade gliomas, current data suggests that microglia lose their capacity to present antigens due to the highly immunosuppressive TME and resemble alternatively activated macrophages (48, 50). For example, TGF-β inhibits microglial proliferation and when microglial cells are co-cultured with glioma stem cells, they phenotypically revert to a M2 status. These microglial cells have reduced phagocytosis and secrete high levels of IL-10 (51). The M2 phenotype microglial cells also have lower MHC-class II and surface co-stimulatory

molecule expression, reducing antigen presenting capacity (52, 53). Indeed, microglia have a large regulatory role in the central nervous system (CNS) immunity and plasticity which is utilized by glioma to promote growth. Upwards of 30% of a GBM tumour mass can include these immune cells and higher numbers are seen at higher grades (54). Microglia release chemoattractants (monocyte chemoattractant protein-1 (MCP-1) and macrophage inflammatory protein-1) when associated with glioma cells promoting further microglial/monocyte recruitment from the peripheral blood and, in combination with the cytokine milieu (IL-10, TGF-β and IL-6), promote further immunosuppression (48, 53). Furthermore, glioma associated microglia can release matrix metalloproteinase-14, which degrades normal brain parenchymal and promotes tumour invasion (55).

Distinct from the role of microglia, T-cell reactivation can occur in several anatomical niches including the choroid plexus, the meninges and the perivascular space within the CNS parenchyma, where co-localisation with distinct antigen presenting cells and T-cells are seen (figure2) (56). For example, classical myeloid dendritic (cDC) type 1 cells have been identified in the CSF space adjacent to subarachnoid vessels and choroid plexus stroma. While cDC type 2 have been identified in post-capillary venules of parenchymal tissue in mouse models (56). These cells are potent antigen presenting cells capable of re-stimulating a T-cell response. There are also distinct macrophage populations at these sites, with perivascular macrophages sharing embryonic origins with microglia, while choroid plexus macrophages replenished by blood-derived monocytes, turnover rate at a higher rate (56). There is also a consensus that lymphatic drainage of the outer lining and subarachnoid space is via dural sinuses and into deep cervical lymph nodes, where MHC class II-expressing cells localize and can present antigen (57, 58). Hence, this route may indeed prove the pivotal source of antigen presentation within the CNS.

Clinical support of antigen detection in the CNS and extracranial de-novo T-cell responses are seen from reports of the abscopal effect following CNS radiotherapy (59, 60). In a series of 13 patients whom received CNS radiotherapy for metastatic melanoma and had disease progression in the brain following ipilimumab, 7 experienced a partial response at extracranial sites including liver, lung, pelvic and cutaneous (60). This provides support to the theory that presentation of glioma antigens can trigger a peripheral immune response, likely via priming and activation in the deep cervical lymph nodes (58).

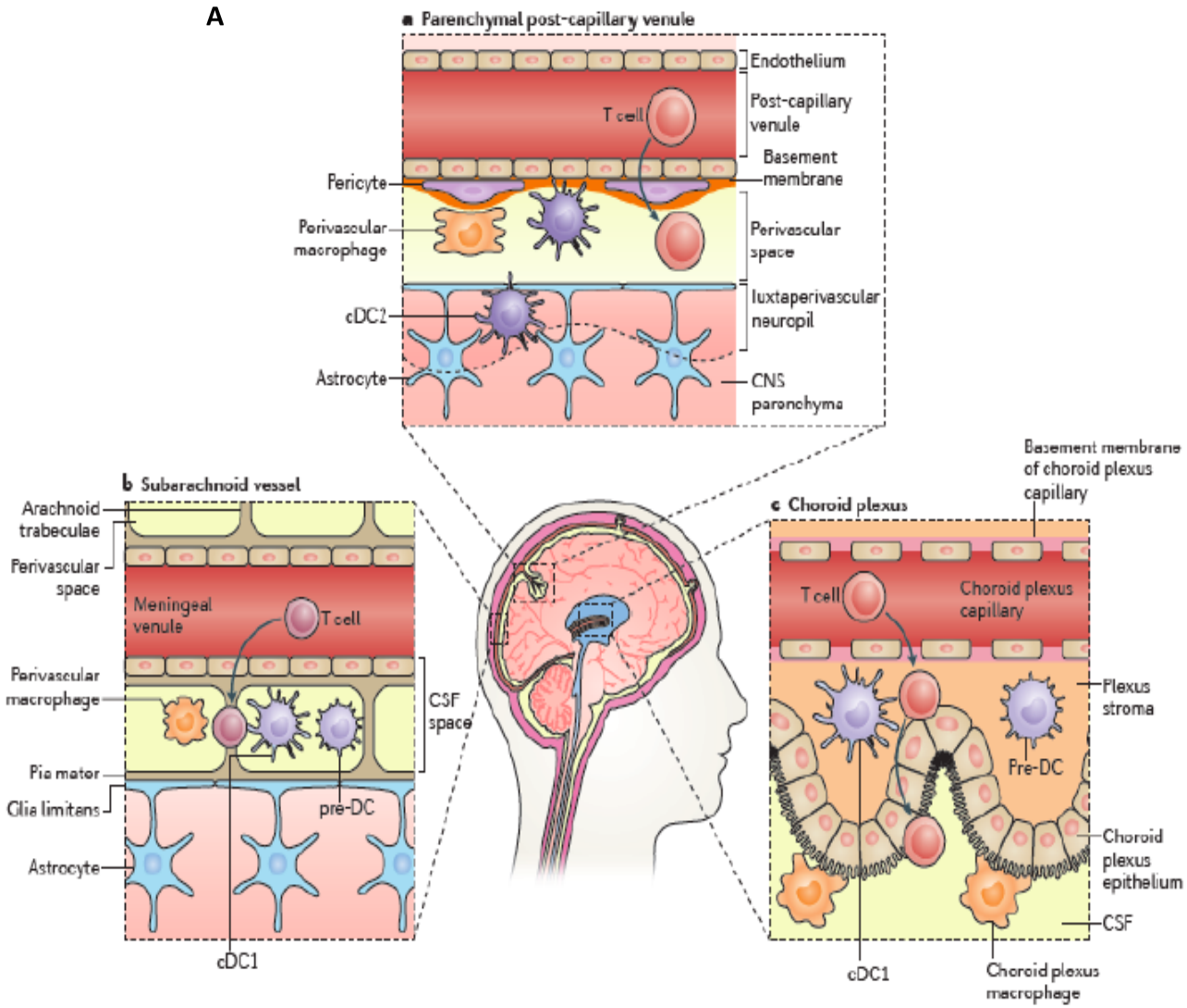
Lymphatics

The lack of traditional lymphatics has led to controversies in regard to the CNS communication with peripheral lymph nodes and therefore the site of antigen presentation and T cell priming. However, the cervical lymph nodes seem to be important with in vivo tracers following CNS antigens draining through CSF, across the cribriform plate and into the nasal mucosa. This subsequently drains into the cervical lymph nodes (61). Recently, dissection of mouse meninges and immunohistochemistry staining has co-localised endothelial cells, T-cells and MHC-II expressing cells with high concentration of immune cells near the dural sinuses. Indeed, intravenous and intracerebral injection of lectin dyes and anti-CD45 fluorescent antibodies have revealed alignment of T-cells and antigen presenting cells along perisinusal vessels (58). Alternatively, soluble antigens have been shown to travel down a separate pathway in the perivascular spaces within the wall of the cerebral arteries and into the cervical lymph nodes (62).

Further support to the importance of the cervical lymph nodes in T-cell priming comes from a mouse model of MS, Experimental autoimmune encephalitis (EAE). This condition occurs in mice after intracranial injection of purified myelin antigen and is exacerbated by an intracranial cryo-lesion. The removal of the cervical lymph nodes, prior to inflicting the cryo-lesion

ameliorates this phenotype (61).

Furthermore, in the perivascular space, along which the cerebrospinal fluid (CSF), circulates T-cells which display a memory phenotype, rather than naive (47). In support of this, homing of CD8+ T-cells towards the brain has been found to occur after presentation of tumour-specific antigens at the cervical lymph nodes (63). Under physiological circumstances, activated memory CD4+ T-cells enter the CSF from the bloodstream and monitor perivascular spaces as part of the immunosurveillance machinery in the CNS. Upon encounter of antigen-loaded APCs, CD4+ T-cells differentiate into effector cells and acquire the competence to invade the parenchyma, thereby triggering local immune responses in the brain (64). In a similar fashion, many CD8+ T-cells that are found in the CNS during neuroinflammation display an effector memory phenotype and are thought to be selectively recruited by α4-integrin-expressing endothelial cells at the BBB (65). This data supports the notion that there is a constant interaction between the extracranial and intracranial immune responses and suggests that the priming and expansion of T-cells occurs outside the CNS in the cervical lymph nodes (figure 2).


A
a Parenchymal post-capillary venule
Endothelium
T cell
Post-capillary venule
Basement membrane
Pericyte
Perivascular macrophage
Perivascular space
Juxtaperivascular neuropil
cDC2
Astrocyte
CNS parenchyma
b Subarachnoid vessel
Arachnoid trabeculae
Perivascular space
Meningeal venule
T cell
Perivascular macrophage
CSF space
Pia mater
Glia limitans
pre-DC
Astrocyte
cDC1
Basement membrane of choroid plexus capillary
c Choroid plexus
T cell
Choroid plexus capillary
Plexus stroma
Pre-DC
Choroid plexus epithelium
CSF
cDC1
Choroid plexus macrophage

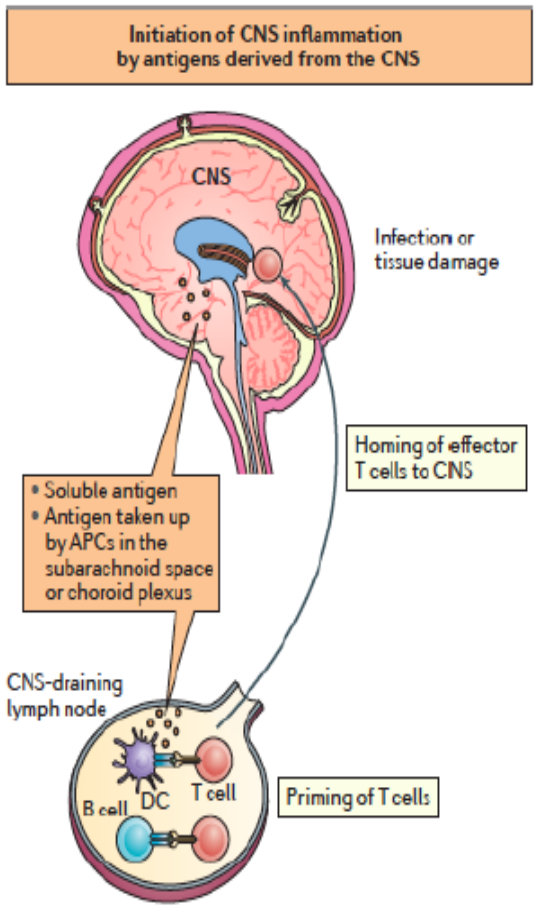

B
Initiation of CNS inflammation by antigens derived from the CNS
CNS
Infection or tissue damage
Homing of effector T cells to CNS
• Soluble antigen
• Antigen taken up by APCs in the subarachnoid space or choroid plexus
CNS-draining lymph node
B cell
DC
T cell
Priming of T cells

Figure 2. A: Antigen presenting cells and T-cells are found in distinct locations within the CNS of mice. B: Antigen from the CNS are captured and drain into cervical lymph nodes.
A: In post-capillary parenchymal venules antigen presenting cells, similar to conventional dendritic cell type 2 (cDC2) and perivascular macrophages have been seen (a). In the subarachnoid space, type 1 cDC (cDC1) and perivascular macrophages, along with pre-DC (CD11c+MHC-II^{low}) associate with T-cells (b). The choroid plexus contains both macrophages and cDC1 and has been proposed as a site of T-cell re-stimulation (c).
B: Antigens, either in a soluble form or via antigen-presenting cell-mediated uptake, drain from the above areas and are transported to the cervical lymph node, where T-cell priming occurs.
Images taken from a review by Korn and Kallies 2017 (56).

Blood Brain Barrier (BBB) and immune privilege

The blood brain barrier is not a static barrier, but dynamic. The integrity of the BBB across CNS microvessels relies on endothelial cells and intact tight junctions between them. This close association reduces permeability and prevents solute exchange to occur paracellularly (66-68). Nevertheless, the endothelial BBB is a dynamic entity that responds to environmental cues. Inflammation and brain pathologies can compromise the integrity of the BBB, thereby increasing its permeability, and thus allowing the infiltration of circulating monocytes and lymphocytes from the periphery (68, 69). As in other tissues, the extravasation of T-cells across the BBB involves the interaction between specific adhesion molecules and chemokines expressed on immune and endothelial cells. However, trafficking into the brain is known to be less efficient than in other organs and may involve transcellular instead of paracellular extravasation, to preserve endothelial tight junctions (68, 70). For example, there is also evidence that inducible metalloproteinases facilitate penetrance of leukocytes migration following perivascular cuffing across the glia limitans and basement membrane, particularly in inflammation such as a diseased pathology of the brain (71). In the inflamed blood brain barrier, monocytes, Th1 and Th17 cells migration across the blood brain barrier is a multistep process involving E- and P- selectin mediated rolling along the surface of the endothelium, followed by chemokine mediated activation and adhesion to the endothelium. This is proceeded by intracellular adhesion molecule-1 (ICAM-1) and vascular adhesion molecule-1 (VCAM-1) and activated leukocyte adhesion molecule (ALCAM) upregulation by pro-inflammatory cytokines. These bind to affiliated T-cell receptors leukocyte function associated antigen-1 (LFA-1), very late antigen-4 (VLA-4) and CD6. BBB endothelial cells and glial cells are an important source of the pro-inflammatory chemokines such as CCL2/MCP-1, RANTES and CXCL10/IP-10 and thus facilitate immune cell recruitment. $CD8^+$ T cells seem to be dependent on α4 integrin, distinct to the aforementioned mechanisms (65, 68, 72, 73). Immunoglobulins can also cross the BBB via the immunoglobulin

receptor, FcRn, by carrier mediated transportation via the cerebral blood vessel and into the brain parenchyma (74-76).

Clinical support of the effective penetration of T-cells into the CNS comes from a phase II trial which included 52 patients with untreated or progressive brain metastases diagnosed with metastatic melanoma or NSCLC. These patients had a similar responses intracranially, as to their extracranial disease following treatment with pembrolizumab, a T-cell immune checkpoint inhibitor, targeting PD-1 (77). Thus, suggesting that these drugs are effective intracranially if the relevant immune signatures against the tumour are present. This has also been observed in GBM, where a recent case report of two patients with recurrent GBM on a background of paediatric biallelic mismatch deficiency, had a deep and durable response to nivolumab (another PD-1 inhibitor) (78). Although a rare subtype of Glioblastoma, in certain countries, where consanguineous rates are higher, biallelic mismatch repair deficiency are estimated to account for 40% of paediatric glioblastoma cases (79).

T-cell dysfunction

GBM patients have been recognised to have severe deficits in cell-mediated immunity, particularly within the lymphocyte population (80, 81). This has been narrowed down to the CD4 compartment. T regulatory cells (Tregs) are highly diverse and plastic subset of T-cells cells and have a universal role of immune tolerance (82). The thymic derived, natural Tregs (nTregs), characterised by high constitutive expression of FoxP3, cause contact dependent cytokine independent immunosuppression through CTLA-4, PD-L1, granzyme/perforin and Fas/FasL pathways (44). Inducible Tregs, have transient or absent FoxP3 expression and induce immunosuppression through IL-10 and TGF-β (83). Fecci et al described suppressed absolute CD4 counts in 20 patients with GBM, however, they noted the fraction containing $CD4^+CD25^+FoxP3^+CD45RO^+$ T cells was increased compared to healthy controls (84). Overall these patients T-cells showed anergy or secreted Th2

polarising cytokines on stimulation. Removal of the Treg population reversed this cytokine signature. Furthermore, in the murine immunocompetent model using the strain mouse strain VM/Dk injected with SMA-560 (mouse glioma cell tumour) intracranially, anti-CD25 was shown to deplete Tregs and increase survival (84).

In support of an important role of Tregs in glioma is an immunohistochemistry study comprising 62 patients, whose tumours were stained for FoxP3 and CD8 and found Treg accumulation at the tumour site was associated with poorer prognosis, while $CD8^+$ TILs were not associated with survival (85). Indeed, the nTreg population may predominate in glioma, with high FoxP3 expression also seen by another group in glioma samples and linked with higher grade and high levels of Helios transcription factor, another nTreg marker (86, 87). This group expanded this theory to a mouse orthotopic model with intracranially injected (i.c.) GL261 mouse cell line of GBM and found thymectomy, prior to i.c., significantly decreased Treg levels (87). This may be through high expression of CCL-2 chemokine by glioma. In 19 GBM patients where $CD4/CD25^{bright}$ cells were isolated, T-regs migrated preferentially to glioma conditioned media and was reversed by using a CCL-2 blocking antibody (88).

A more recent study has quantified the CD4 compartment compromise in newly diagnosed GBM as equal to that in HIV patients. They found GBM patients had CD4+ counts of $\leq$200/µl compared to a healthy adult numbers of >1,000 (89). They proposed a mechanism of sequestration of T-cells in the bone marrow of patients causing a relative lymphopenia through loss of sphingosine-1-phosphate (S1P) receptor on the T cell surface. In health, a S1P ligand gradient directs T-cell chemotaxis to blood and lymph nodes areas and maintains circulating lymphocyte frequency (89). They showed in mice which are S1P1-deficient, T cells accumulated in the bone marrow of glioma-bearing mice. However, S1P1-knockin, glioma-bearing mice did not have T-cell sequestration (89).

T-cell exhaustion is a highly active area of research given the recent success of PD-1/PD-L1 axis blocking antibodies in solid organ cancers (41). The most clinically relevant biomarker for predicting response to PD-1/PD-L1 blockade is PD-L1 immunohistochemistry (IHC), for which there are now four FDA approved assays. PD-L1 correlates with improved objective response rates compared to PD-L1 negative tumours in almost all tumour types (90).

A number of studies had shown PD-L1 expression on GBM tissue albeit at variable levels. A range between 50-90% positive cells was described in a cohort of 10 primary GBM samples, which was later backed by a larger cohort of 135 samples, of which 86% expressed the marker(91, 92). Contrary to this, another study of 92 IHC samples showed that a median of 2.7% of tumour cells expressed PD-L1, despite 61% defined as positive using a threshold of ≥1%. The same study also performed flow cytometry on 5 primary samples, which was supportive of their IHC analysis (93). Hence, although a large proportion of samples are positive by the 1% cut-off, these are of low intensity. Furthermore, the clinical response to PD-1 antibody, in the phase III trial of relapsed GBM, had been disappointing, with a 8% objective response rate and 1.5 month PFS (42).

A recent publication has revealed that the poor response rates seen to PD-1 inhibitor monotherapy may be due to the upregulation of multiple checkpoint and a more severely exhausted T-cell phenotype (94, 95). Woroniecka et al have studied T-cell exhaustion in GBM in more depth. They isolated TIL and PBL from GBM patients in 21 patients and assessed for the presence of multiple immune checkpoint markers including PD-1, CTLA-4, TIM-3, LAG-3, CD160, 2B4, TIGIT, CD39, and BTLA (94). Interestingly, they found $PD\text{-}1^{+}CD8^{+}$ were present in 96% of patient TIL samples. The $CD8^{+}$ T-cells were of an effector memory phenotype ($CD45RA^{-}CD62L^{-}$), however noted LAG-3, TIGIT, TIM-3 and CD39 were all upregulated, in addition to PD-1. They also measured post stimulation levels of intracellular IFN-γ, TNF-α and IL-2 by flow cytometry

and found cytokines levels were severely suppressed in TIL expressing PD-1, TIM-3 and LAG-3 (triple positive), but not PD-1 single positive. Indeed, the $CD8^{+}PD\text{-}1^{+}$ produced more IL-2 than $CD8^{+}PD\text{-}1^{-}$ which the authors reflected demonstrates that PD-1 alone is an activation marker rather than purely a marker of exhaustion. They modelled T-cell exhaustion in two mouse models of GBM and found the TIL population mirrored those found in mouse models of chronic lymphocytic choriomeningitis virus, with the loss of $Tbet^{hi}PD\text{-}1^{int}$ T cells, and the accumulation $Eomes^{hi}PD\text{-}1^{hi}$ exhausted T cells (96). Furthermore, the GBM mouse model TILs had more $CD8^{+}PD\text{-}1^{+}TIM\text{-}3^{+}LAG\text{-}3^{+}$ than equivalent models in melanoma, breast and lung cancer (94). Simultaneously, a second group published supportive findings to these showing that $CD8^{+}$ TILs isolated from GBM showed a severe exhausted phenotype (95). This group also compared relapsed and primary GBM patients' TILs and tumour transcriptomic immune signature which they found were similar. However, the relapsed patients had a restricted TCR repertoire clonality and thereby supports a role of boasting antigen presentation and priming through DC targeted immunotherapies (97).

Immunosuppressive tumour microenvironment

Glioblastoma has a wide variety of mechanisms of immunosuppression, most of which are also common in non-CNS tumours (44). Over 4 decades ago impaired cell mediated immunity was described in brain cancer patients driven by a sera mediated factor likely to be a cytokine (81). Indeed TGF-β isoform 2 was originally described as glioblastoma-derived T cell suppressor factor, given its discovery in GBM cell lines and patient serum, where it was noted to be immunosuppressive to T-cell proliferation through IL-2 dependent and independent pathways (98, 99). TGF-β is pleiotropic and plays a role in both glioma tumorgenicity and immunosuppression. Its receptor is highly expressed on glioma cells and RNA silencing of TGF-β reduces glioma proliferation, migration and invasiveness. TGF-β also inhibits the transcription factors for the activating immunoreceptor NKG2D and its ligand MHC class I polypeptide-related sequence A (MICA), thus suppressing CD8 T-cell and NK function (100). MHC class II expression on glioma cells, microglia and macrophages is also reduced following TGF-β exposure (101). Interestingly, TGF-β2 has been measured pre- and post-op in GBM patients, with a favourable prognosis seen in those with a greater reduction in the cytokine, implying an important role of the cytokine in progression (102).

IL-10 is a potent anti-inflammatory cytokine. IL-10 induces immature and tolerogenic DC and hinders cytotoxic T cell effector function through sustaining the FoxP3 transcription factor on Treg (103, 104). IL-10 messenger RNA has been seen in gliomas, with higher levels associated with higher grades (105). IL-10 production by gliomas seems to polarise the tumour associated macrophages and microglia in the tumour microenvironment (106). IL-10 also promotes expression of the negative checkpoint molecule PD-L1 on glioma associated macrophages and peripheral monocytes (91).

Another important immunomodulatory mechanism of DCs and other immune cells is through indolamine 2,3-dioxygenase 1 (IDO) (44). This

orchestrates response to the cytokine environment, for example it is upregulated in response to interferons (107). IDO is a cytosolic enzyme which controls tryptophan degradation particularly kynurenine and in addition to the above, facilitates Treg expansions and inhibits T effector function. Furthermore, it can also attract and activate circulating Tregs in the TME to mediate immunosuppression (88). Overall it therefore downregulates the immune response (108, 109). It is highly expressed by glioblastoma multiforme (but not normal brain tissue) and levels of IDO expressions by malignant tumours has been correlated to poorer prognosis. Supportive of the above, mice implanted with IDO producing glioma cells (GL261), had increased intra-tumoral Treg accumulation and reduced survival (108). Furthermore, administration of 1-methyl-tryptophan (an IDO inhibitor) in combination with PD-L1 and CTLA-4 inhibitors resulted in 100% glioma mice survival, improved over PD-L1 and CTLA-4 dual inhibitor therapy (110).

Overall the TME in glioma is profoundly immunosuppressive through a number of cell populations and cytokine factors.

Corticosteroids

Corticosteroids are universally used to alleviate symptoms of vasogenic oedema in GBM patients. Vasogenic oedema is a major consequence of BBB disruption and increased vascular permeability in GBM, resulting in accumulation of fluid entering the brain extracellular space (111). Administration of glucocorticoids effectively reduces BBB permeability by reinforcing endothelial tight junctions. In addition, dexamethasone (Dex) can inhibit the effects of tumour-derived VEGF and suppress vascular permeability (112).

This type of oedema is characteristic of brain malignancies that are progressing, but it can also appear after treatment with chemotherapy and radiotherapy due to uncontrolled inflammation of the CNS (113). Owing to tumour location and volume limitation, cerebral oedema increases

intracranial pressure and can compromise neurologic function, causing significant morbidity and mortality (111, 114).

Unfortunately, treatment with glucocorticoids also has several negative effects. Of particular relevance is the anti-inflammatory and immunosuppressive action of steroids (115). Several studies have shown that the use of Dex can lower CD4+ T lymphocytes, as well as exert global immunosuppression by inhibiting the activity of NF-κβ in T-cells (115-117). More recently, studies in GBM animal models and patients indicate that Dex lowers the efficacy of chemotherapy and radiotherapy, resulting in a decreased overall survival (118, 119). Steroids are known to be immunosuppressive and characteristically exert this effect by directing T-cell apoptosis, both at thymic development and in the periphery during activation-induced cell death (120, 121). Indeed clinically, steroids have direct cytotoxic effects on lymphoid origin cancers such as lymphoma and acute lymphoblastic leukaemia whereas have minimal cytotoxic effect on myeloid leukaemias (122). We discuss the detrimental effects of Dex on T-cell and DC function in more detail in chapter 2.

Circulating Dendritic Cells

DCs were first described in the lymphoid organs of mice as unique, stellate, nucleated cells making up 0.1-1.6% of total nucleated cells (123). Subsequently, it has been shown that these cells also have distinct functional properties separating them from macrophages and lymphocytes (124, 125). The key functional features of dendritic cells are their ability to capture antigens and process them with MHC complexes to initiate the adaptive immune response (125). MHC-peptide complexes are 10-100 times higher on DCs than other antigen presenting cells such as B cells and monocytes (125). Furthermore, their array of co-stimulatory molecules and cytokines secreted by DCs, orchestrate T cell differentiation and potent immune responses. In contrast to this DCs also determine tolerance by presenting self-antigens, which in the thymus, leads to deletion of self-reactive thymocytes, while in the lymphoid tissues, results in T cell anergy (125).

Since their description in mice, it was identified that DCs could be derived in humans from monocytes with appropriate cytokine exposure and these showed typical antigen presenting characteristics (126-129). This was shown to occur in-vitro and in a minority of inflammatory monocytes in-vivo (129). Now, it is clear that dendritic cells are a heterogeneous functional group of cells found in the circulation, lymph nodes and organs (130-133). Langerhans cells, found in the epidermis and CD1a DCs, found in the dermis, are examples of human tissue specific DCs (133). Here we focus on human DCs found in the blood namely myeloid $CD1c^{+}$ (cDC2), myeloid $CD141^{high}$ (cDC1), plasmacytoid (pDC) and slan DCs. A definitive DC marker does not exist and human DCs are defined as lineage negative (CD19/20/3/56 –ve) and HLA-DR high.

In the last decade, more distinctive circulating DC markers have been discovered such as Blood dendritic cell antigen (BDCA)-1 or CD1c, BDCA-2 (CD303), BDCA-3 (CD141) and BDCA-4 (CD304) (134). This is significant since the $CD11c^{+}$ myeloid population can be divided into cDC2, cDC1, $CD14^{+}$ and

$CD16^+$ populations (131, 133). We are now beginning to understand each DC have distinct functions. Indeed, the latest single-cell RNA analysis and unbiased surface marker dissection by mass cytometry (CyTOF), suggests further subset discrimination. For example, two transcriptionally distinct $CD1c^+$DC populations have been reported and a new, previously unreported DC population named AS-DC ($AXL^+Siglec6^+$), which transcriptionally fits on a spectrum between a pDC and cDC2 (135, 136).

It is currently not known which DC is most important for orchestrating cancer immunity. DC subsets have shown distinct patterns of TLR and lectin expression and this has led to discrete functions modelled in-vitro. These characteristics are summarised in figure 3.

The cDC2 subset expresses a wide range of lectins and TLR from 1 to 8, with particularly high expression of TLR 1,2,4 and 8 (131, 137). This subset has been shown to present glycolipids from mycobacteria and stimulate responses to fungal infections facilitated by high Dectin 1 and 2 expression (131). They also secrete a range of cytokines including TNF alpha, IL-8, IL-10 and IL-12 (138-141). cDC2s have higher expression of costimulatory molecules CD80, 83 86 and 40 and chemokine CCR7 for lymph node migration, than MoDCs and, furthermore migrate without the need for prostaglandins on maturation. (130, 131, 142, 143). The cDC2 have superior ability to stimulate an allogeneic response in a mixed lymphocyte reaction compared to the other circulating DC (130, 141). When cell ablation of the equivalent $CD11b^+$ DC in mice is performed, Th1, Th2 and Th17 responses are abrogated (131, 144). However, the $CD11b^+$ antigen presenting cells in mice are a highly heterogeneous population and includes macrophages and DC (133). Furthermore, $CD11b^+$ murine DC do not produce large quantities of IL-12, and poorly migrate (130, 141, 145, 146). In man, cDC2 cells are particularly important as they are the major source of IL-12, efficiently cross present antigens and activate Th1 and CD8+ cytotoxic T lymphocyte responses (141).

Phase I clinical trials in prostate cancer and melanoma have demonstrated the ability of cDC2 to induce anticancer immunity (147, 148).

The cDC1 ($CD141^{high}$) is a rare subset of DC making up only 0.1% of mononuclear cells in humans (131). They have been described in typical DC areas of lymph nodes, bone marrow and blood in humans (138, 149, 150). However, their mouse counterparts are more numerous and express $CD8\alpha$ in lymph node and $CD103^{+}$ in tissue which has facilitated research of cDC1 (151, 152). Indeed, the homology between mice and human cDC1 is better defined, where both are reliant on lineage-defining transcription factors IRF8, BAFT3 and IR2 for development and function (146, 153, 154). Furthermore, both human and mice counterparts uniquely express the C-lectin CLEC9A which has been shown to specialize in presenting necrotic tissue (149, 152). They also both uniquely express the chemokine receptor XCR1, which, on binding to its ligand XCL1 on T-cells, increases the antigen specific CD8+ T cell pool and IFN-γ secretion (155). In mouse studies cDC1 are the only high IL-12 and cross-presenting conventional DC, however, in humans cDC2 are at least equally able(138, 141, 156). cDC1 express a restricted TLR receptor expression with high TLR3 and -10, but notably lack TLR4, -5, -7, and -9 (137). Recently, interest in their importance for cancer immunity has grown following data, in mouse models, showing ablation of BAFT3 dependent $CD103^{+}$DC reversed response to immune checkpoint (157). Furthermore, expansion of $CD103^{+}$DC augments response to PD-L1 (158). The clinical utility of cDC1 in a vaccine for adoptive transfer has been restricted by both their low numbers and the lack of GMP-grade isolation kits (159).

Plasmacytoid DCs (pDC) are phenotypically and functionally distinct from myeloid DCs (134, 160). They lack myeloid markers such as CD33, CD11b and CD11c and have morphological plasmacytoid shape, giving them their name (134). Unique surface markers include surface markers CD123, CD303 (BDCA-2) and CD304 (BDCA-4) (134, 160). PDCs are at least as abundant as cDC2 in the circulation, are present in lymph nodes, but are not seen in tissues in

quiescent states (161). The hallmark of these cells is high expression of TLR7 and 9 which recognize viral nucleic acids and leads to high secretion of type 1 interferons (134, 160). PDCs thus control T cell responses to chronic viral infections (162). In the steady state they express low MHC class II, co-stimulatory molecules and induce T-cell tolerance or Th2 immunity, while in other contexts, activation led to efficient priming of both CD4 and CD8 T-cells and tumoricidal properties (133, 156, 163-165). PDCs are in early phase trials in melanoma and have been shown to be safe, have minimal toxicity and increased survival compared to historic controls (166). The same group have also combined pDC and cDC2 in vaccine therapy since there is pre-clinical evidence of synergy (159, 167). For example, recombinant IFN-α and activated pDC strongly enhance cDC2 maturation and increase IL-12 production (168). Contrary to this, a group has recently reported that although pDC are the predominant antigen presenting cell infiltrating glioma tissue they lack the ability to secrete interferon alpha in mice models (169). Depleting pDC resulted in reduced Tregs infiltrating the brain tissue and increased survival in mice. However, cDC2 vaccines were able to stimulate robust CD4 and CD8 responses, tumour eradication and long-term survival in 60% of mice. This was superior to both pDC vaccinated and control mice (169). PDC have not been trialed in high grade glioma patients and the results of a combined vaccine approach in melanoma are awaited.

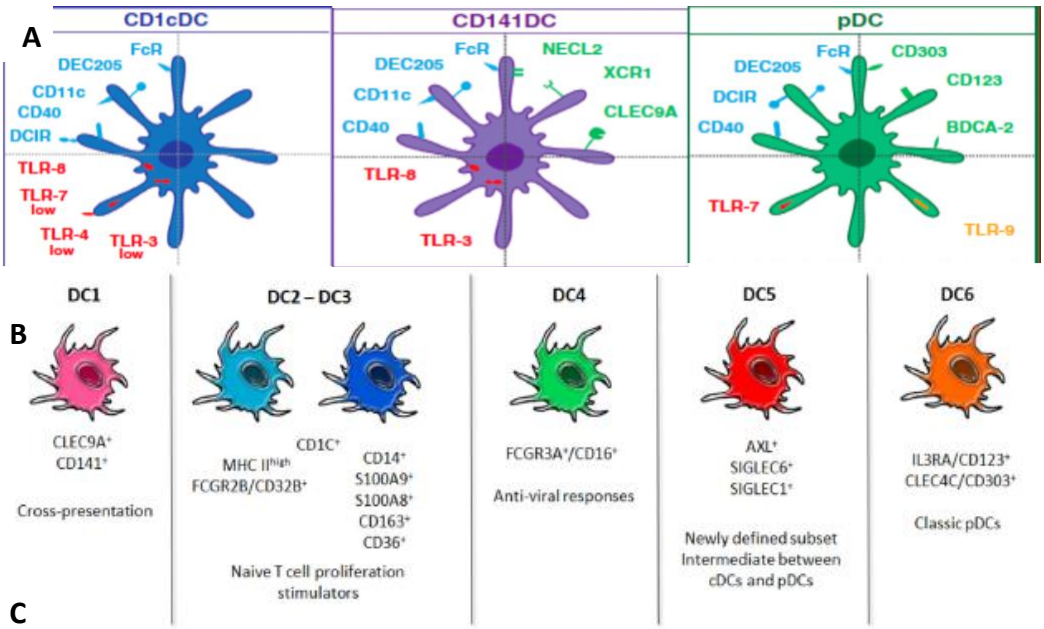
6-Sulpho LacNAc-Expressing Dendritic Cells (Slan DC) have been characterized by their novel surface protein, 6-sulfo LacNAc modification of PSGL-1, recognized by the M-DC8 antibody. They express CD16 and high HLA-DR and CD83 on maturation and were found to avidly phagocytose latex beads and exhibit MHC-restricted specific cytotoxicity against melanoma cells and hence classified as a dendritic cell (170, 171). They have been, in some papers, quantified as more numerous than the cDC2 population (172). Functionally, they release large quantities of pro-inflammatory cytokines, including TNF-alpha, IL-1b, IL-6, IL-23 and IL-12. This is a rapid response to inflammatory stimuli when triggered by TLR 7/8 (172). In one study, Slan DC produced

higher IL-12 on maturation with LPS (TLR 4) or CD40-ligand than cDC2s (173). Interestingly, maturation of the SlanDC, and therefore IL-12 secretion, was inhibited by CD47 expressed on erythrocytes, binding to SIRP-alpha (a signal regulatory protein), on SlanDCs (173). Therefore, it was proposed that this CD47/SIRP-alpha interaction could be a mechanism of controlling systemic IL-12 secretion from SlanDCs and prevent uncontrolled adverse inflammatory reactions (173).

When compared in-vitro to cDC2, SlanDCs were more powerful in programming Th17/Th1 T cells that secrete IL-17, IL-22, TNF-α and IFN-γ (172). Through staining of skin samples and their functional response in-vitro, a study defined SlanDCs as inflammatory dermal DCs which are important in psoriasis pathogenesis, and lupus erythematosus (172, 174). However, Slan DC stimulated with IFN-γ, can directly lyse tumour cells lines, in a TNF-α driven manner and via cell-to-cell contact, can promote NK cells directed cytotoxicity (175). Slan DC therefore can trigger tumour specific T cell responses, direct cytotoxicity and enhance NK cell killing (175). However, this population is debated in the literature as to whether they represent a DC or a non-classical monocyte (132). In the most recent RNA sequencing transcriptomic analysis, these cells may fall into the DC4 subset which are clustered separately from all non-classical monocyte populations (132, 135). This DC4 subset are $lin^{-}HLA\text{-}DR^{+}CD16^{+}$ and needs to be verified as to whether this population functionally matches the SlanDC data described.

Summary

There has been little progress to standard of care since the Stupp protocol was developed in 2005. Standard of care remains maximum surgical resection, 6 weeks of chemoradiation and a further 6 months of adjuvant Temozolomide (13). There are no standard second-line treatments. The immunotherapy wave of optimism has not been realised in GBM with disappointing results seen in the relapsed setting although the first line data in combination with standard of care is yet to mature. However, even though a small proportion of patients responded to PD-1 (8%), the median duration of response was 11.5 months, which in the relapse setting may be worthy of guarded optimism (176). Indeed, although our understanding of brain immunity is not complete, GBM are not like the typical "cold" tumours seen as immunologically inert (177). There are rich population of both myeloid origin innate immune cells and T-cell populations including activated $CD8^+$ T-cells. However, there is a restricted TCR repertoire seen in the TILs and multiple upregulated immune checkpoints which provoke thoughts for future combination treatments (94, 95). In this PhD we focus on the feasibility and utility of circulating dendritic cell, mainly cDC2 subset as the next generation of dendritic cell vaccines. We hypothesised that the abundance and function of circulating DC subsets is suppressed in patients with GBM. Furthermore, inhibiting the p38 MAPK pathway in patients' circulating DC subsets can restore their function. We further extended our work to look at the combination of immune checkpoint blockade with DC therapy to assess for synergy and ultimately guide rationale for successful immunotherapies to treat GBM.



C

Subset	cDC2	cDC1	pDC	SlanDC
Phenotype markers	CD1c CD172a (SIRPα) Dectin 1 Dectin 2	CD141 CLEC9A XCR1	CD303 CD304 CD123	CD16 CD11c M-DC8
TLR Expression	1,2,3(low),4,5,6,8,10	1,2(low),3,6,8,10	1,6,7,8(low),9,10	2(low),4,7,8
Cytokines	IL-1α, IL-1β, IL-6, TNF-α, IL-8, IL-10, IL-12, IFN-β, IFN-γ	IFN-β, IL-8, IL-12	IFN-α, IFN-β, IL-4, IL-10	TNF-α, IL-1β, IL-6, IL-12, IL-23
Function	Cancer Mycobacteria Fungal	Cancer Virus Allergy	Virus Cancer Autoimmunity (Psoriasis, SLE)	Cancer Autoimmunity (Psoriasis, SLE)
Relative prevalence	+++	+	++	+++
Mouse Equivalents	CD11b+ (tissues) CD4+ CD11b+ (lymphoid) ESAM	CD103+ (tissues) CD8+ (lymphoid) CLEC9A XCR1 Langerin	B220 Siglec H	Gr-1/Ly6C low monocyte CX3CR1hi CCR2 negative
Lineage Critical Transcription factors	Irf4, Zeb2, RelB Notch2	Irf8, Batf3, Id2	Irf8, E2-2, Bcl11A	?
References	(130, 131, 133, 137, 140, 146)	(130, 131, 133, 137, 146, 151, 155, 178-181)	(131, 133, 146, 161, 162, 166)	(130, 131, 133, 137, 170, 172-174)

Figure 3: Phenotype and functional classification of circulating Dendritic cells (A) Common surface markers and toll-like receptors (TLR) on cDC and pDC adopted from Radford et al is shown (182). (B) New DC classification based on single cell RNA sequencing, identifying 2 subsets of CD1c$^+$DC (DC2-DC3) and a novel subset (DC5) adapted from Gornati et al (183). (C) Table summarising DC phenotype and function.

Materials and Methods

Ethical Approval

Glioblastoma patients were entered into a study titled “A Study to investigate the effects of cancer and cancer treatment on the immune system over time” and approved by the University of Nottingham Research and Ethics Committee (REC): 13-EM-0218. The study sponsor was the University of Nottingham. Healthy volunteers were recruited to a study titles “Using human blood from normal donors for the study of immune responses” REC approval NB-161-1711.

Methodology and rationale for circulating dendritic cell flow cytometric analysis

Our group had previously published a protocol for enumerating myeloid CD1c^{+} (cDC2) and plasmacytoid DC (pDC) using a 3-colour panel which selected DC lineage markers (CD1c+ and CD303) following exclusion of B-cells (CD19+), monocytes (CD14+) and granulocytes (139). This was expanded to also include the DC subsets Slan and myeloid CD141^{high} (cDC1). Furthermore, we phenotyped each subset for CD86 and PD-L1 expression, which expanded the assay to 6 colours and 9 parameters (see figure 1). The staining antibody-fluorochrome used and respective isotype controls are summarised in table 1.

We aimed to design an assay, which required minimal blood from patients, while providing valid results, quoted as at least 100 events on flow cytometric analysis (194). We anticipated low numbers of cDC1 and found that red blood cell lysis was needed to differentiate this numerically small population on a background of red blood cell events. We chose to stain whole blood, since this was both quicker, needed small volumes of blood and was less likely to result in cell loss, than isolating the peripheral blood mononuclear layer. To do this we used Red blood cell lysis buffer (Biolegend cat: 420301), at a volume ratio

20:1 1Xbuffer:blood, as recommended by manufacturer. In healthy volunteers, this technique resulted in a total event count between 0.5-2.0 x 10^6 and a cDC1 event count greater than 100, in 13 out of 16 individuals screened. The cDC1 population is known to be a rare and makes up approximately 0.1% of mononuclear cells (133). The staining panel (table 2), required 6 separate tubes per analysis and hence 4.2mls of blood from each patient. This quantity was favourable, since only one 5ml tube of blood was required from participating patients.

Another factor, limiting quantitative analysis, was the capacity of the MACS Quant software on the flow cytometer. A data limit for acquisition per file was exceeded, even using 700µl of blood, unless a trigger was set. We used a forward scatter trigger of 100 to exclude debris. A final cell suspension volume of 460µl was chosen for flow cytometric analysis, since the maximum uptake by MACS Quant v10.0 is 450µl. This maximised the recorded flow events.

Protocol for circulating dendritic cell subset analysis

6 separate tubes containing 700µl of whole blood were stained using the antibody panel summarised in table 2. This allowed 9 parameters to be investigated with isotype controls. The quantity of antibodies used (table 1) were added to whole blood and incubated for 15 minutes. The blood was stained in tubes rested on ice and in the dark to protect fluorochromes. We then added 14mls of 1X red blood cell lysis buffer per tube and incubated the tubes in the dark for a further 15 minutes. The 15ml falcon tubes were then immediately spun at 1000 RPM for 5 minutes and the supernatant was discarded. The cells were then transferred to 5ml FACS tubes and resuspended in 3ml of staining buffer for washing. The cells were then spun again at 1000 RPM for 5 minutes. The supernatant was then discarded, and the cells were resuspended in 460µl of staining buffer for flow cytometric analysis. A multicolour compensation profile (see later) was created to correct for fluorochrome spectra emission overlap.

The MACS Quant Analyser 10 Flow cytometer is able to enumerate cells without the need for counting beads. The absolute number of dendritic cells were calculated using the following formulae:

$$Dendritic\ cell/ml\ blood = \frac{Events\ x\ Total\ Count/ml}{Total\ Events}\ x\ \frac{Volume\ Suspended}{Volume\ Blood\ Stained}$$

Flow cytometric gating strategy for identifying circulating dendritic cell populations

Using our 6 colour, 9 parameter flow panel, we identified 4 distinct population of dendritic cells (DCs). Initially cells were selected after doublet exclusion and by forward and side scatter. Cells with low side scatter (SSC) and CD19/14 negative events were selected to exclude granulocytes, B cells and monocytes respectively (figure 1a). DCs are characterised by high MHC class II expression and therefore HLA-DR positive cells were selected against isotype control (figure 1b). Lineage markers for cDC2 ($CD1c^{+}$), pDC ($CD303^{+}$), Slan (M-$DC8^{+}$) and cDC2 ($CD141^{high}$) were gated against isotype controls (figure 1c).

The 4 distinct populations were sub-gated to identify the CD86 and PD-L1 expression. Both molecules are vital to the co-stimulation axis of T-cells and are the target of cancer immunotherapies. The median fluorescence intensity (MFI) was calculated as a surrogate for relative expression by subtraction of the MFI of the marker of interest from the MFI of the respective isotype.

To test variance of the assay, four healthy donors gave a single blood donation. From this single donation, the assay was performed on three separate occasions. This negated the potential natural dynamic variance in an individual's immune system and the health of the donor at blood acquisition. The results are shown in figure 2.

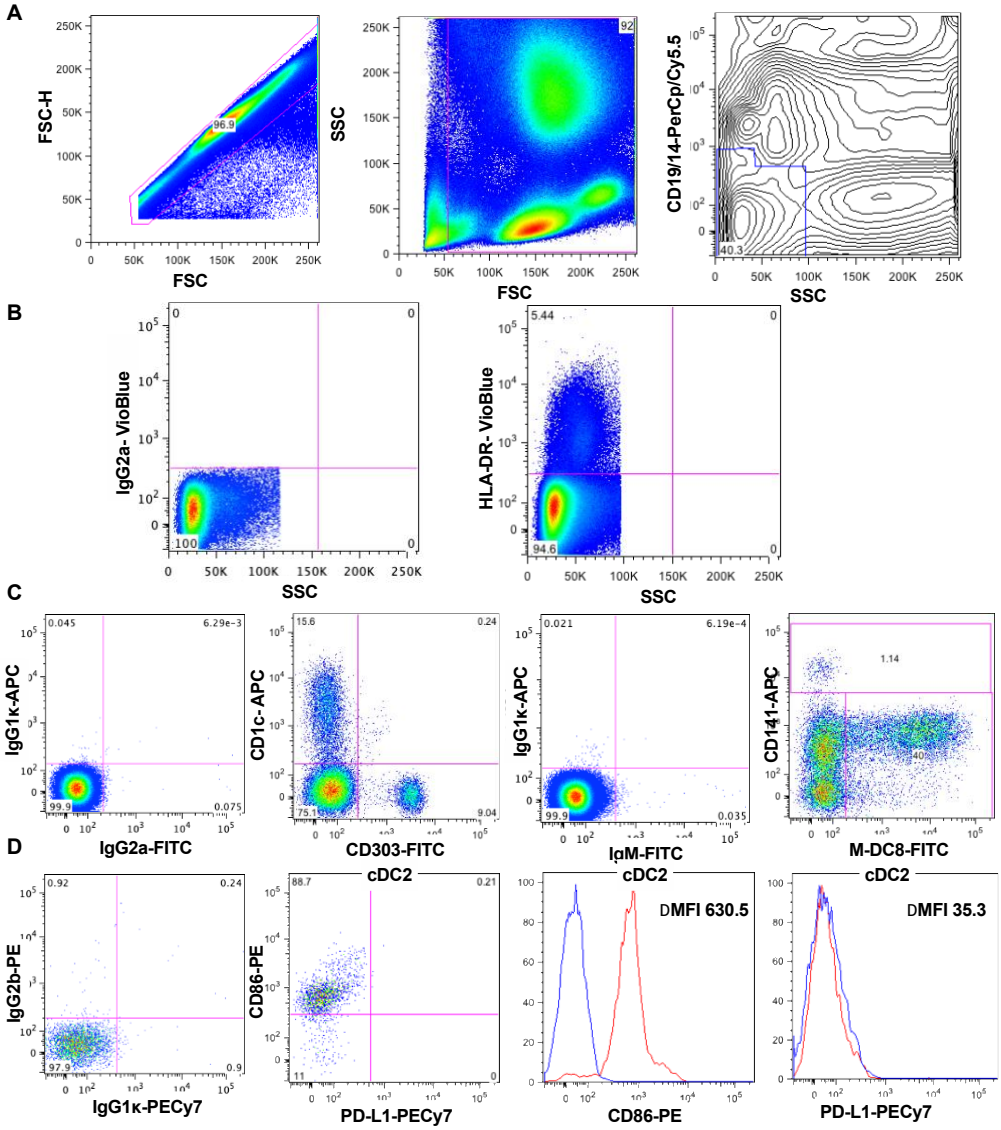
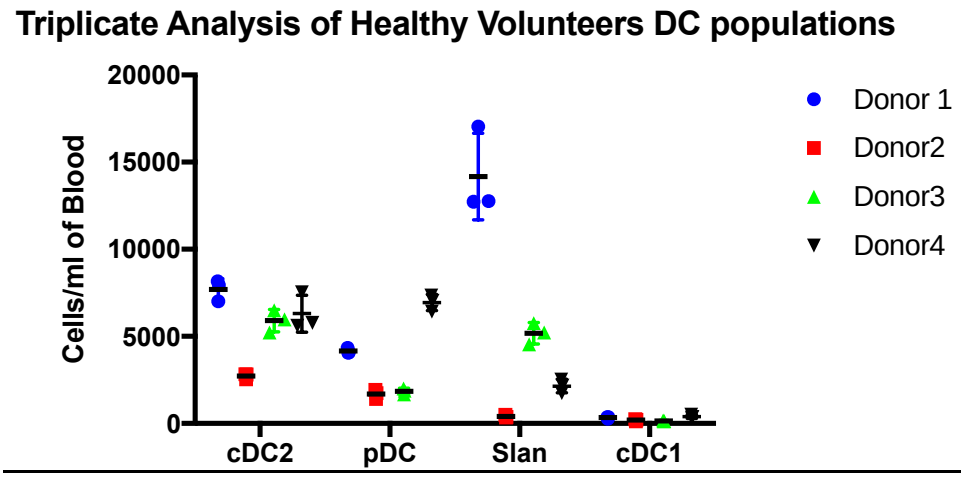


Figure 1: Gating strategy for enumerating and phenotyping circulating dendritic cells. (A) Doublet cells were first excluded by selecting cells with proportional forward scatter (FSC) height and area. A typical plot of white blood cell populations was subsequently seen when side scatter (SSC) and FSC were plotted. CD19/CD14-PerCP/Cy5.5 against SSC were plotted on a contour plot to exclude Granulocytes, B-cells (CD19) and monocytes (CD14). The subsequent cells were gated against a HLA-DR isotype control to select HLA-DR^{+} cells, characteristic of DC (B). Lineage markers for cDC2 (CD1c+), pDC (CD303+), Slan (M-DC8) and CD141^{high} (cDC1) were gated against isotype controls. The CD141^{high} populations was a clear group and manually gated (C). Each DC subset was then sub-gated for CD86 and PD-L1 expression on a dot-blot graph against isotype controls and plotted on histograms to calculate the MFI.



DC Subtype	Coefficient of Variance %				
	Donor 1	Donor 2	Donor 3	Donor 4	Mean
cDC2	7.90	5.96	10.84	16.84	10.39
pDC	3.80	15.35	9.22	6.77	8.76
Slan DC	17.5	18.12	11.87	18.2	16.42
cDC1	14.4	28.7	13.2	26.5	20.70

Figure 2: **The co-efficient of variance for four healthy volunteers' circulating dendritic cells.** Experiments were performed in triplicates from a single blood donation. The actual cells/ml are shown in the scatter plot and % co-efficient of variance in the table.
FSC= forward scatter; SSC= side scatter; FSC-H forward scatter height; FSC-A= forward scatter area; DC= dendritic cell; cDC2=Myeloid DC type 2, pDC= plasmacytoid DC; Slan= Slan DC; cDC1= Myeloid DC type 1; pink line = isotype control

Table 1: Antibody-Fluorochromes and isotypes with respective quantities used for whole blood enumeration of circulating dendritic cells assay

Antibody	Fluorochrome	Manufacturer	Catalogue No.	Clone	Working Conc µg/mg	Volume /700µl
CD303	FITC	Biologend	354208	201A	200	5.0
Mouse IgG2a (CD303 isotype)	FITC	Biolegend	400210	MOPC-173	200	5.0
M-DC8	FITC	Miltenyi	130-093-027	DD-1	33	10.0
Mouse IgM (M-DC8 isotype)	FITC	Miltenyi	130-093-178	ISS-20C4	44	10.0
CD1c	APC	Biolegend	331524	L161	100	5.0
Mouse IgG1κ (CD1c and CD141 isotype)	APC	Biolegend	400122	MOPC-21	100	5.0
CD141	APC	Biolegend	344106	M80	150	5.0
CD19	PerCP/Cy5.5	Biolegend	302230	HIB19	100	5.0
CD14	PerCP/Cy5.5	Biolegend	325622	HCD14	400	5.0
HLA-DR	VioBlue	Miltenyi	130-095-293	AC122	82.5	10.0
Mouse IgG2a (HLA-DR isotype)	VioBlue	Miltenyi	130-094-671	S43.10	55	10.0
CD86	PE	eBioscience	12-0869-42	IT2.2	100	5.0
Mouse IgG2b (CD86 isotype)	PE	eBioscience	12-4732-42	ebMG2b	200	5.0
CD274 (PD-L1)	PECy7	eBioscience	25-5983-42	MIH1	50	5.0
Mouse IgG1κ (CD274 isotype)	PECy7	eBioscience	25-4714-42	P3.6.2.8.1	50	5.0

Table 2: Staining Panel for whole blood enumeration of circulating dendritic cells assay

	Fluorochrome and Antibody					
Tube	**PerCp/Cy5.5**	**APC**	**FITC**	**VioBlue**	**PE**	**PECy7**
1	CD19/14	CD1c	CD303	HLA-DR	CD86	PD-L1
2	CD19/14	CD141	M-DC8	HLA-DR	CD86	PD-L1
3	CD19/14	CD1c	CD303	HLA-DR Isotype	CD86 Isotype	PD-L1 Isotype
4	CD19/14	CD141	M-DC8	HLA-DR Isotype	CD86 Isotype	PD-L1 Isotype
5	CD19/14	CD1c Isotype	CD303 Isotype	HLA-DR	-	-
6	CD19/14	CD141 Isotype	M-DC8 Isotype	HLA-DR	-	-

Multi-colour Compensation

When multi-colour staining of a single well or FACS tube was used and where the fluorochrome emission spectra overlapped, a compensation profile was created prior to analysis. Miltenyi MACS Comp beads (130-097-900) were used. 100µl of MACS Running buffer was added to 5ml FACS tubes. Antibodies, used at the expected experimental concentration, were added to separate tubes. One drop of positive beads and negative beads were added to each tube with antibodies. A further blank tube was created with 100µl of Running buffer and negative beads only. The beads and antibodies were incubated in the dark for 15 minutes. The beads were then analysed on MACS Quant 10.0 on the multicolour automatic compensation setting. A visual inspection of the profile prior to saving ensured satisfactory compensation. These settings were saved, and only the forward/ side- scatter parameters were changed at cell acquisition, according to cell phenotype.

Isolation of Peripheral Blood Mononuclear cells (PBMC)

The required blood volume (typically 50-200ml) was transferred from heparinised syringes to a T75. Buffy Coats were diluted 1:1 with Dulbecco's phosphate buffered saline solution (DPBS). Fresh blood was made up to a final volume 210ml with DPBS. The blood was then pipetted gently over a 15ml Ficoll gradient per 50ml falcon tube, which separates blood cells by their density. Red blood cells and granulocytes penetrate the Ficoll, while the lymphocytes, monocytes and platelets do not. Centrifugation at 800g, acceleration 9 and brake 1 over 25 minutes was used to divide cells by their density, resulting in the characteristic appearance seen in figure 3.

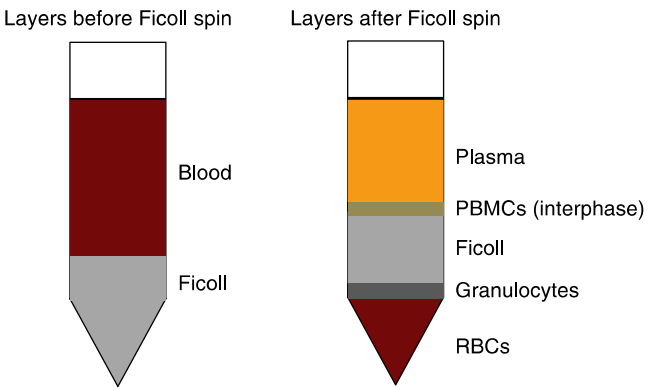


Figure 3: Illustration of the PBMC layer from blood before and after centrifugation over a Ficoll gradient. Adapted from Lin et al 2014 (184).

The PBMC layer was then isolated and the cells were washed 3 times (1400 RPM for 8 minutes, 1400 RPM for 7 minutes and 1000 RPM for 5 minutes) to improve purity and remove platelets. The final isolated PBMCs were counted prior to use. The typical numbers from fresh blood were 0.75-2.5 x 10^6/ml .

Generation of Monocyte Derived Dendritic Cells (MoDCs)

Monocytes were isolated through positive CD14+ve microbead selection of PBMCs using Miltenyi Biotec isolation kit (Cat 130-050-201). For 5-7x10^8 PBMC cells were resuspended in 800µl MACS buffer and 150µl of CD14

microbeads. When using buffy coats, filters were used and placed above the column. Following 15 minutes incubation at 5^{o}C, cells were washed by adding 20ml MACS buffer to cells, and then centrifuged at 1000 RPM for 5 minutes. The supernatant was discarded and cells were resuspended in 1ml MACS buffer. Meanwhile, a Miltenyi LS column, which has a capacity for 2 x10^{9} total cells and a maximum 10^{8} labelled cells, was prepared. This required rinsing with 1 ml MACS buffer. The cells were then passed through the LS column, 500µl at a time. To elute the cells from the column, 5 ml of MACS buffer was applied to the column away from the magnet into a 50ml falcon tube. This protocol had been modified in our group giving consistent purities >94%. The effluent cells were kept for peripheral blood lymphocytes (PBLs).

To make MoDCs, CD14 +ve cells (monocytes), were washed in MACS buffer by centrifugation for 5 min at 1000 RPM and the supernatant was discarded. The monocytes were then resuspended in 15ml (T75 flask) or 30ml DC media (T175 flask), depending on cell number (≤15 x10^{6} cells in T75 flask or > 15 x10^{6} but ≤30 x 10^{6} T175). Prior to transfer, IL-4 and GMCSF were added at 1:1000. The cells were cultured for 5-7 days in a 5% CO_2 35^{0}C incubator.
On day 3 of culture, half the initial volume of DC media +IL-4+ GMCSF 1:1000 were added to avoid cytokine exhaustion. The cells were routinely checked by electron microscopy for typical appearances of monocyte-derived dendritic cell appearances and by flow cytometry for upregulation of HLA-DR and CD14 negativity (figure 2).

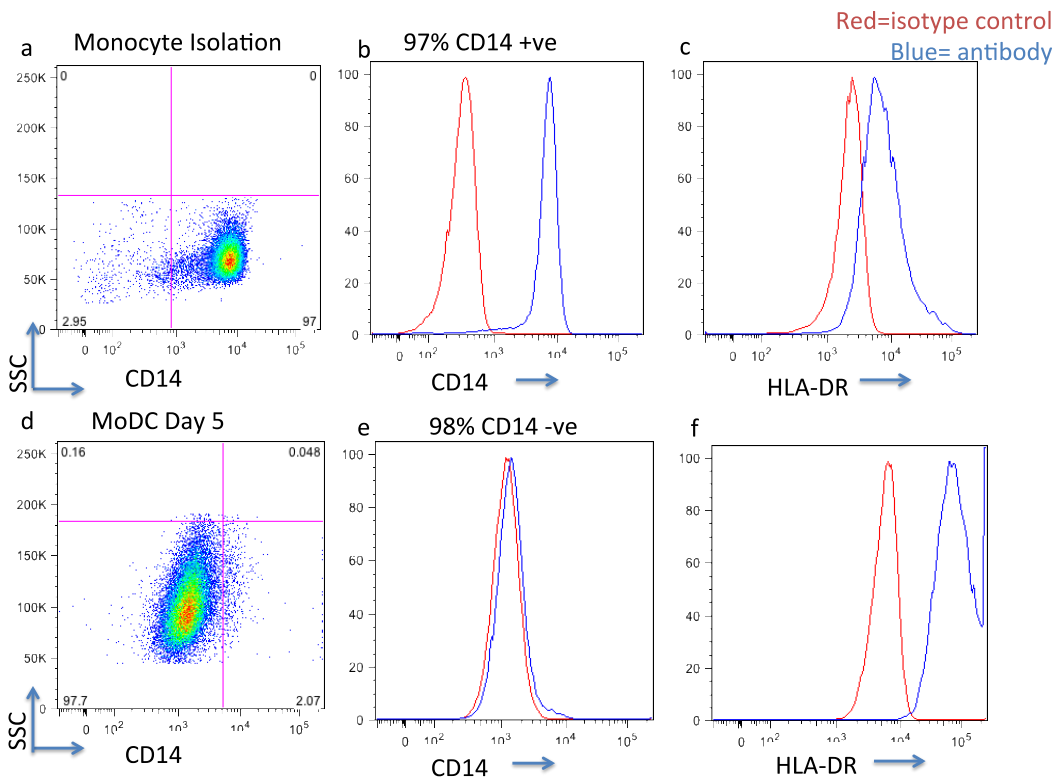


Figure 4: A comparison of the phenotype of monocytes post isolation by flow cytometry (top row) and MoDC (bottom row). Monocytes show 97% purity post isolation represented on dot plot (a). CD14 expression compared to isotype control (b) and HLA-DR (c) are shown on histogram plots. Monocytes are CD14+ and have low HLA-DR expression. MoDCs, however, when differentiated, downregulate CD14 (negative 97.7%) represented by dot plot (d) and by histograms (e). They have also high HLA-DR expression characteristic of a DC (f).

Isolation of myeloid CD1c$^+$ (cDC2)

cDC2s were isolated from fresh blood using the validated Miltenyi CD1c isolation kit (130-090-506) from peripheral blood lymphocytes (PBL). The principle of the protocol is to deplete B cells, since they weakly express CD1c, and then positively select the remaining CD1c$^+$ cells.

PBLs were counted and quantities adjusted according to cell number as advised by manufacturer. The quantities given are for a starting number of 10^8 cells.

CD19 (B-cell) depletion was performed by suspending cells in MACS buffer (200µl) proceeded by the addition of FcR blocking reagent (100µl), CD19 microbeads (100µl) and CD1c-biotin (100µl). The cells were then mixed by gentle pipetting and incubated at 5^{o}C for 15 minutes. Subsequently, 20mls of MACS buffer was added for washing the cells followed and centrifuged at 1000 RPM for 10 minutes. The supernatant was discarded and the cells were resuspended in 500µl MACS buffer. The cell suspension was passed through a Miltenyi LD column attached to a magnet, which has a maximum capacity of removing 10^8 B-cells. The column was then washed with 2x1ml of MACS buffer. Effluent cells were collected for the subsequent CD1c selection steps. The B-cells were saved for PBL by eluting the column cells away from the magnet.

The effluent cells (CD19 deplete) were then washed in 10mls of MACS buffer and centrifuged at 1000 RPM for 10 minutes. The cells are resuspended in 400µl MACS buffer, labelled with 100µl of anti-biotin and incubated at 5^{o}C for 15 minutes. For this selection, a Miltenyi MS column was used with a capacity of 2 x10^8 cells and a maximum selection of 10^7 labelled cells. An anticipated range of 0.3-1.5 x10^6/200ml cDC2 from a donor was expected. The column was rinsed with 500µl of MACS buffer, followed by the cell suspension in 500µl of MACS buffer. The cell suspension is proceeded by 3x 500µl of MACS buffer for washing. To achieve high purities, the cells in the MS column are eluted directly onto a second MS column. This results in consistent cell purity of >98% and 6-7% cell death (on PI stain, see figure 3). Effluent (T-cells)

were kept and added to previously isolated B-cells for later use.

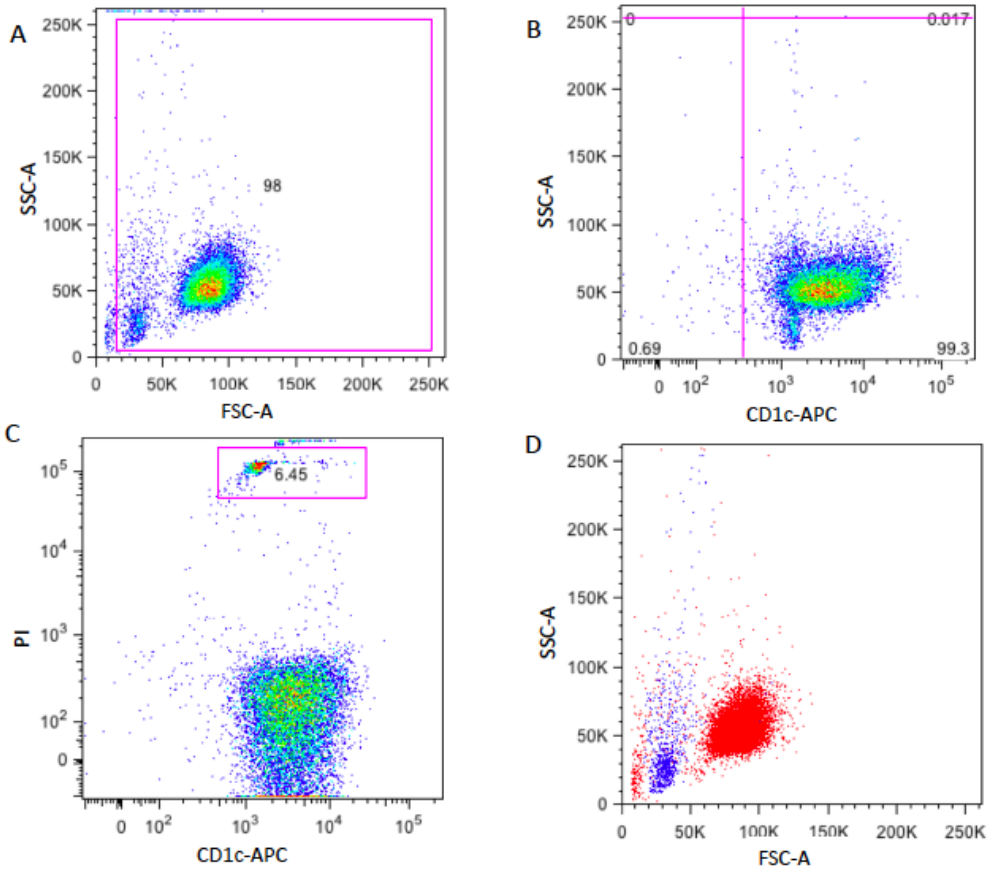


Figure 5: Purity and viability of cDC2 post isolation. (A) Side scatter (SSC-A) vs Forward scatter (FSC-A) of cDC2 post isolation; (B) Typical dot plot assessing purity of cDC2, in the example shown there was 99.3% purity (pink lines gating based on isotype control). (C) Viability assessed by Propidium iodide (PI) staining showing 6.45% dead cells which have been back gating onto original SSC-A vs FSC-A and shown as blue dots (D).

Phenotyping isolated dendritic cells MoDC or cDC2

Isolated cells were phenotyped for purity, activation state and effect of p38 MAPK inhibition in a number of experiments. 10^5 MoDC or $5x10^4$ Myeloid DC were typically stained. The concentration of antibodies used are listed in table 3. Post isolation, cells were stained in FACS tubes immediately following isolation. Where MoDC or cDC2 phenotype was compared in the immature, matured and p38 inhibited states, cells were analysed in a 96 well plate. The cells were washed in MACS running buffer followed by resuspension in 200µl MACS running buffer. Antibodies were added at the concentrations stated in table 3 and incubated at 5^oC in the dark. Samples were analysed by MACS Quant flow cytometry and multi-colour compensation profiles (as previously described) were created prior to analysis, which allowed multiple stains to be added to the same cells.

Table 3 Phenotype antibodies and fluorochromes for MoDC and cDC2

Antibody	Fluorochrome	Manufacturer	Catalogue No.	Clone	Stock Conc µg/ml	Volume/ 200µl
CD80	APC	Miltenyi	130-097-204	2D10	110	1.0
Mouse IgG1κ (CD80 isotype)	APC	Miltenyi	130-092-214	IS5-21F5	22	1.0
CD86	PE	eBioscience	12-0869-42	IT2.2	100	0.5
Mouse IgG2b (CD86 isotype)	PE	eBioscience	12-4732-42	ebMG2b	200	0.5
CD1c	APC	Biolegend	331524	L161	100	5.0
Mouse IgG1κ (CD1c isotype)	APC	Biolegend	400122	MOPC-21	100	5.0
CD14	PerCP	Miltenyi	130-094-969	TÜK4	55	1.0
Mouse IgG2a (CD14 isotype)	PerCP	Miltenyi	130-094-967	S43.10	11	1.0
HLA-DR	VioBlue	Miltenyi	130-095-293	AC122	82.5	0.5
Mouse IgG2a (HLA-DR isotype)	VioBlue	Miltenyi	130-094-671	S43.10	55	0.5
CD273 (PD-L2)	PE-Vio770	Miltenyi	130-105-828	MIH18	55	1.0
Mouse IgG1 (CD273 isotype)	PE-Vio770	Miltenyi	130-096-654	IS5-21F5	11	1.0

IL-12 ELISA

The stock concentration for the ELISA reagents are recorded in table 4.

The IL-12p70 ELISA was performed as BD Biosciences protocol and product (555183). Briefly, 96 well ELISA plates coated with capture antibody diluted in DPBS (1:250) 100µl/well and was sealed overnight at 5^{o}C. The plates were washed in Washing buffer (PBS+0.05% Tween-20) three times on the day of use. Initially, the plates were blocked with Assay diluent (DPBS+10%FBS) 200µl/well and incubated for 1hr. The samples and standards were plated to make final volume 100µl/well. The typical sample dilutions were 1:20-1:50. The standards were prepared by serial dilution to detect a range up to 1000pg/ml. Following the addition of the samples and standards, the plates were sealed and incubated for 2hrs. The plates were then washed with 300µl/well Washing buffer 5 times. 100µl/well of Working detector (detection antibody 1:500 + SAv-HRP 1:250) was subsequently added. The plate was left to incubate for 1hr and then washed. Following this, 100µl/well of Substrate solution (see table 4) was added and observed for a colour change from clear to yellow. The standards and samples changed colour gradually, typically over 20 minutes. Stopping solution (1M of $2NH_2SO_4$) was added (100µl/well) when the standards were clearly visible. The plates were then read on an ELISA reader (Infinite F50 Tecan). A standard curve was plotted using the standard ELISA values and known concentrations in Microsoft Excel and a formula acquired from a trend line. The actual IL-12 levels from the samples were calculated by inputting the light intensity into the formula to output an IL-12 value and multiplied by the dilutions factor.

IL-10 ELISA

IL-10 cytokine secretion was analysed using ELISA R&D Systems protocol and product (DY217B). A 96 well ELISA plate was coated with capture antibody diluted in DPBS (1:180) and added at 100µl/well. The plates were left overnight at room temperature. On the day of use, plates were washed in

Washing buffer thrice, and subsequently blocked with reagent diluent (DPBS+1%BSA) 300µl/well. This was incubated for 1hr. Following 3 washes, 100µl/well of sample or standards were added. The samples were diluted 1:1 with reagent diluent. The standards were diluted to detect up to 2000pg/ml with serial halving dilutions. The sample and standards were incubated for 2hrs and subsequently washed three more times with washing buffer. Detection antibody added (1:180) 100µl/well was then added, incubated for 2hrs, and then washed. Following this streptavidin, horseradish peroxidase (1:200) was added and incubated in the dark for 20 minutes. To finish the ELISA, substrate and stopping solution was added as in IL-12 and the plates analysed as aforementioned.

IFN-γ ELISA

IFN-γ cytokine secretion was analysed using ELISA R&D Systems protocol and product (DY285B). A 96 well ELISA plate was coated with capture antibody diluted in DPBS (1:180) and added at 100µl/well. The plates were left overnight at room temperature. On the day of use, plates were washed in Washing buffer thrice, and subsequently blocked with reagent diluent (DPBS+1%BSA) 300µl/well. This was incubated for 1hr. Following 3 washes, 100µl/well of sample or standards were added. The samples were diluted with reagent diluent depending to expected signal (typically 1:50-1:100). The standards were diluted to detect up to 2000pg/ml with serial halving dilutions. The sample and standards were incubated for 2hrs and subsequently washed three more times with washing buffer. Detection antibody added (1:180) 100µl/well was then added, incubated for 2hrs, and then washed. Following this streptavidin, horseradish peroxidase (1:200) was added and incubated in the dark for 20 minutes. To finish the ELISA, substrate and stopping solution was added as in IL-12 and the plates analysed as aforementioned.

Cell lines

The U87 GBM cell line was acquired from the American Type Culture Collection (ATCC) deposit. A recent publication has stated that this differs from the original cell line deposited from a male in 1966, by using single tandem repeat and mitochondrial DNA analysis to compare the current ATCC deposit to the original. However, by comparing the transcriptome profile to the Cancer Cell Line Encyclopedia, confirmed it is genetically GBM from a male patient (185). These cells were expanded in Eagles minimum essential medium (EMEM)+10% FBS and cultured at $0.5x10^6$ cells/ml. Cells were split bi-weekly and grown in a T75 flask. The LN-299, was also acquired from the ATCC and this cell line has a mutation in p53 (TP53) and a deletion in p16 tumour suppressor gene, typical of GBM. This cell line was originally from a female GBM patient in 1979. These were grown in Dulbecco's modified eagles medium supplemented with 5% FBS. These were cultured at $0.5x10^6$ cells/ml in T75 and split bi-weekly.

The Jurkat T-cells transduced with CD8 and the complete α- and β-chains of a TCR specific for the HLA-A2.1-restricted peptide $gp100_{(280–288)}$ (E6.1 fl296) were acquired from the Carl Figdor Tumour Immunology laboratory, Radboud University, Netherlands as part of a collaboration. This cell line has been described and validated in previous publications (186, 187). Cells were cultured in RPMI with 1% L-glutamine and 10% FBS and kept between 0.2 and $1x10^6$ in 10ml in a T75. IL-2 (5ng/ml) was added each week and cells were split bi-weekly.

All cell lines were mycoplasma tested and negative prior to use in co-culture experiments.

Tumour Lysate

To make tumour lysate, cells were placed in a 50ml falcon tube at 10^7 cells/ml in a final volume of 10mls. 5 cycles of freeze-thawing between liquid nitrogen and 50^{o}C water bath was then applied. Lysate was obtained by pipetting the supernatant following centrifugation at 1000 RPM for 5 minutes. The

resultant tumour lysate was stored at -80^{o}C until use.

Co-culture DC, Tumour Lysate (TDL) or Dexamethasone (Dex) +/- p38 MAPK inhibitor

Following cDC2 or MoDC isolation, cells had 1:1000 GMCSF added and were rested in a 96 well plate. They were seeded at 10^4 cells per well for one hour in 100µl DC media prior to co-culture. MoDC, following 5-7 day generation, were washed, phenotyped and plated at 10^4 cells per well, for direct comparison experiments with cDC2, or $5x10^5$ for MoDC only experiments.

Cells were incubated with Dex at concentrations 10^{-6}M,10^{-7}M and 10^{-8}M. U87 TDL was used at ratios 1:1, 1:3 and 1:10. BIRB0796, a p38 MAPK inhibitor, was used at 1µM at which concentration it is known to block all 4 subunits of p38 (α, β, σ and λ) and we have previously shown that at 0.1 µM, BIRB0796 does not fully inhibit downstream MK2 phosphorylation (139). For co-culture of 3 conditions, DC were seeded in a volume of 100µl DC media, with Dex/TDL/DC media/BIRB0796 added at 4X concentration in a volume of 50µl. Finally, the TLR agonist R848 (4X 2.5µl/ml) and PolyI:C (4X 20µl/ml) were added for maturation or media, for immature DC (iDC), in 50µl. Therefore, all wells had a final volume of 200µl. BIRB0796, DEX and TL were co-cultured with MoDC/cDC2 for 1 hr prior to PolyI:C and R848 maturation. Cells were then incubated at 35^{o}C and 5%CO_2 for 24 hrs.

The supernatant was collected for cytokine analysis at this time and cells phenotyped by flow cytometry where stated. Previously, in our group, the optimal PolyI:C and R848 concentrations were titrated and therefore not repeated. It was also shown that dual TLR agonists were required for high cDC2 IL-12 production (139). Indeed, others have identified that dual TLR produce high IL-12 and are required for cross-priming, particularly the combination of TLR3/4 and TLR 7/8 (141, 188). This may highlight the non-redundant specialised roles of different DC subsets. We had previously seen similar levels of IL-12 from cDC2 stimulated with either LPS (TLR4) or PolyI:C

(TLR3) in combination with R848 (TLR7/8) and therefore PolyI:C and R848, were used for all experiments, where maturation was required, to allow direct comparisons between MoDC and cDC2.

Mixed Lymphocyte Reaction (MLR)

In the mixed lymphocyte reactions untreated or treated (Dex- or TDL-exposed) DCs were co-cultured with peripheral blood lymphocytes (PBL). Firstly, immature, mature (+/- Dex or TDL) p38 inhibited DCs were made.

DC were washed, after 24hrs of maturation, in DC media to remove TLR agonists, Dex, TDL and BIRB0796. They were then plated at specified stimulator to responder ratio, as stated in the results, in round bottom 96 well plates. Meanwhile, PBL were rested overnight at 10^6/ml in T175 flask in T-cell media. PBLs were used at a concentration of 10^5 /100µl for 'responders' in all experiments. DCs and PBLs were co-cultured for 5 days. At day 5, tritiated thymidine was added at 10µl of 250UmCi per well for 18hrs. Plates were then washed and left overnight to dry. Scintillating fluid was then added and the plates sealed. The plates were analysed on a TopCount NCT reader.

When the combination of DC and checkpoint blockade were combined in an MLR, the method was as above, but with CD4 T-cells as responders, as opposed to PBL. In our preliminary data a proliferative effect with CTLA-4 inhibitor was seen in only the CD4 responders and not with PBMC and PBL in a MLR. This was supported by data on CD4 and PD-1 inhibitors initiating a proliferative response between DC and CD4 T-cells in a MLR by Wang et al (305). Anti-CTLA-inhibitor (ipilimumab) 50µg/ml, anti-PD-1 (pembrolizumab) 50µg/ml or a combination of both were added with CD4 T-Cells to appropriate conditions on Day 1.

Western blotting of cDC2 p38-MK2 pathway

The activity of BIRB0796 was confirmed by western blotting for the downstream target phospho-MK2. Isolated cDC2 cells were plated in DC medium containing GM-CSF. After resting, cells were treated with 1µM BIRB0796 for 1hr, stimulated with Poly I:C/R848 then lysed in radio-immunoprecipitation assay buffer (RIPA) (Sigma) containing protease inhibitor cocktail, phosphatase inhibitor cocktail 2 and 3 and Benzonase endonuclease (all Sigma) on ice for 1h. Proteins were resolved by SDS-PAGE electrophoresis in 10% Tris/glycine gels and transferred to nitrocellulose. Membranes were blocked (5% milk powder (w/v) in PBST (PBS-0.1% (v/v) Tween 20)), probed with primary antibodies overnight at 4°C whose binding was detected with secondary antibodies in 1% milk powder (w/v) in PBST. Rabbit anti-human phospho-MK2(T334) and mouse anti-human β-actin (Sigma) were detected with donkey anti-rabbit-800 and anti-mouse-680 (LiCor) and imaged by LiCor Odyssey SA. Semi-quantitative analysis was undertaken with Odyssey software normalising to β-actin.

Migration Assay

cDC2 were isolated as previously described, rested and matured +/- p38i. Following 24hr maturation overnight, cDC2 were counted both manually and through FACS. 5 healthy donor cDC2 immature, matured (mDC) and p38i mDC were compared. A CCL21 concentration of 250ng/ml was chosen based on other DC migration studies and media (RPMI+ 1%FCS) was used as a control (189). Briefly, the lower chamber of a 24-well transwell 5µm pore membrane plate (Costar 3421) was filled with 600µl of media (RPMI+1%FBS) or CCL21 (250ng/ml diluted in RPMI+1%FBS). The upper chambers were then filled with 50µL of media to moisten membrane for 15 minutes prior to the addition of cells, which facilitated even distribution of cells across the membrane. $5x10^5$ cDC2 were resuspended in 50 µL of media per well. The upper chambers were placed over the lower chambers containing media or CCL21 and left in an

incubator for 4 hours 37° 5%CO_2. Cells were harvested from the lower chamber by agitation with media cells and PBS+EDTA (cold). Wells were inspected by light microscopy to ensure maximum yield from plate. Cells were then counted by FACs. Cells were also phenotyped for CCR7 expression.

Cross-Presentation Assay

cDC2 were isolated and plated as iDC, mDC or p38i mDC, as previously described, in a 96 well plate at 10^4 cells/well in 100 µl of DC media. Long gp100 peptide ($gp100_{272-300}$ 50µM in 25µL) was added simultaneously with maturation factors in test wells. Blank wells with DC only were also left for controls (added on day 2). Cells were incubated overnight at 37°C 5%CO_2 to allow processing of the long peptide. On day 2, E6.1 fl296 Jurkat T cells, a transfected Jurkat cell line for TCR $gp100_{280-288}$, were added at $5x10^4$ cells per well in 25µL, which were activated by long peptide processing to short peptide ($gp100_{280-288}$). The transfected cell line has been validated in similar assays (186). The short peptide (1µM in 50µL $gp100_{280-288}$) was added as a positive control to appropriate wells for iDC, mDC and p38i mDC. A $gp100_{154-167}$ irrelevant peptide (1µM in 50µL) was added to appropriate wells as a negative control. The final volume in the wells was 200µL. After 24 hrs cells were washed twice with PBS and stained with TCR-gp100-eFluor780, CD3-FITC and CD69-APC to assess $gp100_{280-288}$ specific Jurkat activation. PMA was used as a positive control for Jurkat staining with CD3 and CD69. All conditions were stained in duplicate.

cDC2-peptide specific cytotoxic T-cell generation

3 healthy HLA-A2 donors' cDC2 were isolated, rested, and then treated with or without p38i and matured overnight with dual TLR (R848 and PolyI:C). After 24 hours DC were washed with serum free media and pulsed with peptide (EGFRvIII, TRP-2 or Flu-matrix - see table 4) at 10μg/ml for 4 hours. Following which, cells were then washed and re-plated in a 24 well plate with autologous PBL at DC:PBL ratio of 1:50. IL-7 (5ng/ml) was added on Day 1 and then every 7 days to support the culture. IL-2 was added at 66IU/ml on day 3 and then with IL-7 every 7 days. The PBL stimulated with DCs were co-cultured for 15-21 days prior to the analysis by IFN-γ ELISPOT. A peptide boost was performed on day 7, 14 and with the ELISPOT in the appropriate wells. The ELISPOT was performed with 250,000 cells per well and cells activated with media (control), relevant or irrelevant peptide (EGFRvIII, TRP-2, CEF1) or phytohaemagglutinin (PHA - positive control for ELISPOT). The manufacturer's protocol (MABTECH 3420-2A) was used to complete the IFN-γ ELISPOT assay.

IFN-γ ELISPOT

The method was carried as per manufacturer's instructions. Briefly, PVDF plate (Milipore #MAIPSWU) were activated with 35% ethanol for one minute and immediately washed 5x with sterile water. 100μl of coating antibody (1-DIK) 15μg/ml, was added to each well and left overnight sealed at 5^{o}C. The following day, wells were washed and blocked with whole media for 30 minutes. 10^5 PBL was placed in wells and incubated with titrating doses of the peptide of interest (0.05, 0.5 and 5μg/ml), PHA control and 5μg/ml of irrelevant peptide. Cells were wrapped in clingfilm and placed in 37^{o}C humidified 5% CO_2 incubator for 24 hours. Cells were subsequently washed and incubated with detection antibody (7-B6-1-biotin 1μg/ml) for 2 hours at room temperature. The plate was then washed and diluted streptavidin-ALP (1:1000) added and incubated for a further hour. Following a further wash,

substrate solution (BCIP/NBT) was added to the wells and the plate was incubated in the dark until spots developed. The reaction was terminated by washing the plate under water. The plate was read on ELISPOT plate reader.

PD-1 inhibited CD4-Tcell co-culture with GBM cell lines

Here 10^4 GBM tumour cells lines (U87 or LN229) were plated in a 96-well plate for 24 hours, which allowed adherence and expansion in the well. They were then irradiated at 4Gy to halt further proliferation without causing significant cell death. CD4 T-cells, isolated by direct magnetic labelling with CD4 microbeads from fresh blood of healthy donors, were then added. The simultaneous addition of increasing concentrations of PD-1 (0, 5, 50μg/ml) and 5μg/ml of phytohemagglutinin were added to stimulate proliferation. Following 3 days of culture, the supernatant was analysed for IFN-γ by ELISA.

Statistical analysis

The statistical tests used are stated in the results section. If not stated, student's t-test was used, when data had a parametric distribution or parametric when transformed using either ln x or 1/x. Otherwise Mann-Whitney analysis was used for non-parametric data. Freidman tests was used, where multiple paired comparisons of non-parametric cytokine data were required (with Dunn's correction) and Wilcoxon test for single group non-parametric paired analysis. A *p-value* less than 0.05 was interpreted as statistically significant.

Table 4: Summary of Reagent.

Product	Information
Dulbecco Phosphate Buffered Solution (DPBS) 1X	Gibco 14190-094
Roswell Park Memorial Institute medium (RPMI)	Sigma R8758
Eagles Minimum Essential Medium (EMEM)	Sigma M5650
FCS (Dendritic /T cell media)	Sigma 14M134
FCS (Cell line media)	Gibco 10270
BSA	Sigma A/906-100G
Dendritic cell media	RPMI (500ml) + 10% FCS (50ml) + 1% Sodium Pyruvate (5ml)
T cell Media	RPMI (500ml) + 10% FCS (50ml) + 2% Hepes Buffer (10ml) + 1% Sodium Pyruvate (5ml) + 1% L-Glutamine (5ml) + 1% Non-essential amino acids (5ml)
MACS Buffer	DPBS (500ml) + EDTA (2mM) + 1% FCS
Red Blood Cell Lysis Buffer 10X	Biolegend 420301; Working concentration 1X
R848 (TLR 7/8)	Invivogen; Working Concentration: 2.5µl/ml
PolyI:C (TLR 3)	Invivogen; Working Concentration: 20µl/ml
LD Column	Miltenyi 130-042-901 (CD19 depletion)
LS Column	Miltenyi 130-042-401 (CD14 selection)
MS Column	Miltenyi 130-042-201 (CD1c selection)
Pre-Separation Filters (30µl)	Miltenyi 130-041-407 (Buffy Coat)
FlowJo Software 8.7	For flow cytometry analysis
Magnetic Separation kit	Miltenyi Minimac 291100115/018999
Flow Cytometer	MACS Quant Analyser 10.0 and MACS Quantify software
MACS Comp beads kit	Miltenyi 130-104-187 (anti-human Igk)
Dexamethasone	4mg/ml Organon, UK (Clinical grade)
GMCSF	Peprotech 300-03; Working Concentration 1:1000
IL-4	Immunotools 11340042; Working Concentration 1000U/ml
CCL21	R&D Systems 366-6C-025
BIRB0796	Selleck chemicals S1574; Working Concentration 1µM
ELISA IL-12	BD Bioscience 555183
ELISA IL-10	R&D Systems DY217B

ELISA ILN-γ	R&D Systems DY285B
ELISA Reader	Infinite F50 Tecan + Magellan F50 Software
Washing Buffer	PBS + 0.05% Tween-20
Substrate Solution	1:1 Substrate Reagent A (Hydrogen Peroxide in buffered solution: 51-2606KZ) + Substrate Reagent B (Tetramethylbenzidine: 51-2607KZ)
Stop Solution	1M $2NH_2SO_4$ Made in house
IL-10 Capture Antibody	Working Conc 2.0ug/ml
IL-10 Detection Antibody	Working Conc 150ng/ml
U87	U-87 MG (ATCC HTB-14) glioblastoma; astrocytoma; classified as grade IV
MM418	Malignant Melanoma Cell line
Jurkat Cell line $gp100_{280-288}$-TCR	E6.1 fl296 Jurkat T-cell, Radboud University, Nijmegen
Scintillating Fluid	Microscint PerkinElmer 86-15071
Radioisotope Reader	TopCount NCT PerkinElmer
24-Transwell Plate	Costar 3421
Influenza Matrix $Protein_{58-66}$, CEF1	Alta Bioscience (#Q8915) sequence GILGFVFTL. Stock 5mg
EGFRvIII peptide	Genscript (#RP20356) Sequence LEEKKGNYVVTDHC. Stock 5mg
TRP-$2_{180-188}$ peptide	Genscript (#RP20250) Sequence SVYDFFVWL. Stock 1mg
$gp100_{280-288}$	YLEPGPVTA; Working concentration 10 µM; Genscript
$gp100_{272-300}$	Working concentration 10 µM; JPT peptides
$gp100_{154-167}$	Sequence KTWGQYWQV; Working concentration 10 µM; Genscript
IFN-γ ELISPOT kit	MABTECH 3420-2A IFN-γ monoclonal coating ab 1-D1K 1mg/ml Biotinylated monoclonal antibody 7-B6-1 Streptavidin-Alkaline Phosphatase 1:1000

Results: Chapter 1 – Circulating dendritic cells in glioblastoma patients

Introduction

Circulating DC have been measured in a number of cancer types including pancreatic, breast, prostate, glioma, Kaposi sarcoma and renal cancer (190-192). Dendritic cells have historically been defined as lineage (lin) negative ($CD3^-$, $CD56^-$, $CD19/20^-$) and $HLA\text{-}DR^+$ cells. Early studies into circulating DC subdivided these into myeloid-like ($CD11b^+CD11c^+$) and lymphoid-like ($CD11c^-$ and or $CD11c^-CD123^+$) or immature ($CD11c^-CD123^-$) (193).

In the introduction, we introduced the newer DC markers which better differentiate functional properties of DC in health and disease. The Monocyte-derived DC have been used in a number of vaccine trials to treat GBM. A review summarized 19 phase I/II trials with a median number of 12 patients per trial (194). It noted these were mainly single centre trials, recruiting patients with relapsed disease post-surgery either on no or low dose maintenance steroids (194). Despite the number of MoDC trials, the optimum route of DC loading, maturation, route of administration and timing of administration is unknown (194, 195). For example, tumour loading with autologous tumour lysate, RNA or peptides, maturation with a cytokine cocktail including IL-4, TNF-α, IL-1β, to IL-6 and vaccine adjuvants such as tetanus toxoid or imiquimod cream (a TLR-7 agonist) have all been used without defining comparative outcomes (195). Overall there has been no dose limiting toxicities reported in these trials and a response rate of 11.4% has been estimated (194). This data is consistent with DC vaccine responses and varied protocols seen in the treatment of other cancer types (196).
One MoDC trial of note, which has just reported initial survival data, is a multicentre, international, phase III trial using autologous tumor lysate-pulsed MoDC vaccine (called DCVax®-L) as an adjuvant with standard therapy

treating newly diagnosed glioblastoma patients (197). This is the largest DC trial in any tumour type. In this trial 331 patients were randomized after surgery and 6 weeks of chemoradiation (if stable disease) to DCVax®-L or placebo (PBMC) with adjuvant Temozolomide as standard of care. Vaccines were administered after randomization on days 0, 10 and 20, then on months 2, 4 and 8, and thereafter at 6-monthly intervals (197). In the first analysis in the intention to treat group median overall survival was 23.1 months and 3-year survival rate of 25.4%, which compares favorably to other first line trials with an apparent heightened tail of the curve on the Kaplan-Meier survival plots. However, nearly 90% of the ITT population received DCVax®-L at some point due to cross-over. The authors have not published a direct comparison between the arms. Of note, only 20% of patients screened enter the trial. The screening took place pre-operatively, therefore the most common exclusion was histology not consistent with GBM (24%), but more importantly disease progression (20%), insufficient tumour lysate (16%), patient declined leukopheresis (10%) or manufacturing difficulties of product (10%) (197). We await further maturation of data to guide whether a true survival benefit was observed in this trial.

We proposed studying the circulating dendritic cell frequency in an unselected patient group with GBM. It is currently not known which DC is most important for orchestrating cancer immunity. cDC2 vaccine therapy has been trialled in metastatic melanoma and prostate cancer and found to be safe and has a signal for efficacy (147, 148).

Our main objective was to assess the feasibility of leukopheresis for potential adoptive transfer of circulating DC. Since little is known about these cells in GBM patients, an unselective approach was taken. Given that the multimodal approach in the 1st line treatment of GBM includes a number of potential immunosuppressants such as chemotherapy, radiotherapy and dexamethasone, this approach would likely be explorative.

In addition to frequency, it is important to know the functional capacity of circulating DC in terms of maturation markers such as HLA-DR, CD86 and cytokine secretion, like IL-12 and IL-10. This is because DC orchestrate the direction of the immune response from a cytotoxic and Th1 helper response, to immune tolerance, dependent on co-stimulatory molecule expression and cytokine secretion, when priming T-cells (125, 198). We would aim to promote a Th1 interferon-gamma polarised T cell response, which is dependent on mature DC with high HLA-DR expression, B7 molecules (such as CD86) and secretion of IL-12 (198).

Results

Patient characteristics for immunophenotyping circulating DC

We recruited 16 unselected patients who attended the Oncology outpatients for management of glioblastoma and consented to take part in our study titled "Investigating the function of the immune system during cancer" (NRES 13/EM/0218; Nottingham University). The patient characteristics are summarised in Table 1.

The median age of the cohort was 59, which is similar to the phase III Stupp trial (registration trial for current standard of care), where the median age was 56 years (13). In our cohort there was a skewed male predominance (4.3:1) which is higher than average in most studies approximately 1.6-1.7:1 (13, 199). The most likely explanation for this disparity in our cohort is the small sample size. There was only 1 patient who had a WHO Performance Status (PS) score of 0, indicating no restriction to activity compared to pre-disease status. This is not surprising, given the high proportion of patients whom had symptomatic neurology (9 out of 16 patients). The vast majority of patients were PS1, which reflects referral for adjuvant treatments to oncologists. However, it must be noted that the Stupp trial did include a higher proportion of PS0 (39%), which better reflects a selected cohort for a

1st line treatment trial. Two patients were PS2, one of which was having daily RT treatment, which was for symptom control in a palliative regime. The other patient was having second line treatment with procarbazine, lomustine and vincristine chemotherapy, and thus PS2 represents the disease status and also the toxicity of second line therapy. There may be worse PS patients with GBM however, these are unlikely to either receive aggressive surgery and/or adjuvant oncology treatment. This is reflected by epidemiological survival statistics, where median survival of all patients registered in the UK is 6 months compared to phase III trials 1st line trial where in the chemoradiation group median survival is 14.6 months.

10 of the 16 patients were undergoing 1st line treatment with chemoradiation, radiation or adjuvant chemotherapy. At the time of investigation, radiotherapy monotherapy was given to patients who had a poorer performance status over 3 weeks as opposed to 6 weeks with chemoradiation, to achieve some symptom control without exacerbating further decrease in health from side effects of chemotherapy.
Chemoradiation consists of daily Temozolomide taken at a dose 75mg/m^2 and daily radiotherapy (5 days out of 7 per week) at 2Gy per fraction. This is followed by adjuvant Temozolomide at higher doses of (150mg-200mg/m^2) for 5 consecutive days, repeated every 4 weeks for 6 months to complete the Stupp protocol. In these patients we measured DC frequency prior to their next cycle of Temozolomide, when their bone marrow was likely to be least affected by the chemotherapy.
Secondary GBM represents a better prognostic group whom have had a previous low-grade glioma with aggressive transformation. One of these patients was in long-term remission, having completed successful surgery and chemoradiation in 2005. The second patient was undergoing chemoradiation and was the only known IDH1 mutated glioblastoma, typical of secondary transformation.

A potential factor to consider when studying the immunity of patients with glioblastoma is the number of patients receiving steroids. In our cohort 11/16 (69%) of our patients were taking steroids, which is comparable to the Stupp trial, where 71% of patients were taking steroids at the point of randomisation, post-surgery and prior to chemoradiation/ radiotherapy (13). However, a proportion of patients will generally wean off these during the course of chemoradiation.

The rate of symptomatic neurology seen in approximately 56% of patients in our cohort is a reflection of the disease. Indeed, symptomatic neurology at baseline is a features of local tumour effects or effects following extensive debulking surgery. The development of new neurology during treatment is an indicator of progression, which usually is detrimental to performance status and corresponds with increasing oedema, hence the clinician is likely to prescribe dexamethasone. These factors are all therefore linked.

IDH1 status is associated with better survival. *IDH1* and *IDH2* mutations occur in a mutually exclusive manner in nearly 80% of grades II and III oligodendrogliomas and astrocytomas and also secondary GBM. Conversely, IDH mutations are found in only 6% of patients with primary GBM. Molecular studies of IDH-mutant gliomas have established that the IDH mutation is an early causative event in the pathogenesis of this brain tumour subset (200). There was one known IDH1 mutated patient in our cohort, whom had transformed from previous low-grade astrocytoma, resected 5 years previously, and was undergoing chemo-RT with radical intent.

Table 1: Patient characteristics whom were recruited for circulating DC analysis

Glioblastoma Patients n=16	
Age (years)	
Median (Range)	59 (37-74)
Sex	
Male	13
Female	3
ECOG Performance Status	
0	1
1	13
2	2
Treatment at DC analysis	
Chemoradiation	5
Radiotherapy	2
Adjuvant Temozolomide	3
PCV chemotherapy	4
Remission	2
Type	
Primary	14
Secondary	2
Dexamethasone dose	
None	5
0.5-2mg	4
>2mg-4mg	6
>4mg	1
Residual Disease	
Yes	10
No	6
Symptomatic Neurology	
Yes	9
No	7
Survival (months)	
Median (range)	14.0 (3.8-138.5)
IDH1 status	
Unknown	5
Mutated	1
Wild type	10

ECOG= Eastern co-operative oncology group; PCV= procarbazine, lomustine and vincristine chemotherapy
IDH1= isocitrate dehydrogenase 1

Alterations in circulating DC numbers in patients with GBM

We determined the abundance of the major circulating DC subsets using a 6 colour, 9 parameter flow panel in GBM patients (n=16) and healthy adults (n=16). The analysis required less than 3ml of whole blood was initially lysed to remove red blood cells and then analysed resulting in the expected populations of lymphocytes, monocytes and granulocytes. DC are defined broadly as lineage negative and MHC class-II high expressing cells (133). Figure 1.2 shows the gating strategy and is further described in the materials and methods section. Briefly, HLA-DR positive cells were gated following exclusion of granulocytes, CD14 and CD19 populations. Subsequently, the four circulating DC populations were identified by specific surface markers: CD1c (cDC2), CD303 (pDC), $CD141^{high}$(cDC1) and M-DC8 (Slan). CD86 and PD-L1 expression was then measured against isotype controls for each DC population (figure 1.2).

As expected, cDC2 and slanDC cells were the most frequent circulating DC subsets identified in both the healthy volunteers and the patient population. The cDC1 cell population were 10-fold less abundant than cDC2 population in heathy volunteers which limits their use for adoptive transfer. The cDC2 and pDC subsets were significantly reduced in patients (cDC2 median 1736 vs 4975 cells/mL p=0.028, pDC 893 vs 2287 cells/mL p<0.001, patients vs controls respectively). In contrast, there were equivalent numbers of the slanDC in patients and controls (3296 vs 3936 cells/mL respectively; P=0.379). The myeloid cDC1 subset had a non-significant trend towards lower numbers in patients (135 vs 228 cells/mL, patients vs controls p=0.078). Even in the context of the relatively small sample size, it was possible to identify a proportion of patients with similar numbers of circulating DC as healthy controls (Figure 1.3).

We undertook a preliminary univariate analysis and found that patients with higher circulating DC numbers had increased survival (cDC2

p=0.019; pDC p=0.004; and cDC1 p=0.009). Higher numbers of cDC2 were associated with no steroid use at time of blood acquisition (p=0.005), no residual disease (p=0.028), a secondary GBM (p=0.002) and in remission (p=0.010).

Higher pDC was associated with younger age (<50yrs, p=0.009), secondary GBM (p<0.001), in remission (p=0.037), and no use of Dex (p=0.017). The absence residual disease (p=0.007) and Dex use (p=0.014) was associated with greater Slan numbers. Higher numbers of cDC1 was associated with younger age (<50yrs, p=0.014), secondary GBM (p=0.002), in remission (p=0.022) and the absence of residual disease (p=0.004) and Dex use (p=0.005).

Despite the small sample size, this cohort represents a typical range of patients that would be candidates for adoptive immunotherapy and highlights the extent of reduction in circulating DC in GBM patients.

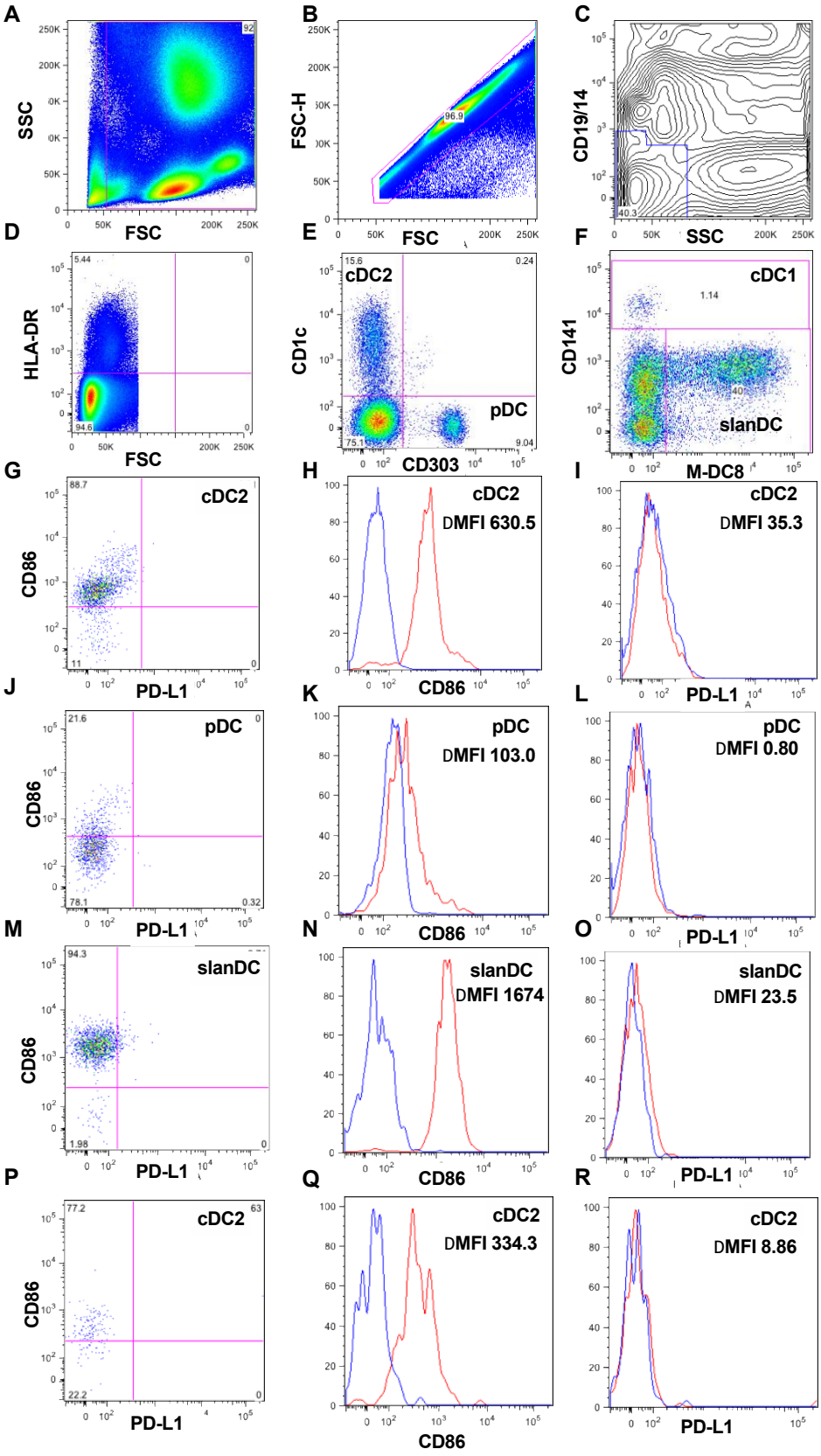


Figure 1.2: Flow cytometry analysis of circulating DC in GBM patients and healthy controls. Flow cytometry was used to enumerate circulating DC. Briefly, whole blood was stained and red blood cells lysed prior to acquisition on a flow cytometer. (A) Shows the typical forward (FSC) and side scatter (SSC) of the

leukocyte populations. Doublet events were excluded by plotting FSC height against area (B). The exclusion of B cells, monocytes and granulocytes was achieved by gating CD14-/19- and side scatter low events (C). HLA-DR high events, a hallmark of DC, were then selected (D). Surface markers for cDC2 (CD1c+), pDC (CD303+) (E), cDC1(CD141^{high}) and slanDC (Slan+) (F) were then identified against isotype controls (purple gates). CD86 and PD-L1 expression was assessed in dot plots and histograms to measure MFI on cDC2 (G-I), pDC (J-L), slan DC (M-O) and cDC2 (P-R)**.**
FSC= forward scatter; SSC= side scatter; FSC-H forward scatter height; FSC-A= forward scatter area; DC= dendritic cell; ΔMFI= Median Frequency Intensity of Cells (red) – Isotype (blue)

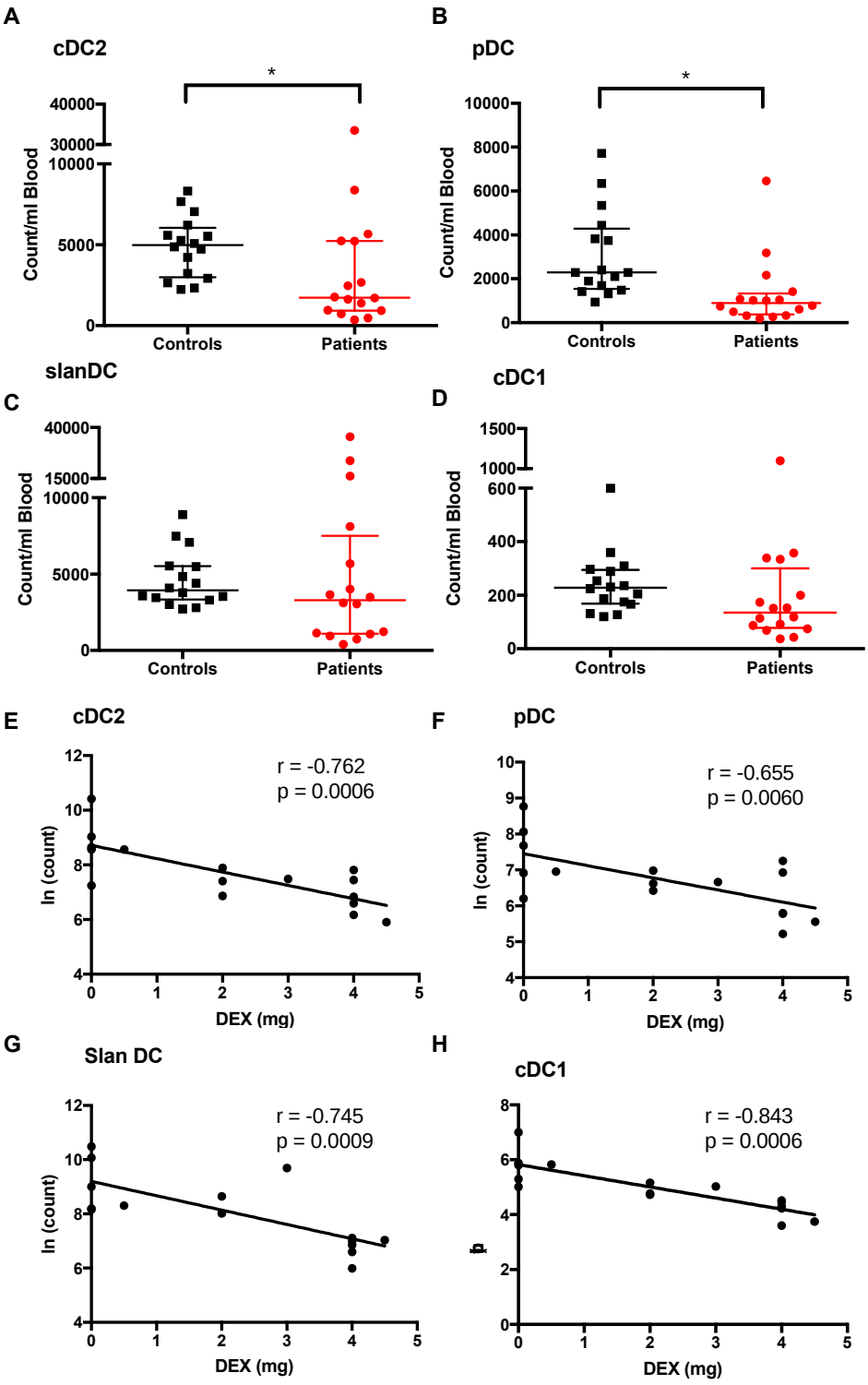


Figure 1.3 Enumeration of circulating DC in GBM patients and healthy controls and correlation to dexamethasone dose. (A-D) Absolute numbers of circulating DC in GBM patients compared with healthy controls. A significant decrease in cDC2 and pDC is seen in GBM patients compared to healthy controls.
(E-H) Correlation of steroid dose on day of blood acquisition to DC counts (in natural log for parametric analysis). Pearson's correlation coefficient (r) and significance is shown. Dexamethasone dose is associated with lower numbers of all subsets of circulating DC *=p<0.05

Association between reduced number of DC and dexamethasone

An association existed between the number of circulating DC subsets and the Dex dose at the time of blood acquisition. In all DC subsets, there was a significant linear relationship between increasing dose of Dex and reduced number of DC; cDC2 P=0.0006; pDC P=0.0060; slanDC P=0.0009 and cDC2 DC P=0.0009 (Figure 1.3). In the cDC2 subset the Pearson coefficient was -0.762, indicating a strong correlation between cell number and dose of Dex. This remained significant after adjusting for confounders of primary or secondary GBM and current treatment. Age, sex, residual disease, overt neurology and performance status were not significant confounders in this analysis.

Altered phenotype of circulating DC

Phenotyping was also performed on circulating DC in addition to the enumeration reported above (figure 1.4). We analysed CD86 (B7-2) co-stimulatory molecule expression since this provides signal 2 for stimulating antigen-specific T-cell activation via ligation to CD28. In the absence of co-stimulation at priming, T-cells become anergic or tolerogenic (198). PD-L1 expression, alternatively, downregulates the T-cell response principally by attenuating CD28 signalling (201).

In healthy volunteers, all four DC populations have low to negative PD-L1 expression. CD86 co-stimulatory molecule is expressed particularly high by SlanDC then, cDC2 and cDC1. CD86 expression in the resting state is low on pDC.

The expression of HLA-DR on patients' circulating cDC2, cDC1 and pDC cells was significantly lower than with healthy controls (P=0.009, 0.029 and 0.047 respectively; Figure 1.4). Additionally, CD86 expression was significantly lower on patients' cDC2 cells compared to controls (P=0.01). The expression of PD-L1, was also significantly lower in GBM patients in both the cDC2 (P= 0.003) and cDC1 (P=0.015) subsets. Overall, low HLA-DR and/or CD86 represent a less mature phenotype of the DC. Furthermore, immature DC

stimulate T cell tolerance, and hence this is a potential mechanism for tumour tolerance in GBM (125, 202). In contrast to the other subsets studied, the phenotype of slanDC was unaffected in GBM patients.

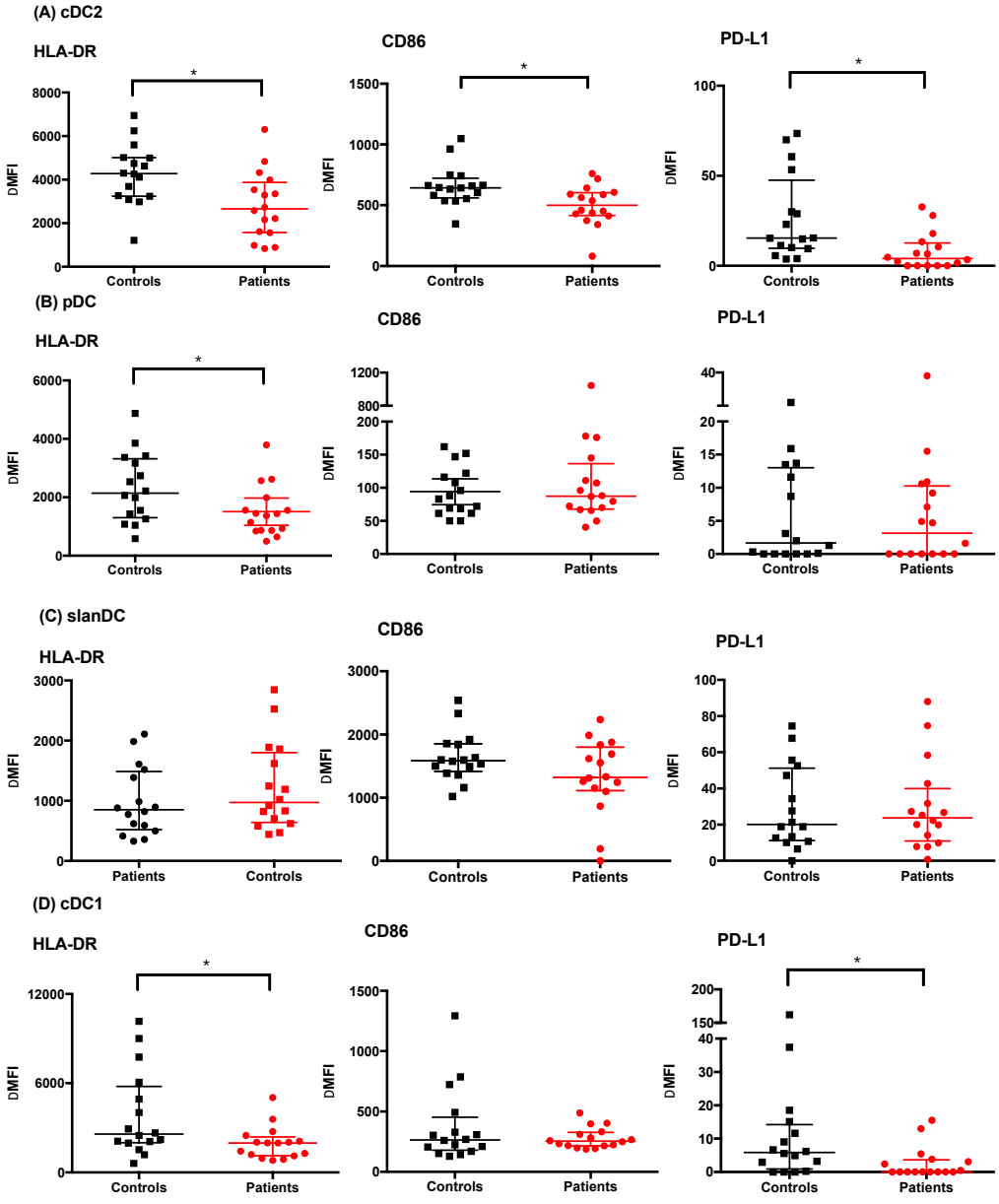


Figure 1.4: Circulating DC have altered phenotype in GBM patients compared to healthy controls. DC were analysed by flow cytometry as in figure 1.2. Subsequently, the expression of HLA-DR, CD86 and PD-L1 was determined. The change in median fluorescence intensity (MFI) was calculated by subtracting the MFI of the phenotype marker from its isotype control. (A) There was lower HLA-DR, CD86 and PD-L1 expression on cDC2 of patients compared to controls. There was also lower HLA-DR expression in pDC (B) and cDC1 (D). PD-L1 expression was also significantly lower on patient cDC1 compared to healthy controls. *p<0.05

cDC2 cytokine release in GBM patients is suppressed compared to healthy controls.

Clinical grade isolation of the cDC2 subset is now possible and the utility of these cells is under investigation in prostate cancer and malignant melanoma (147, 148). Therefore, given these are the most numerous cDC2 subset we further investigated cDC2 functional activity. For such analysis a further 6 patients were recruited and magnetic bead cell isolation was used, requiring 200ml of blood per patient (Table 2). An important feature of cDC2 in humans is their capacity to produce IL-12 to support Th1-dependent CTL responses (203, 204). Following isolation, cDC2 were rested in media and GM-CSF for 1 hr prior to maturation with TLR agonists (polyI:C and R848). A range of IL-10 and IL-12 levels were secreted by isolated cDC2 from both patients (n=6) and healthy controls (Figure 1.5). IL-12 secretion from cDC2 was significantly impaired in GBM patients (median 6541 vs 322pg/mL respectively; P=0.0245). However, IL-10 secretion was equivalent, with a median 108pg/mL in healthy volunteers compared to 41pg/mL (ns). Overall, the ratio of IL-12 : IL-10, which determines CD4+ T cell polarisation, significantly favoured Th1 response in healthy controls compared to GBM patients (P=0.032, see figure 1.5) (205). This represents an impairment to orchestrate appropriate anti-tumour immune responses in GBM patients.

Table 2: Patient characteristics for analysis of cDC2 cytokine release.

Patient	Age	PS	Sex	Tx	DEX dose	Residual disease	%cDC2 of PBMC	cDC2/ml
GBM01	33	0	M	RT/TMZ	3.0	Y	0.36	2,400
GBM02	68	1	M	RT/TMZ	2.0	Y	1.25	5,813
GBM03	39	0	M	RT/TMZ	0.0	N	0.66	7,160
GBM04	61	1	M	RT/TMZ	2.0	Y	1.50	4,000
GBM05	71	1	M	RT	4.0	Y	0.35	1,125
GBM06	55	1	M	TMZ	0.0	Y	0.38	3,250

PS= performance status; Tx= treatment; DEX= dexamethasone; M=male; RT= radiotherapy; TMZ temozolomide; Y=yes; N=no

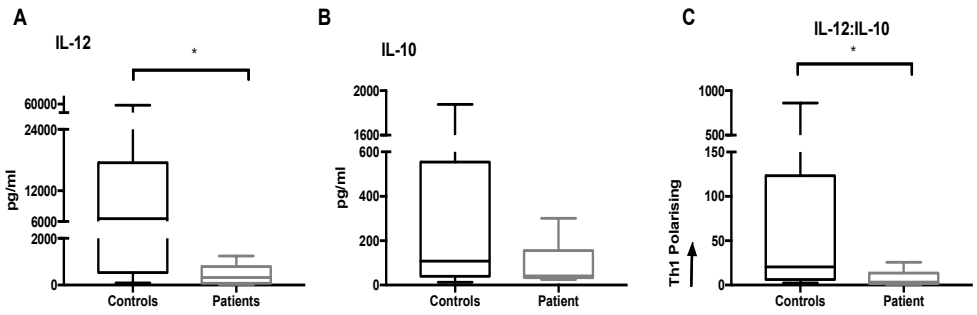


Figure 1.5: cDC2 cytokine release in GBM patients is suppressed compared to healthy controls. cDC2 were isolated from whole blood of healthy controls (n=9) and GBM patients (n=6), then matured ex-vivo with polyI:C and R848. Cytokine release was determined after 24hrs by ELISA. IL-12 secretion was significantly suppressed (A) and IL-10 has a trend to lower levels (B) in patients compared to healthy controls. Overall the ratio of IL-12 to IL-10 would skew away from Th1 polarisation (C). *$p<0.05$

Discussion

Here we show the first detailed analysis focusing on the abundance, phenotype and function of circulating DC in GBM. We found distinct differences between the circulating DC in GBM patients and healthy volunteers.

The most abundant circulating DC and the interest of the next generation of vaccines, cDC2, were numerically significantly suppressed in GBM patients. They also had a lower HLA-DR expression, CD86 and PD-L1 expression compared to healthy controls. Lower expression of co-stimulation and MHC-class II would likely reduce the T-cell priming activity of the DC. MHC-class II proteins are vital for presenting peptides to CD4 T helper cells, which also requires co stimulation provided by CD80/86 to induce activation (198). For optimum CD8 cytotoxicity Th1 help is required through CD40-CD40L interactions which licence DC to prime CD8, particularly of exogenous antigens (206-210). Furthermore, CD4 help is required for generating and maintaining CD8 T-cell memory (211-214).

Plasmacytoid DC were also numerically suppressed and had low HLA-DR expression. The SlanDC population was relatively comparable to healthy controls and would be an important area for further research. However, there seem to be a bimodal distribution with some patients having high numbers and others suppressed, although overall the median was similar to the healthy population. These DC are thought to be principally important in inflammatory diseases such as Psoriasis, where patient slanDC produced high quantities of IL-23, TNF-α and drive a Th17 and Th1 response. Similarly, in Systemic Lupus, patients produced high levels of single stranded RNA binding TLR 7 and 8 which induced high quantities of pro-inflammatory cytokines TNF-α and IL-12 from SlanDC. There is still some debate as to whether this subset is a non-classical monocyte or true DC population (132, 135).

The cDC1 population is numerically low in healthy adults and, although did not quite meet statistical significance (p=0.078), showed a trend towards

suppression in GBM patients. With a median cell count of 135 cells/ml of blood in the GBM population, it is unlikely that sufficient numbers would be feasible to isolate for research or clinical adoptive transfer with current technologies (159).

In all 4 DC subsets there were patients with numerically comparable DC numbers to healthy controls. Interestingly one patient had higher numbers of all 4 subsets of circulating DC, even when compared to healthy controls. He had originally had a low-grade glioma, which relapsed 5 years later as a GBM. He was 11.5 years since radical treatment and was in remission. Similarly, the next patient with numerically higher proportions of DC had a previous low-grade glioma who had again relapsed 5 years later with GBM and now undergoing adjuvant chemoradiation. The aforementioned case is intriguing because survival at 5 years is less than 10% (215). However, even with the acknowledgement of small sample size, univariate analysis of the whole cohort, revealed the absence of residual disease, being in remission and no Dex use was associated with higher DC numbers. Furthermore, higher Dex dosage at time of phlebotomy was strongly correlated to decreasing DC numbers in a dose dependent manner for all 4 DC subsets. One other group has studied circulating DC numbers and steroids in autoimmune disease. This group defined myeloid cDC as $Lin^{-}HLA\text{-}DR^{+}CD11c^{+}$, which would include both cDC2 and cDC1 population and pDC as $Lin^{-}HLA\text{-}DR^{+}CD123^{+}$, in 5 patients with autoimmune disease. They measured DCs at baseline and after 3 days of high dose methylprednisolone. Prior to starting corticosteroids, these patients had comparable circulating DC to healthy controls. However, following 3 days of corticosteroids, they found myeloid DC were significantly reduced and pDC abolished in individuals compared to baseline (216). This is similar to the pattern seen in our GBM patient cohort, where both cDC and pDC are suppressed, particularly the pDC population.

Although we are the first group to directly compare these 4 subsets in GBM patients, others have studied circulating DC in cancer, although many of these studies predated the blood dendritic cell antigen antibodies (BDCA 1-4).

Yanagitmo et al studied $CD11c^{+}Lin^{-}DR^{high}$ and $CD11c^{-}Lin^{-}DR^{high}$ cells in pancreatic cancer pre- and post-treatment with chemoradiation. They found that DC were significantly lower in patients than healthy controls (patients n=29, controls n=20) at baseline and patient derived-DC had poorer allostimulatory activity than controls. Following treatment with chemoradiation, the allostimulatory activity significantly improved. Furthermore, this correlated with a significant reduction in serum TGF-β, suggesting a mechanism for improved DC function with chemoradiation treatment (190).

Pinzon-Charry et al also investigated circulating $Lin^{-}HLA^{-}DR^{+}$ DC in circulating blood of 136 cancer patients suffering from breast (n=120), prostate (n=10) or glioma (n=6). DC were separated into cDC ($CD11c^{+}$), pDC ($CD123^{+}$) and a third group named HLA-DR immature cells (DR+IC) defined as $CD11c^{-}CD123^{-}$. They found that in all cancers cDC and pDC were suppressed at baseline. However, the $CD11c^{-}CD123^{-}$ DR+IC cells were expanded compared to controls and increased with advancing stage of breast cancer. Similarly, in the 6 glioma patients, expansion of DR+IC correlated with disease relapse and progression. The DR+IC DC had low expression of CD80, 83 and 86, poor antigen uptake ability and allostimulatory capacity (191). Hence, the authors concluded that advanced cancer leads to a relative expansion of circulating DC with immature phenotype (191).

Another study looking specifically at glioma patients investigated the effect of glioma grade on circulating immune cells, including DC (all grades, n=29). They investigated the $CD11c^{+}$ myeloid DC population as a whole, but also specific subgroups ($CD1c^{+}$, $CD141^{+}$ and $CD16^{+}$ DC). They found that $CD1c^{+}$ cDC2 and $CD123^{+}$ pDC were significantly suppressed in glioblastoma (grade IV, n=17) compared to grade I-III glioma (n=12). CD16+ DC and $CD141^{+}$ cDC1 were not significantly different. Patients with a higher $CD11c^{+}$ myeloid DC had a trend

towards better survival. In a similar manner to the Pinzon-Charry study, the authors found an expansion in $Lin^{-}HLDA\text{-}DR^{+}CD11c^{-}CD123^{-}$ DC which they also concluded represented immature DC (192). Thus, these studies further support the notion that cancer patients have an immature DC phenotype.

Larger studies have also been carried out in head and neck cancer, breast cancer, non-small cell lung cancer, chronic lymphocytic leukaemia, acute myeloid leukaemia and Kaposi sarcoma and all show suppression of circulating DC with increasing stage and an immature DC phenotype (217-220).

In another interesting series of patients with renal cancer (n=26), the cDC2 (CD1c+), cDC1 (CD141+) and pDC (CD303+) subsets in addition to the monocytes, myeloid derived suppressor (MDSC), neutrophils, immature myeloid cells and lymphocytes populations were measured in patients on treatment (221). Patients had a higher baseline level of monocytes, neutrophils and MDSC than healthy controls. All three DC subsets, however, were significantly decreased compared to healthy controls prior to treatment for their cancer. The cDC2 also had lower expression of HLA-DR and CD86. Those with higher baseline cDC2 numbers had improved survival. Patients responding to the pan-VEGF/PDGF/kit tyrosine kinase inhibitor, Sunitinib, also had a significant increase in cDC2 levels relative to other myeloid cells. This was not correlated to VEGF plasma levels or IL-10, but to plasma IL-6 levels. Hence tumour burden and IL-6 seemed important factors determining the cDC2 fraction of the myeloid compartment and suggests a previously unreported beneficial off-target effect of Sunitinib treatment for renal cancer by reversing immune suppression (221).

An important advantage of our enumeration assay over the studies mentioned above, is that we employed a methodology with minimal manipulation in which cells were stained in whole blood and avoided errors introduced by PBMC isolation. Importantly, we required less than 4mls of

blood for our study, therefore this allowed more accurate measurement of both the relative frequency and absolute number of DC in blood. To test variance of the assay, four healthy donors gave a single blood donation. From this single donation, the assay was performed on three separate occasions and mean coefficient of variance was 10% and 8% for cDC2 and pDC respectively (see materials and methods).

Since the acquisition of this data in GBM patients, more heterogeneity is being understood in regard to circulating DC which has not been investigated here. For example, a landmark unbiased single cell-RNA sequencing analysis of DC $Lin^{-}HLA\text{-}DR^{+}$ cells revealed at least two cDC2 subpopulations, named as DC2 and DC3. Furthermore, a novel DC subset DC5 (or AS-DC) was described and had transcriptomic signatures in common with both $CD1c^{+}$ DC and pDC. The two cDC2 transcriptomic clustering was validated by isolation using novel surface markers for cluster A (DC2) using CD32B and CD163 and CD36 for cluster B (DC3) (135). Both clusters were potent stimulators of naïve T cell proliferation, however differences were seen in cytokine secretion with TLR agonists, with cluster A secreting higher levels of immune mediators such as IL-10, IL-12β and CCL-19 (135). Prospectively this study may also be able to better define the mice homologous $CD11b^{+}$ DC population.

Another group, prior to this publication had identified the expansion of $CD1c^{+}CD14^{+}$ DC population in melanoma patients which suppress CD4 T cells in an antigen-specific manner (222). This subpopulation of cDC2 had high expression of PD-L1, lower CD86 expression and released higher levels of IL-6 and IL-10. Transcriptomics and proteomics shared features with both DC and monocytes (222). During our flow cytometry data, we excluded the CD14 cell and therefore this immunosuppressive subpopulation.

A further group has recently identified that the cDC2 population can be subdivided by $CD5^{high}$ or $CD5^{low}$. Those $CD1c^{+}CD5^{high}$ cDC2 showed typical cDC2-specific genes such as IFN regulatory factor 4, while $CD5^{low}$

preferentially expressed monocyte related genes (189). These two subsets showed differential migration to CCL21, cytokine release and naïve T-cell activation phenotype and function (189).

All three studies highlight the increasing heterogeneity understood about circulating DC, with implications for cDC2 adoptive transfer. For example, the group investigating $CD1c^{+}CD14^{+}$ DC found a higher proportion of this subset in vaccine non-responder in their melanoma clinical trial and subsequently modified their isolation protocol to exclude this subset (222).

Obtaining sufficient cell numbers remains a persistent challenge in the development of adoptive immunotherapy with circulating DC. Given that leukopheresis typically yields $7x10^{9}$ PBMC, and in our hands isolated cDC2 by manual magnetic bead isolation comprised 0.52% of PBMC, we could expect $3.6x10^{7}$ cDC2 per leukopheresis (Table 2) (223). To extrapolate our flow cytometry data prospectively to determine leukopheresis outcomes, we can compare this to the clinical bone marrow transplantation protocols. In such patients a target minimum of 10 - $20x10^{3}$ $CD34^{+}$ cells/ml is used as a threshold before leukopheresis is planned, whereas comparatively the median of cDC2 in our GBM patient cohort was $1.7x10^{3}$, 10-fold less (224, 225). However, for successful bone marrow engraftment a minimum 2-$5x10^{6}$/kg of $CD34^{+}$ cells is required, hence for a 70 kg human this would amount to $350x10^{6}$ cells (224). In the melanoma phase I trial between 3 - 10 x 10^{6} total cDC2 were delivered per vaccination (147). Hence, it is likely that even with low circulating cDC2 numbers in GBM patients successful leukopheresis will be possible. Of note in the melanoma trial the yields ranged from 27 - $96x10^{6}$ per leukopheresis, with an average purity of 93%. However, yields after antigen pulsing and overnight maturation dropped and ranged from 25-95% with a median of approximately of 55%. This research group accepted yields >50% for clinical release of vaccine and therefore these numbers must be anticipated when considering translational feasibility. They did not publish comparative flow cytometry and leukopheresis data yields (147).

In addition to enumeration we tested the cytokine release from 6 patients with GBM. Both IL-12 and IL-10 secretion was suppressed on ex-vivo maturation of cDC2. Pro-inflammatory IL-12 was suppressed to a greater extent relative to IL-10 leading to a polarised IL-12:IL-10 ratio away from Th1 response. The ratio of cytokines contribute to signal 3, to determine T-cell fate (198).

Overall, we have therefore discovered that for cDC2 adoptive therapy, cell numbers are likely to be sufficient. However, the subsequent viability after antigen pulsing and maturation must be considered when compared to other cDC2 trials. The isolated cells also were functionally impaired with low cytokine secretion, in addition to low HLA-DR and CD86 expression. Explorative analysis indicated that Dex and tumour associated factors were likely contributing to suppressed numbers, therefore we explore this in more depth in chapter 2. We concluded that mechanisms to rescue cDC2 function are essential prior to considering adoptive transfer in GBM patients and are the focus of chapter 3-5.

Results: Chapter 2 – Dexamethasone and Tumour-derived factors inhibit MoDC and cDC2 function

Introduction

DC dysfunction is a mechanism of tumour evasion from immune detection. Such tumour-derived factors which directly inhibit DCs includes secretion of VEGF, IL-6 and IL-10 (226). However, studies demonstrating this have mainly focussed on human MoDC and murine DC. Little is known about circulating human DC in GBM patients. We had discovered in our patient cohorts that there were differences in circulating DC numbers between healthy controls and GBM patients. The major findings included cDC2 and pDC populations were significantly decreased. Indeed, decreasing DC numbers of all subsets was correlated with increasing dexamethasone (Dex) dose. In our exploratory univariate analysis, residual disease was also associated with lower counts of cDC2. Furthermore, patient derived MoDC and cDC2 secreted low IL-12 and IL-10 (see chapter 1). Therefore we sought to investigate if GBM tumour derived factors and Dex, did induce DC dysfunction in a controlled in-vitro model.

Since the functional capacity of DC is vital for the direction of the immune response, particularly signal 3 provided by cytokines, we focussed on IL-12 and IL-10 secretion (125, 205). This is because the ultimate goal of our DC vaccine would be to drive a Th-1 response, dependent on IL-12 at the DC:T-cell synapse, to provide CD4 help and support effective cytotoxicity (227). IL-10 is associated with immunosuppression and T-cell tolerance. Indeed IL-10 was originally known as cytokine synthesis inhibitory factor for its negative regulation on Th1 responses (228). It has long been recognised that this action required the presence of antigen presenting cells (229). For example,

immature MoDC cultured with IL-10 produces anergy in an alloantigen MLR with T-cells that secrete low IL-12 and IFN-γ (230).

The effect of dexamethasone on MoDC has been previously studied, however, little information is available about the effects of Dex on cDC2. One group has studied cDC2 as a tool for promoting tolerance to prevent transplantation rejection using dexamethasone (231). They found Dex cultured with cDC2 after isolation and during 24-hour maturation with LPS (dex cDC2) produced a tolerogenic DC which poorly stimulated an allogeneic response and the resulting supernatant showed a significant decrease in IFN-γ and IL-2 and a significant increase in IL-10. (231).

To study the effect of Dex on DC, we modelled the effect initially on MoDC and cDC2 from 8-9 healthy volunteers' blood and performed a dose finding exercise to discover the effect of Dex. In adults with GBM, doses are initiated at 16mg per day to combat cerebral oedema and weaned down over weeks. Dex is rapidly absorbed by all body tissues and has high protein binding capabilities (77% protein bound) hence estimating a serum levels exposure is difficult (232). In a previous study by Piemonti et al, they studied Dex, principally at a dose of 10^{-8}M to investigate the effects on monocyte differentiation to MoDC in conjunction with IL-4 and GMCSF. At higher doses (10^{-7}M and 10^{-6}M) they had low yields of MoDC so didn't investigate this effect further (233). Bosma et al, who to our knowledge are the only other group to investigate the effect of Dex on cDC2, used 10^{-6}M and hence a range between 10^{-6}M- 10^{-8}M was used.

We have also previously showed that melanoma-derived tumour lysate can inhibit both MoDC and cDC2 IL-12 secretion, when incubated pre-maturation with immature DC (139, 234). We have previously identified targeting the MEK pathway reversed melanoma cell line (MM418) induced MoDC IL-12 suppression (234). In cDC2, a MEK inhibitor reduces IL-12 suppression. Furthermore, we found an inhibition of an alternate MAPK pathways, p38,

increased IL-12 in cDC2 but acted in the reverse action on MoDC. Overall, we can conclude that tumour lysate from melanoma patients induces DC dysfunction, however, this is through different MAPK signalling depending on DC type.

We therefore investigated the effect of GBM cell line tumour lysate and Dex, comparing both MoDC and cDC2 IL-10 and IL-12 secretion.

Results

Dexamethasone suppresses IL-12 and increases IL-10 in MoDC

We isolated and differentiated monocytes from 9 healthy donors to make MoDC as described in materials and methods. We found that there was a wide range in IL-12 secretion from healthy donors when immature DC (iDC) were stimulated with Poly:IC and R848 TLR agonists, from 174pg/ml – 272149 pg/ml. For each donor triplicates of iDC, mDC, and mDC with Dex at 10^{-8}M, 10^{-7}M and 10^{-6}M was used. The addition of Dex decreased IL-12 secretion when added 1hr prior to stimulation and co-cultured with TLR agonists for 24 hours prior to cytokine analysis. The analysis of significance was performed using Friedman test, the non-parametric equivalent to ANOVA with pairing of parameters per donor. Multiple comparisons were set for statistical significance against mDC.

There was a dose-dependent decrease in IL-12 secretion when Dex was added. Stimulated DC (mDC) and mDC + Dex 10^{-8}M had no significant effect on secretion (median 18930 vs 16781 pg/ml; p=0.6037). However, at 10^{-7}M (median 70774 pg/ml, p=0.0016) and 10^{-6}M (median 2715 pg/ml, p<0.0001) significant suppression of IL-12 was seen.

Dex had less of an effect on IL-10 secretion from MoDC. The median IL-10 secretion from stimulated DC (mDC) was 457 pg/ml. With increasing Dex dose of 10^{-8}M, 10^{-7}M and 10^{-6}M the median IL-10 concentration compared to mDC was 339 (p=0.8200), 269 (p=0.2037) and 174 pg/ml (p=0.0030) respectively. Overall there was a decreasing trend of IL-10 secretion with increasing Dex concentration, reaching statistical significance at 10^{-6}M concentration (figure 2.1).

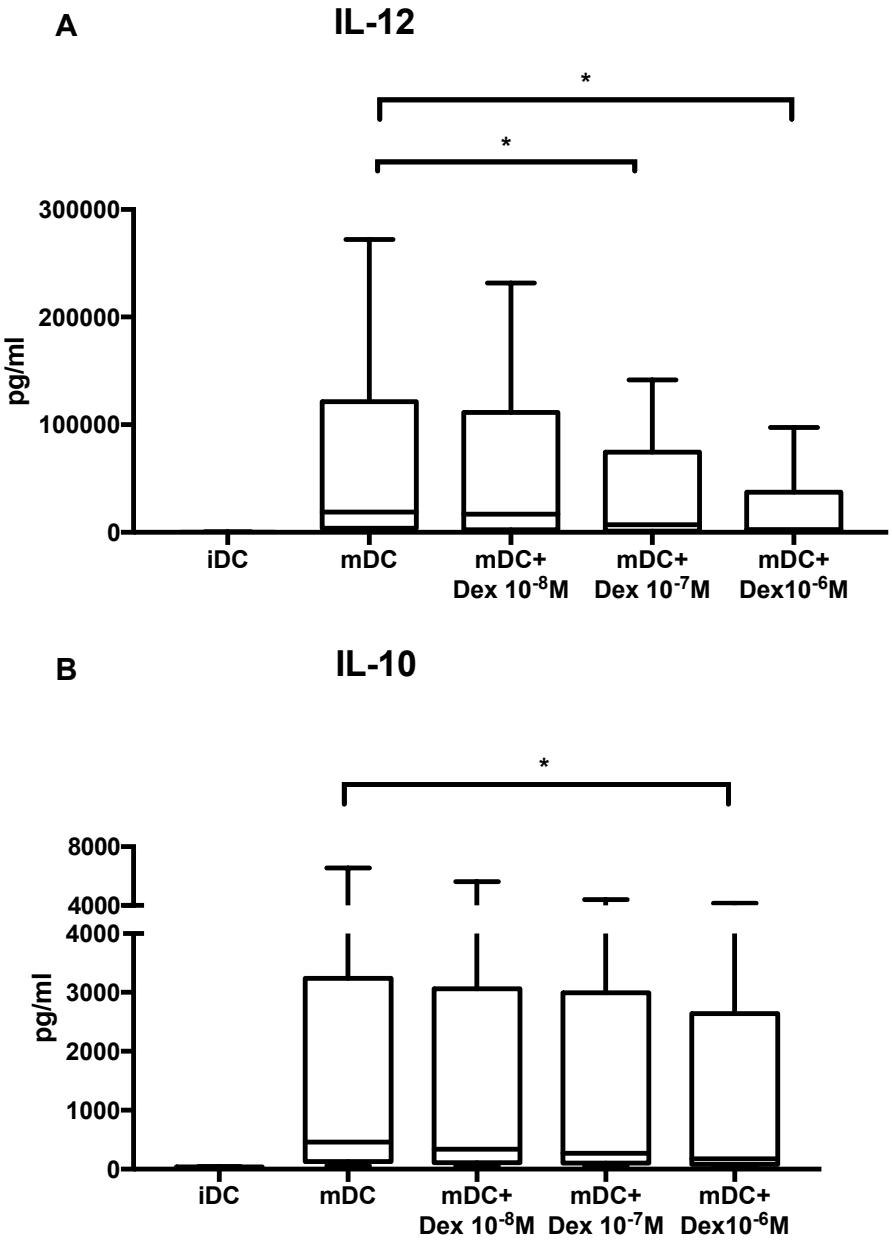


Figure 2.1: Dexamethasone suppresses IL-12 and IL-10 from Monocyte-derived DC. MoDC were isolated from healthy volunteers (n=9). Immature DC were rested in GM-CSF overnight as a control and produce little IL-12 and IL-10. DC were also matured with TLR dual agonists (polyI:C and R848) following 1hr of resting and then left for 24hours (mDC). Alternatively, mDC + Dex were treated as mDC, however exposed ex-vivo to Dex 1hr prior to maturation. Cytokines were measured in the supernatant after 24hrs by ELISA. Dex exposed MoDC had significantly suppressed IL-12 secretion at Dex concentrations of 10^{-7}M and 10^{-6}M compared to mature DC (mDC) (A). Dex exposure also significantly increased the immunosuppressive cytokine IL-10 secretion from MoDC at 10^{-6}M (B).*$p<0.05$

Dexamethasone suppresses the allo-stimulatory activity of mature MoDC and alters the PBL cytokine signature

A further vital characteristic of a DC is its ability to trigger an allo-stimulatory response in peripheral blood lymphocytes (PBL) in a mixed lymphocyte reaction (MLR) assay. We therefore tested 3 healthy individuals MoDC which had been created under standard conditions for normal differentiation (see materials and methods). The immature DC (iDC) were then exposed to Dex at 10^{-6}M 30min prior to maturation with polyI:C and R848. For each individual, iDC, matured DC (mDC) were compared to mDC with Dex. Increasing numbers of DC were incubated with 10^{5}PBL, in a standard MLR. Increasing PBL proliferation was seen with increasing DC numbers, validating the stimulator dependency of the assay. The cumulative data of the three donors is summarised in (figure 2.2 D). As expected, mDC significantly increased proliferation compared to iDC (p=0.0004). The addition of Dex significantly decreased proliferation to levels similar to iDC. Indeed, there was no significant difference between the proliferation of iDC and mDC + Dex 10^{-6}M (figure 2.2 D).

We also analysed the resulting supernatant from the 5 days MLR (figure 2.2 E,F). The mDC exposed to Dex prior to co-culture with peripheral blood lymphocytes, showed a trend towards decrease in median IFN-γ from 3086 pg/ml to 1413 pg/ml which was not significantly different (p=0.3146) and a small but significant increase in IL-10 from a median 76 pg/ml to 91 pg/ml (p=0.0267)

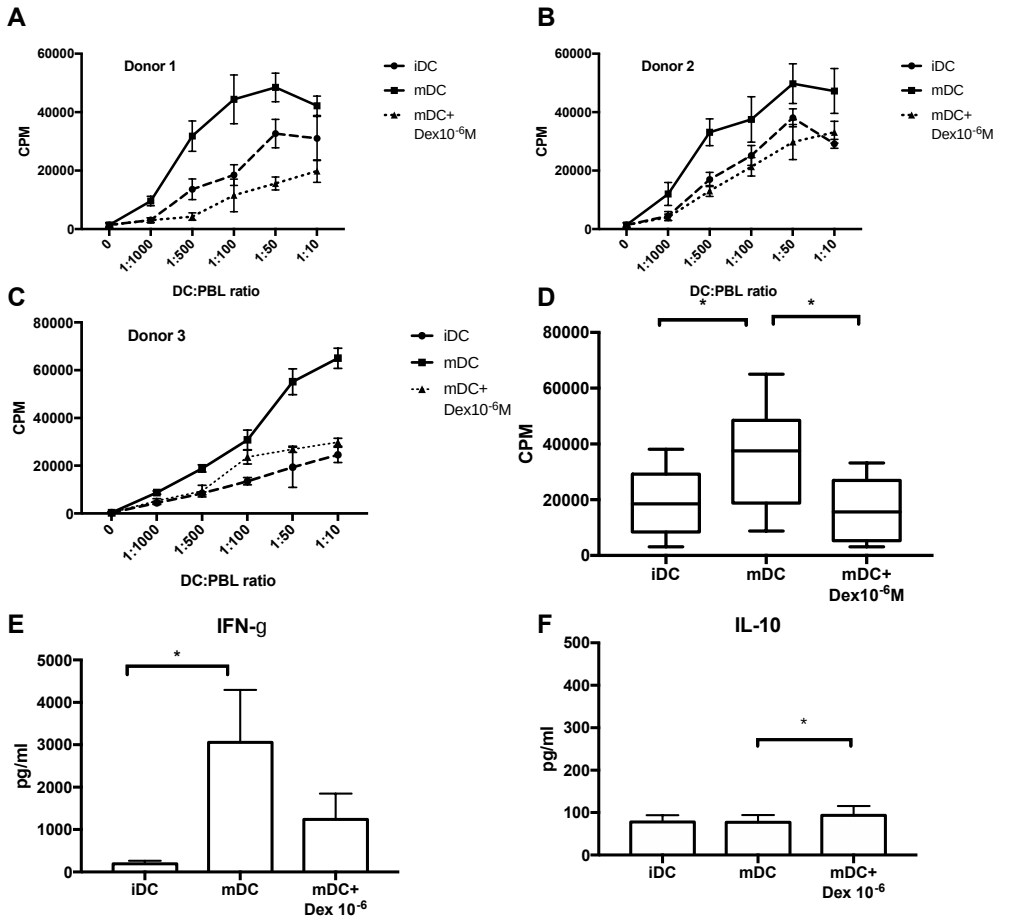


Figure 2.2 Dexamethasone suppresses the allo-stimulatory activity of mature MoDC and alters the PBL cytokine signature. Immature (iDC), matured with polyI:C and R848 (mDC) and matured MoDC exposed to Dex 10^{-6}M 1hr prior to maturation (mDC + Dex) were co-cultured with 10^5 peripheral blood lymphocyte responders (PBL) for 5 days. Proliferation was measured by recording tritillated thymidine levels, added for the final 18hrs of culture. With increasing DC numbers (DC:PBL ratio), there was increased proliferation of PBL for all condition and donors (A-C). D shows the cumulative proliferation data from the three donors. Maturation significantly increased PBL proliferation compared to iDC. In all three donors Dex significantly suppressed proliferation induced by mDC back to the level seen with iDC (A-D). At day 5, supernatant from the co-cultures were analysed for IFN-γ and IL-10 by ELISA. Dex decreased IFN-γ from PBL stimulated by mDC but did not reach statistical significance. IL-10 was low in all conditions but significantly higher from PBL stimulated by mDC + Dex. *p<0.05; CPM= count per minute

Dexamethasone suppresses IL-12 and increases IL-10 in cDC2

cDC2 were isolated, rested and stimulated as stated previously. The mean values are plotted from triplicate repeats in figure 2.3. Each of the 8 donors had either no stimulation with TLR agonists, hence immature (iDC) or matured with polyI:C and R848 (mDC) +/- Dex, added 1hr prior to maturation (mDC) at titrating doses. There was a large range in IL-12 secretion from 316 pg/ml – 57393 pg/ml from mDC. The addition of dexamethasone decreased IL-12 secretion significantly at a dose 10^{-6}M (p=0.0058). The effect was dose dependent with the median IL-12 secretion from mDC of 15764 pg/ml and with the addition of Dex 10^{-8}M 10009 pg/ml, Dex 10^{-7}M 5274 pg/ml and Dex 10^{-6}M 2771 pg/ml.

The median IL-10 secreted from stimulated cDC2 was also significantly increased compared to mDC from a median of 90 pg/ml to 115 pg/ml at 10^{-7}M (p=0.0355) and 123 pg/ml at 10^{-8}M Dex (p=0.0058).

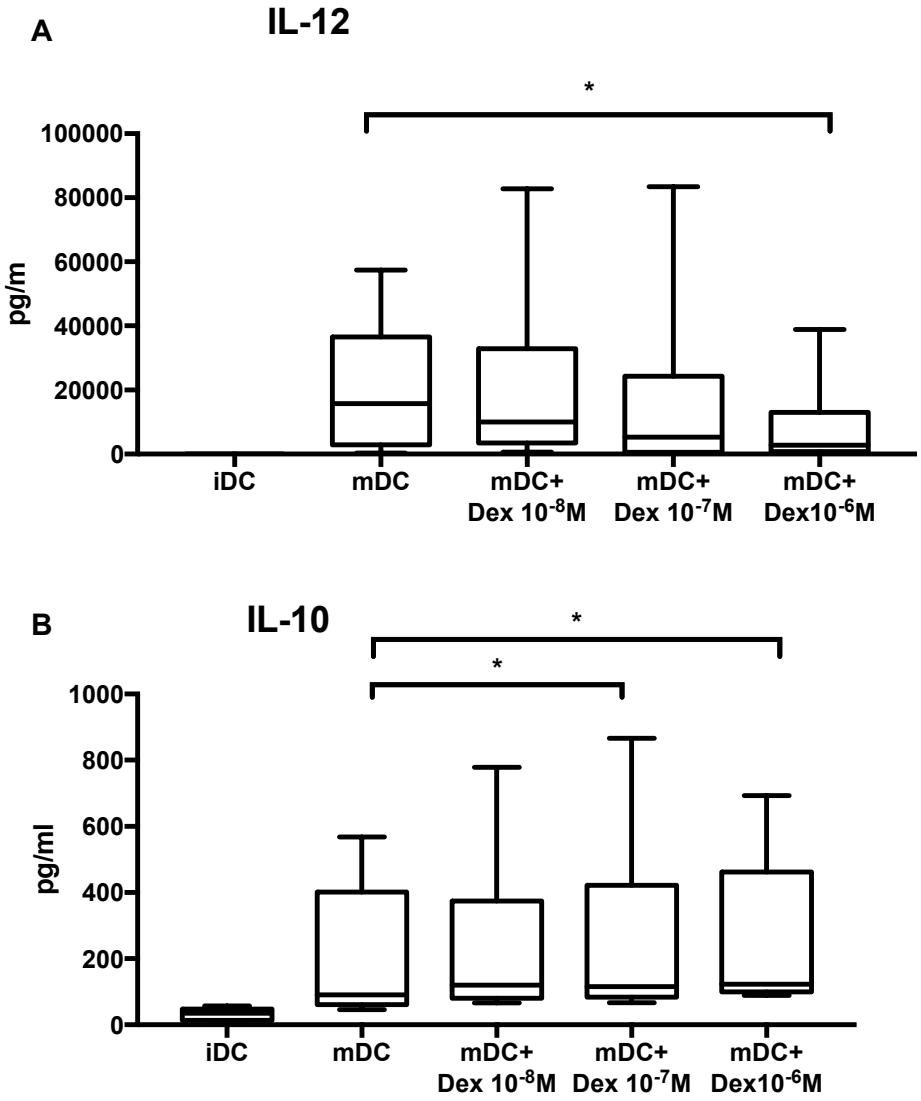


Figure 2.3: Dexamethasone suppresses IL-12 and IL-10 from cDC2. CD1c+ DC were isolated from healthy volunteers (n=8). Immature DC were rested in GM-CSF overnight as a control and produce little IL-12 and IL-10. DC were also matured with TLR dual agonists (polyI:C and R848) following 1hr of resting and then left for 24hours (mDC). Alternatively, mDC + Dex were treated as mDC, however exposed ex-vivo to Dex 1hr prior to maturation. Cytokines were measured in the supernatant after 24hrs by ELISA. With increasing dose of Dex exposure, there was decreasing IL-12 secretion which reached statistical significance at 10^{-6} M compared to mature DC (mDC) (A). Dex exposure also significantly increased the immunosuppressive cytokine IL-10 secretion from cDC2 at 10^{-7}M and 10^{-6}M (B).*$p<0.05$

Dexamethasone suppresses the allo-stimulatory activity of cDC2 and alters the PBL cytokine signature

We next evaluated the effect of Dex on the allo-stimulatory ability of cDC2 by an MLR. Following isolation of cDC2 from three healthy donors, cDC2 were rested overnight either immature (no TLR agonists added), matured (with TLR agonists polyI:C and R848 for 24 hrs) or had Dex 10^{-6}M added 1hr prior to TLR agonist addition. With increasing cDC2 ratios compared to responders (PBL), there was increased proliferation demonstrating the sensitivity of this assay to the stimulators (figure 2.4 A-C). In a cumulative analysis of the three donors, there was no significant difference seen between PBL proliferation stimulated by iDC or mDC (p=0.2969, figure 2.4 D). In a traditional MLR, alloreactivity is driven by foreign MHC recognition by lymphocytes (235). Indeed, the majority or reaction involved in a MLR are through TCR-MHC binding (236). In this context of DC:T-cell co-culture – MHC concentration is therefore a key determinant of proliferation. In immature cDC2 unlike rested immature MoDC, have high HLA-DR expression, equal to that of mature cDC2. This may account for the similar iDC and mDC stimulation of lymphocyte proliferation. However, a difference in the T-cell expanded populations was apparent between iDC and mDC as demonstrated by the PBL cytokine signature. The resulting supernatant was analysed from the MLR after 5 days of co-culture and maturation of the cDC2 significantly increased the IFN-γ production from PBL compared to iDC, from a median of 490 pg/ml to 1907 pg/ml (p=0.0187).

The addition of Dex significantly decreased proliferation compared to mature cDC2 (p=0.0002). The addition of Dex to DC also decreased IFN-γ with a median of 757 pg/ml compared to mDC 1907 pg/ml (p=0.1665). There was a small, but statistically significant increase in IL-10 with maturation of DC from a median 68 pg/ml to 77 pg/ml (p=0.0094), however no significant difference between mDC and Dex exposed mDC (median 77 vs 71 pg/ml, p=0.3146)

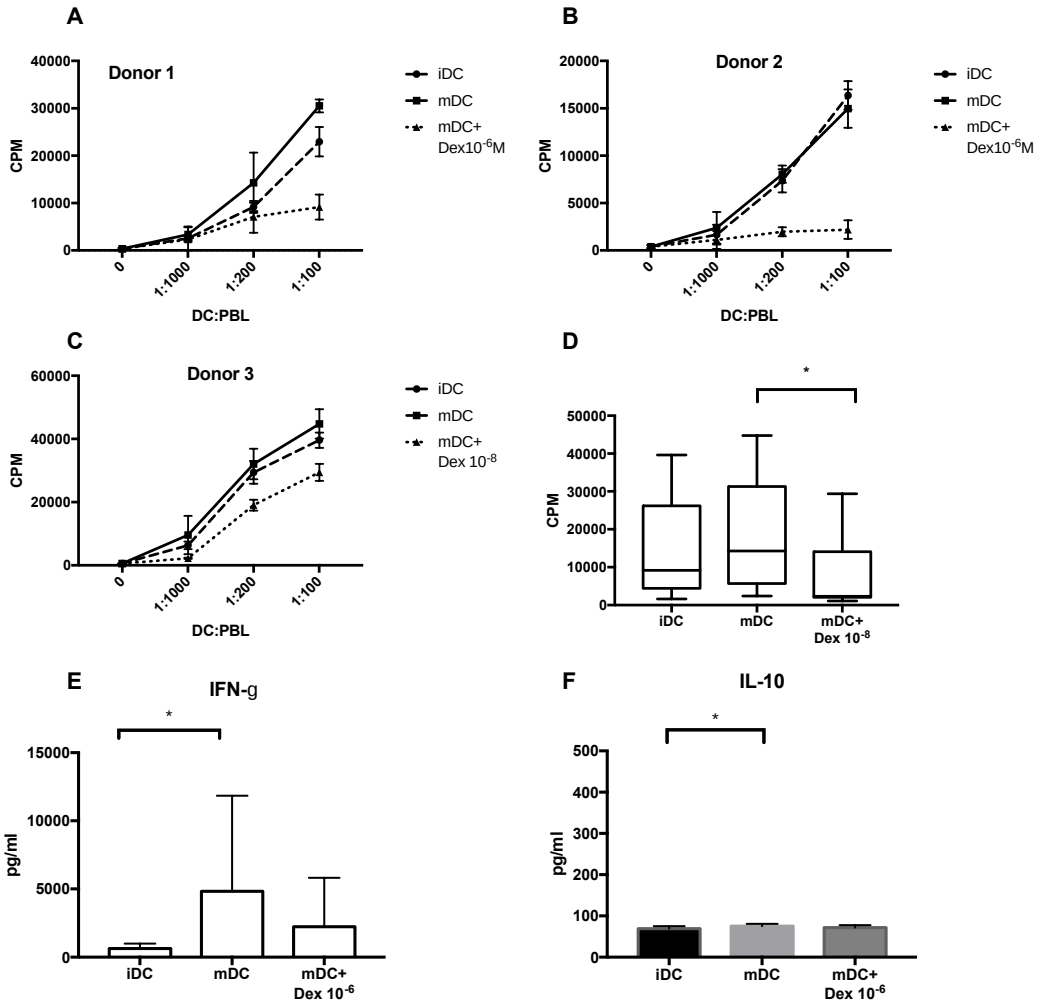


Figure 2.4 Dexamethasone suppresses the allo-stimulatory activity of mature cDC2 and alters the PBL cytokine signature. Immature (iDC), matured with polyI:C and R848 (mDC) and matured cDC2 exposed to Dex 10^{-6}M 1hr prior to maturation (mDC + Dex) were co-cultured with 10^5 peripheral blood lymphocyte responders (PBL) for 5 days. Proliferation was measured by recording tritillated thymidine levels, added for the final 18hrs of culture. With increasing DC numbers (DC:PBL ratio), there was increased proliferation of PBL for all condition and donors (A-C). (D) shows the cumulative proliferation data from the three donors. iDC and mDC induced similar PBL proliferation, although mDC induced a greater IFN-γ secretion from PBL (E). In all three donors Dex significantly suppressed proliferation induced by mDC (A-D). At day 5, supernatant from the co-cultures were analysed for IFN-γ and IL-10 by ELISA. Dex decreased IFN-γ from PBL stimulated by mDC but did not reach statistical significance. IL-10 was low in all conditions but significantly higher from PBL stimulated by mDC. *p<0.05; CPM= count per minute

GBM tumour-derived lysate suppresses IL-12 and increases IL-10 in MoDC

In our 16 patient GBM cohort, described in chapter 1, our explorative analysis, in a univariate analysis also found a significant association with residual disease, proposing tumour-derived factors affecting DC function.

To establish an in-vitro model to study tumour suppression on DCs, we used tumour lysate derived from the U87 cell line, representative of GBM, to measure the effect on DC cytokine secretion post activation.

We found that with increasing doses of tumour-derived lysate (TDL), there was a decrease in IL-12 secretion from matured MoDC (figure 2.5A). On maturations the median IL-12 secretion was 20226 pg/ml, while with increasing ratio TDL:DC median IL-12 was 7992 (1:1), 4152 (3:1) and 2243 pg/ml (10:1) respectively. Using Freidman's statistical test, a non-parametric equivalent to ANOVA with repeated measures, we compared the medians IL-12 secretion from TDL exposed DC to mDC and found that at both 3:1 and 10:1 TDL:DC ratios, IL-12 was significantly suppressed ($p=0.0016$ and $p<0.0001$ respectively, figure 2.5A). Whereas IL-10 secretion did not significantly change from mDC producing a median 369 pg/ml, compared to the addition of TDL at a ratio of 1:1 of 353, 3:1 of 326 and 10:1 of 266 pg/ml ($p>0.9999$) (figure 2.5B).

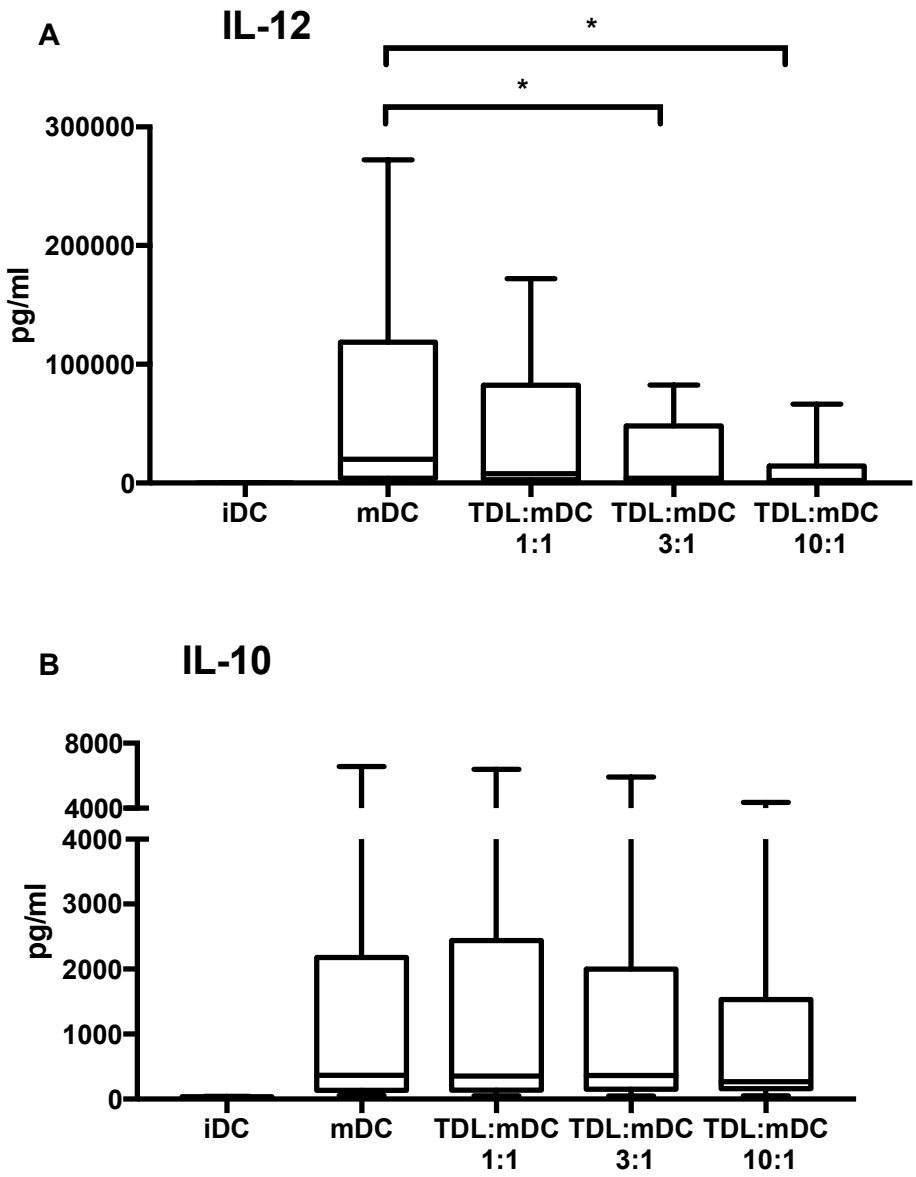


Figure 2.5: GBM tumour lysate suppresses IL-12 and IL-10 from MoDC. DC from 9 healthy volunteers were isolated and left immature DC (iDC), matured with TLR dual agonists (mDC) or matured following 1hr of co-culture with U87 tumour-derived lysate (TDL:mDC). Cytokines were measured in the supernatant after 24hrs by ELISA. With increasing TDL:DC ratio exposure, there was decreasing IL-12 secretion which reached statistical significance at TDL 3:1 compared to mDC (A). TDL exposure did not significantly change IL-10 secretion (B).*$p<0.05$

GBM tumour-derived lysate suppresses the allo-stimulatory activity of mature MoDC and alters the PBL cytokine signature

Three healthy donors' monocytes were isolated and differentiated under standard conditions to produce MoDC. We then tested the allostimulatory activity of immature DC (iDC) versus mature DC (mDC) and mDC cultured with TDL one hour prior to maturation with polyI:C and R848 (figure 2.6 A-D). DC were then harvested after 24 hrs and plated with allogeneic PBL. The allostimulatory activity was measured in an MLR and the results of the three donors is shown along with a cumulative analysis (figure 2.6 A-D). A TDL:DC ratio of 10:1 was chosen since the higher ratio are more reflective of in-vivo conditions and we had demonstrated the suppressive IL-12 changes in our model similar to our patient cohort.

As expected with an MLR, increasing DC numbers, increases PBL proliferation. Immature DC is a useful control in MoDC, since these they have a lower HLA-DR expression and have a significantly lower propensity to drive an allo-reaction as shown in our healthy volunteers (iDC vs mDC $p<0.0001$). The addition of TDL to mDC also significantly decreased proliferation ($p=0.0016$) supporting the notion that TDL is immunosuppressive to DC.

The analysis of the MLR supernatant after 5 days of co-culture of DC and PBL showed a significant increase in IFN-γ production with maturation from 176 to 3086 pg/ml ($p=0.0094$). There was a trend towards decreased IFN-γ production with TL exposed DC decreasing the median IFN-γ to 719 pg/ml ($p=0.3146$). There was no significant difference in IL-10 secretion from the MLR supernatant between any of the conditions (figure 2.6 E,F).

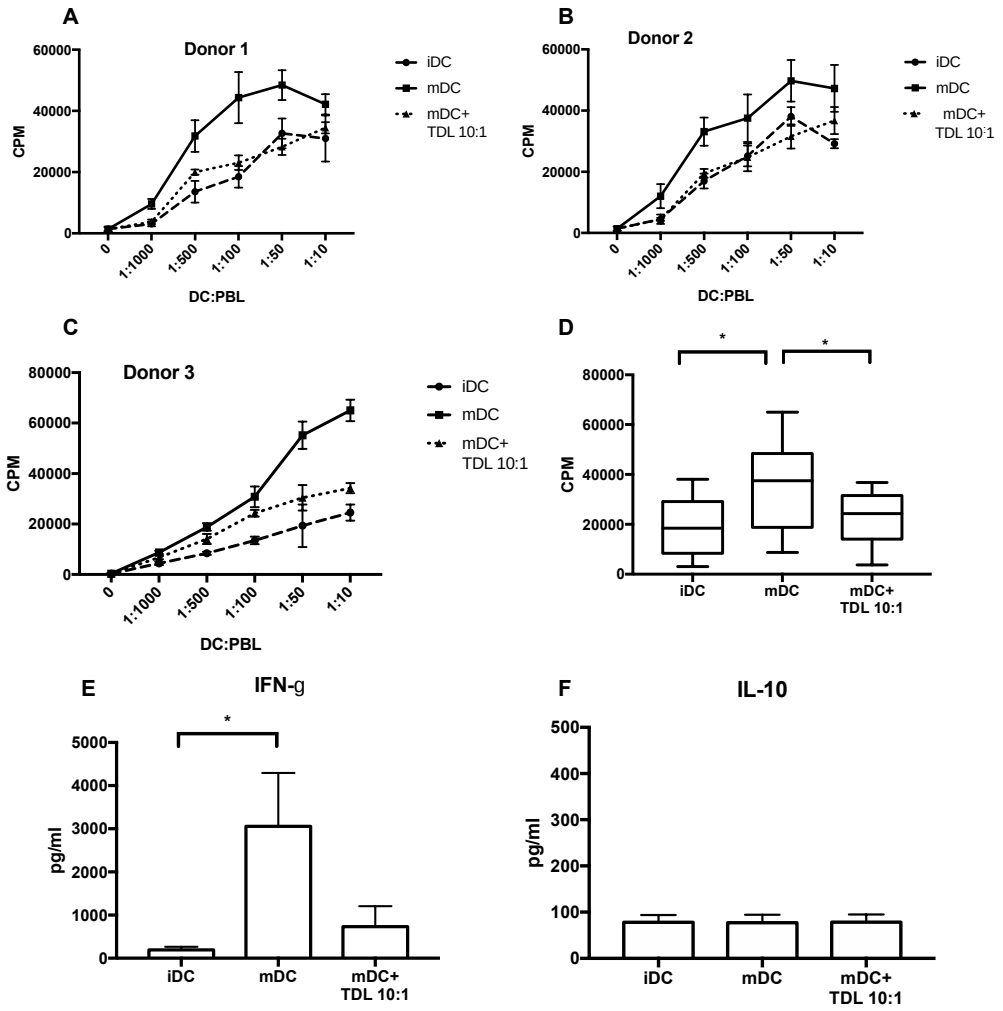


Figure 2.6 GBM tumour-derived lysate suppresses the allo-stimulatory activity of mature MoDC and alters the PBL cytokine signature. Immature (iDC), matured with polyI:C and R848 (mDC) and matured MoDC exposed to Dex 10^{-6}M 1hr prior to maturation (mDC + Dex) were co-cultured with 10^5 peripheral blood lymphocyte responders (PBL) for 5 days. Proliferation was measured by recording tritillated thymidine levels, added for the final 18hrs of culture. With increasing DC numbers (DC:PBL ratio), there was increased proliferation of PBL for all condition and donors (A-C). D shows the cumulative proliferation data from the three donors. Maturation significantly increased PBL proliferation compared to iDC. In all three donors TDL significantly suppressed proliferation induced by mDC back to the level seen with iDC (A-D). At day 5, supernatant from the co-cultures were analysed for IFN-γ and IL-10 by ELISA. TDL decreased IFN-γ from PBL stimulated by mDC but did not reach statistical significance. IL-10 was low in all conditions. *p<0.05; CPM= count per minute

GBM tumour-derived lysate suppresses IL-12 and increases IL-10 in cDC2

We found that with increasing tumour-derived lysate exposure, cDC2 IL-12 secretion was suppressed in a dose dependent manner (figure 2.7 A). The median IL-12 secretion from mDC was 9663 pg/ml, which decreased to 3109, 2363 and 963 pg/ml with increasing TDL:DC ratios of 1:1, 3:1 and 10:1. This reached statistical significance at TDL:DC ratio 3:1 and 10:1 ($p=0.0459$ and $p<0.0001$ respectively).

We also found that with TDL, there was significant increase in IL-10 secretion (figure 2.7 B). Matured cDC2 (mDC) produced a median IL-10 secretion of 90 pg/ml, whereas with a TDL:DC ratio of 1:1, 3:1 and 10:1 there was a median secretion of 123, 124 and 126 pg/ml ($p=0.0008$, $p=0.0004$ and $p=0.0097$ respectively). Among all conditions there was a large range in IL-10 secretion, for example in the mDC population the range was 37 pg/ml to 977 pg/ml. Overall, at the DC:T-cell synapse, the effect of tumour derived factors would lead to suppressed IL-12 and increased IL-10 skewing the T-cell phenotype away from Th1.

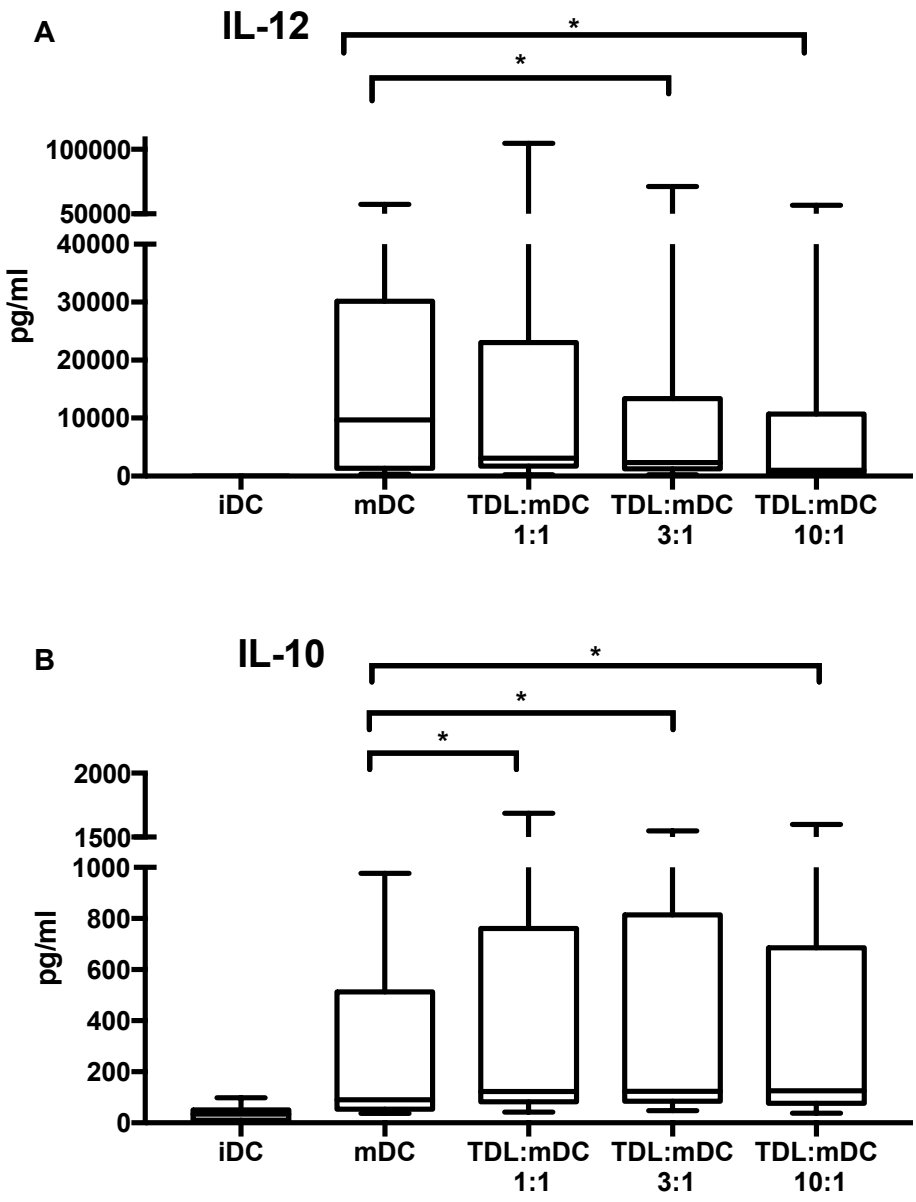


Figure 2.7: GBM tumour-derived lysate (TDL) suppresses IL-12 and IL-10 from cDC2. DC were isolated from healthy volunteers (n=8). Immature DC were rested in GM-CSF overnight as a control and produce little IL-12 and IL-10. DC were also matured with TLR dual agonists (polyI:C and R848) following 1hr of resting and then left for 24hours (mDC). Alternatively, mDC + TDL were treated as mDC, however exposed, ex-vivo, to TDL 1hr prior to maturation. Cytokines were measured in the supernatant after 24hrs by ELISA. With increasing dose of TDL exposure, there was decreasing IL-12 secretion which reached statistical significance at TDL:mDC ratio 3:1 compared to mDC (A). TDL exposure also significantly increased the immunosuppressive cytokine IL-10 secretion from cDC2 at all TDL:mDC ratios (B).*$p<0.05$

GBM tumour-derived lysate suppresses the allo-stimulatory activity of cDC2 and alter the PBL cytokine signature

Further to our findings of skewed cytokine profile from cDC2 with suppressed IL-12 and increased IL-10 secretion with TDL exposure, we investigated the effects on TDL exposed mDC allo-stimulatory ability. We isolated cDC2 from three healthy and compared iDC, mDC and mDC cultured with TDL at a ratio 10:1, 1hr prior to maturation. As previously seen iDC and mDC stimulate an MLR equally with cDC2 stimulators. However, the addition TDL to mDC decreased proliferation in all three donors (figure 2.8 A-C). Overall, using Freidman test, to analyse variance between the three groups confirmed a statistically significant decrease in proliferation with TDL exposed cDC2 as stimulators in the MLR ($p=0.0005$) (figure 2.8 D).

The resultant MLR supernatant was analysed after 5 days of co-culture and maturation of DC showed a significant increase in IFN-γ production from a median 454 pg/ml to 2538 pg/ml ($p=0.0267$), compared to iDC. The mDC exposed to TDL prior to co-culture with
PBL, showed a trend towards reduction in IFN-γ to 973 pg/ml ($p=0.1542$) (figure2.8 D). The median production of IL-10 was similar between the conditions with a median 68, 77 and 68 pg/ml from PBL stimulated by iDC, mDC and TDL exposed mDC (iDC vs mDC $p=0.0678$; mDC vs mDC +TDL $p=0.5777$, figure2.8 E)

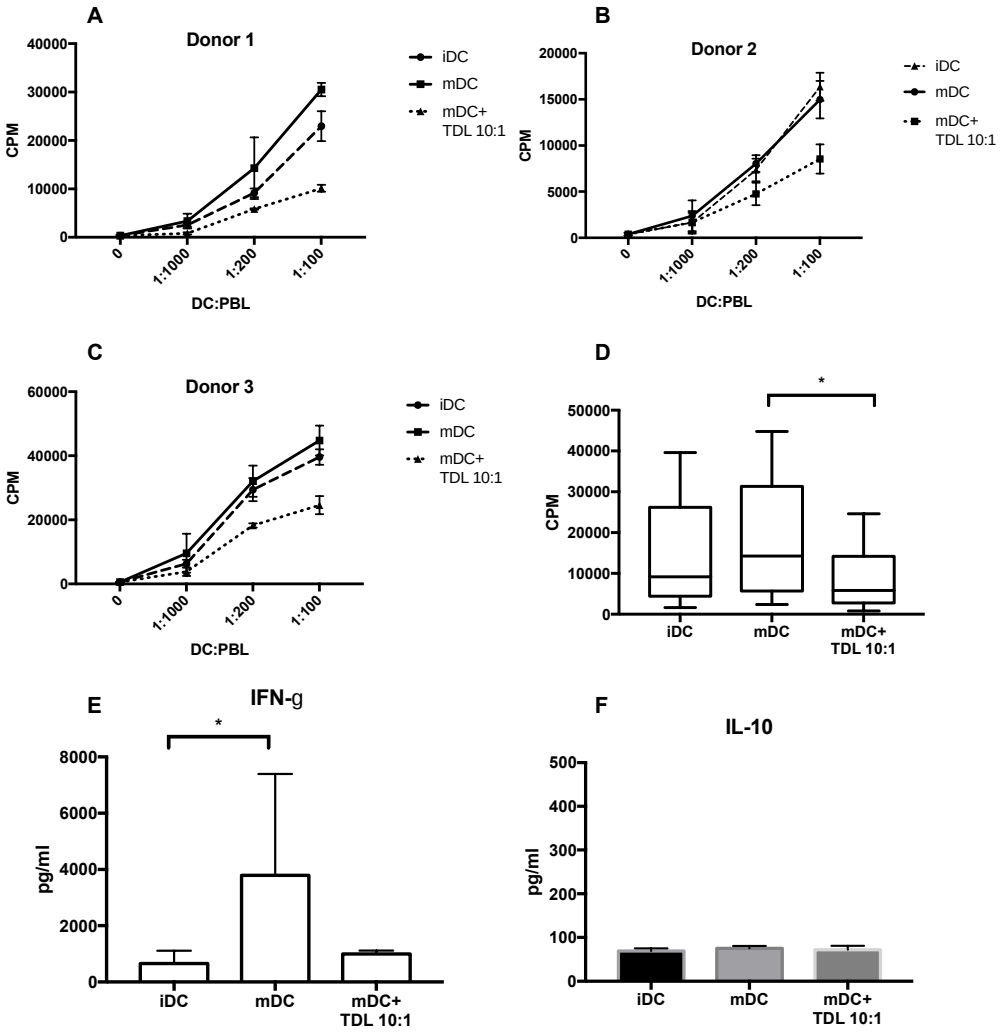


Figure 2.8 GBM tumour-derived lysate (TDL) suppresses the allo-stimulatory activity of mature cDC2 and alters the PBL cytokine signature. Immature (iDC), matured with polyI:C and R848 (mDC) and matured cDC2 exposed to TDL 1hr prior to maturation (mDC + Dex) were co-cultured with 10^5 peripheral blood lymphocyte responders (PBL) for 5 days. Proliferation was measured by recording tritillated thymidine levels, added for the final 18hrs of culture. With increasing DC numbers (DC:PBL ratio), there was increased proliferation of PBL for all condition and donors (A-C). D shows the cumulative proliferation data from the three donors. IDC and mDC induced similar PBL proliferation, although mDC induced significantly greater IFN-γ secreting PBL (E). In all three donors TDL significantly suppressed proliferation induced by mDC (A-D). At day 5, supernatant from the co-cultures were analysed for IFN-γ and IL-10 by ELISA. TDL decreased IFN-γ from PBL stimulated by mDC but did not reach statistical significance. IL-10 was low in all conditions. *p<0.05; CPM= count per minute

Discussion

Dendritic cells are central to adaptive immunity and can direct between anticancer immunity, T-cell tolerance and anergy (198). The conventional immune response involves DC processing of antigens and presentation of peptides on major histocompatibility molecules to T-cell receptors restricted to specific MHC alleles. This is referred to as signal 1 in T-cell activation (198). Signal 2 requires co-stimulation signals, the most studied axis been CD80/86 binding to CD28 on T-cells. This axis has been the successful target of the recent cancer immunotherapy revolution targeting immune checkpoints which modify the signal strength of this axis through inhibition of Programme death-1 (PD-1) and Cytotoxic T-lymphocyte activatory-4 (CTLA-4) (41). The combination of signal 1 and 2 allow T-cells to become effector cells, however signal 3, concerns the high level expression of selective sets of cytokines to determine T-cell fate (198). For example, IL-12 secreted from DC has been shown to drive Th1 responses, whereas IL-10 is directly inhibitory to this signal and can induce T-cell anergy (201, 237). Indeed, signal 3 strongly depends on the conditions under which the DC is primed. For example, ligation of pattern recognition receptors, through TLR agonists polyI:C and R848 have both been shown to stimulate MoDC to produce IL-12 and direct Th1 responses (198). The vast majority of vaccine efforts, particularly in GBM have focused on tumour lysate loading which we have shown here to inhibit both MoDC and cDC2 (194, 238). Although others have recognized this, efforts to overcome DC tumour mediated suppression have focused on danger signal stimulants (239).

Here we show there is a large range in cytokine secretion by healthy individuals from both MoDC and cDC2 is consistent with similar studies (139, 240). Nevertheless, Dex suppressed matured DC IL-12 secretion and increased IL-10 in a dose dependent manner. Further functional assessment revealed these Dex exposed MoDC and cDC2 had significantly impaired allo-stimulatory activity and reduced the IFN-γ secretion in stimulated PBL. Of note, this assay

focussed on Dex effects on DC, since the Dex (along with TLR agonists) were washed off DC prior to plating with allogeneic PBL. Although only 3 donors were used for assessment of allo-stimulation, each donor had 3 different DC:T-cell ratios and were plated in triplicate, giving strength to the findings. Furthermore, all donors showed the same activity trends.

Steroids are known to be immunosuppressive and characteristically exert this effect by directing T-cell apoptosis, both at thymic development and in the periphery during activation-induced cell death (120, 121). Indeed clinically, steroids have direct cytotoxic effects on lymphoid origin cancers such as lymphoma and acute lymphoblastic leukaemia whereas have minimal cytotoxic effect on myeloid leukaemias (122).

A group studied the systemic immune suppression in glioma patients (n=37) including T-cells, myeloid derived suppressor cells and monocytes and compared patients on and off Dex, to elicit tumour versus corticosteroid induced immune changes (241). They found Dex exacerbated lymphopenia in patients compared to healthy controls particularly to the T-cell compartment. In the patients on steroids, although they had similar numbers of monocytes, there was an increase in CD14+HLA-DR$^{-/lo}$ monocytes, which inhibited T cell proliferation and failed to differentiate into MoDC. These cells were also negative for CD80 and had reduced CD86 co-stimulatory molecule expression. Furthermore, these immature cells made up to a third of the monocyte population and were distinct from other CD14^{+} immune cells such as MDSC (241). Serum from GBM patients could induce the same changes to healthy monocytes from healthy controls and the authors proposed this to be CCL2 driven. Dex could not induce the loss of HLA-DR+ expression on healthy monocytes, but reduced CCL2 expression in a series of GBM cell lines and, furthermore, inversely correlated with serum CCL2 levels in a dose dependent manner. Therefore, the authors concluded that tumour induced factors led to the low HLA-DR expression in the monocyte phenotype, however, Dex reduced CCL2 secretion by the tumour, reducing tumour recruitment of

monocytes and resulting in increased peripheral CD14+HLA-DR$^{-/lo}$ monocytes (241). Therefore, this groups suggests the immunosuppressive effects of Dex and tumour-derived factors are additive.

Piemonti et al first described the changes seen to monocytes with the addition of Dex during differentiation to MoDC. They described similar morphology on differentiation, however, on detailed phenotyping, found low levels of CD1a, CD86, and CD40, with high levels of CD14 and CD16 (233). Similarly, molecules involved in antigen uptake (mannose receptor, CD32) and cell adhesion (CD11/CD18, CD54) were up-regulated. Furthermore, on exposure to TNF-alpha and CD40L, Dex exposed DC failed to upregulate B7 molecules. The secretion of pro-inflammatory cytokines TNF-alpha, IL-1β and IL-12 was reduced in response to a number of stimuli including LPS, while maintaining similar levels of immunosuppressive IL-6 and IL-10(233). Overall, they concluded Dex differentiated MoDC had high endocytic activity and lower antigen presentation ability consistent with an immature state, which has been supported by other groups (216, 233).

These early works on the effect of Dex on monocyte differentiation are vital for GBM vaccine trial protocols, where the majority of patients having adjuvant treatment will be on steroids. Indeed, this has been recognised as a limiting factor in the GBM MoDC vaccine trials (216). A large European consortium leading MoDC trials in GBM stated they were unable produce good-quality DCs out of monocytes isolated at the time of corticosteroid use and hence restricted inclusion criteria to the absence of Dex (194). Although, our data here would support this approach, selecting a small good prognostic group, has therefore likely exaggerating overall survival results, especially when such data is compared to historic controls.

Less is known in regard to the effect of Dex on circulating DC. A group studying tolerogenic DC for clinical utility in transplant medicine, found cDC2 cultured with Dex pre-maturation with LPS (cultured for 18h with Dex and

then washed), partially prevented maturation. However, Dex cultured with cDC2 after isolation and during 24-hour maturation with LPS (dex cDC2) produced a tolerogenic DC with low CD83 and CD86 expression and produced low IL-12, IL-10 and IL-6. In co-culture with T-cells, Dex cDC2 poorly stimulated an allogeneic response and the resulting supernatant showed a significant decrease in IFN-γ and IL-2 and a significant increase in IL-10. Hence, the authors concluded that Dex cDC2 stimulated IL-10 producing T-cells and therefore Dex was capable of producing tolerogenic cDC2 (231). Our data presented here partially agrees with this group although our Dex exposed cDC2 did not result in a large increase of IL-10 from stimulated PBL.

Tumour-lysate also had inhibitory effects on both MoDC and cDC2. IL-12 was supressed in both DC groups and IL-10 was significantly increased in secretion from matured cDC2. As discussed above, this is likely to skew the immune response away from a Th1 response. This was supported by the DC-PBL co-culture experiments where a reduction in IFN-γ was seen from PBL stimulated by DC exposed to TDL. Although data for U87 cell line only is shown here, the same effect has been seen using LN18 and LN229, both GBM cell lines, by others in our laboratory (data not shown). In GBM patients there is a hostile tumour microenvironment secreting cytokines, such as IL-10 and TGF-β and catabolites, like IDO, which are suppressive to DC function (44, 202, 242). Indeed TGF-β isoform 2 was originally described as glioblastoma-derived T-cell suppressor factor, given its discovery in GBM cell lines and patient serum, where it was noted to be immunosuppressive to T-cell proliferation through both IL-2 dependent and independent pathways (98, 99). More recently, GBM have been shown to lead to sequestration of T-cells in the bone marrow of patients causing a relative lymphopenia through loss of sphingosine-1-phosphate (S1P) receptor on the T-cell surface. In health, a S1P ligand gradient directs T-cell chemotaxis to blood and lymph and maintains circulating lymphocyte frequency (89). However, the DC mechanisms of immunosuppression have not been well defined in GBM and are extrapolated from those known in other cancer types (226). The data here supports that

tumour-derived factors also induce immunosuppression. However, to expand on this data we need to dissect the exact mechanisms in the tumour-lysate inducing DC dysfunction which was beyond the scope of this hypothesis generating analysis.

Overall, our data here confirms that both tumour-derived factors and Dex can replicate the DC specific poor cytokine secretion seen in our patient cohort in chapter 1. It confirms the challenge of residual disease in GBM patients which induces DC dysfunction, in addition, the immunosuppressive effect of tumour-lysate for DC pulsing. Here, Dex is also shown to affect both MoDC and cDC2 function with reduced IL-12 cytokine secretion and allo-stimulatory ability.

Results: Chapter 3: p38 mitogen-activated protein kinase (p38i) enhances cDC2 function in healthy individuals

Introduction

There is great interest in the use of circulating DC as the next generation of DC vaccines (147, 159). This stems from the improved migration and stimulatory properties of myeloid DC compared to monocyte-derived DC (146). However, as we have discussed in chapters 1 and 2, that DC are impaired by tumour related factors and immunosuppressive drugs such as Dex, used to treat cerebral oedema in GBM patients (202, 216). The ex-vivo optimisation of DC for vaccine therapies have thus far focussed on antigen pulsing and maturation(243). Our group, however, have explored the novel idea of targeting the MAPK pathways to reverse DC dysfunction (139, 240).

The p38 MAPK pathway was first recognized for its role in inflammation and regulating the biosynthesis of pro-inflammatory cytokines from monocytes namely IL-1 and TNFα (244). Subsequently, it was found to regulate the secretion of many other cytokines (244, 245). The canonical understanding of the p38 MAPK pathway is that it promotes expression of inflammatory genes (246). BIRB0796 is a potent inhibitor of all 4 p38 isoforms with 330-fold greater selectivity versus c-Jun N-terminal kinase 2, weak inhibition for c-RAF and insignificant activity against extracellular regulated kinase (247). It also has a particularly slow dissociation rate constant and this is thought to contribute to its potency. However, when used as an anti-inflammatory to treat rheumatoid arthritis and Crohn's disease, it failed to show meaningful clinical activity (248).

The limited clinical benefit may be explained by the differential signalling role of the p38 MAPK pathway in human innate immune cells and our group have previously shown that p38 inhibition in MoDC, decreased IL-12 secretion, while in cDC2, IL-12 was increased (139). Also, in collaboration with another group, we have shown that the p38 MAPK pathway downregulates the immuno-stimulatory properties of Slan-DCs (249). Taken together, we conclude that p38 MAPK inhibitor (p38i) is of interest at enhancing the cDC2 subset only.

We therefore explored whether p38i could reverse the tumour derived and Dex- induced impaired phenotypical and immune dysfunction to the cDC2 population.

Results

The p38i, BIRB 796, successfully blocks downstream MK2 signalling

The activity of BIRB0796 was confirmed by western blotting for the downstream target of p38, phospho-MK2. Isolated cDC2 cells were plated in DC medium containing GM-CSF. After resting, cells were treated with 1μM BIRB0796 for 1hr, stimulated with Poly I:C/R848**.** Activation with Poly I:C / R848 increased phosphorylation of p38 MAPK and its downstream target, MK2, by 30 minutes. As expected, BIRB0796 does not inhibit p38 phosphorylation but inhibited p38 function as shown by the absence of MK2 phosphorylation (see figure 3.1).

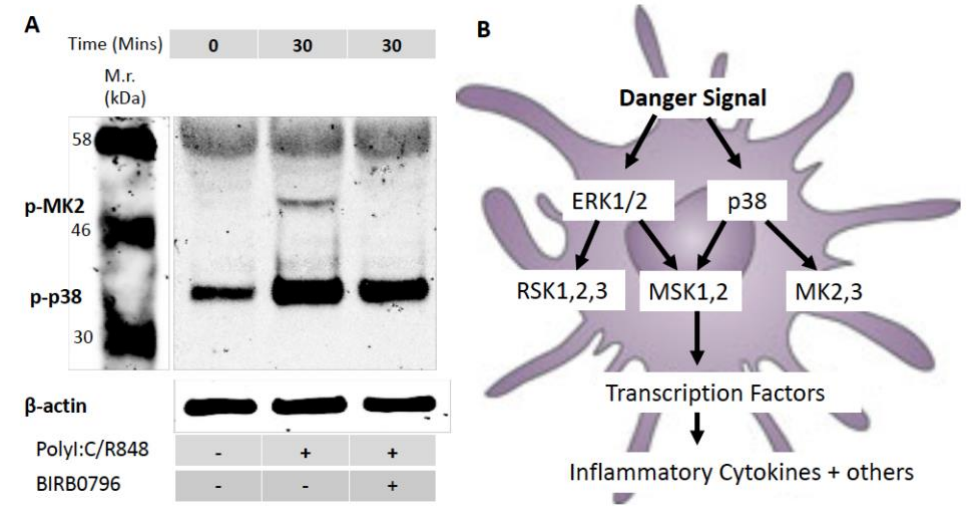


Figure 3.1: Signalling pathway of the p38 Mitogen-activated kinase (MAPK) pathway

(A) Western blot showing that by 30 minutes post maturation with polyI:C and R848, cDC2 phosphorylate p38 and MK2. BIRB0769 inhibited p38 MAPK function thus preventing MK2 phosphorylation. **(B)** A pictorial representation of the signalling pathways controlling cytokine production within cDC2. Danger signals such as TLR agonists trigger ERK1/2 and p38 activation. Downstream of p38, MSK1,2 and MK2,3 regulate transcription factors of inflammatory cytokines such as IL-12 and IL-10.

Inhibition of the p38 MAPK (p38i) pathway enhances the phenotype of cDC2

In our GBM patient cohort, cDC2 were shown to have significantly lower expression of CD86 and HLA-DR than seen in healthy controls. We therefore investigated whether p38i could improve this immature phenotype. There have been no previous reports analysing surface expression effects by p38i. We phenotyped cDC2 in the immature (iDC), matured (mDC with R848 and Poly:IC) and with p38i added to mDC. An example of a healthy donor is shown below in figure 3.2.

A selection of markers was analysed including HLA-DR, CD86, CD80, PD-L1, PD-L2, HLA-ABC, CD40, CD209, CD83 in 6 healthy donors. A summary of fold change in expression is shown in figure 3.3 comparing the median frequency intensity of staining from the isotype (IgG1-PE) expression on mDC. The primary focus was the comparison between mDC and p38i mDC and we found a significant increase in the co-stimulatory molecules CD86 ($p=0.003$), CD80 ($p<0.001$) and CD40 ($p<0.001$). Indeed, CD86 showed a 6-fold increase in expression, CD80 2-fold and CD40 a 7-fold increase. There was also a significant increase (7-fold) in the expression of the C-lectin CD209 (DC-SIGN, $p=0.001$). Of note, was a significant decrease in PD-L1 expression ($p=0.001$). There was also a small but significant decrease in CD83 expression ($p=0.027$). Overall, however, the large increase in p38i mDC co-stimulatory expression favours inducing T-cell activation, as oppose to tolerance and anergy.

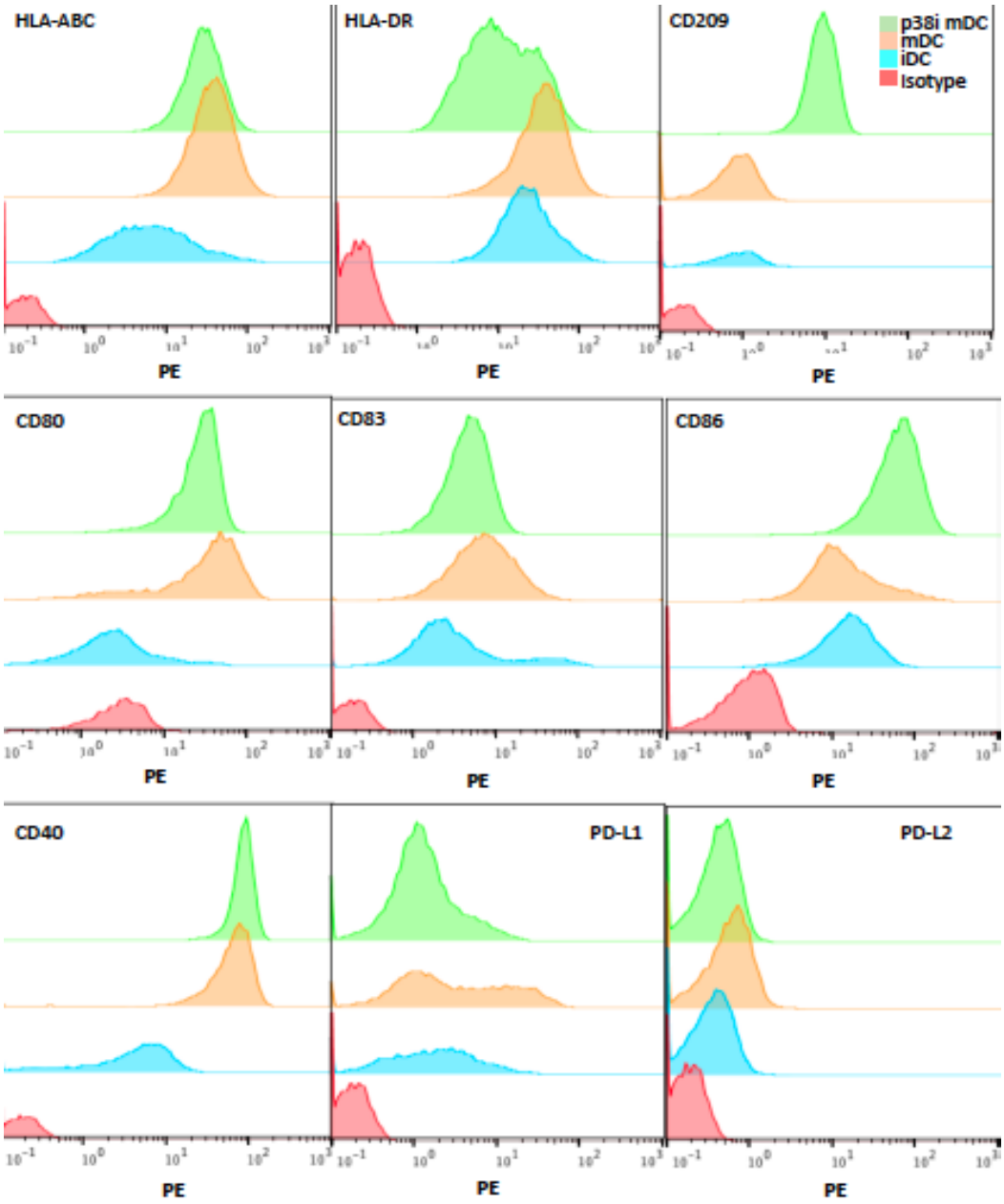


Figure 3.2. Phenotype of cDC2 comparing immature, matured and matured with p38i cDC2

A representative cDC2 stained with phenotype labelled fluorophore antibodies and analysed by flow cytometry. Histograms are shown with isotype controls (red), immature DC (blue), mature (orange) and p38i matured cDC2 (green).

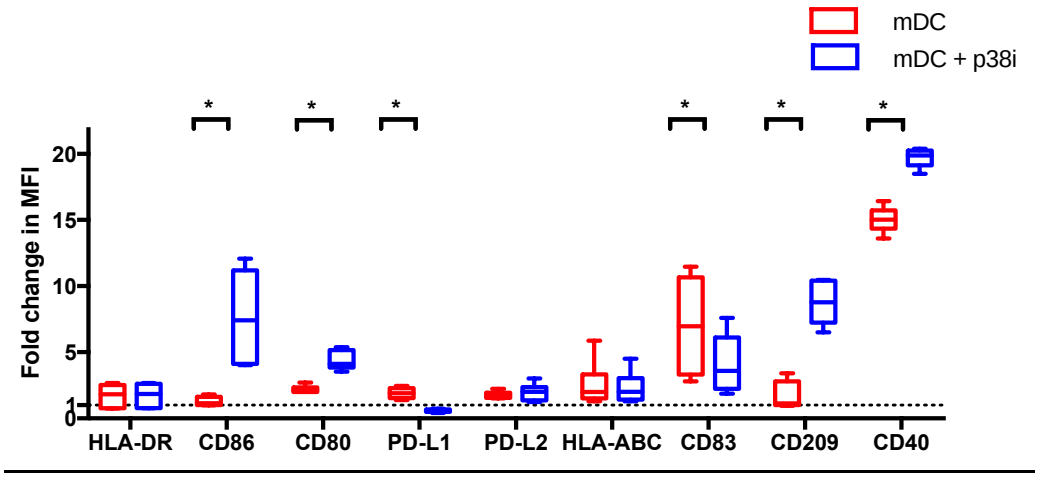


Figure 3.3 Summary of phenotype change comparing matured cDC2 and p38i cDC2

cDC2 were isolated and treated with PolyI:C and R848 +/- p38i as previously described. cDC2 were stained with PE-conjugated antibodies to respective surface markers and analysed by flow cytometry. The MFI was calculated by fold change from IgG1-PE stained mDC. There was a significant increase in CD86, CD80, CD209 and CD40 expression in p38i mDC compared to mDC. There was also a significant decrease in PD-L1 and CD83 expression.

Inhibition of p38 MAPK reverses Dex and TDL induced cytokine dysfunction in cDC2

Previously we established that activation of the p38 MAPK pathway downregulates IL-12 secretion from cDC2 cells and p38i increases IL-12 secretion. This is opposite to what we showed in MoDC and slanDC, whereby p38i inhibits IL-12 secretion (139, 249). We therefore hypothesised that inhibition of p38 MAPK in cDC2 would reverse the immunosuppressive effects of Dex and TDL shown in chapter 2.

Therefore cDC2 were isolated from 9 healthy volunteers exposed to Dex at 10^{-6}M or TDL at ratio 10:1, as used in chapter 2, with or without p38i. Inhibition of p38 MAPK significantly increased IL-12 expression in both Dex (from median 3050 to 8555pg/mL; p=0.0011) and TDL treated DC (from median 1294 to 9314 pg/mL; p=0.0175). Furthermore, p38i reduced secretion of the regulatory cytokine IL-10 (Dex median 176.9 to 39 pg/mL; p=0.0019, TDL median (200.3 to 45.3 pg/mL; p=0.0006). As such, inhibition of p38 MAPK skewed the cytokine release profile of cDC2 towards a pattern associated with Th1 responses (Figure 3.4).

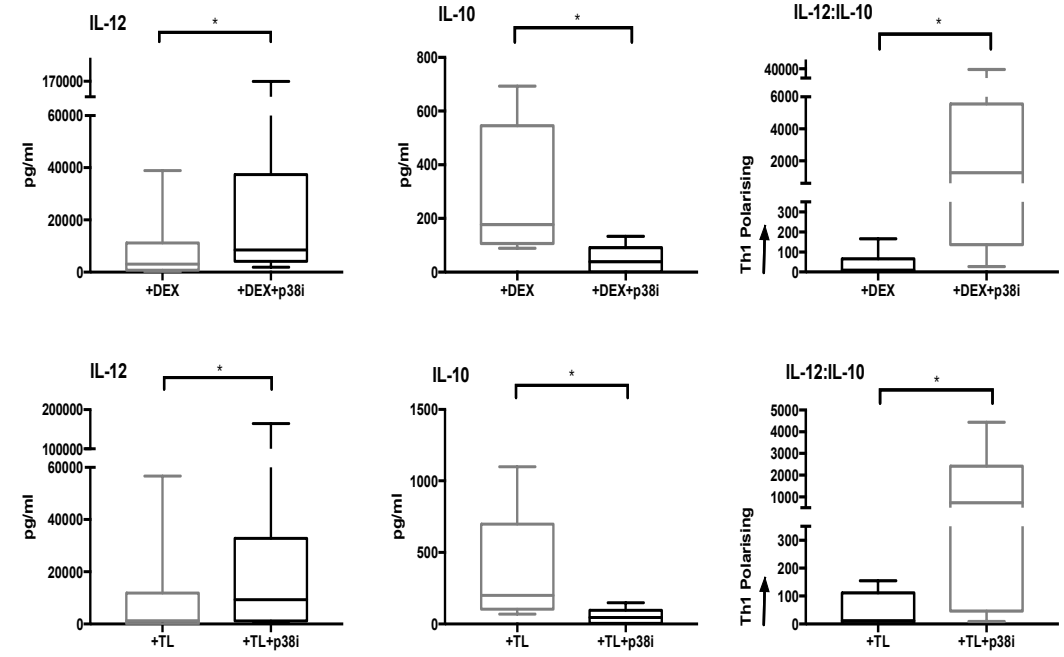


Figure 3.4: p38i restores TDL and Dex-exposed cDC2 IL-12 secretion and suppresses IL-10

cDC2 were isolated from healthy volunteers (n=9). DC were matured with TLR dual agonists (polyI:C and R848) following TDL or Dex exposure (mDC) +/- p38i. Cytokines were measured in the supernatant after 24hrs by ELISA. cDC2 exposed to p38i significantly increased IL-12 in both TDL and Dex exposed DC, suppressed IL-10 and increased the ratio of IL-12:IL-10. This would favour Th1 polarisation. *p<0.05

The allo-stimulatory activity of cDC2 exposed to Dex and TDL is enhanced by p38i and the resulting PBL supernatant is IFN-γ rich

The functional activity of p38i cDC2 in terms of allo-stimulation was also shown to be impaired in chapter 2. We therefore investigated whether p38i could reverse this immunosuppression to cDC2.

Three healthy donor cDC2 were isolated and exposed to TDL, as previously. The results for the three donors are shown in figure 3.5. TDL-exposed DC had a significantly impaired ability to drive an allo-reaction in an MLR, compared to mDC ($p=0.0059$). However, p38i co-culture was able to reverse this immunosuppression and improve allo-stimulation compared to TDL exposed DC ($p<0.0001$). Furthermore, this significantly improved allo-stimulation compared to mDC ($p<0.0001$). The resulting cytokine analysis of supernatant from the 5-day MLR showed a significant increase in IFN-γ from p38i cDC2 exposed to TDL (972.5 pg/ml to 9412 pg/ml, TDL vs TDL+p38i $p=0.0400$). The IL-10 secretion from the MLR was not significantly changed (see figure 3.5).

The same 3 donors cDC2 were also exposed to Dex. As seen, in chapter 2, Dex significantly inhibited the allo-stimulatory activity of mDC ($p=0.0357$). The addition of p38i treatment with Dex increased the allo-stimulatory activity significantly ($p<0.0001$). Furthermore, this was increased above that of mDC without Dex exposure ($p<0.0001$) as shown in figure 3.6.
The resulting supernatant was IFN-γ rich with p38i treatment compared to Dex treated cDC2 (Dex+p38i - median 7157 pg/ml compared to 757 pg/ml in Dex only $p=0.0045$). There was also a trend towards increase IFN-γ secretion from PBL stimulated by p38i Dex-mDC compared to mDC without Dex exposure (p38i+Dex vs mDC - 7157 vs 1907 pg/ml $p=0.1299$). There was a small but significant increase in IL-10 in p38i and Dex treated cDC2 from a median with Dex exposure of 70.76 pg/ml increased to 79.11 pg/ml compared to Dex-mDC. Relative to the 10-fold increase in IFN-γ there is a predominant Th1 signature consistent with the DC cytokine showing IL-12 rich secretion

skewing for Th1 polarisation (figure 3.6). The Friedman's statistical test for paired, non-parametric, (one-way) ANOVA was used to analyse cytokines secretion and 2-way ANOVA for MLR proliferation analysis.

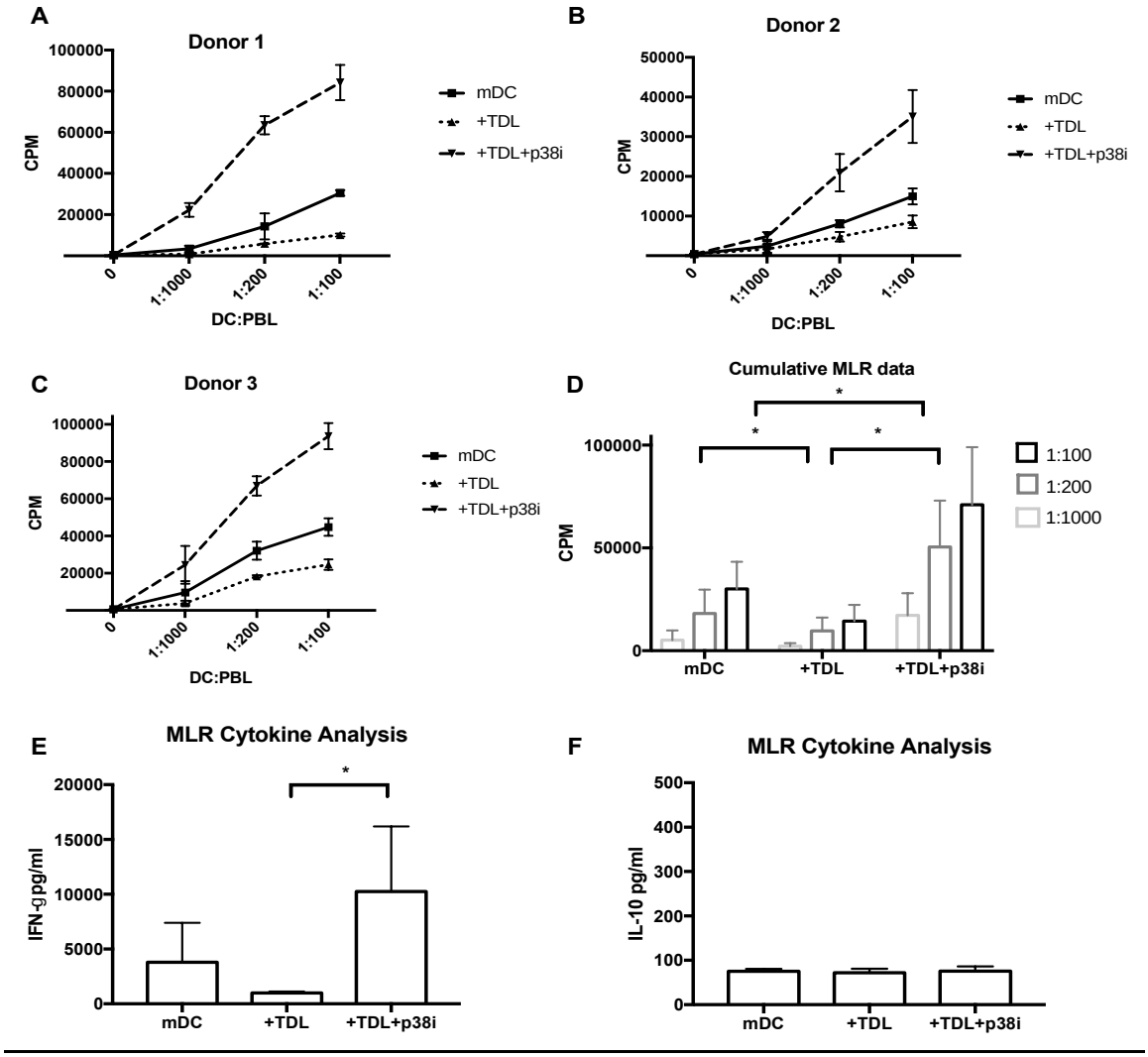


Figure 3.5 p38i improves TDL-exposed cDC2 allo-stimulatory ability and induces IFN-γ rich supernatant: Matured (mDC), mDC exposed to TDL 1hr prior to maturation (mDC + TDL) and p38i mDC + TDL were co-cultured with 10^5 peripheral blood lymphocyte responders (PBL) for 5 days. Proliferation was measured by recording tritillated thymidine levels, added for the final 18hrs of culture. With increasing DC numbers (DC:PBL ratio), there was increased proliferation of PBL for all condition and donors (A-C). (D) shows the cumulative proliferation data from the three donors. p38i significantly improved proliferation in all three donors, while TDL significantly suppressed proliferation (A-D). At day 5, supernatant from the co-cultures showed increased IFN-γ from PBL stimulated by p38i TDL-mDC. IL-10 was low in all conditions. *p<0.05; CPM= count per minute

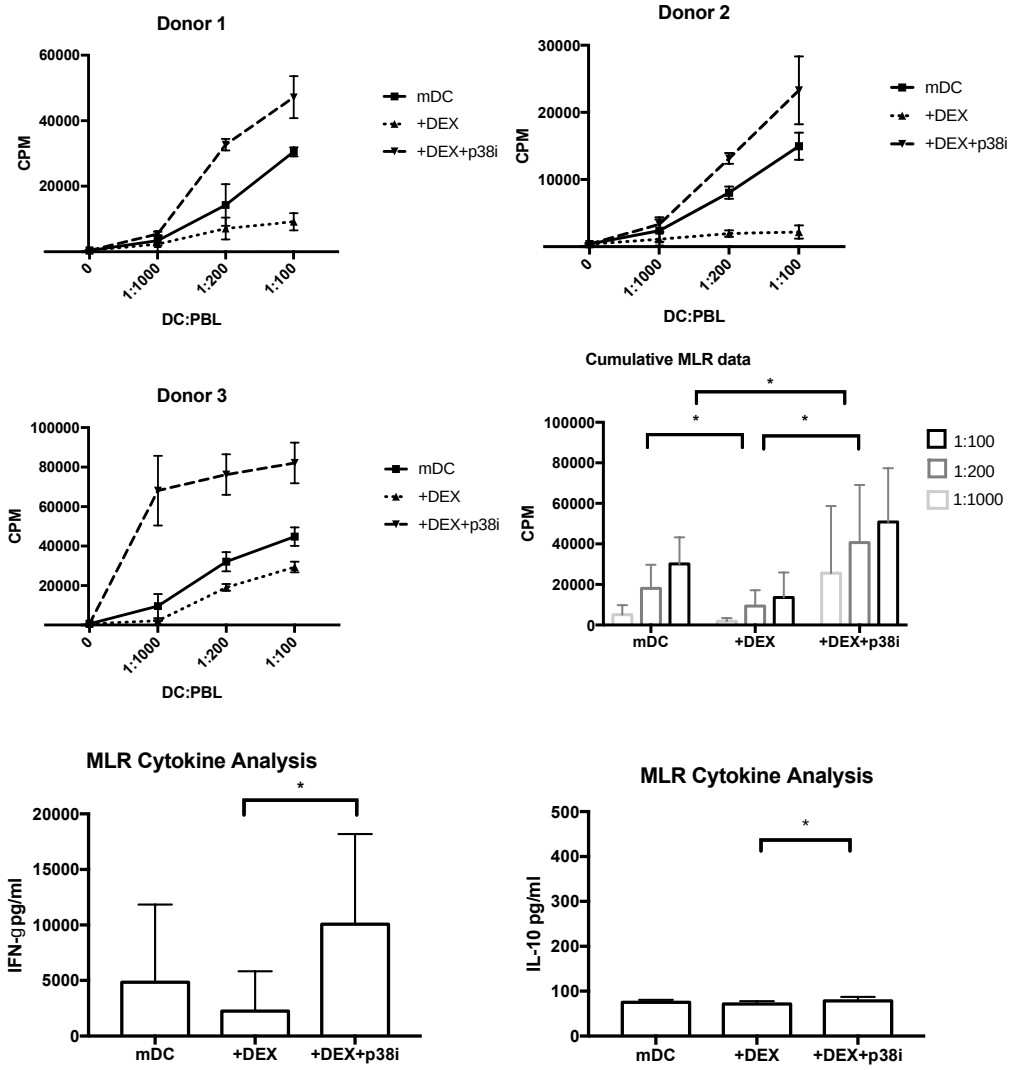


Figure 3.6 p38i improves Dex-exposed cDC2 allo-stimulatory ability and induces IFN-γ rich supernatant: Matured (mDC), DC exposed to Dex 10^{-6}M 1hr prior to maturation (+DEX) and p38i (+DEX+p38i) were co-cultured with 10^5 peripheral blood lymphocyte responders (PBL) for 5 days. Proliferation was measured by recording tritillated thymidine levels, added for the final 18hrs of culture. With increasing DC numbers (DC:PBL ratio), there was increased proliferation of PBL for all condition and donors (A-C). (D) shows the cumulative proliferation data from the three donors. p38i significantly improved proliferation in all three donors, while Dex significantly suppressed proliferation (A-D). At day 5, supernatant from the co-cultures showed increased IFN-γ from PBL stimulated by p38i Dex-mDC. IL-10 was low in all conditions, but significantly higher in p38i Dex-mDC compared to Dex-mDC. *p<0.05; CPM= count per minute

The migration of cDC2 towards a CCL21 gradient was superior with p38i treatment. This is independent of CCR7 expression on cDC2.

The success of DC based immunotherapy is critically dependent on migration. All DC vaccine immunotherapy uses ex-vivo antigen education via either RNA, tumour lysate or peptides. Therefore, the key migration is from the injection site to the local lymph node where T-cell priming and activation takes place (125).

CCR7 is a chemokine receptor expressed on DC and upregulated on maturation and discovered to be vital for DC migration (250). CCL21, a natural ligand, is a chemokine found on endothelial cells that guides a DC initially into the terminal lymphatics from its cells of interest by haptotaxis (251). CCL21 also guides a migratory DC to the T-cell rich paracortex of the lymph node, for T-cell priming (252). CCR7 deficient mice showed a number of immunodeficiencies, which include abnormal secondary lymphoid morphology and a failure of mature DC to migrate to draining lymph nodes (253). Both CC21 and CCL19 are known ligands to CCR7, however some studies suggest CCL21 is the more critical (254). Hence, we investigated whether p38i matured DC could migrate better across a Boyden chamber to a CCL21 gradient.

We took 5 healthy donor cDC2 and compared iDC, mDC and p38i mDC. A CCL21 concentration of 250ng/ml was chosen based on other DC migration studies and media (RPMI+ 1%FCS) was used as a control (189). Figure 3.7 shows a representative donor and a summary of the 5 donors' cDC2 migration.

The mean percentage of DC migration was dependent on DC state with iDC, mDC and p38i mDC giving 17.1, 39.5 and 65.6% migration to the CCL21 pool in the bottom of the Boyden chamber (overall p=0.0041). There was a significant

difference in migration between CCL21 and media ($p<0.0001$) as would be expected. Consistent with other published data mDC migrated significantly better than iDC to CCL21 ($p=0.0274$). Furthermore, p38i mDC migrated significantly better to both iDC ($p<0.0001$) and mDC ($p=0.0099$).

Given the favourable phenotypic changes in costimulation molecule expression on cDC2 described earlier in the chapter with p38i mDC, we hypothesized that the superior migration of p38i mDC was from increased CCR7 expression. However, of the five donors analysed, the CCR7 expression on p38i mDC was lower than mDC with a median MFI of 11.3 on p38i mDC compared to 59.1 on mDC. This did not reach statistical significance ($p=0.1156$, figure 3.8). Therefore, the mechanism of improved migration to CCL21 gradient by p38i mDC is unknown and is the focus of future studies.

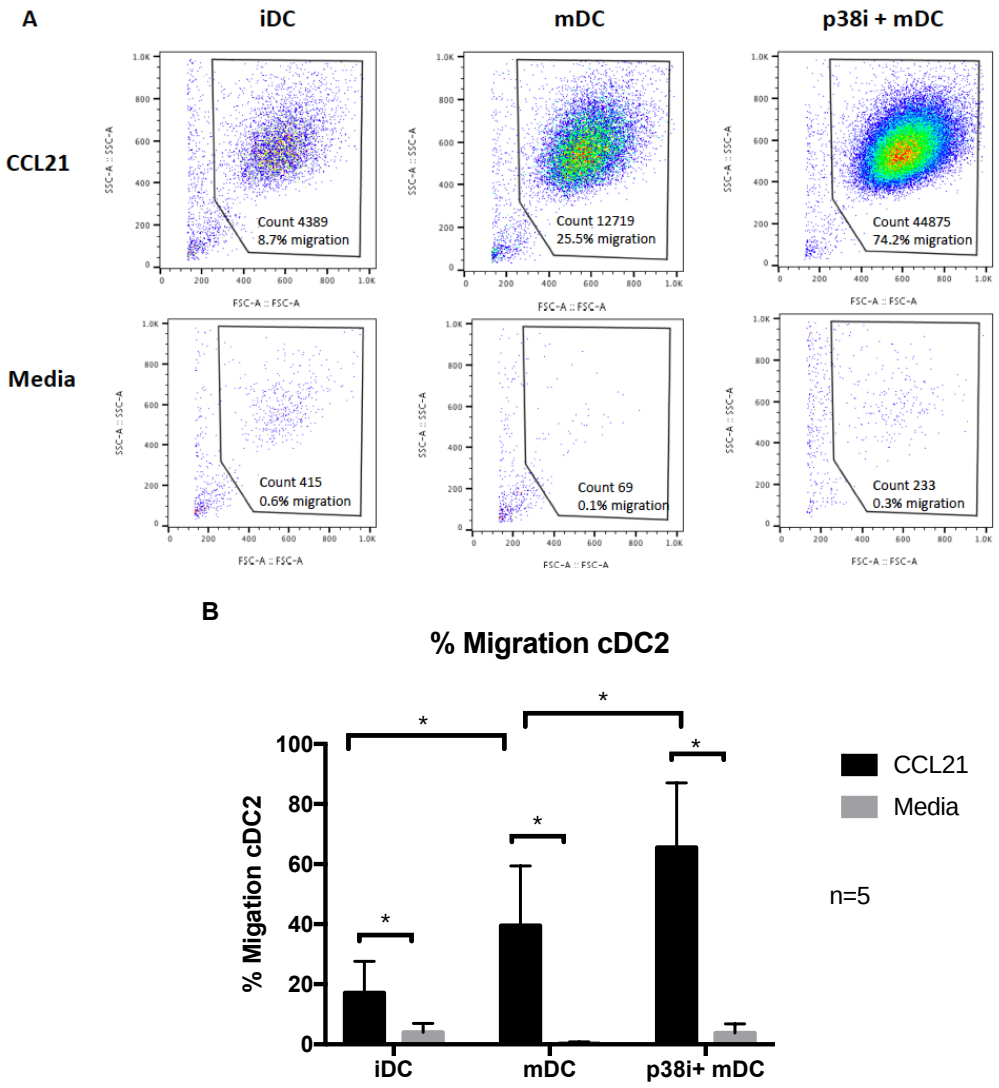


Figure 3.7: Migration of cDC2 towards CCL21 is improved by p38i. cDC2 were isolated from healthy individuals and either left immature (iDC), matured (mDC) or matured with prior p38i (p38i + mDC) before harvesting after 24 hours. A 24-well transwell plate with 5µM pore membrane separated cDC2 in the upper chamber from either media (control) or CCL21 (250ng/ml) in the lower chamber. (A) An example of migration of iDC, mDC and p38i mDC from a healthy donor. (B) Cumulative data from 5 healthy donors. cDC2 migration was superior towards CCL21 than media in all conditions. Maturation of cDC2 significantly improved CCL21-migration compared to iDC, while p38i mDC had significantly greater migration towards CCL21 than both mDC and iDC.

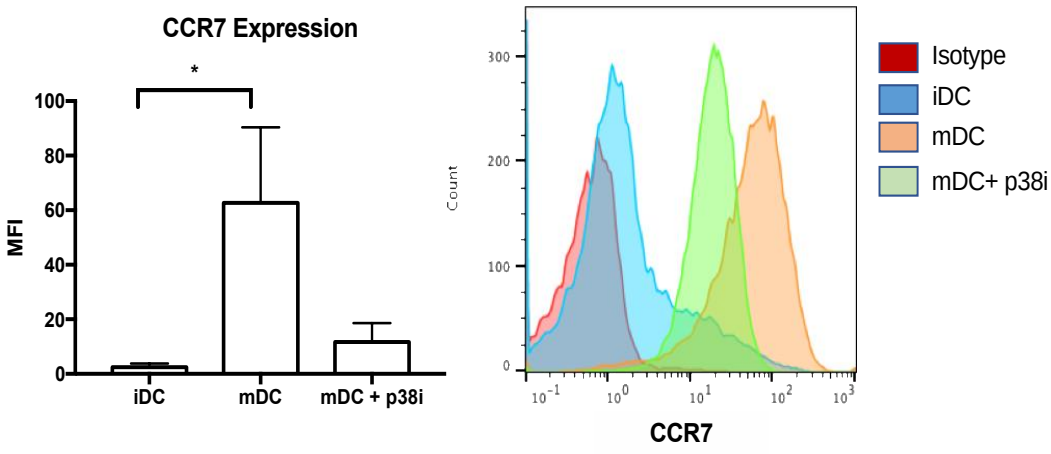


Figure 3.8: CCR7 expression on cDC2 is reduced in p38i. Following isolation, immature, mature and p38i matured cDC2 were stained with CCR7-PE-Vio770 and analysed by flow cytometry. On maturation CCR7 is upregulated as expected, however p38i mDC have a trend of lower expression than mDC.

Mature and p38i cDC2 are able to cross-present antigens

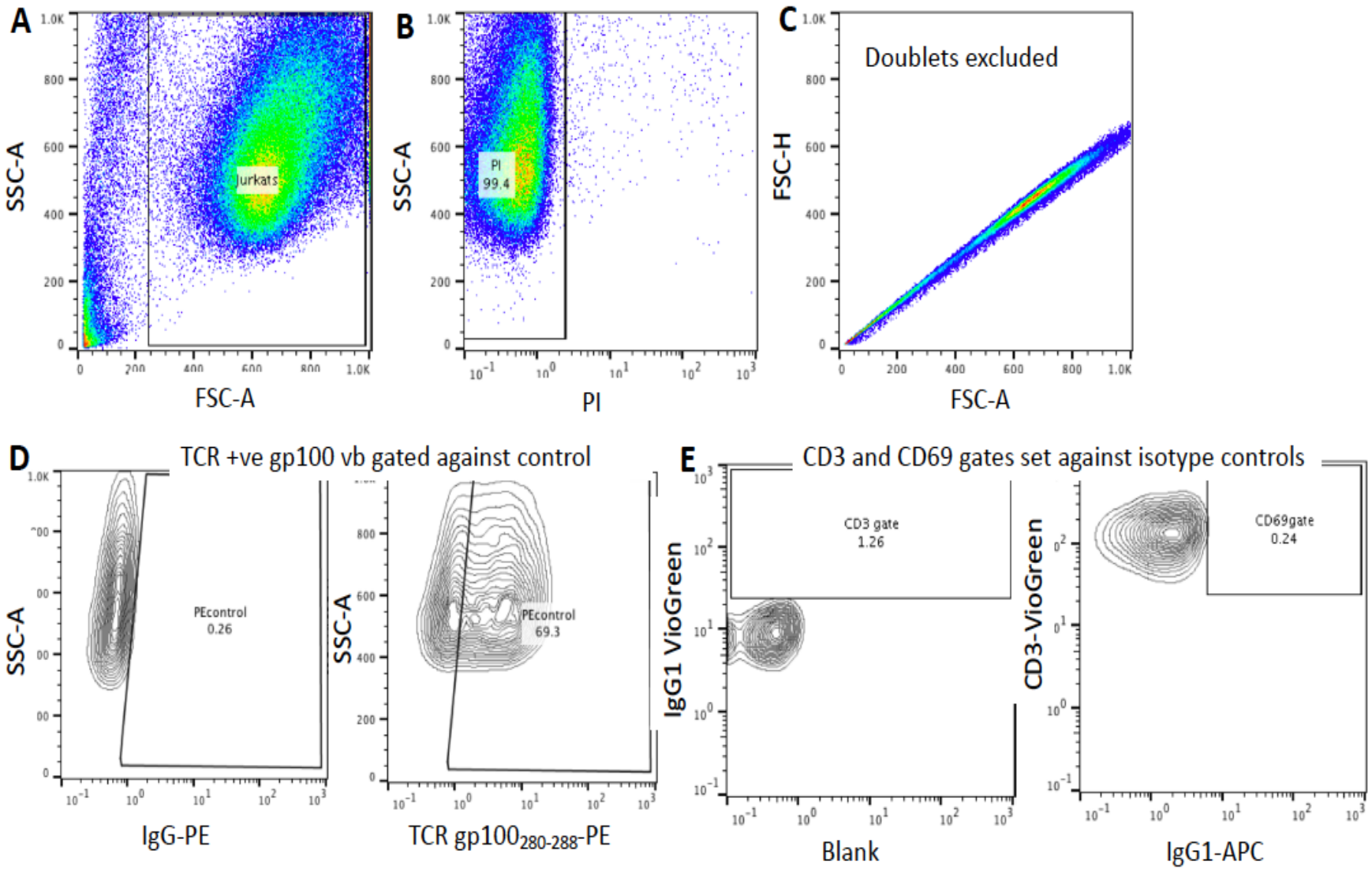
For a successful adaptive immune response to an antigen, a DC delivers 3 vital signals, to a T-cells (198). Signal 1 comprises the presentation of a peptide, in the context of MHC complex to T-cell receptor (TCR). Signal 2 involves the co-stimulatory B7 complex (CD80/86) binding to CD28 on the T-cell, which provides survival and proliferation signal to support signal 1 and avoids T-cell anergy or tolerance. While, signal 3 is produced by the secretion of cytokines from the DC, which polarize the T-cell effector phenotype (198).

We have shown that p38i mDC can strengthen signal 2 by increasing expression of B7 molecules (CD80, 86) and polarise towards a Th1 response, vital for facilitating cytotoxicity. We therefore set to test p38i cDC2 ability to present antigens, pivotal for signal 1. Our initial investigating involved cross presentation.

In mice, the major cross presenting DC is $CD103^{+}Clec9A^{+}XCRX1$ ($CD8\alpha^{+}$ in lymph nodes) equivalent to the human cDC1 ($CD141^{high}$), while $CD11c^{+}CD11b^{+}MHC\text{-}II^{+}$ DC in mice, most closely associated with cDC2, are unable to. However, given the heterogeneity of the murine $CD11b^{+}CD11c^{+}$MHC-II antigen presenting cell population which includes macrophages, monocytes and $CD14^{+}$ DC-like cells, the antigen presenting abilities of the cDC2 population is likely underestimated (145). Equally, when cDC1 were first isolated in humans to assess cross-presenting capacity in comparison to cDC2, suboptimal TLR agonist stimulation of cDC2 was used (149). Subsequent studies of human cDC2 have demonstrated both cDC1 and cDC2 efficiently cross present, however they have different TLR agonist requirements (141, 156).

A system developed by our collaborators was able to assess the ability of a DC to cross present peptides (186). In this assay long $gp100_{272\text{-}300}$ peptide requires intracellular processing by cDC2 to release the $gp100_{280\text{-}288}$ cognate epitope

and activate the transfected $gp100_{280-288}$ TCR on a Jurkat cell line. The readout was the early activation marker CD69 expression after 24 hours of co-cultured DCs and Jurkats. An irrelevant peptide, $gp100_{154-167}$, was used as a negative control and $gp100_{280-288}$ (short) peptide, used as a positive control. The short $gp100_{280-288}$ peptide was known to be presented by HLA-A2 and hence 4 HLA-A2 buffy coats were selected to isolate cDC2. DCs were isolated and rested following isolation. The addition of BIRB 796 was added to one third of the DCs to create our enhanced DCs as previously described for one hour, prior to maturation. One third of DC were left Immature (iDC) and the final third matured with R848 and polyI:C only. Simultaneous to the addition of the TLR agonists, long $gp100_{272-300}$ peptide was added and DC left overnight to mature and process antigen. After 18 hours DC were then washed and co-cultured with transfected $gp100_{280-288}$ TCR-Jurkats ($5x10^4$ per well). In addition, the irrelevant, short gp100 peptides and phytohaemagglutinin (PHA) were added to appropriate control wells. After 24 hours of co-culture, cells were washed and stained for CD3 and CD69 and relevant isotypes control for gating (see figure 3.9).


A
SSC-A
FSC-A
Jurkats
B
SSC-A
PI
PI
99.4
C
FSC-H
FSC-A
Doublets excluded
D
TCR +ve gp100 vb gated against control
SSC-A
IgG-PE
PEcontrol
0.26
SSC-A
TCR gp100280-288-PE
PEcontrol
69.3
E
CD3 and CD69 gates set against isotype controls
IgG1 VioGreen
Blank
CD3 gate
1.26
CD3-VioGreen
IgG1-APC
CD69gate
0.24

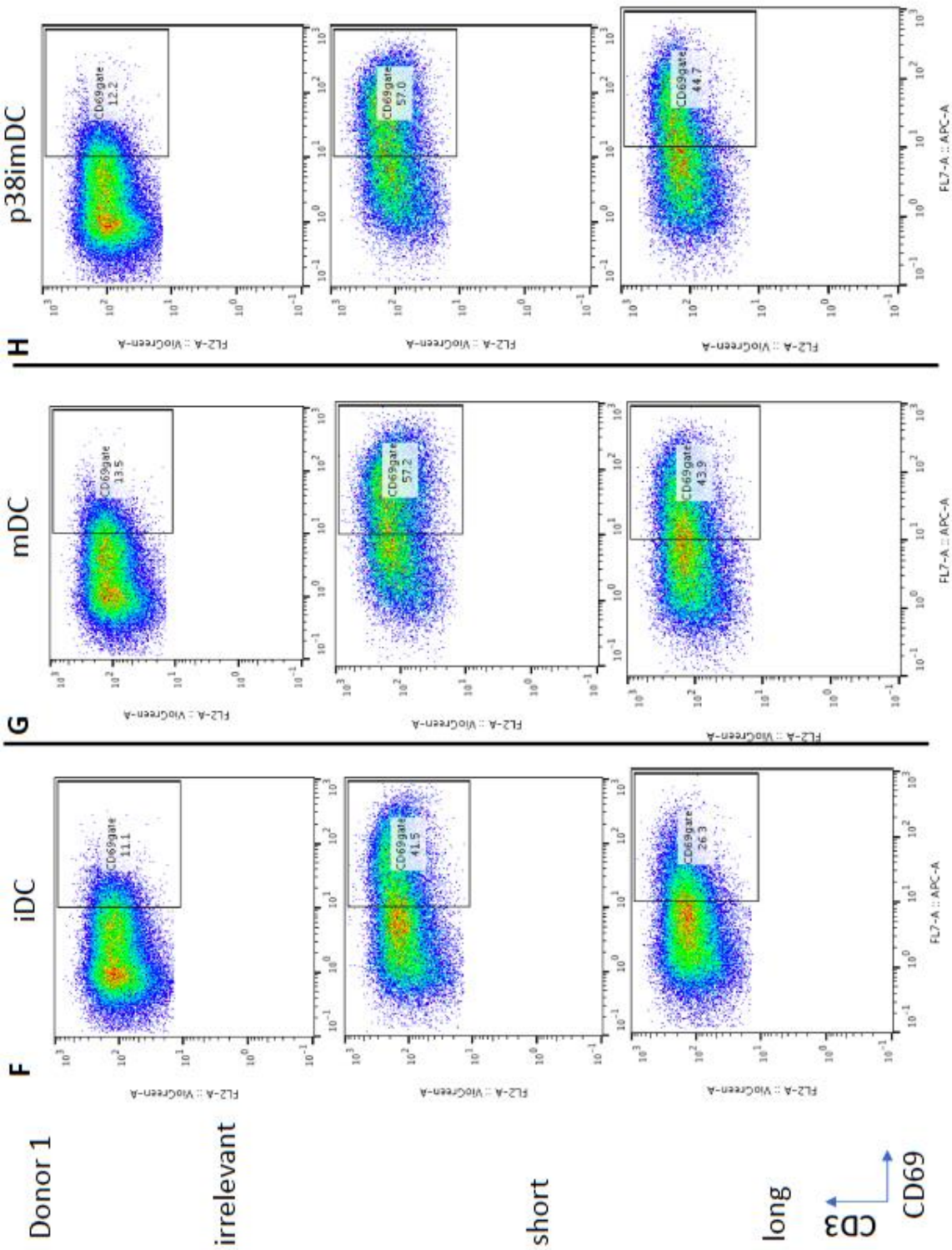

F
G
H
iDC
mDC
p38imDC
Donor 1
irrelevant
short
long
CD3
CD69
CD69gate 11.1
CD69gate 41.5
CD69gate 26.3
CD69gate 13.5
CD69gate 57.2
CD69gate 43.9
CD69gate 12.2
CD69gate 57.0
CD69gate 44.7
FL2-A :: VioGreen-A
FL7-A :: APC-A

Figure 3.9: Flow cytometry of transfected $gp100_{280-288}$ TCR on a Jurkat following co-culture with cDC2 +/- p38i and $gp100_{272-300}$ and $gp100_{280-288}$ peptides. The long ($gp100_{272-300}$) peptide was co-cultured with cDC2 +/- maturation +/- p38i. Successful processing of the $gp100_{272-300}$ to the short peptide led to activation of transfected $gp100_{280-288}$ TCR on a Jurkat. A $gp100_{280-288}$ peptide was used as a positive control and $gp100_{154-167}$ as a negative control (irrelevant peptide). (A) Shows forward (FSC) and side scatter (SSC) of the transfected jurkat cell line and (B) gating of live cells and doublet exclusion in (C). (D) shows the PE-control and PE-$gp100_{280-288}$ staining of Jurkat cell line showing approximately 70% successful transfection. CD3 and CD69 isotype control are also shown (E). A representative donor iDC (F), mDC (G) and p38i mDC (H) stimulated transfected Jurkats were stained for CD3 and CD69 after 24 hours. The activation was significantly higher in mDC and p38imDC stimulated transfected Jurkats, compared to iDC. PMA – Phorbol myristate acetate.

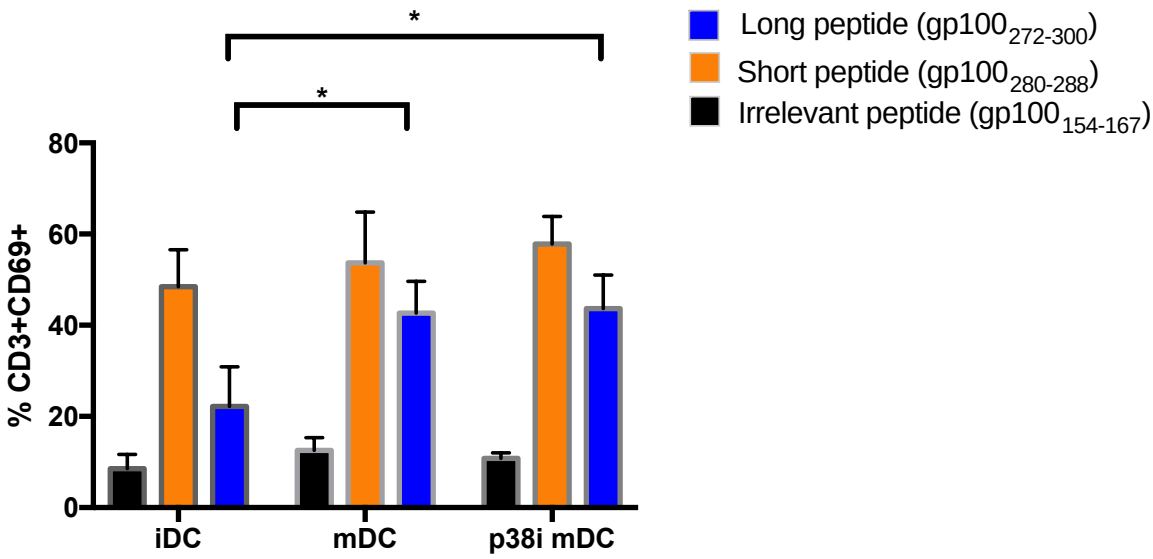


Figure 3.10: Cumulative analysis of 4 healthy donors' stimulation of transfected gp100$_{280-288}$ TCR-Jurkat cell line following co-culture of cDC2 and gp100 peptides. The irrelevant peptide (gp100$_{154-167}$) triggered low activation (8-12%) in all DC conditions as expected of a negative control. The short peptide (gp100$_{280-288}$) activated 49%,54% and 59% Jurkats, by iDC, mDC and p38i mDC respectively and was a positive control. The long peptide (gp100$_{272-300}$) was processed by both mDC and p38i mDC and activated significantly more Jurkats than iDC.

There was a significant increase in the percentage activated ($CD3^+CD69^+$) $gp100_{280-288}$-Jurkat cells by long peptide compared to irrelevant peptide activation for all DC conditions; iDC ($p=0.0233$), mDC ($p<0.0001$) and p38i mDC ($p<0.0001$). This proves the antigen specificity of the assay and that cDC2 can cross present antigens. Both mDC and p38i mDC were superior at cross presentation than iDC, as demonstrated by a significantly higher antigen-specific Jurkat activation seen (both $p<0.0001$). There was, no difference between mDC and p38i mDC of percentage activated $gp100_{280-288}$-Jurkat cells with long peptide stimulation, suggesting p38i does not interfere with cross-presentation ($p=0.9460$). The short peptide stimulation (positive control) of $gp100_{280-288}$-Jurkat cells was also similar between mDC and p38i ($p=0.3897$).

Enhanced p38i cDC2 are capable of inducing de-novo peptide-specific T-cell responses

A vital functional requirement of enhanced cDC2 is their ability to prime cytotoxic T-lymphocytes (CTL) responses. This is the most critical function of DC therapy in order to direct the immune system to recognise the tumour as foreign and reverse tumour-induced DC dysfunction.

Initially the optimum dose of peptide to pulse cDC2 remained to be determined. This was extrapolated by investigating the immune response to influenza matrix protein$_{58\text{-}66}$ (GILGFVFTL), known to be presented on HLA-A2. Two assays were performed with this intent, firstly peripheral blood mononuclear cells (PBMCs) were incubated with influenza peptide (5-100μg/ml) over 14 days with cytokine support (IL-2 and IL-7). At day 14 an ELISPOT was performed with titrating dose of influenza peptide (5, 15 or 50μg/ml) or an irrelevant HLA-A2 (EGFRvIII 15μg/ml). The results are shown below in figure 3.11. In these two donors the optimal pulsing peptide concentration was between a dose of 5-15 μg/ml to achieve a recall influenza response.

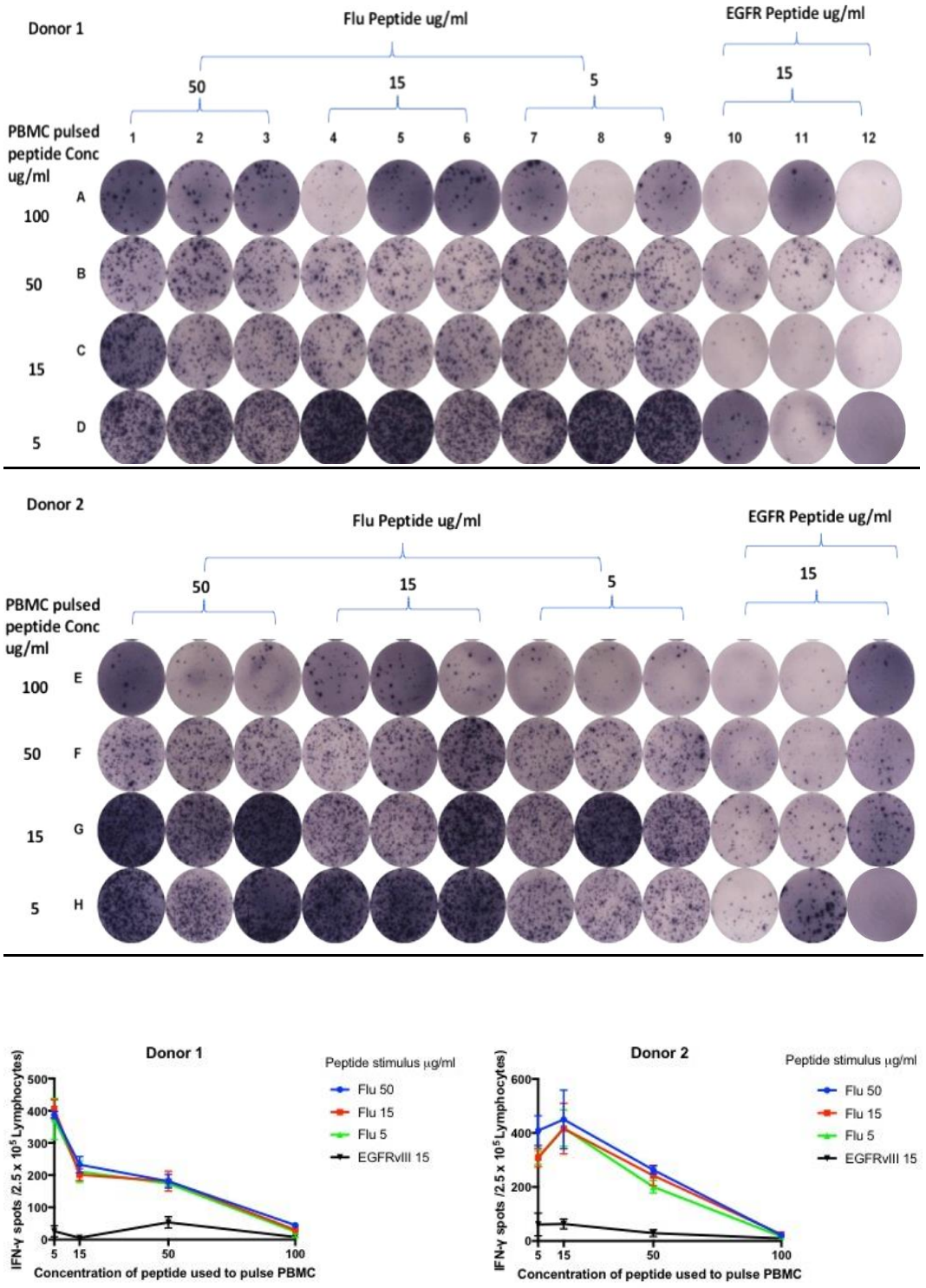
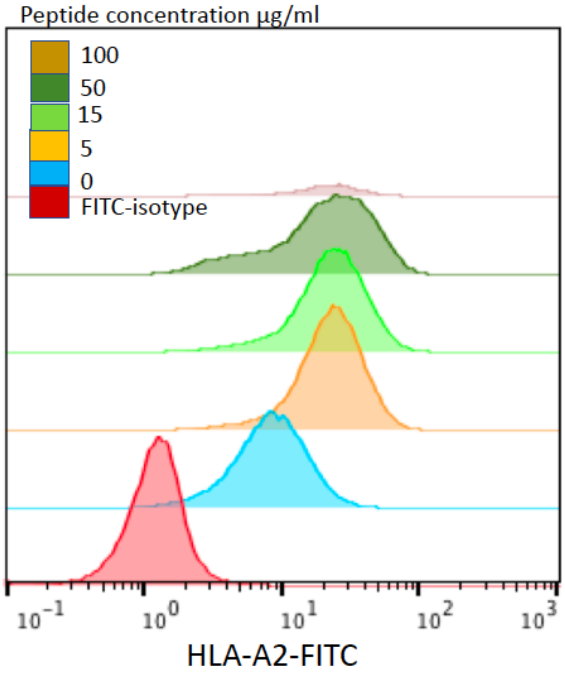
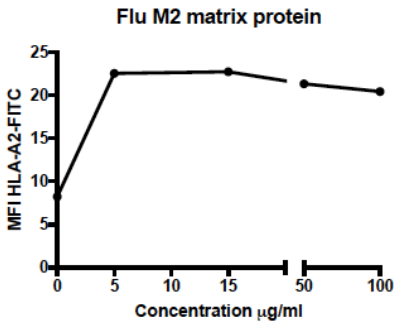


Figure 3.11 IFN-γ ELISPOT response from PBMC pulsed with influenza M2-matrix peptide. PBMC were isolated from 2 HLA-A2 healthy donors, pulsed with influenza matrix protein$_{58\text{-}66}$, IL-7 and IL-2 cytokines for 14 days. Peptide pulsing concentration (5-100μg/ml) is shown on y-axis and ELISPOT peptide concentration (5-50 μg/ml) on the x-axis. EGFRvIII peptide (15μg/ml) was used as a negative control. A graphical representation shows peak IFN-γ between 5-15μg/ml.

Secondly, a T2 cell line was also used to discover the optimum peptide dose. T2 cells are deficient in the peptide transporter associated with antigen processing (TAP) and therefore fails to present endogenously processed peptides. However, exogenous peptides, capable of binding to MHC class I, can bind in a non-competitive environment and form stable MHC-peptide complexes (255). Below are the results of T2 cells pulsed with influenza matrix protein$_{58\text{-}66}$ (GILGFVFTL) at 0-100 μg/ml peptide concentration. A HLA-A2-FITC antibody was then used to measure HLA-A2 expression by median fluorescence intensity (MFI). The higher the MFI, the greater the stable MHC-peptide complex. The highest MHC-peptide concentration was achieved by a dose 5μg/ml, while at the highest dose 100μg/ml, this seemed to be toxic to cells (figure 3.12).

Concluding from both the PBMC influenza peptide recall response and T2-peptide binding assay, we chose a peptide dose of 10μg/ml to carry forward to cDC2 peptide pulsing.





Influenza Peptide dose	HLA-A2-FITC MFI
Isotype	1.21
0.0	8.22
5.0	22.5
15.0	22.7
50.0	21.3
100.0	20.4

Figure 3.12. Staining of HLA-A2 in T2-influenza matrix protein$_{58\text{-}66}$. T2 cell-line is deficient in transporter associated with antigen processing (TAP) and therefore only makes stable MHC complexes with exogenous peptides. Pulsing of influenza matrix protein$_{58\text{-}66}$ with T2-cells shows maximum presentation from 5µg/ml of peptide. Increasing the peptide concentration makes no difference to MFI. At 100 µg/ml peptide, there was less viable cells hence the lower area under the curve.

cDC2 peptide pulsing to achieve a naïve CTL response in healthy donors

With the view of comparing p38i cDC2 and matured cDC2, three healthy donors' cDC2 were isolated, rested, and then treated with or without p38i and matured overnight with dual TLR agonists (R848 and Poly:IC). After 24 hours DC were washed with serum free media and pulsed with peptide at 10μg/ml for 4 hours. Following which, cells were then washed and re-plated in a 24 well plate with autologous PBL, which had been rested overnight. DC: PBL ratio was 1:50. The peptides EGFRvIII, TRP-2 and influenza matrix protein were used to pulse cDC2. EGFRvIII is the most common known neo-antigen shared in approximately 25-30% of GBM patients (256). Neoantigens have the potential to trigger strong immune responses if able to be presented by host MHC, since there should be no prior host negative selection during central tolerance (257). In a single centre study, EGFRvIII was thought to be presented on HLA-A2 (258).

TRP-2 is also a tumour associated antigen, which is known to be overexpressed in two-thirds of glioblastoma patients, presented on HLA-A2 and immunogenic (259). Influenza matrix protein is also presented on HLA-A2 and should trigger a recall response in almost every individual and therefore a positive control.

Peptide specific responses were achieved in all three donors as shown in figure 3.13. In all 3 donors, there was a clear increase in the IFN-γ producing lymphocytes re-stimulated with the peptide of interest in the ELISPOT, compared to the irrelevant peptide. However, this was inconsistent between donors. All three donors showed a negligible response to EGFRvIII presented by mDC or p38i cDC2. In the T2 assay aforementioned, EGFRvIII, did not form a stable complex with HLA-A2, casting doubt whether this neoantigens is truly presented by HLA-A2 (data not shown).

Donor 1's cDC2 pulsed with TRP-2 resulted in no CTL response, however there was a robust response with p38i cDC2-TRP-2 pulsing. The flu responses were greater in the mDC stimulated lymphocytes in this donor. In donor 2, there was a strong response to flu in the p38i cDC2 stimulated cells, however the mDC gave a better generation TRP-2 specific CTL. Finally, in donor 3 the generation of flu and TRP-2 specific CTLs were greater in lymphocytes stimulated with p38i cDC2 compared to mDC.

Overall the TRP-2 peptide was able to elicit an immunogenic response in all three donors when presented with cDC2 (either mDC or p38i mDC). In 2/3 of the donors this response was superior in the p38i cDC2 population.

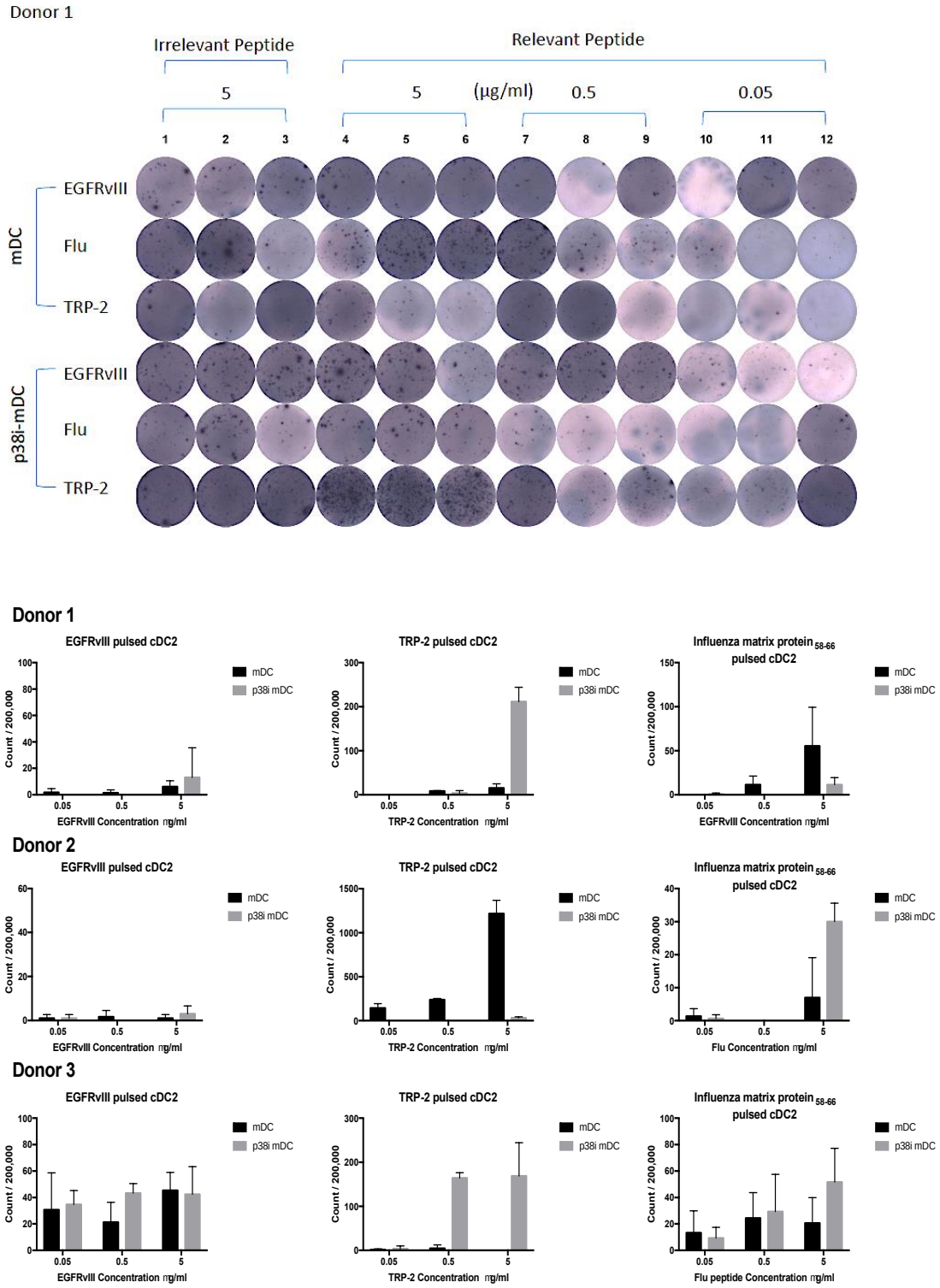


Figure 3.13: cDC2 can present tumour-associated antigens to autologous PBL and trigger de-novo CTL response. cDC2 were matured with or without p38i. Following overnight incubation they were washed and pulsed with either TRP-2, EGFRvIII or influenza matrix protein$_{58\text{-}66}$. IL-7 (day1 and every 7 days) and IL-2 (day 3, 7 and every 7 days) were added to support CTL expansion. A peptide boost was added on day 7 and 14. An IFN-γ ELISPOT was performed at day 21 to assess response. (Top) shows an ELISPOT plate from a representative donor, while below shows the summary of peptide response from the 3 donors.

Discussion

DC are pivotal to orchestrating the immune response (125). However, GBM induces DC dysfunction through a variety of mechanism including IL-10 and transforming growth factor-beta (TGF-β), and catabolites, including indoleamine 2,3-dioxygenase (IDO) (202, 242). We have demonstrated that DC dysfunction occurs through both tumour-related factors and Dex exposure both in-vivo, by our flow-cytometry data on circulating DC phenotype and function and in-vitro with MoDC and cDC2 co-culture experiments.

Although, DC vaccines have shown some efficacy in clinical trials to date, the autologous harvesting of patient DC which are dysfunctional at outset, likely contributes to limited efficacy. The ex-vivo maturation with TLR agonists and tumour antigen associated education greatly improves antigen presentation, however, further mechanisms to reverse immunosuppression and enhance DC function do not exist. Such compromised DC functions include poor migration, low cytokine secretion and expression of co-stimulatory proteins. Here, we demonstrate the inhibition of the p38 MAPK pathway in cDC2 reverses both tumour- and Dex-induced DC dysfunction.

Firstly, we confirmed that the p38i BIRB0796, is active at 1μM concentration as used by our group previously (139). After 30 minutes, the downstream protein MK2 is no longer phosphorylated confirming inhibition in the pathway (figure 1).
The effect of p38i on cDC2 is of particular interest since these are the DC of choice in the next generation of vaccines (159).

The phenotype of p38i matured DC were studied in comparison to steady state matured DC from healthy individuals. Remarkably, an increase in the expression of co-stimulation molecules was seen, such as a six-fold increase in CD86 and two-fold increase in CD80. The co-stimulation axis is vital for anti-tumour T-cell responses and indeed both cytotoxic T-lymphocyte associated

protein-4 (CTLA-4) and programme death-1 inhibitor antagonist inhibitors which have revolutionised cancer treatment, principally modify these signals (260, 261). The MHC-peptide receptor complex is not, on its own, sufficient to activate a naive T- or B-cell. The co-stimulation provided by DC expressed CD80 and CD86 to CD28 on naïve CD4 and CD8 T-cells are essential for T-cell priming, growth, and development of memory function (262, 263). Indeed, expression of CD86 is expressed constitutively low on all antigen presenting cells and upregulated during infection or cellular stress and provides one form of modulation regulating activation against self-antigens (264). Therefore, as demonstrated in chapter 1 the significantly lower expression of CD86 on patient cDC2 is not surprising and may limit T-cell responses induced by patient DC. Hence this six-fold upregulation in expression could be predicted to improve T-cell priming of tumour associate antigens.

There was also a seven-fold increase in p38i matured cDC2 in CD40 expression. While naive T cells primarily utilize CD28 as the co-stimulatory receptor, naive B cells use the TNF receptor family member CD40. Indeed, the initiation and progression of both the cellular and humoral adaptive immune response are dependent on CD40-CD40L ligation (265). Furthermore, CD40 expressed on an activated 'exhausted' DC can bind to CD40L on an activated T-cell and can provide a second surge in IL-12 (266, 267). This is likely a significant mechanism for Th1 priming in-vivo of DC vaccines given the ex-vivo maturation of DC is now standard of care due to superior migration of matured DC (268). Hence, a second cytokine surge in-vivo on CD40-DC40L ligation is key. In a mouse model of an immunologically cold tumour, pancreatic adenocarcinoma, a single dose of CD40 antibody agonist lead to clonal expansion of T-cells and is developing a therapeutic interest (269). DC-SIGN (CD209) was also upregulated 7-fold higher. This is a vital c-lectin integral to viral and tumour antigen capture and processing by DC (270). There was also a significant decrease in PD-L1 expression which is a negative regulator of CTL responses. The role of tumour myeloid compartment PD-L1 on macrophages and DC has recently been described as predictive of response to PD-1 immunotherapy, emphasising it role in effector tumour

immunity as a negative regulator (271). Indeed, blockade of PD-L1 with monoclonal antibodies on MoDC increases T-cell activation and T-cell cytokine secretion (272). There was a significant decrease in CD83 expression, which although is commonly used as a DC activation marker, its role in the function of DC remains unclear and its soluble extracellular component has been described a negative regulator of DC:T-cell activation (273, 274).

In chapter 2 we modelled the poor IL-12 secretion from patient-derived DC by co-culture of cDC2 and MoDC with Dex and U87 cell line-derived tumour lysate (TDL). We also discussed the importance of signal 3 at directing the phenotype of T-cells at priming and activation, whereby an IL-12 rich cytokine environment would support a Th1 and CTL expansion against the presented peptide (198). Here, we show that p38i matured cDC2 reverses Dex and TL- induced IL-12 suppression. Furthermore, the immunosuppressive cytokine, IL-10 was further quenched and thereby the ratio of IL-12:IL-10 at the DC:T-cell synapse was greatly skewed in favour of Th1 priming. This was supported by the resultant MLR between p38i Dex- or TDL-exposed cDC2 and allogeneic PBL, whereby the resultant supernatant after 5 days of proliferation, was rich in IFN-γ. The IFN-γ production was greater than mDC controls without exposure to Dex and TDL, emphasising the success of p38i at enhancing the cDC2. The allo-stimulatory was also restored by p38i of Dex- and TDL- co-cultured DC and was superior than control mDC. The combination of phenotypical (co-stimulatory molecule) and functional improvement identify p38i as an important adjuvant to signal 2 and 3 of T-cell priming and activation.

We next set to investigate whether migration of cDC2 was affected by p38i. Early MoDC vaccines identified that the maturation status of the DC was critical, with mDC migrating 10-fold more than iDC counterparts. Furthermore, only mDC migrated to multiple lymph nodes (268). This is thought at least partly due to maturation status determining upregulating the chemokine receptor CCR7 which is critical for DC migration to lymph node

areas (253, 275). However, studies comparing intradermal and intranodal injection concluded that equal numbers of CTL were measured by both routes, despite maximally only 4% of intradermal injected DC reaching lymph node areas when measured by in-vivo scintigraphy imaging through DC labelling with indium and superparamagnetic iron oxide (276). There is no clear consensus on the best route of vaccine administration in GBM trials with intradermal, intravenous, intracranial routes having all been trialled (195, 277). The canonical view is that DC migration is dependent on CCR7 chemokine expression dependent migration towards both CCL19 and CCL21 gradients. Hence, we investigated the migration of DC towards CCL21 since this chemokine is adequate in the absence of CCL19 to induce DC migration and used in recent publications investigating cDC2 migration (189, 254, 278). We found that p38i mDC were significantly superior at migration than iDC and mDC. However, this was independent of CCR7 expression, since expression was lower in p38i mDC than mDC. Therefore the mechanism of this superior effect is currently unknown and the subject of current investigation in our laboratory. Recently, Van Rijn et al, described a GPI-anchored protein, semaphorin 7A, which is highly expressed on activated cDC2 and vital for adhesion strength to the extracellular matrix and actin cytoskeleton organisation (278). Both $Sem7A^{-/-}$ mice and siRNA deficient Sem7A DC ex-vivo showed impaired migration to CCL21, without altering CCR7 expression (278). It is therefore clear that CCR7 alone is insufficient to explain DC migration success to lymph node areas. Indeed, CCR7 expression alone is insufficient for DC migration and requires inflammatory signals such as prostaglandin E2, leukotriene C4 transporter MRP1 and CD38 to sensitise CCR7 to its ligands (279). The mechanism by which these mediators alter CCR7 is not known (279). More recently, an important role of lysosome signaling via TFEB-TRPML1 axis, activated following microbial sensing during micropinocytosis, is required for DC chemotaxis to lymph nodes (280). It must also be noted that much of the DC migration studies have mainly investigated MoDC and skin-associated DC migration and therefore, much needs to be learnt in regards to DC mechanism of migration, particularly cDC2 (279).

We next set to investigate antigen presentation by p38i cDC2. As previously discussed, the goal of DC vaccines is to provide antigen recognition of the cancer associated peptides. DC vaccines are hypothesised to be superior to peptide-based vaccine strategies since they simultaneously provide the peptide and also the accompanying physiological co-stimulation and cytokine instruction for an appropriate adaptive immune response. We have shown we can improve signal 2 and 3 and therefore set to demonstrate that p38i cDC2 can still present peptides without detriment. The assay used gp100 TCR-transfected Jurkat cell line (E6.1 fl296) developed by our collaborators which is activated by $gp100_{280-288}$ peptide (186). The $gp100_{272-300}$ long peptide was then used to test whether DC could process and cross present the long peptide into $gp100_{280-288}$ epitope and thus activate the antigen specific Jurkat cell line. The readout was the early activation ($CD69^+$ expression). It is important to note that the simultaneous timing of long peptide addition with TLR agonists to DC, since antigen uptake and processing can only occur in the immature state. Therefore, the addition of the peptide with the TLR agonists, allowed enough antigen processing time. This is also supported by the superior short peptide activation by mDC and p38i cDC2, compared to iDC suggesting better stimulatory capacity of these DC. In this assay p38i cDC2 were not superior to mDC, despite previously showing enhanced activation of lymphocytes in MLR assays. This may be because Jurkats are an acute lymphoblastic leukaemia cell line and are partially activated and less dependent on the B7-CD28 co-stimulation pathway, than endogenous lymphocytes. In this scenario, a transfected autologous CD8 responder may be superior to Jurkats to represent the in-vivo activation. However, our main objective was reached to show that p38i mDC could cross present antigens and this is equal to mDC. This assay also confirmed that human cDC2 cross present antigens and that this is not a unique feature of cDC1 (141, 149, 156).

Furthermore, we were able to show that cDC2 could induce and expand antigen-specific de-novo T-cell responses when co-cultured with peptides and

autologous PBL. The EGFRvIII responses were poor, which is disappointing given this is a neo-antigen. However, the work on EGFRvIII peptide been restricted to HLA-A2 has not been completely established. One group identified through predictive peptide software that a number of peptide sequences from EGFRvIII peptide could evoke a HLA-A2 response particularly LEEKKGNYV sequence (258). However, in a phase II peptide vaccine trial using the 13 amino acid EGFRvIII created by an in-frame deletion, like that used in this assay (LEEKKGNYVVTDHC), no correlation was found between HLA type and progression-free and overall survival (256). Indeed, a phase III EGFRvIII-peptide vaccine trial recruiting 745 GBM patients failed to show a survival advantage above standard treatment (281). A more well established tumour associated antigen TRP-2, however consistently produced a dose dependent expansion of CTL response on ELISPOT. In 2/3 donors the TRP-2 response was greater in p38i mDC. The influenza control responses were not as marked as expected. Indeed this was weaker in all 3 donors than we had seen in our PBMC recall response assay (figure 3.11). Therefore, this assay still requires further optimisation before conclusion in regard to the superiority of mDC or p38i mDC at inducing de-novo T-cell responses. Ideally, instead of re-stimulating with peptide only, a cDC2-peptide re-stimulation may increase expansion and reduce background levels of non-specific IFN-γ activation. A tetramer to monitor response would likely help guide optimum expansion, however, this significantly increases the cost of the assay.

With further optimisation the target would be for 6 tumour associated antigens to be pulsed in combination, such as HER2, TRP-2, gp100, MAGE-1, IL13Ra2, and AIM-2 used by Phuphanich and Wheeler et al in a MoDC vaccine trial. The rationale here is that, in pre-clinical studies of GBM fresh frozen tumour samples, at least three peptides was expressed by all GBM tumours and 75% expressing all six (282, 283). The group also rationalized that these epitopes are reported to be overexpressed on glioma stem cells, seen as a driver of therapy resistance and relapse to multimodal treatment (284). They supported this by demonstrating a loss of tumour $CD133^+$ cells in relapsed

tumour specimens compared to pre-vaccine samples, where tumour samples were available on relapse (282). By targeting multiple epitopes, the hope is to have a consistent antigen loading material, at reduced cost of manufacture and negating the need for autologous tumour material. Furthermore, it creates an increased chance of a tumour-antigen specific response, with resultant epitope spreading and avoiding epitope escape by targeting a single antigen.

Overall in this chapter we have shown p38i cDC2 have improved co-stimulation expression, IL-12:IL-10 ratio, migration to CCL21 gradient and are capable of antigen cross presentation. Therefore, p38i are a promising adjunct for the next generation of cDC2 vaccine therapy.

Results: Chapter 4 - Enhanced p38 MAPK inhibited cDC2 is a novel immunotherapy strategy to restore cytokine dysfunction in GBM patients

Introduction

We described in chapter 1 a number of quantitative and functional deficits in circulating DC from GBM patients. This included reduced numbers of cDC2 and pDC. The cDC2 population had significantly lower HLA-DR, CD86 and PD-L1 expression than healthy controls. Both Dex and residual disease were associated with lower numbers. We also found in a cohort of 6 patients, that IL-12 and IL-10 cytokine secretion was significantly reduced. This was modelled in-vitro in chapter 2 and shown to be induced by both tumour-derived factors and Dex exposure. In chapter 3 we were able to reverse tumour-derived lysate and Dex induced IL-12 cytokine suppression in healthy donors using p38 MAPK inhibition and to skew the IL-12:IL-10 ratio towards Th1 polarisation.

We therefore wanted to test the reversibility of IL-12 suppression in our patients with GBM. We did a comparison between MoDC and cDC2 in both healthy controls and patients. We focussed on the cohort of 6 GBM patients analysed in chapter 1.

Results

MoDC and cDC2 in healthy volunteers produce equivalent levels of IL-12, but cDC2 produce less IL-10. Overall IL-12:10 favours cDC2

As before, 100ml of blood was used to isolate cDC2, which were then rested in media and GM-CSF for 1 hr prior to maturation with TLR agonists (PolyI:C and R848). Monocytes were also isolated and differentiated to make MoDC as previously described. Cytokines were analysed by ELISA after 24 hrs from maturation.

5 of the 9 healthy volunteers' IL-12 secretion was higher from MoDC, whereas the other 4 were higher in the cDC2 subset. The range of IL-12 from healthy MoDC was large between 174.4 – 272149.2 pg/ml and a median of 18930.0 pg/ml (IQR 3891.0-121251.0 pg/ml). In comparison, the range of IL-12 from healthy control derived cDC2 was 316.9 – 84495.0 pg/ml and a median of 19219.0 pg/ml (IQR 4246.0-48547.0 pg/ml). Wilcoxon statistical test for paired, non-parametric analysis, showed there was no significance difference between MoDC and cDC2 IL-12 secretion from healthy controls (p=0.734, figure 4.1A).

There were, however, differences seen in the healthy population between MoDC and cDC2 IL-10 secretion. The range in IL-10 secretion from MoDC was 57.2-6551.0 pg/ml compared 46.3-567.8 pg/ml from cDC2. The median IL-10 secretion from MoDC was 457.0 (IQR 130.8-3241.0) pg/ml which was significantly higher than cDC2 (median 94.27 IQR 64.9-308.2 pg/ml; p=0.0391, figure 4.1B).

Given the large physiological range in both IL-12 and IL-10 secretion in healthy control DC, the relative abundance of cytokines may be more important than the absolute value. We therefore, compared the relative IL-12:IL-10 secretion (figure 4.1C). The highest ratio of IL-12:IL-10 was seen in the cDC2 control population. The median IL-12:IL-10 ratio in cDC2 population was 130.6

compared to 31.2 in the MoDC subset (p=0.039), indicating a 4-fold greater polarisation favouring IL-12.

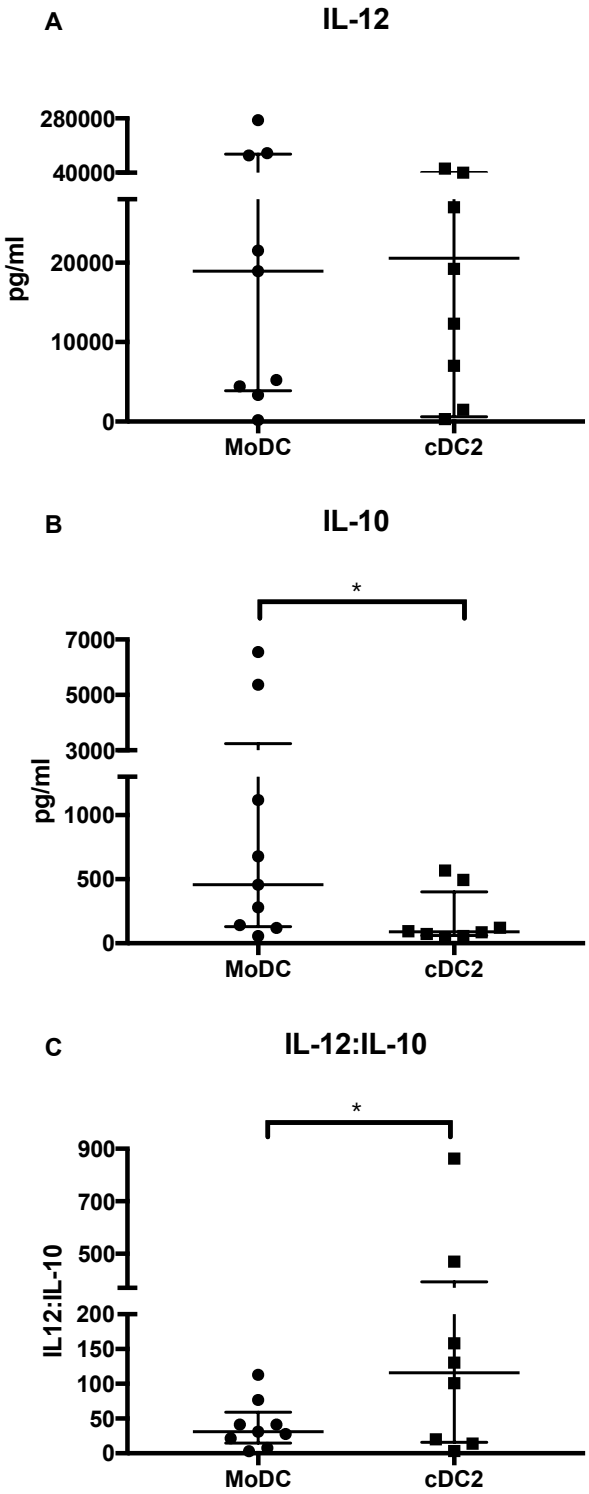


Figure 4.1. MoDC and cDC2 from healthy adults secrete similar IL-12, lower IL-10 and overall higher IL-12:IL-10 from cDC2. MoDC and cDC2 were isolated from 9 healthy volunteers. Following maturation with TLR dual agonists (R848 and PolyI:C), cytokines were measure by ELISA. (A) IL-12 levels were similar between MoDC and cDC2, whereas IL-10 was lower from the cDC2 subset (B). Overall the ratio of IL-12:IL-10 favoured the cDC2 subset for Th1 polarisation (C).

GBM patients produce low levels of IL-12 from MoDC and cDC2. cDC2 showed marked IL-12 and IL-10 suppression

The 6 GBM patients whom cDC2 secreted suppressed IL-12 levels previously described were compared to MoDC derived from the same patient. These patients were all undergoing first-line treatment with either radiotherapy (1 patient), chemoradiotherapy (4 patients) or adjuvant Temozolomide.

The range in IL-12 secretion from patient-derived MoDC was 60.1-7336.0 and greater than cDC2 subset which was 2.2-1250 pg/ml. The median IL-12 in MoDC was higher than cDC2, median 1454.0 (IQR 371.8-3639.0) pg/ml compared to 321.1 (IQR 76.1-795.0) in the cDC2 subset, although not statistically significant (p=0.219, figure 4.2A).

A comparison between the patients-derived MoDC and cDC2 populations showed MoDC secreted more IL-10 (median 194.1 pg/ml, IQR 51.9-513.9) than the cDC2 subset at 41.13 pg/ml (IQR 33.3-155.5 pg/ml), although not statistically significant (p=0.240, figure 4.2B).

Overall, there was comparable secretion of IL-12 and IL-10 between patient derived MoDC and cDC2, which was supported by similar IL-12:IL-10 ratio. The median was 6.7 (IQR 1.6-23.3) in MoDC compared to 3.4 (IQR 1.6-13.5) in the cDC2 subset (p>0.999; figure 4.2C).

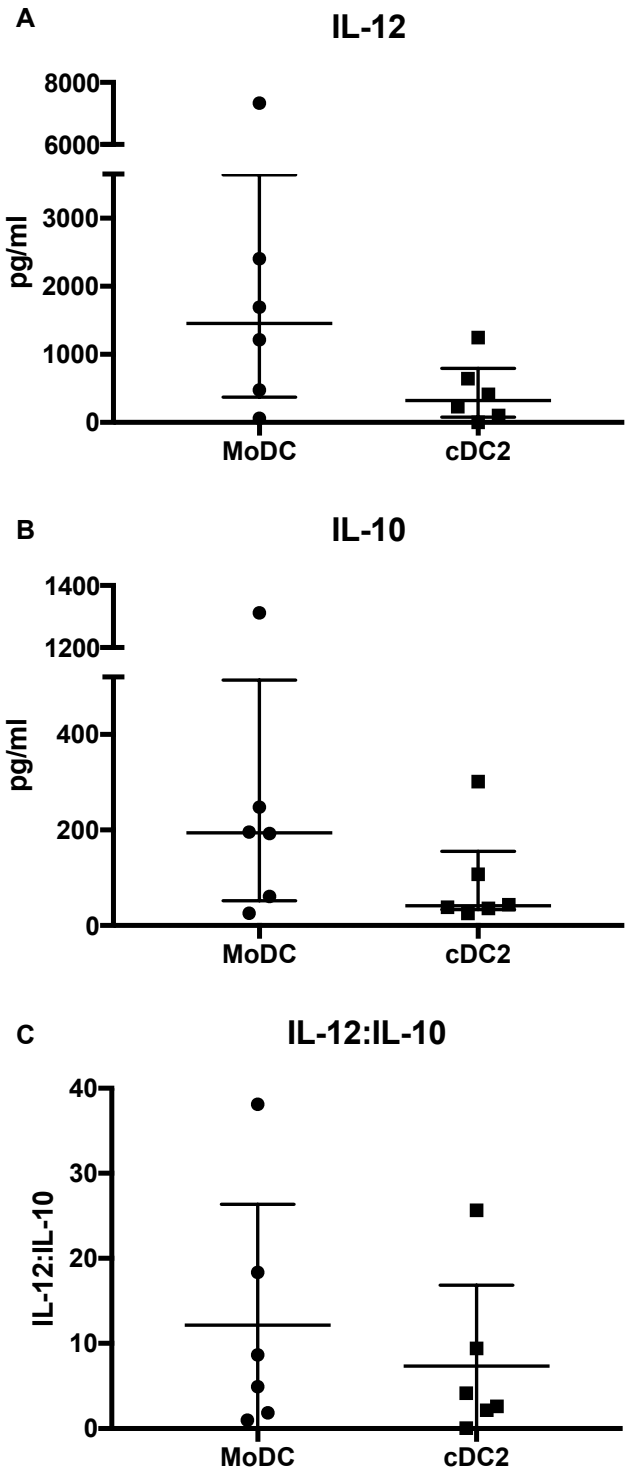


Figure 4.2. Patient-derived MoDC and cDC2 secrete similar IL-12 and IL-10. MoDC and cDC2 were isolated from 6 GBM patients. Following maturation with TLR dual agonists (R848 and PolyI:C), cytokines were measure by ELISA. (A) IL-12 levels were higher MoDC compared to cDC2, whereas IL-10 was lower (B). However, neither reached statistical significance (p=0.219 and p=0.313 respectively). Overall the ratio of IL-12:IL-10 was similar (C).

Patient-derived p38i cDC2 show increased IL-12 levels and ablated IL-10 . The ratio is similar to healthy controls' cDC2.

The addition of p38i 1hr prior to maturation with TLR agonists (R848 and PolyI:C) ex-vivo, significantly increased IL-12 in the cDC2 subset, from a median of 321.9 to 920.6 pg/ml (p=0.031, figure 4.3A). This was comparable to the patient MoDC IL-12 secretion level (p=0.818) however, significantly lower than that seen from both healthy controls cDC2 and MoDC (p=0.018 and p=0.012 respectively; figure 4.3B).

The cDC2 IL-10 secreted from patients-derived cells had a trend towards lower secretion compared to healthy controls (median 41.1 compared to 90.6 pg/ml, p=0.107, figure 4.2D).
Furthermore, with p38i prior to maturation, IL-10 levels were ablated to a median 35.5 pg/ml (IQR 16.2-56.4 pg/ml, figure 4.3C). This was significantly lower compared to control cDC2 (p=0.012), control MoDC (p<0.001) and patient-derived MoDC (p=0.041; figure 4.3D).

In both the patient MoDC (p=0.029) and cDC2 (p=0.013) subset the IL-12:IL-10 was significantly lower, than in the control cDC2 population, indicating a shift away from Th1 population. However, since there was a significant increase in IL-12 and decrease in IL-10, this restored the balance of IL-12:IL-10 to comparable levels of control cDC2 (p=0.529; figure 4.3E&F).

Overall, although p38i improved IL-12 secretion in patient-derived cDC2 consistent with our results in healthy volunteers, the absolute IL-12 secretion remained significantly lower. However, the balance of IL-12:IL-10 from patient-derived p38i cDC2 was comparable to healthy control cDC2, mainly due to the ablation of IL-10. In this context, signal 3 is restored to healthy levels.

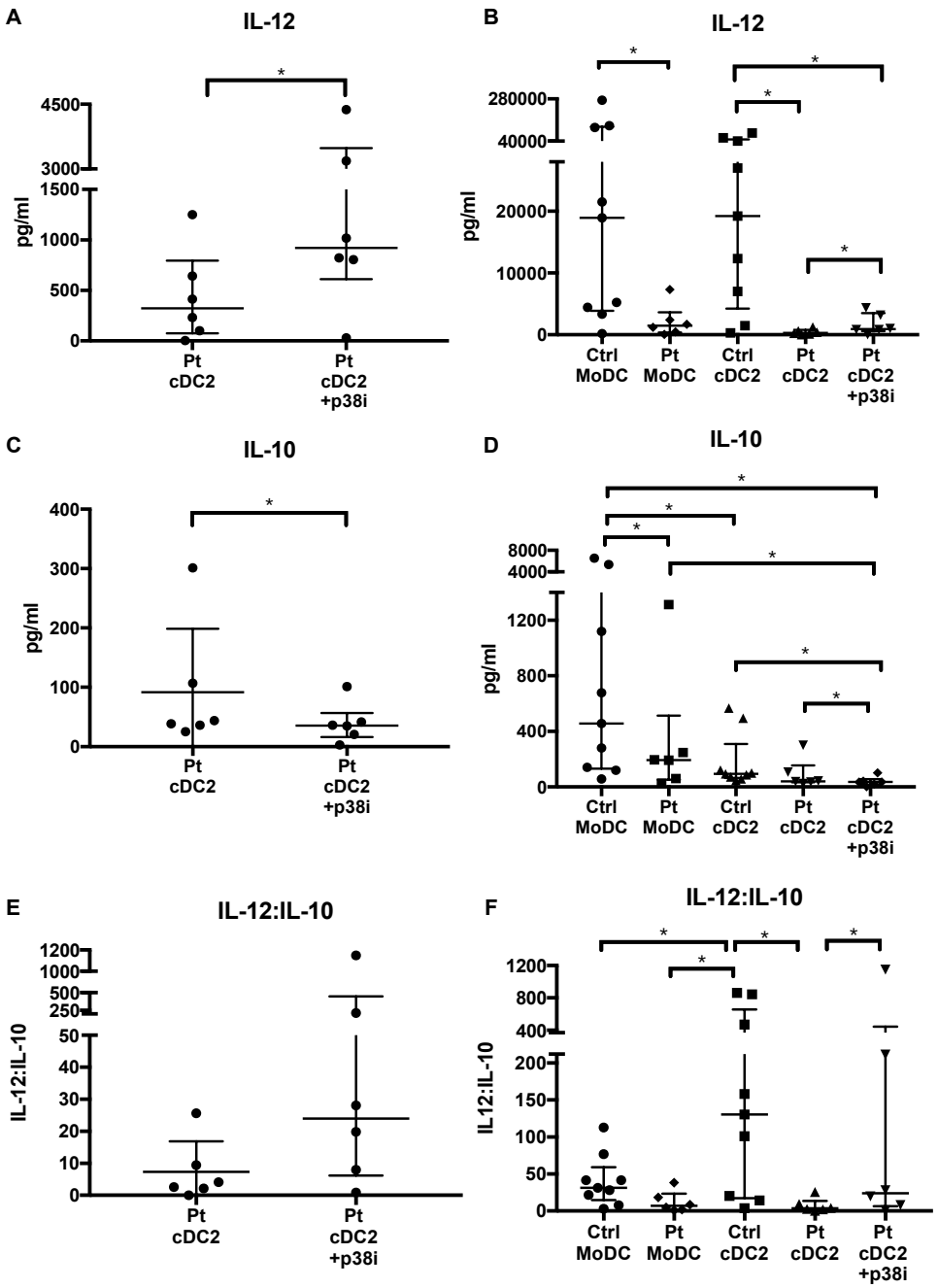


Figure 4.3 Comparisons between the IL-12 secretion from MoDC, cDC2 and p38i-cDC2 from GBM patients and healthy controls. MoDC and cDC2 from healthy volunteers were isolated and treated as above. The patient-derived cDC2 subset were also treated with p38i. Cytokines were measured after 24 hours from maturation by ELISA. (A) The IL-12 secretion was significantly increased by p38i addition to patient-derived cDC2. However, IL-12 levels still remained significantly lower than healthy control MoDC and cDC2 levels (B). (C) Patient-derived cDC2 IL-10 was significantly suppressed with p38i and was lower compared to healthy control DC subsets and patient MoDC (D). The IL-12:IL-10 ratio in patient-derived cDC2 was higher following p38i and this was comparable to healthy control cDC2 ratios.*$p<0.05$; Pt= patient; Ctrl= Controls

Discussion

In chapter 3 we showed that p38i cDC2 could increase IL-12 secretion significantly in healthy controls and, furthermore, reverse the IL-12 suppression induced by Dex and tumour lysate. A decrease in IL-10 was also seen.

Here, in an in-depth analysis of both GBM patient-derived MoDC and cDC2, we were able to show that both DC subsets have suppressed IL-12 and IL-10 secretion. We discussed in chapter 2, the importance of signal 3 to determine T-cell fate (198). IL-12 secreted from DC has been shown to drive Th1 responses, whereas IL-10 is directly inhibitory to this signal and can induce T-cell anergy, hence we focussed our analysis on these two cytokines (201, 237). Indeed, the IL-12 secretion from cDC2 was at the limits of detection. However, the addition of p38i, prior to maturation significantly improve IL-12, but not back to levels seen in controls. Nevertheless, the secretion of IL-10 in p38i enhanced cDC2 was effectively ablated. Therefore, when comparing IL-12:IL-10 ratios in p38i cDC2 from GBM patients to healthy donors, IL-12:IL-10 ratios were restored.
The data shown here both highlights the immune dysfunction of both DC subsets in GBM patients, however the use of p38i as a vaccine adjunct is supported.

The fate of Th1 cells has long been shown to be driven by T-bet upregulation which is dependent on IFN-γ and signal transducer and activator of transcription (STAT)-1, at activation. T-bet then upregulates IL-12Rß2 and thereby gains sustained reliance on IL-12 to maintain differentiation, through STAT-4 pathway (285, 286). IL-12 also represses GATA3 transcription factor facilitating T-bet dominance and Th1 polarization (287). Thereby IFN-γ and IL-12 are both essential cytokines for Th1 differentiation.

What is unknown in immunology is whether there is a minimum threshold of IL-12 required to orchestrate a Th1 response. This is unlikely to be dependent on a single variable, such as IL-12, given that the initial T-cell priming of antigenic presentation on MHC to the T-cell receptor and co-stimulation thresholds need to be adequate in the first instance. These signals are also not static and therefore difficult to capture this process over time. This is highlighted by the fact T-cell activation occurs hours after TCR signalling implying either a threshold of magnitude or duration of signal are required (288). Indeed, the number of triggered TCRs were shown to determine a threshold after which IFN-γ and proliferation could occur by Viola et al in 1996 (289). They used three different ligand complex systems - toxic shock syndrome toxin, MHC specific peptide complex and anti-CD3 - to stimulate T-cells and found approximately 8000 TCR were required to be triggered for an IFN-γ response. This was lowered to 1500 TCRs when ligation of CD28 by B7 molecules on antigen presenting cells provided co-stimulation (289). More recently, Au-Yeung et al, used a fluorescent reporter gene that was activated by TCR stimulation, to determine the threshold for proliferation. Using a transgenic mouse containing the Nur77–eGFP transgene, antigen signal strength was measured by GFP expression. Furthermore, they created an engineered mutant zeta-chain associated protein (Zap70) which they could modify by titrating a selecting kinase inhibitor and thus modifying the TCR downstream signaling. They thereby showed that a sharp signal through the TCR could activate proliferation and was independent of the magnitude of antigenic stimulation. Furthermore, the addition of IL-2 did not change this threshold. They therefore concluded that short and sharp stimulation is all that is required for proliferation (288).

Further demonstrating the sensitivity of MHC-peptide:TCR ligation, another group used a single molecule imaging quantum dot-labelling technique to identify that a single MHC:peptide complex can trigger detectable increases in intracellular CD4 calcium concentration and subsequent IL-2 and TNF-α production (290). The cytokine milieu, such as IL-12 threshold has yet to be

determined in priming, however it has a number of roles in both CD4 and CD8 T-cell responses. In an OT-1 DC-OVA mouse model the addition of Listeria and lymphocytic choriomeningitis virus, which secrete multiple inflammatory cytokines, was used to study the effects of cytokines, in the presence of stable antigen load. Through a series of experiments, they found pro-inflammatory cytokines improved CD8 cytotoxicity and antigen clearance. Furthermore, in an IL-12 KO mice responding to OT-1 DC-OVA and listeria infection, antigen sensitivity was reduced, emphasising the role of IL-12 in the CD8 directed response (291). In another study which used a series of adoptive transfer of functionally differentiated or memory CD4 responding to Listeria, IL-12 was shown to change the functional avidity when the antigen was re-challenged (292). Thereby demonstrating that IL-12 modifies the secondary effector T-cell response.

In addition to changing the sensitivity of the TCR, earlier studies of gene expression profiles of CD8 activation during a 3-day interval, showed that IL-12, maintained a 350 gene profile initiated by signal 1 and 2. Without IL-12 this gene expression profile returned to baseline within 72 hours. A histone deacetylase inhibitor could mimic this effect, hence suggesting that IL-12 allowed sustained expression of a number of genes in CD8 activation through, at least part, chromatin remodelling (293).

Our results show that by adding p38i at maturation to patient-derived cDC2, we increase IL-12 secretion and return the balance of IL-12:IL-10 to physiological levels. This analysis is limited by the 2-cytokine analysis of the cytokine milieu, when a broader spectrum of cytokines may be present at the DC:T-cell synapse. While acknowledging this limitation, the low absolute IL-12 secretion from patient-derived cDC2 even after p38i enhancement, may be a concern. Clearly there are a number of variables determining T-cell activation and fate and we feel the rescue of some IL-12 is of significance.

Of course, the complexity of T-cell fate does not stop at the lymph node and CD4 cells have increasingly been shown to be plastic in phenotype and function, including Th1 cells (294). A good example is from Liu et al, whom were studying the role of CD4 cells in autoimmune mouse models of inflammatory bowel disease (295). They used IFN-$\gamma^{Thy1.1}$ CBir1TCR Tg reporter mice, whose TCRs are specific for an intestinal microbiota antigen, CBir1 flagellin. By using adoptive transfer of these mice Th1 specific CD4 into $Rag^{-/-}$ mice, they were able to recapitulate autoimmune colitis. On sacrificing the animals and performing immunohistochemistry and flow cytometry of cells they were able to establish that the previous pure CD4 IFN-γ^{+}IL-17^{-} were now a mixture of CD4 IFN-γ^{+}IL-17^{-}, CD4 IFN-γ^{-}IL-17^{+} and CD4 IFN-γ^{+}IL-17^{+}. Hence, a plasticity in effector phenotype and a spectrum from Th1 to Th17. They found elevated levels of TGF-β and IL-6 cytokines in the inflamed colon and by measuring a number of transcription factors regulating IL-17, found Runx1 expression was induced by TGF-β in CD4 IFN-$\gamma^{Thy1.1+}$. Runx1 induces transactivation of the rorc promoter and IL-17, and they found TGF-β and IL-6 induced histone modification at these promoter sites. Furthermore, when Runx1 was knocked down using siRNA it could stop Th1 to Th17 conversion (295).

In the GBM tumour microenvironment TGF-β and IL-6 are known to be key immunosuppressants of the antitumor response (44, 102). Both the rich innate immune cell infiltrate and tumour cells release cytokines which have numerous deleterious effects, such as to NK cell and CD8 T-cell cytotoxicity and may also include Th1 functional plasticity (100). This highlights the challenge of immunotherapy in treating all solid organ cancers.

Results: Chapter 5 - The combination of immune checkpoint blockade with enhanced p38 MAPK inhibited cDC2 can improve either monotherapy immune strategy

Introduction

Immune checkpoint inhibitors have revolutionized solid organ cancer, particularly the treatment of Metastatic Melanoma and NSCLC (296, 297). The best response rates with Programme death-1 (PD-1) blockade monotherapy are 45%, which increases to 58% with dual Cytotoxic T-lymphocyte associated antigen-4 (CTLA-4) and PD-1 blockade in melanoma (296). However, augmentation of the response is still a key area to achieve higher response rates and a cure. Furthermore, in the treatment of relapse GBM, PD-1 blockade achieves response rates of 8% and progression free survival of 1.5 months, hence does not show sufficient activity to warrant routine use (42). The combination of CTLA-4 and PD-1 blockade has also shown poor activity but high toxicity (298).

We hypothesized that improved antigen presenting therapy, like p38i cDC2, may promote superior immune responses in combination with checkpoint blockade therapy. This rationale is supported by the cancer-immunity cycle hypothesis, which describes the stepwise events required for successful immunity against cancer (299). In this model antigen presentation to T-cells is a vital initial step, which p38i cDC2 would aim to improve. This can potentiate further antigen-specific T cell expansion in combination with drugs targeting T-cell priming, such as the anti-CTLA-4, ipilimumab. Furthermore, the greater number of antigen specific T-cells can combine with PD-1 blockade to

overcome negative checkpoints in the tumour microenvironment, which may have limited previous DC immunotherapy attempts (300).

We therefore studied the combination of p38i cDC2 and immune checkpoint blockage using a model in-vitro system. We used both the aforementioned MLR and the TCR-gp100 transfected Jurkat cross presentation assays to test this hypothesis.

Results

Improved activation of a Th1 response by Dex exposed p38i-cDC2 and immune checkpoint blockade combination

Previously, we showed that DCs in GBM patients are dysfunctional with reduced numbers of circulating cDC2 and suppressed secretion of the Th1-polarising IL-12. Furthermore, the treatment of DCs with p38i reversed this tumour- and Dex- induced IL-12 secretion. We also found that in GBM patients, the dose of Dex was correlated with decreased numbers of all circulating dendritic cell subsets. However, whether immune checkpoint blockade could further restore immune function, is unknown.

To test this, we initially isolated cDC2 using direct magnetic labelling of CD19 depleted PBMCs from fresh blood of healthy volunteers. DCs were pretreated with a p38i, BIRB 0796 (1μM), where specified. We then cultured DCs with Dex at 10^{-6}M for 24 hours in addition to maturation signals (PolyI:C 20μg/ml and R848 2.5μg/ml). The subsequent DCs were then harvested, washed and plated with 10^5 allogeneic peripheral blood CD4 T-cells with or without immune checkpoint blockade antibodies (50μg/ml of anti-CTLA-4 - ipilimumab and/or anti-PD-1-pembrolizumab) in a 96-well plate. The co-culture was incubated for a total of 5 days, with tritiated thymidine added for the final 18hrs. The supernatants were also collected on day 5 of co-culture for cytokine analysis by ELISA. The proliferation results are shown in figure 5.1.

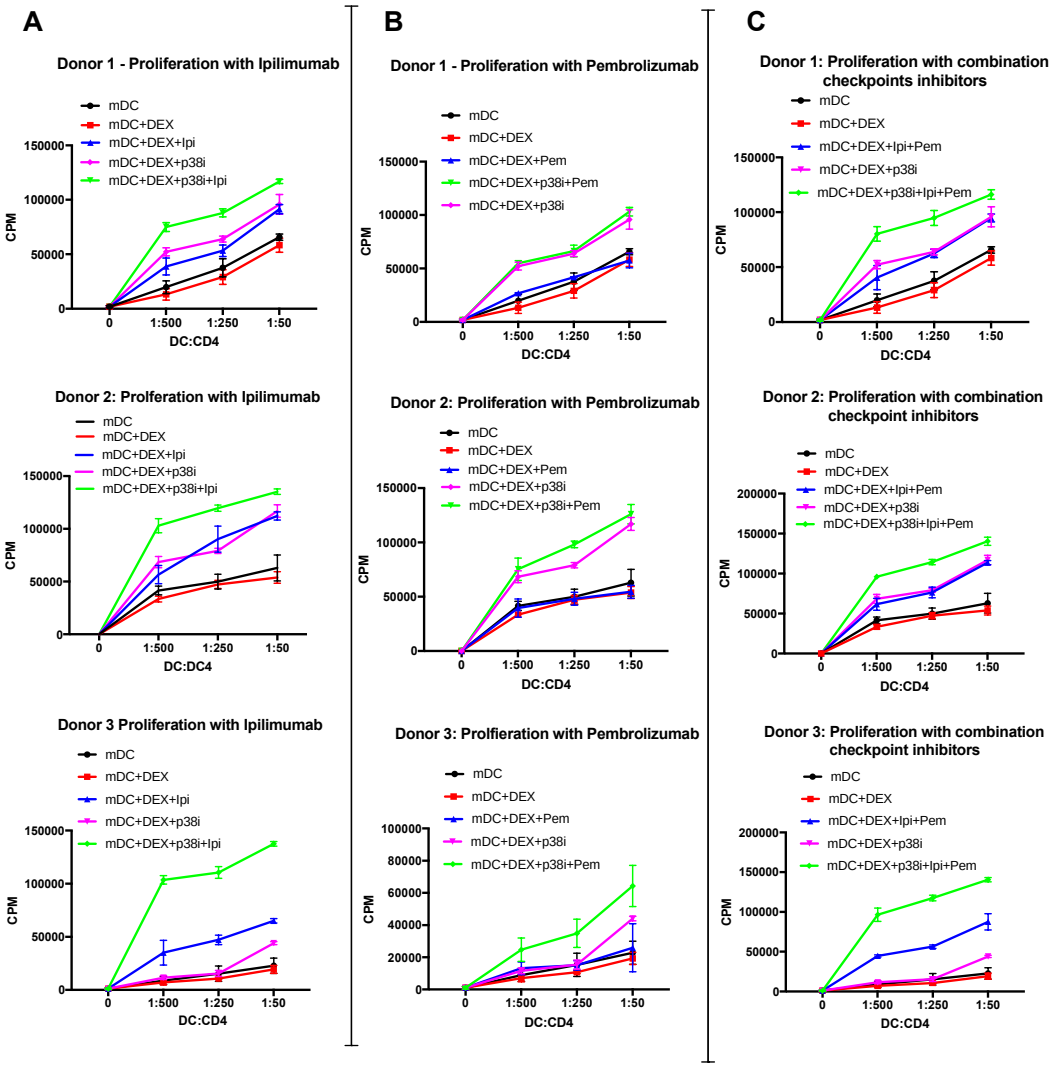


Figure 5.1: The proliferative effect of p38i pre-treatment on dexamethasone-exposed cDC2 in a mixed lymphocyte reaction with CD4 T-cells and checkpoint blockade antibodies in 3 donors.

The proliferative response separated into columns with ipilimumab based combination (column A); pembrolizumab combinations (column B) or dual checkpoint blockade (column C). The conditions for each donor have been separated onto 3 graphs to allow clear visualisation of the groups. Briefly, 10^5 CD4 T cells were incubated with cDC2 exposed to Dex +/- p38i at varying DC:CD4 ratios (x-axis). All DCs were matured with PolyI:C and R848 for 24 hrs and washed prior to re-plating with CD4 T-cells. Checkpoint blockade antibodies were added to the MLR at this point. Proliferation was recorded after 5 days with tritiated thymidine incorporation for the final 18hrs of the assay. mDC= matured DCs; DEX=10^{-6}M dexamethasone; p38i=BIRB 0796 1μM; Ipi=Ipilimumab 50μg/ml; Pem=Pembrolizumab 50μg/ml.

The proliferation results from the three donors were analysed using Friedman's statistical test, used for non-parametric, paired and for multiple matched grouped data. Using Dunn's method, which corrects for multiple group comparisons, Dex exposure to DC did not affect the proliferation of CD4 T-cells ($p=0.999$). Both ipilimumab and p38i pre-treatment, significantly improved the T-cell proliferative response to DCs exposed to Dex ($p=0.027$ and $p=0.016$ respectively). Pembrolizumab had no effect on proliferative response as a monotherapy ($p=0.999$), however was significant in combination with ipilimumab ($p=0.005$), pre-treatment with p38i ($p<0.001$) or both therapies ($p<0.001$). In fact, the combination of p38i pre-treated DCs and ipilimumab was highly significant ($p<0.001$) and the addition of pembrolizumab added little. The cytokines from the supernatant, taken on day 5 of the MLR, was analysed for IFN-γ and IL-10 and is shown in figure 5.2.

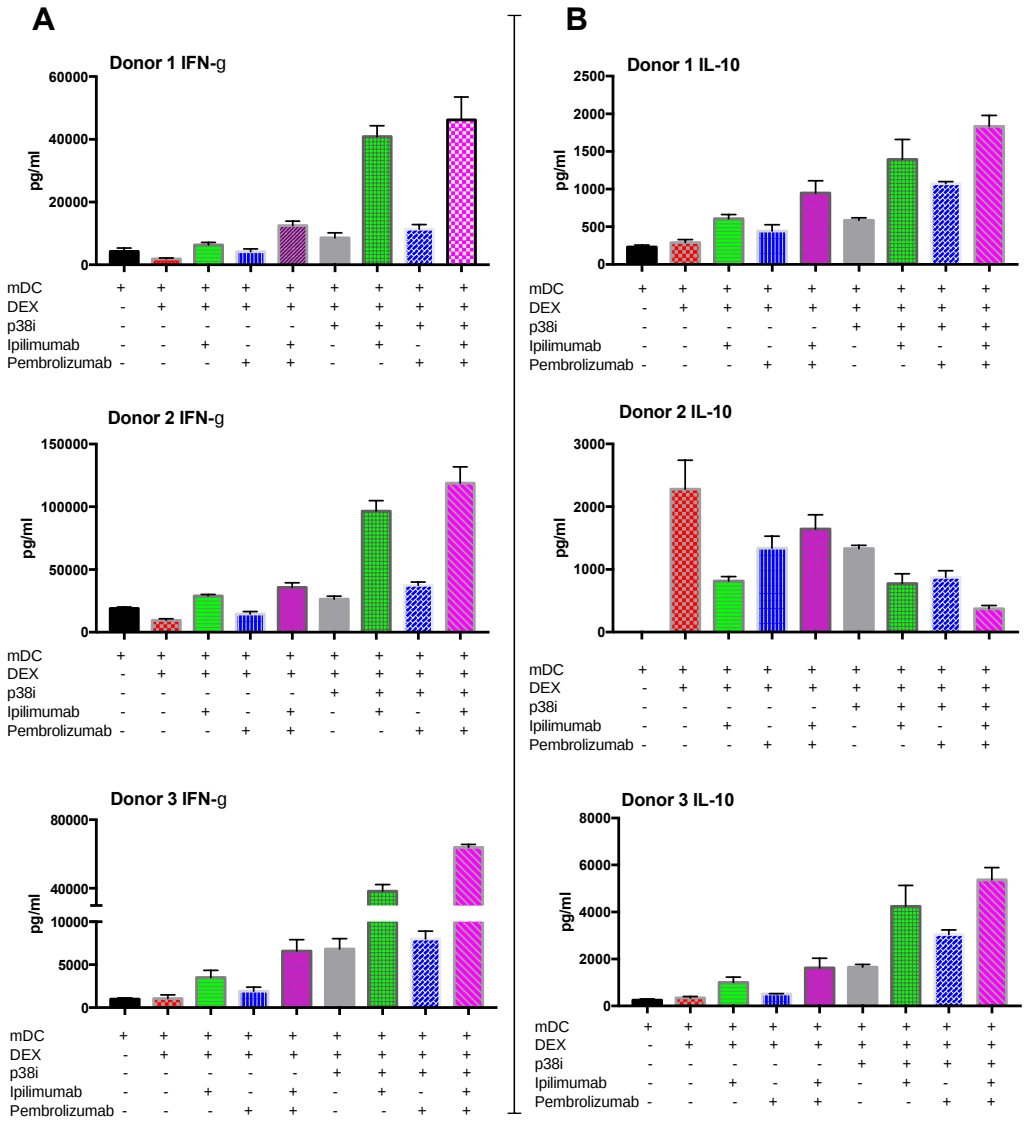


Figure 5.2: The cytokine profile from supernatant taken at day 5 of a MLR involving p38i on Dex-exposed cDC2 and CD4 T cells with checkpoint blockade antibodies in 3 donors.

The figure shows the cytokine analysis of IFN-γ (column A) and IL-10 (column B) from the supernatant collected on day 5 of the MLR described in figure 5.1. The cytokines were analysed by ELISA. The highest IFN-γ was seen from p38i-cDC2 combined with ipilimumab either with or without pembrolizumab. There was little additional benefit of adding pembrolizumab compared to p38i-cDC2 and ipilimumab. There was also a higher IL-10 secretion in these conditions. However, the relative increase of IFN-γ was far greater in the p38i-cDC2 and CD4 T-cells ipilimumab +/- pembrolizumab conditions, compared to IL-10.

mDC= matured DCs; DEX=10^{-6}M dexamethasone; p38i=BIRB0796 1μM; Ipi=Ipilimumab 50μg/ml; Pem=Pembrolizumab 50μg/ml.

The three donors' cumulative cytokine secretion was also analysed using Friedman's statistical test and Dunn's method for group comparisons. Here, Dex exposed DCs did not significantly reduce the IFN-γ production from CD4s ($p=0.999$). Likewise, pembrolizumab ($p=0.999$) and ipilimumab ($p=0.128$) monotherapy had no significant improvement to the MLR IFN-γ production in Dex exposed cDC2. However, the combination of checkpoints ($p=0.001$) and pre-treatment with p38i ($p=0.011$) did improve IFN-γ production. Furthermore, p38i cDC2s, in combination with ipilimumab ($p<0.001$), pembrolizumab ($p<0.001$) or both checkpoint inhibitors ($p<0.001$) all had significant improvements to total IFN-γ production. The combination with ipilimumab and p38i DCs, is synergistic. By contrast, the production of the immunosuppressive cytokine, IL-10 was low in comparison to IFN-γ, with between 10-40x more IFN-γ in the combination treatment groups, compared to Dex exposed cDC2 stimulated CD4 T-cells. IL-10 secretion was more variable between the three donors. This may account for why Friedman's statistical test for multiple matched groups and Dunn's multiple comparator test showed that no group had produced significantly more IL-10 than the Dex-treated DC condition.

Improved activation of a Th1 response from tumour-derived lysate exposed cDC2 by combination p38i and immune checkpoint blockade

We extended our Dex cDC2 assay to investigating the effect of U87, a GBM cell line lysate (TL), on cDC2. Previously, we had shown that TL suppressed IL-12 and the allo-stimulation of PBL by cDC2, but this could be rescued by p38i added prior to maturation.

In this assay cDC2 were isolated as before and rested in 24 well plate with or without the addition of TL (ratio 1:10 DC:TL). In the test wells, the p38i BIRB796, is added one hour prior to maturation with dual TLR agonists R848 and polyI:C. The MLR was performed as described before and the results of proliferation shown in figure 5.3. The supernatants from the co-culture was also collected for cytokine analysis by ELISA (figure 5.4).

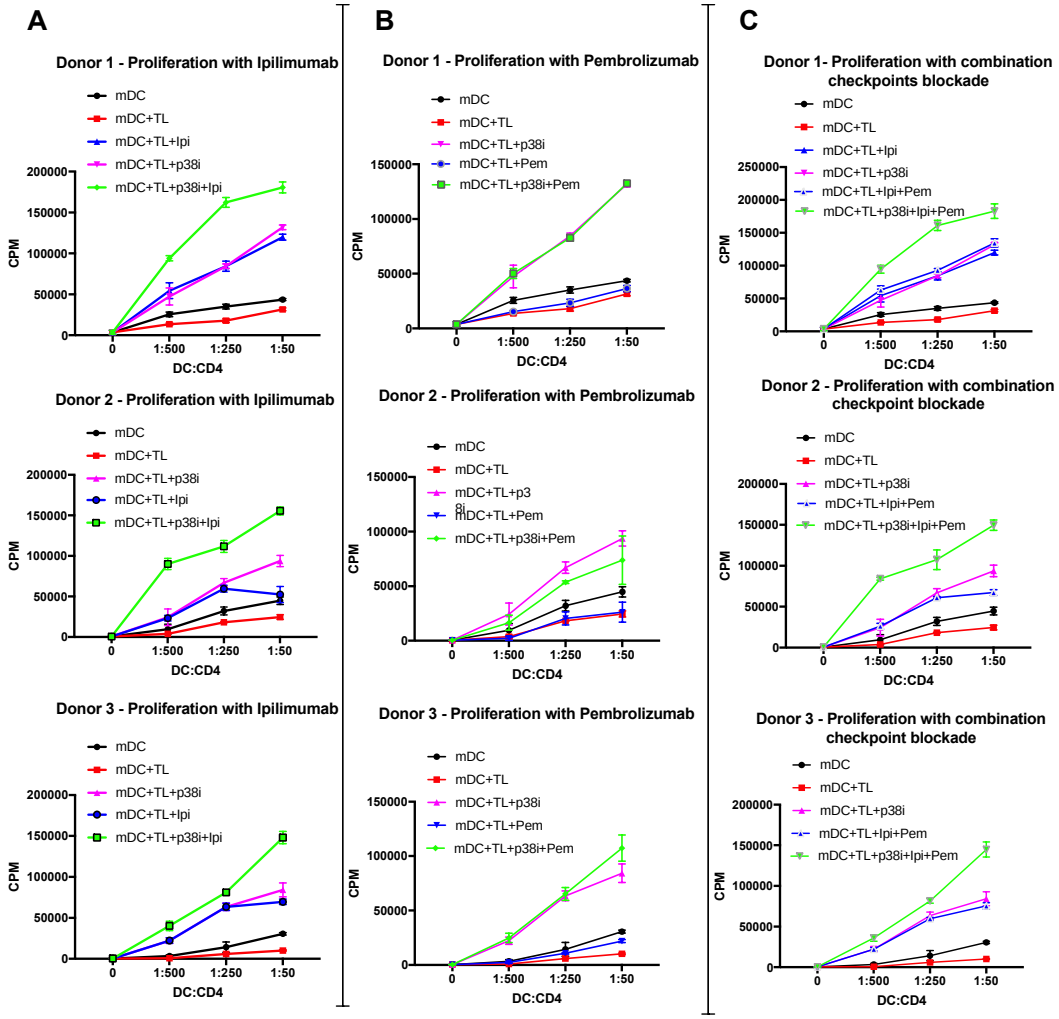


Figure 5.3: The proliferative effect of p38i pre-treatment on U87 derived tumour lysate-exposed cDC2 in a MLR reaction with CD4 T-cells and checkpoint blockade antibodies in 3 donors.

The proliferative response separated into columns with ipilimumab based combination (column A); pembrolizumab combinations (column B) or dual checkpoint blockade (column C). The conditions for each donor have been separated onto 3 graphs to allow clear visualisation of the groups. Briefly, 10^5 CD4 T cells were incubated with cDC2 exposed to TL +/- p38i. All DCs were matured with PolyI:C and R848 for 24 hrs and washed prior to re-plating with CD4 T-cells. Checkpoint blockade antibodies were added to the MLR at this point. Proliferation was recorded after 5 days with tritiated thymidine incorporation for the final 18hrs of the assay.

mDC= matured DCs; TL= U87 tumour derived lysate; p38i=BIRB 0796 1μM; Ipi=Ipilimumab 50μg/ml; Pem=Pembrolizumab 50μg/ml.

We used the non-parametric form of ANOVA - Friedman's and Dunn's multiple comparator test, to compare each group to the standard, selected as matured cDC2 exposed to TL (mDC +TL) group. There was no significant decrease in proliferation seen in CD4 T-cells stimulated by mDC exposed to TL (mDC+TL) compared to stimulation from mDC ($p>0.999$). However, there was a significant increase in CD4 T-cell proliferation stimulated by p38i cDC2 (mDC+TL+p38i $p=0.025$), p38i cDC2 combined with ipilimumab (mDC+TL+p38i+Ipi $p<0.001$), dual checkpoint blockade (mDC+TL+Ipi+Pem; $p=0.006$) and combination of p38i cDC2 and dual checkpoint blockade (mDC +TL +p38i +Ipi+Pem; $p<0.001$). The greatest stimulator of CD4 proliferation was the combination of p38i pre-treated cDC2 and ipilimumab added to the T-cell co-culture and was greater together, than with either treatment alone.

Analysis of the supernatant for IFN-γ and IL-10 from the DC:CD4 ratio 1:50 at day 5 was also performed on the 3 donors. The greatest IFN-γ secretion was seen from the mDC +TL +p38i +ipilimumab (median 86862 pg/ml) and from mDC +TL +p38i +Ipilimumab and pembrolizumab (median 106871 pg/ml) which were both significantly higher compared to mDC +TL (median 1043 pg/ml; $p=0.014$ and $p=0.003$ respectively). There was also a small but significant increase in IL-10 from both these groups compared to mDC +TL ($p=0.023$ and $p=0.005$). As seen with the Dex exposed DC, the greatest increase in IFN-γ was from CD4 T-cells stimulated by p38i TL-cDC2 and ipilimumab combination, producing 80x greater IFN-γ than CD4 T-cells stimulated by TL exposed cDC2. Whereas the IL-10 secretion was only 2-2.5x greater.

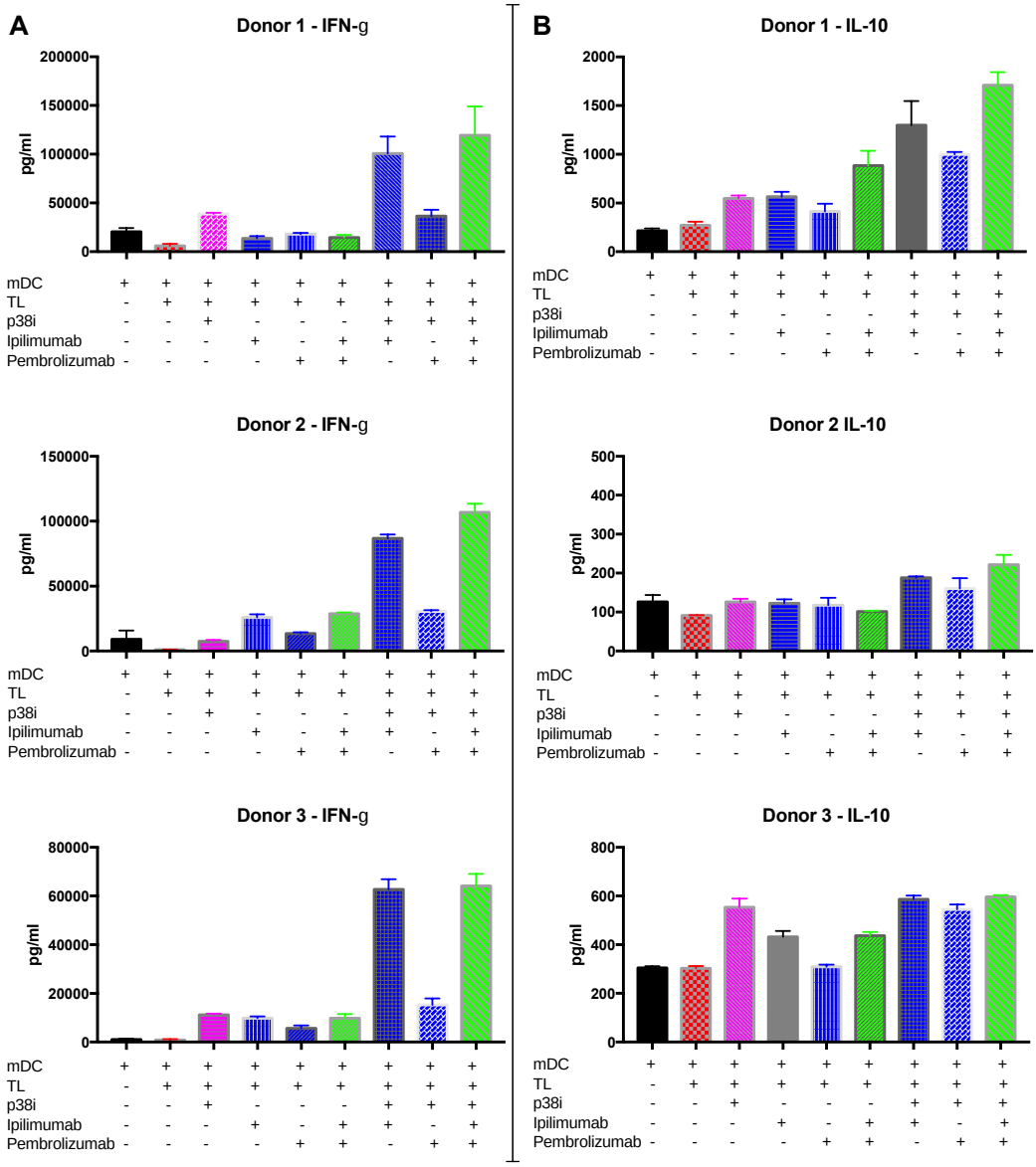


Figure 5.4: The cytokine profile from supernatant taken at day 5 of a MLR involving p38i on U87 tumour lysate (TL)-exposed cDC2 and CD4 T-cells with checkpoint blockade antibodies in 3 donors.

The figure shows the cytokine analysis of IFN-γ (column A) and IL-10 (column B) from the supernatant collected on day 5 of the MLR described in figure 5.1. The cytokines were analysed by ELISA. The highest IFN-γ was seen from p38i-cDC2 combined with ipilimumab either with or without pembrolizumab. There was little additional benefit of adding pembrolizumab compared to p38i-cDC2 and ipilimumab. There was also a higher IL-10 secretion in these conditions. However, the relative increase of IFN-γ was far greater in the p38i-cDC2 and CD4 T-cells ipilimumab +/- pembrolizumab conditions, compared to IL-10.

mDC= matured DCs; TL= U87 tumour derived lysate; p38i=BIRB0796 1μM; Ipi=Ipilimumab 50μg/ml; Pem=Pembrolizumab 50μg/ml.

Pembrolizumab can promote IFN-γ secretion in CD4 exposed to GBM tumour cell lines

To model the effect of PD-1 blockade in the tumour microenvironment, we developed an in-vitro system in which CD4 T-cells, GBM tumour cells and pembrolizumab were co-cultured. Here 10^4 GBM tumour cells lines (U87 or LN229) were plated in a 96-well plate for 24 hours, which allowed adherence and expansion in the well. They were then irradiated at 4Gy to halt further proliferation without causing significant cell death. CD4 T-cells, isolated by direct magnetic labelling with CD4 microbeads from fresh blood of healthy donors, were then added. The simultaneous addition of increasing concentrations of pembrolizumab and 5μg/ml of phytohemagglutinin were added to stimulate proliferation. Following 3 days of culture, the supernatant was analysed for IFN-γ by ELISA and the results are shown in figure 5.5.

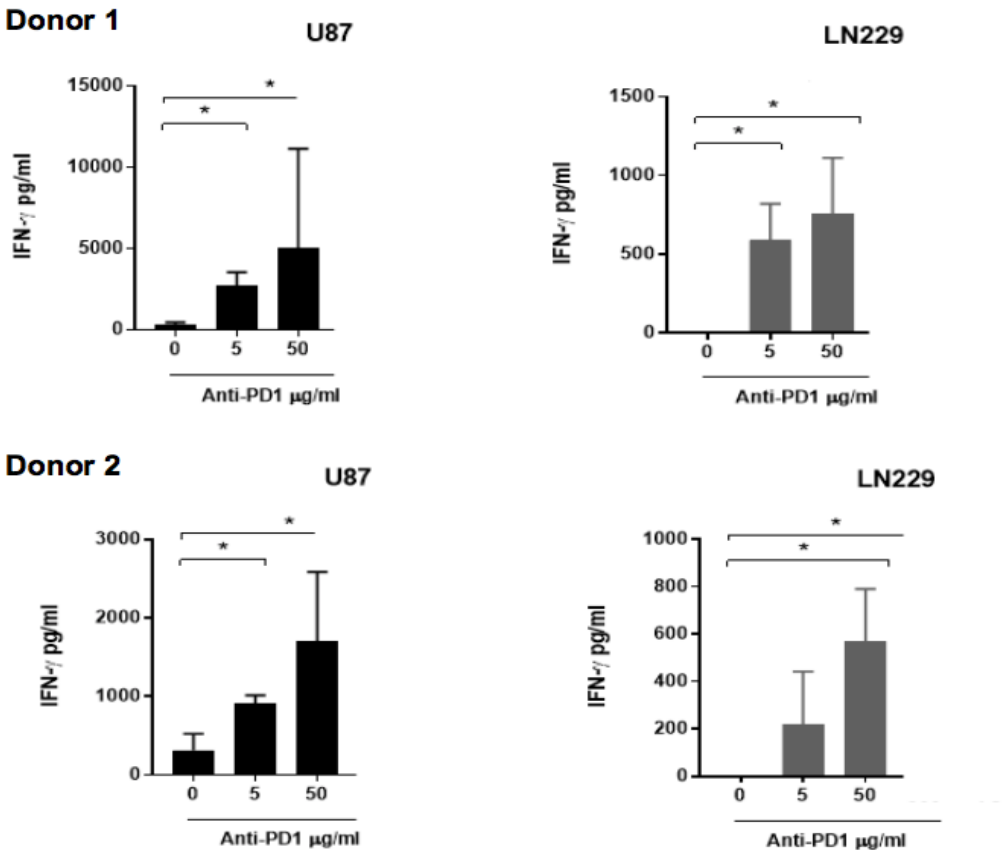


Figure 5.5: IFN-γ secretion from CD4 T-cells co-cultured with GBM cell lines (U87 and LN229) and the effect of an anti-PD-1 inhibitor.

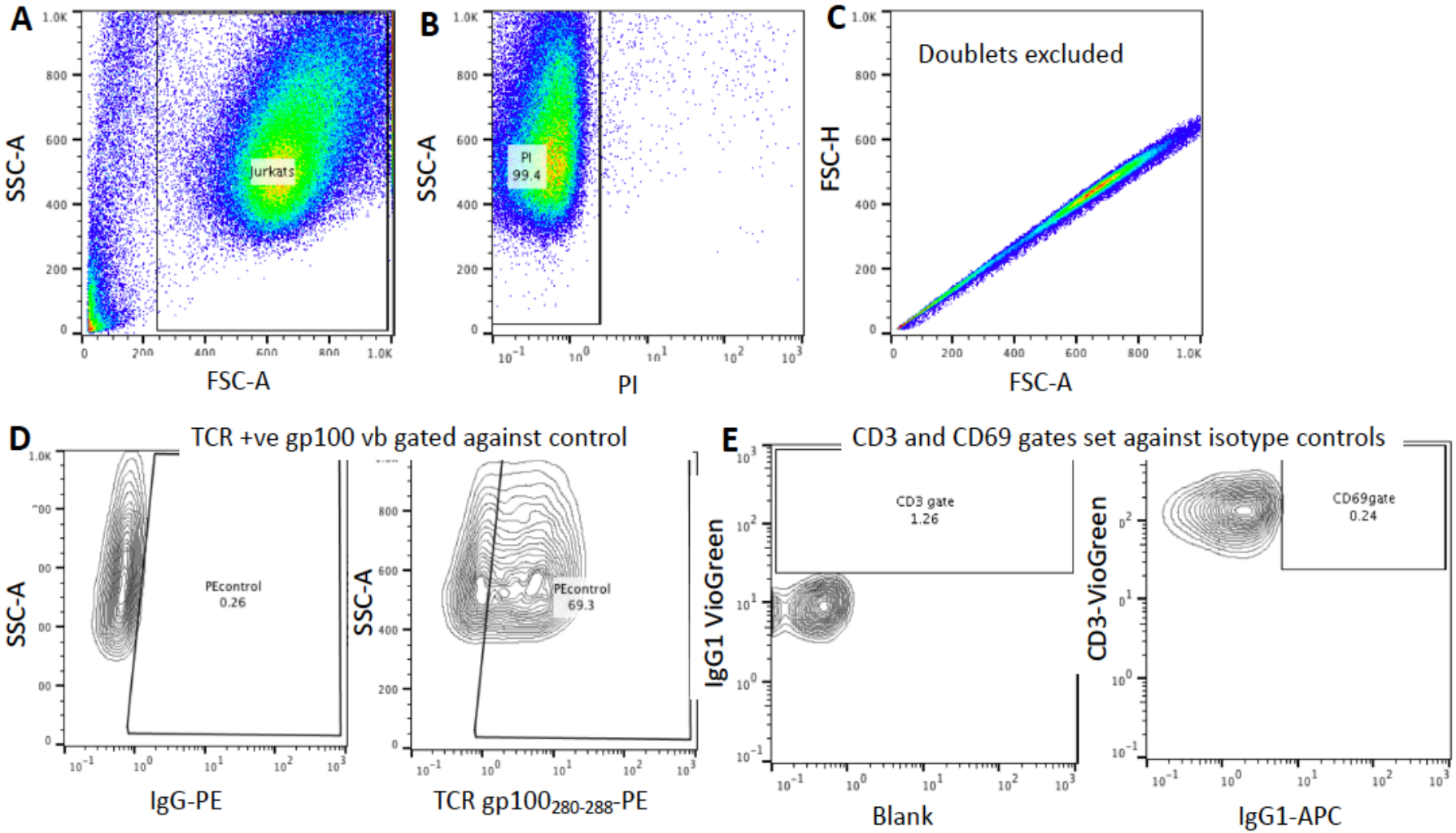
10^4 tumour cells were seeded in a 96 well plate and allowed to proliferate and adhere over 24 hours**.** The cells are then irradiated to halt proliferation (4Gy). CD4 T cells were then added $5x10^4$/well +/- pembrolizumab. CD4 T cells were stimulated with phytohemagglutinin and supernatant collected for ELISA analysis after 3 days. *= $p<0.05$

Pembrolizumab enhanced IFN-γ in both donors. CD4 T lymphocytes, co-cultured with U87 cell line, significantly increased the IFN-γ secretion in the presence of 5 and 50μg/ml of drug, compared to untreated CD4 T cells (p= 0.0088 and p=0.0083 for donor 1; p=0.0114 and p=0.0014 for donor 2). In a similar manner, CD4 T-cells co-cultured with LN229 significantly increased IFN-γ release at both doses of pembrolizumab for donor 1 (p=0.0118; p=0.0211 for 5, 50μg/ml respectively), and donor 2 (p=0.0111 and p=0.0022). These results show the importance of tumour cells in the co-culture model to demonstrate the effectiveness of PD-1 blockade therapies in-vitro, to match in-vivo results.

The combination of p38i cDC2 and immune checkpoint does not alter cross presentation

The cross-presentation assay described in chapter 3 was also used to investigate the effects of immune checkpoint on this assay. In this assay long $gp100_{272-300}$ peptide requires intracellular processing by cDC2 to release the $gp100_{280-288}$ cognate epitope and activate the transfected $gp100_{280-288}$ TCR-Jurkat cell line. The readout was the early activation marker CD69 expression after 24 hours of co-cultured DCs and transfected-Jurkats. An irrelevant peptide, $gp100_{154-167}$, was used as a negative control and $gp100_{280-288}$ (short) peptide, used as a positive control. The short $gp100_{280-288}$ peptide was known to be presented by HLA-A2 and hence 4 HLA-A2 buffy coats were selected to isolate cDC2. Checkpoint blockade antibodies, anti-CTLA-4 and -PD-1, were also added to wells, to assess synergy. After 24 hours of co-culture, cells were washed and stained for CD3 and CD69 and relevant isotypes control for gating.

The results of flow cytometry results of one representative donor is shown below (figure 5.6) and the cumulative results of all 4 donors summarised (figure 5.7).


A
SSC-A
FSC-A
Jurkats
B
SSC-A
PI
PI
99.4
C
Doublets excluded
FSC-H
FSC-A
D
TCR +ve gp100 vb gated against control
SSC-A
IgG-PE
PEcontrol
0.26
TCR gp100280-288-PE
PEcontrol
69.3
E
CD3 and CD69 gates set against isotype controls
IgG1 VioGreen
Blank
CD3 gate
1.26
CD3-VioGreen
IgG1-APC
CD69gate
0.24

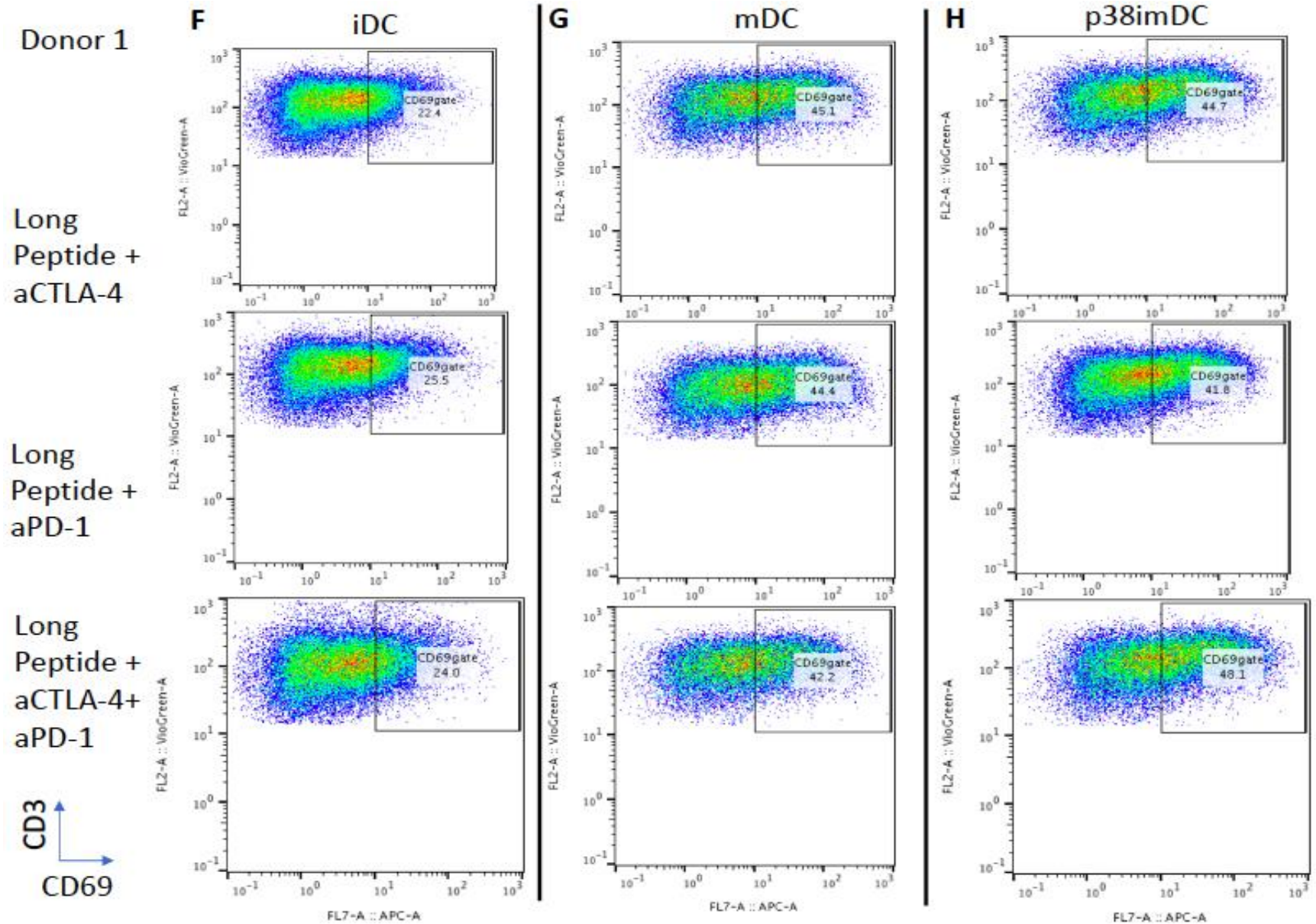

Donor 1
Long Peptide + aCTLA-4
Long Peptide + aPD-1
Long Peptide + aCTLA-4+ aPD-1
F
iDC
G
mDC
H
p38imDC
CD69gate 22.4
CD69gate 45.1
CD69gate 44.7
CD69gate 25.5
CD69gate 44.4
CD69gate 41.8
CD69gate 24.0
CD69gate 42.2
CD69gate 48.1
FL2-A :: VioGreen-A
FL7-A :: APC-A
CD3
CD69

Figure 5.6 Flow cytometry of transfected $gp100_{280-288}$ TCR on a Jurkat following co-culture with cDC2 +/- p38i and ipilimumab, pembrolizumab and $gp100_{272-300}$ and $gp100_{280-288}$ peptides. The long ($gp100_{272-300}$) peptide was co-cultured with cDC2 +/- maturation +/- p38i. Successful processing of the $gp100_{272-300}$ to the short peptide led to activation of transfected $gp100_{280-288}$ TCR-Jurkat cell line. A $gp100_{280-288}$ peptide was used as a positive control and $gp100_{154-167}$ as a negative control (irrelevant peptide). (A) Shows forward (FSC) and side scatter (SSC) of the transfected jurkat cell line and (B) gating of live cells and doublet exclusion in (C). (D) shows the PE-control and PE-$gp100_{280-288}$ staining of Jurkat cell line showing approximately 70% successful transfection. CD3 and CD69 isotype control are also shown (E). A representative donor iDC (F), mDC (G) and p38i mDC (H) stimulated transfected-Jurkats were stained for CD3 and CD69 after 24 hours. The activation was significantly higher in mDC and p38imDC stimulated Jurkats, compared to iDC. The addition of anti-CTLA-4 (ipilimumab) or anti-PD-1 (pembrolizumab), did not change the early acitvation of transfected-$gp100_{280-288}$ Jurkats.
PMA – Phorbol myristate acetate; aCTLA-4 – anti-Cytotoxic T-Lymphocyte Antigen-4 inhibitor; aPD-1 - anti-Programme-death-1

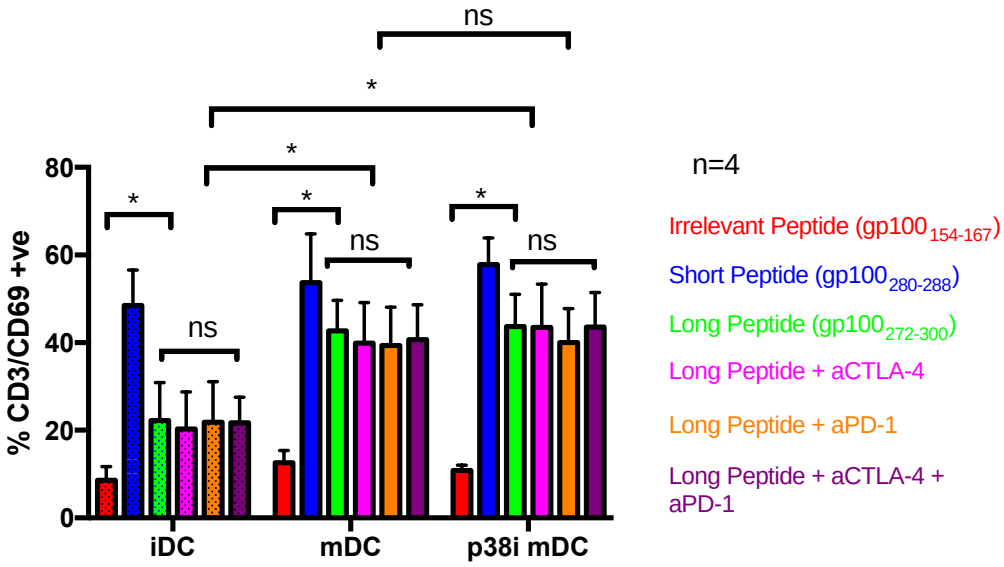


Figure 5.7 Cumulative analysis of 4 healthy donors' stimulation of transfected gp100$_{280-288}$ TCR on a Jurkat cell line following co-culture with cDC2 +/- p38i and ipilimumab, pembrolizumab and gp100$_{272-300}$ and gp100$_{280-288}$ peptides. The percentage CD3+CD69+ Jurkat cells show no significant difference of immune checkpoint blockade to all cDC2 conditions.

We can see that cDC2 were able to process the long peptide, present the short peptide and activate the Jurkats in a TCR specific manner as shown in chapter 3.

In this assay p38i cDC2 were not superior to mDC, despite previously showing enhanced activation of lymphocytes in MLR assays. This may be because Jurkats are an acute lymphoblastic leukaemia cell line and are partially activated and less dependent on the B7-CD28 co-stimulation pathway, than endogenous lymphocytes. In this scenario, a transfected autologous CD8 responder may be superior to Jurkats to represent the in-vivo activation. Also of note, the checkpoint blockade antibodies failed to improve activation, despite reports that Jurkats express PD-1. Immune checkpoint molecules primarily are upregulated after 48 hours to dampen physiological activation and any beneficial effects may not therefore be seen on early activation markers. A CD8 transfected line, co-cultured for a longer duration, may again be better to test combination immunotherapies.

Overall the results show that p38i cDC2 have equal ability to cross present antigens as mDC, supporting their role as vehicles to present tumour associated-/neo-antigens to the immune system to create de-novo T-cell responses. We can conclude that immune checkpoints do not alter the initial activation status of a transfected-Jurkats cell line.

Discussion

We have shown that both p38i cDC2 and the addition of anti-CTLA-4 significantly improves CD4 proliferation induced by TL- and Dex-exposed cDC2. Furthermore, the CD4 T-cell proliferation was superior than matured DC without Dex or TL exposure. The use of p38i on cDC2 and ipilimumab in the MLR was synergistic, producing high levels of IFN-γ from CD4 T-cells. There was also a non-significant increase seen with pembrolizumab, however this effect was less dramatic. This may indicate the greater efficacy of p38i cDC2 at polarising a Th1 response and CTLA-4 upregulation being vital to regulation of the CD4 subtype of T-cells. Likewise, it may indicate a depletion of Treg cells, although the depletion of Treg by CTLA-4 in the human system is debated and less clear than in the animal models (301). The better synergy with ipilimumab may, however, equally be the consequence of the assay design, where in the absence of active tumour, PD-1/PD-L1 axis is a less relevant immune checkpoint (302). PD-1 is a transmembrane protein that binds to its ligands PD-L1 and PD-L2. This interaction is inhibitory to the T-cell through numerous mechanisms, which control T-cell activation, exhaustion and tolerance. This includes, but is not limited to, recruitment of SHP-2 phosphatase reducing phosphorylation of the TCR and subsequent downstream signalling, attenuating T-cell activation and cytokine production. The ligation of PD-1:PD-L1, also decreases production of cytotoxic molecules, limiting T-cell killing activity. There is also reduced anti-apoptotic and increased pro-apoptotic gene expression, thereby decreasing T-cell survival. In addition, metabolic reprogramming within T-cells, further contributes to T-cell inhibition (303).

In figure 5.5 we show that IFN-γ release from CD4 is increased, with increasing PD-L1 antibody, when CD4 are co-cultured with two different GBM cell lines. These results are limited by the small donor number, however, are consistent with the putative mechanism of PD-1 blockade, which is to release the negative regulation of T cells within the tumour microenvironment. The PD-L1 interaction with the DC at the priming step in lymphoid organs seems

less significant. This is supported by the association in most tumours of higher PD-L1 tumour expression, correlating with response to anti-PD-1 and PD-L1 (304).

DCs do express low levels of PD-L1, however our p38i cDC2 have decreased PD-1 expression (see chapter 3), hence the DC:T-cell PD-1 axis is even less active. The significance of DC derived PD-L1 expression in the lymph node is also debated (302). Therefore, the effects of PD-1 are not best demonstrated in our DC-CD4 co-culture. We have also not tested the effect on CD8 T-cells in this assay, and although all effector cells express PD-1, it may be that PD-1 blockade is superior in this subset predominately.

Overall both our Dex and TL exposed enhanced p38i cDC2 in combination with immune checkpoint blockade provide proof of the advantage of targeting different aspects of the cancer-immunity cycle. More importantly, the immuno-oncology community are increasingly targeting so called immunologically ignorant tumours, which currently derive no benefit from immune checkpoint blockade (305). Here, enhanced p38i cDC2 can provide the required stimulus to activate and prime tumour specific CD8 T-cell responses, resulting in greater tumour infiltrating lymphocytes, tumour PD-L1 expression and IFN-γ gene signature, all of which are biomarkers of response to anti-PD-1 therapy (177).

We also wanted to test whether in our transgenic TCR-gp100 Jurkat cell line model, whether any synergy would be seen. The total CD69 positive cells after 24 hours, was unaltered by the addition of checkpoint either as monotherapies or combination. This again would suggest a lower role of PD-1/PD-L1 at the priming site. Physiologically CTLA-4 upregulation usually peaks at 48hrs and hence unlikely to capture any synergistic effect, using the antibody, ipilimumab, since this assay focusses on an early activation marker. Given Jurkat are an immortalised cell line this physiology may be different and was not assessed. Likewise, IFN-γ and IL-2 were not measured in this assay,

which principally focussed on cross presentation. However, we can conclude that immune checkpoint blockage does not interfere negatively with cross presentation.

The challenge for immunotherapy now is how best to combine immunotherapeutic strategies. The cancer-immunity cycle provides a 7-step cycle required for successful anti-tumour immunity. In this cycle antigen capture and presentation by antigen presenting cells, like cDC2, is a key initiating step in the cycle (299). The addition of anti-CTLA-4 and -PD-1 antibodies, then augment response by targeting T-cell priming, activation and cytotoxicity respectively. There is therefore good rationale to combining DC targeting therapies with immune checkpoint blockage therapies.

There have been over 25 FDA approvals for PD-1/-L1 targeting drugs in the last 5 years and while monotherapy has been unsuccessful in the treatment of GBM, there has been a rapid opening of immune checkpoint blockade combination trials. For example, nivolumab, a programme death 1 (PD-1) inhibitor is in phase I trials with stereotactic radiation (NCT02468633), anti-LAG or anti-CD137 (NCT02658981) and dendritic cell vaccines (NCT02529072), all recruiting GBM patients. The most advanced combination trial using PD-1 blockade in GBM is Checkmate-143, which has multiple cohorts of treatment. The combination with ipilimumab thus far has only reported data on toxicity, which is similar to those experienced in other tumours (306). The cohort of PD-1 blockade in the relapsed setting showed inferior survival compared to Bevacizumab (42).

Hence the data described here a combination of immune checkpoint and DC therapies may yield even greater results. However, there will be cost implication to using combination immune checkpoint blockade strategies. For example, NICE have agreed a price of £3750 per 50mg vial of ipilimumab and £439 per 40mg vial of nivolumab, another anti-PD-1 antibody. Hence, for just one cycle of dual checkpoint blockade in a 70kg person, would cost over

£16500. In the melanoma trials this was repeated for 4 cycles and then followed by fortnightly nivolumab monotherapy infusions indefinitely. The cost of combination therapy also needs to consider the higher toxicity, hospital admission, long-term survival, and outpatient appointments, all of which, increase the cost of treatment exponentially.

Another, limiting factor restricting immunotherapy research is the lack of an in-vitro assays to test PD-1 combination therapies such as DC vaccines. Replicating both the priming and activation of T-cells and the immunosuppressive tumour environment is a limiting factor in our tumour-free MLR. Indeed, the basis of using a MLR to show clinical activity in PD-1 blockade was based on a similar study using CD4 stimulated by human MoDC, where increased proliferation was seen measured by tritiated thymidine and increase IFN-γ (307). The mouse models of immune checkpoint blockade also have limitations. For example, the syngeneic models described in the introduction, although have a fully competent immune system, lack the chronic inflammatory characteristics seen in TIL exhaustion from human tumours and also the co-existing inflammation-induced TME remodeling. Furthermore, MC38 is a colon carcinoma cell line and has a low mutational burden, features of which would predict non-responsiveness to immune checkpoint blockade in human patients. However, when grafted onto C57BL/6 mouse, represents a checkpoint blockade sensitive mouse model (157, 308). Hence, even the in-vivo systems have major limitations. Taken together, although there are ambitions to rationalizing immunotherapy combination trials through preclinical models, to prioritize the thousands of ongoing trials and reduce costs, sufficient models do not exist.

It is our thoughts that promoting antigen presentation with DC targeted therapy and immune checkpoint is an investigational treatment strategy which needs clinical testing. To borrow a phrase from a recent editorial, our enhanced p38i cDC2, aim to rev up the cancer-immunity cycle engine, while

combining with immune checkpoint inhibitors cells will dampen the brakes (309).

Overview Discussion

Dendritic cell immunotherapy to treat Glioblastoma

There is an urgent need for novel treatment strategies to combat the poor prognosis for patients suffering with GBM. The UK national statistics identifies the 5-yr survival rate at only 3% (2). The backbone of treatment has remained the Stupp protocol for over a decade which includes maximum surgical resection, chemoradiation and adjuvant chemotherapy (13).

Immunotherapies such as DC vaccines as monotherapy or combined with immune checkpoint blockade are a promising approach. The later has revolutionised the treatment of solid organ cancers, notably in treatment refractory cancers such as metastatic melanoma and lung cancer (296, 297). This has been recognised with the Nobel prize in medicine awarded to the pioneers of immune checkpoint blockade (310).

Immunotherapy for cancer has therefore been at the forefront of research. In tumours with the appropriate immune signatures, targeting these negative regulators of T-cell function alone can have dramatic responses. For example, the median survival for advanced melanoma patients pre-2010 was 7-9 months with dacarbazine chemotherapy (19). Now with treatment using dual checkpoint blockade agents first line, the median survival is greater than 4-years (actual median not reached from the checkmate-67 trial) (296). However, if there is an absent of pre-existing immunity characterised by low PD-L1 expression, low $CD8^+$ TILs, lack of IFN-γ gene signatures and low mutational burden, then responses are low or absent (177). The majority of solid organ malignancies lack most of these characteristics and in GBM, PD-1 inhibitors in the second line setting have had disappointing results, with a median progression-free survival of 1.5 months and response rates of 8%. This was inferior to Bevacizumab, a drug which is not approved by NICE due to lack

of efficacy, in a phase III randomised trial. This trial recruited 369 patients and overall survival was the same between both groups (42). However, of those who responded, the duration of response was significantly longer in the nivolumab arm, median 11.1 months compared to 5.3 months in the Bevacizumab, suggesting a small number of GBM patients did have the relevant immune signatures for a response (42).

GBM has some immune signatures which would predict a response to immune checkpoint blockade. On the mutation burden scale of solid organ malignancies, it lies somewhere in the lower third on the spectrum from high to low burden. Mutational burden correlates with neoantigens load and is predictive of TCR repertoire and response to checkpoint blockade (311). Indeed, clonal neoantigen load has been found to be highly predictive of response in both melanoma and lung cancer patients and is the best biomarker currently available (312).

GBM also express PD-L1 albeit at variable and low levels (91, 92). The TILs from GBM patients however, express multiple immune checkpoints (TIM-3, LAG-3, TIGIT) and therefore show a more severely exhausted phenotype (94).

For tumours with low neoantigen burden, such as GBM, boasting endogenous immunity would intuitively make sense. Dendritic cell vaccine therapy is therefore an attractive treatment strategy. There have been previous dendritic cell vaccine attempts in GBM and a meta-analysis of over 500 patients enrolled in Glioma phase I/II trials reported response rates of 15% and a median 20% increase in overall survival (196, 313).

One phase III MoDC vaccine (DCVax®-L) trial, previously discussed, reported median overall survival of 23.1 months and 3-year survival rate of 25.4%, which compares favorably to other first line trials with an apparent heightened tail of the curve on the Kaplan-Meier survival plots (197).

However, the limitations of this analysis include high trial crossover, lack of treatment arm comparisons and a highly selected patient population.

The next generation of DC vaccines are likely to include circulating DC oppose to in-vitro differentiated monocytes using cytokines as in MoDC. cDC2 are an interesting candidate for the DC of choice to stimulate an anti-tumour response. In-vitro, cDC2 have superior migration and T-cell stimulating activity than MoDC (146, 159). They also secrete a range of cytokines including TNF-α, IL-8, IL-10 and IL-12, have higher expression of costimulatory molecules CD80, 83 86 and 40 and chemokine CCR7 for lymph node migration (138-141). When cell ablation of the equivalent $CD11b^{+}$ DC in mice is performed, Th1, Th2 and Th17 responses are abrogated (131, 144). Indeed, our collaborators in the Netherlands have shown clinical and immunological responses to DC vaccines using cDC2 in a phase I melanoma trial. The cDC2 population are capable of producing high levels of IL-12, stimulate strong T-cell responses and are present in sufficient numbers in melanoma patients to consider adoptive transfer (139, 141, 147, 314). The most important DC for orchestrating anti-tumour immunity in humans is unknown.

This PhD has therefore focused on the cDC2 population given the favourable characteristics described for vaccine development to treat GBM. In the initial evaluation we focused on the 4 major circulating DC subsets (cDC1, cDC2, pDC and SlanDC). Our data, shown in chapter 1 aimed at clarifying whether measurable levels of circulating DC could be seen in GBM patients. We found that patients cDC2 were numerically suppressed in comparison with healthy controls. Furthermore, they had significantly lower HLA-DR and CD86 expression, consistent with a more immature phenotype. Both suppressed numbers of circulating DC and an immature phenotype has been seen in a number of cancer studies, including breast, head and neck, lung cancer, leukaemia and Kaposi sarcoma (191, 218-220). In our cohort we found an association with all subtypes of DC was associated with residual disease and

Dex. Indeed, Dex was strongly correlated in a linear correlation of decreasing numbers with increasing dose.

cDC2 have also been shown in transplantation medicine studies to stimulate a tolerogenic T-cell phenotype when co-cultured with Dex prior to maturation in-vitro (231). Furthermore, Dex directly causes T-cell apoptosis, both at thymic development and in the periphery during activation-induced cell death (120, 121). Indeed, the lymphocyte immune populations are particularly sensitive to steroids as demonstrated in cancers such as lymphoma and acute lymphoblastic leukaemia, where direct cytotoxic effects are seen, contrary to minimal effect in myeloid leukaemias (122).

In chapter 1 we also observed the Th1 polarising cytokine, IL-12, was almost unmeasurable in our cohort of 6 patient whom cDC2 were isolated and stimulated with dual TLR agonists ex-vivo. We confirmed this detrimental effect in chapter 2 where we modelled both tumour-lysate (TL) and Dex exposure in healthy cDC2 from volunteers. Here we confirmed cDC2 impairment of IL-12 secretion and allo-stimulatory activity was attributed to residual disease and Dex. These factors also were immunosuppressive to MoDC.

Therefore, it was clear that for successful use of cDC2 therapy in GBM, we would have to enhance cDC2 phenotype and function. On the basis of previous work by our group using a selection of MAPK inhibitors targeting p38, ERK and MEK, the p38 inhibitor BIRB0796 (p38i) was the most active agent at increasing IL-12 from healthy volunteers. We previously showed that in resected stage 3 melanoma patients circulating cDC2 levels were equivalent to healthy controls and the use of p38i cDC2 could increase IL-12 in this patient group whom were free of cancer and immunosuppressive treatment (139).

Therefore, prior to this study, it was unclear whether p38i could optimise cDC2 function in the setting of profoundly immunosuppressed palliative patients. This included patients with high disease burden and immunosuppressants, which in addition to Dex discussed above, also included chemoradiation and adjuvant chemotherapy.

However, despite the low numbers of cDC2 seen in GBM patients compared to controls, a reasonable number would be expected from leukopheresis which we have estimated from a flow cytometry and PBMC isolation studies to be in the range of 10-50x10^6 cells. The optimum number of DC required in a vaccine is unknown. Pre-clinical studies using a combination flow cytometry, 2-photon imaging and computational modeling to quantify the probability of T cell–DC encounters from mouse popliteal lymph nodes estimated the minimal DC number as 85 to initiate T-cell response starting from a precursor frequency of 10^{-6} T-cells. The aforementioned phase I melanoma trial used between 3 - 10 x 10^6 total cDC2 per vaccination with an average purity of 93%. Hence, it is likely that even with low circulating cDC2 numbers in GBM patients, successful leukopheresis for vaccine development would be possible. However, yields after antigen pulsing and overnight maturation dropped in this trial and ranged from 25-95% with a median of approximately of 55% (147). It is unknown if GBM patients' cDC2 will have similar viability vulnerabilities.

In chapter 3, we extended on our previous findings by showing further phenotypical improvements in healthy volunteers DC. These included a 6-fold increase in CD86 expression, a 7-fold increase in CD40 and CD209 (C-lectin) and 2-fold increase in CD80. The importance of the co-stimulation pathway in DC:T-cell priming are likely to divert a T-cell away from anergy and tolerance towards a more favourable phenotype, given the correct signal 3 provided by local cytokine secretion. As previously seen, IL-12 levels were significantly increased with p38i treatment prior to maturation compared to maturation alone. Furthermore, an increase in allo-stimulatory T-cell proliferation was

seen and an increase in PBL IFN-γ signatures. Hence, confirming that the superior IL-12 and co-stimulation in p38i cDC2 can drive a favourable Th1 immune response.

Using a TCR transfected jurkat cell-line specific to gp-$100_{280\text{-}288}$ peptide, we were able to show that p38i cDC2 also efficiently cross presented peptides equal to matured cDC2. Furthermore, work using healthy volunteers' cDC2, pulsed with glioma-associated peptides and autologous PBL, confirmed that de-novo T-cell responses could be achieved particularly against the antigen TRP-2.

In chapter 4 we showed that cytokine dysfunction in GBM patients could be partially rescued. A 6-patient GBM cohort with barely measurable IL-12 on stimulation ex-vivo at baseline, showed measurable IL-12 levels with the addition of p38i prior to maturation. Furthermore, this decreased the immunosuppressive cytokine, IL-10 and overall the ratio of IL-12:IL-10 in GBM patients was comparable to healthy controls. However, IL-12 levels in these enhanced p38i patient-derived cDC2 was still significantly suppressed compared to healthy controls. It is unknown whether the relative ratio of cytokines determines the T-cell fate following signal 3, or whether a minimal threshold of IL-12 is required to drive a Th1 phenotype in-vivo. This question remains unanswered, however others have shown, following the formation of a single MHC-peptide TCR complex, the sensitivity of the TCR is such that detectable increases in intracellular $CD4^+$ T-cell calcium concentration and subsequent IL-2 and TNF-α cytokines are produced (290). This emphasises the sensitivity of the adaptive immune response to small changes in the environment.

Therefore, impaired cytokine secretion from patient-derived cDC2 could limit the success of vaccine translation in this patient group. However, immune monitoring of T-cell responses in the context of a clinical trial is the best way to answer this question.

Another approach to optimise DC vaccination is to combine this with checkpoint blockade. As discussed earlier, this has revolutionized cancer treatment in solid organ cancers, but lacks success in GBM. The recent evidence of an exhausted TIL phenotype would add weight to this argument. Indeed, if a larger range of glioma specific TCR CD8 could be created, the success of removing exhaustive markers on these will be greater.

In chapter 5 we show that DC co-cultured with anti-CTLA-4 (CTLA-4i) have greater proliferation and IFN-γ secretion. Furthermore, Dex and GBM TL exposed DC which are functionally compromised, when treated with p38i at maturation, trigger superior proliferative responses in $CD4^+$ T-cells. In a MLR the combination of enhanced p38i cDC2 with anti-CTLA-4 and anti-PD-1 resulted in the greatest $CD4^+$ T-cell proliferation. Even more impressively, the IFN-γ measured at day 5 of co-culture was 10-80 times higher than in $CD4^+$ T-cells triggered by Dex- or TL- exposed cDC2. Furthermore, proliferation of IFN-γ producing $CD4^+$ was also far superior than in $CD4^+$ triggered by matured cDC2 without exposure to Dex or TL.

The majority of the synergistic effect seemed to be driven by the anti-CTLA-4, rather than the anti-PD-1, however, the MLR assay favoured testing this immune checkpoint. For, example, there was an absence of $CD8^+$ T-cells and tumour present promoting exhaustion in the MLR, whereas CTLA-4 is more critical at the priming site. Indeed, as discussed previously, testing immune checkpoint blockade combinations in-vitro has the challenge of limited assays with meaningful outputs. The multiple innate and adaptive cells and cytokines involved in the immune response and the tumour microenvironment limits interpretation.

There have been a number of potential vaccine adjuncts which have been described in the DC trials to date including the maturation cocktail, cytokines and antigen stimulant (313). The target of cancer vaccines is to educate the

immune system to the presence of the foreign tumour, usually by presenting tumour-associated antigens or neoantigens. However, for a successful adaptive immune response to be initiated, signal 1, 2 and 3 need to be present (198). Therefore the advantage of DC vaccine is that signal 1, the presentation of an antigen on MHC complex to the T-cell receptor, signal 2, co-stimulation from B7 molecules and signal 3, cytokines such as IL-12 are all provided in one vaccine. This has the theoretical advantage over peptide or protein-based vaccines.

Efforts to improve the efficacy of DC vaccines have therefore focussed on improving these 3 signals. For example, how best to stimulate antigen presentation is unknown. Attempts have used tumour associated peptides either multiple or single, whole tumour lysate, RNA and fusion proteins. However, with new knowledge of mutational burden and clonal neo-antigens, newer DC vaccines efforts are focussing on novel individualised neo-antigen discovery platforms. This has only recently been made possible through improvements in sequencing technology and predictive models of HLA binding to peptides (315). Neo-antigens have the advantage of inducing high affinity T-cell responses, oppose to tumour-associated antigens which usually induce low-affinity T-cell, due to previous central thymic exclusion (257). Unfortunately, the majority of tumour neo-antigens may be unique to an individual, further complicating DC vaccine design, cost and delivery. However, a group investigating neoantigens in melanoma found 2 neoantigens could kill 90% of autologous melanoma cells in-vitro, hence there is hope that targeting limited numbers of neoantigens can still produce meaningful clinical responses (316). Contrary to this, in a study of 18 NSCLC patients who had acquired resistance to anti-PD-1 or anti-PD-1i+CTLA-4, seven had loss of neoantigens identified in the biopsy at progression compared to the origin biopsy. These neoantigens could still promote T-cell responses on exposure to autologous PBL. Hence the authors concluded that widening the breadth of neoantigen reactivity may mitigate the development of acquired resistance (317). Another group developed a platform which

targeted up to 20 personalised neoantigens per patient. In-vitro they were able to show expansion of polyfunctional $CD4^+$ and $CD8^+$ T-cells. When vaccinated into 6 melanoma patients, all 4 whom had resected stage III disease had no recurrence at 25 months. The other 2 patients with stage IV disease (lung metastasis) had progression following vaccination, but experienced complete remission with subsequent PD-1 blockade and measurable expansion of neoantigen-specific T-cells (315).

Signal 2 and 3 can be improved with appropriate maturation cocktails, classically with TNF-α, IL-1ß, IFN-γ, IFN-α and polyI:C known as the α-type 1 DC polarising cocktail (201). However, European trials using DC vaccines have been limited by GMP-approved TLR agonists and novel approaches have been used. For example, a European consortium whom used MoDC vaccines injected intradermally, used topical Imiquimod, a TLR-7 agonist, licensed to treat genital warts, as a mechanism of adding this danger signal. Others have used a licensed travel vaccine, FSME©, developed to protect against Tick-borne encephalitis to mature pDC vaccine, when alternate GMP-approved maturation factors were insufficient (166, 318). Migration to the lymph node is also an important factor determining DC vaccine success. The optimum route of DC delivery be that intranodal, intra-tumoural, intravenous or subcutaneous has not been fully established. One group showed that maturation was superior at migration using ^{111}In-labeled MoDCs compared to immature DC in stage III melanoma patients who subsequently underwent lymph node dissection (n=7-10). However, migration overall was poor with a mean of 0.2% and 1.8% of injected intradermal DC detected in draining lymph nodes from respective immature and mature DC vaccine preparations. Intranodal injection was superior with a mean 19.3% mature DC seen in the lymph nodes and furthermore, on immunohistochemistry, mature DC localized to the T-cell zones within the lymph node (268). However, the same group later carried out a larger trial comparing intradermal and intranodal DC injections in 43 stage III melanoma patients scheduled for lymph node dissection and found, in skin biopsied DTH samples taken for immune

monitoring, higher frequencies of peptide specific T-cells via the intradermal vaccination route (319). This was despite higher number of DC in resected lymph node from intranodal injection, although this was highly variable and 7 of 24 patients injected via this route had a complete absence of DC in lymph node dissection samples. On this basis the research group took forward intradermal injection to phase II/III trials (319).

The future DC immunotherapy trials we propose will therefore include p38i cDC2 combined with immune checkpoint therapy. A future trial design is discussed in our concluding remarks.

Limitations of this study

We acknowledge there are a number of limitations to the data presented in this PhD.

The principle aim in chapter 1 was to enumerate circulating DC subsets in an unselected GBM patient population as a feasibility study. Therefore, the subsequent interpretation of the data for treatment related effects on DC function, is limited. A larger, more uniform patient population pre-surgery, post-resection and during chemoradiation and adjuvant chemotherapy would better quantify the relative changes to DC by treatment and reveal important information on the timing of leukopheresis and/or of functional DC defects. In this regard serial monitoring of patients' DC would also reveal novel characterisation of treatment and disease related DC dysfunction. This information would also impact on future DC vaccine trial design. The low numbers of patients in our cohort means our univariate analysis of factors associated with DC numbers are, at best, exploratory. The nature of GBM patient population, however, means that even a larger cohort, would likely still have variable use of Dex as a confounder. Although our data shows the detrimental effects of Dex on DC numbers and function, the exclusion of its use in a clinical trial design would select a small, good prognostic group. For

example, 75% of patients in the current 1st line standard-of-care defining Stupp trial, were on corticosteroids at randomization (13).

To expand on our DC flow cytometry data, a more comprehensive immune marker panel to include T-reg, T-helper, CD8, NK cells and MDSC populations would give a contextual view of immune dysfunction in GBM patients. At the initiation of this study the restrictions of fluorescent spectrum overlap on conjugated antibodies restricted our analysis to 6-colours. A larger assay panel would require higher quantities of blood, analysed in separate tubes and a less detailed analysis of DC. We therefore focussed on our principal aim of enumeration to identify whether leukopheresis of DC subsets for adoptive therapy would be possible in this patient group. However, newer technologies such as mass cytometry allow the simultaneous analysis of 40 immune markers without such limitations. This would be a great expansion to this study and also identify biologically optimal combinations. For example, although Temozolomide causes lymphopaenia, it also has important immunomodulatory effects, which includes T-reg depletion. This may be advantageous for combination with DC therapy (320).

We also acknowledge, in chapter 2 that the tumour lysate model has the exclusive use of the cell line U87. Cell lines do have a cautionary relevance to in-vivo translation, indeed emphasised by U87, where recent genetic analysis has shown the ATCC banked cell line is of different genotype than originally described. However, the same study confirmed it had features of a GBM from a male donor (185). To support the data presented here, others in our group have replicated the reduced IL-12 and increased IL-10 induced on DC using the tumour-lysate derived from other GBM cell lines including LN229 and LN8. An important addition to this data would be to use autologous patient samples which would be individualised to the patient and better replicate the in-vivo tumour.

Conclusions into the mechanisms driving tumour-lysate induced DC dysfunction are also absent from our experiments. As previously discussed, known tumour associated factors include TGF-β and CCL2 (99, 202, 241). An alternate mechanism also includes tumour secreted exosomes containing microRNA (miRNA) inhibiting DC function. There are a number of miRNA overexpressed in GBM specimens, linked to stem-cell-like properties, tumour invasion and prognosis (321, 322). Ideally, we would investigate blocking antibodies against TGF-β, CCL2 and/or analysing tumour secreted exosomes. This would also infer important information for the use of tumour-lysate for antigen education of DC. Ultimately, performing transcriptomics on tumour-exposed and patient-derived DCs and comparing to healthy individuals will identify other pathways involved in DC dysfunction.

All our in-vitro models are restricted by the absence of supportive in-vivo models. The major restriction here is the lack of phenotypical homology of surface protein expression and transcriptome between mice and human cDC2 population. The complexity of human DC subsets has been recently emphasised by single-cell whole-exome transcriptome analysis of HLA-$DR^{high}Lin^{-}$ immune cell population, showing there are subsets of $CD1c^{+}$DC, which were classified as cDC2 at the time of this PhD (135). The equivalent mouse data set is yet to be completed. It is clear in previous publication that the $CD11b^{+}$ cell population in mice do not functionally represent cDC2 population in humans since they do not migrate, cross present or secrete IL-12 (146). All these are key characteristics of the cDC2 subset in humans and confirmed in this PhD. However, a subset of the heterogenous $CD11b^{+}$ population in mice may indeed be homologous to human cDC2 and our group is currently embarking on isolating the mice $CD11b^{+}CD4^{+}$ splenic DC for further characterisation and functional analysis.

A further expansion to the work presented here would be to inhibit the p38 MAPK pathway through other methods to confirm the effects seen are due to p38i. Previously, we have published the use of the p38i, SB203580, in healthy

individuals and resected stage 3 melanoma patients, which has replicated our findings using BIRB0796 (139). Our group has since expanded our analysis to include VX-745, which has a 20-fold selective p38α inhibition and blood-brain barrier penetration (323). This has replicated the increased IL-12 and decreased IL-10 secretion from matured cDC2 presented in this PhD (data not shown). However, all MAPK inhibitors have off target effects and therefore to affirm these effects, alternate strategies such as siRNA or CRISPR/Cas-9 could be used. The latter has not been done on cDC2 and this would require an increase in expertise and expense beyond this study's remit. The p38 MAPK inhibitors have the advantage of been pharmacologically available products for translation.

We do have concerns in regard to the level of IL-12 secretion from patient-derived DC. However, as previously discussed, it is unclear whether there is an absolute threshold or a relative abundance of IL-12 that is required at the DC:T-cell synapse to polarise T-cell fate. A wider breath of cytokine analysis using multiplex bead analysis would identify the relative proportion of cytokines secreted by p38i cDC2. In our patient population both IL-12 and IL-10 were severely supressed following TLR agonist stimulation and it remains unknown whether this is true for all cytokines or for only a specific family.

Finally, we acknowledge that in chapter 5, the data shown includes 2-3 donors per experiment and therefore more repeats would increase the power of the data.

Targeting DC in-situ

Although progress has been made with DC vaccine therapy, limitations such as poor migration of MoDC to lymph nodes, the variable levels of measurable immune response correlating with clinical responses and viability of cells after manufacturing remain. Furthermore, only a limited number of centres worldwide have the expertise to manufacture these individualised vaccines at

high cost. This makes targeting DC in-situ an attractive approach. One such phase I trial used CDX-1401 vaccine composed of a human monoclonal antibody specific for DEC-205 fused to the full-length tumor antigen NY-ESO-1 and combined with TLR agonists, Resiquimod (TLR7/8 agonist) and Hiltonol (Poly-ICLC; TLR3 agonist) to target in-vivo DC populations (324). DEC-205 is highly expressed on DC, but also on a number of immune cells including monocytes, T-cells and B-cells. The trial recruited any patient where NY-ESO-1 antigen is known to be overexpressed and included 45 patients, half with melanoma, while the rest had a range of cancer including non-immunogenic cancer such as sarcoma, colorectal, and ovarian cancer. There were 13 patients who had stable disease and two partial responses (both patients with melanoma). Within 3 months six melanoma patients received ipilimumab and 4 had either objective or complete response, which is much higher than the expected rate of 15%. All these patients had an expansion in NY-ESO-1-specific T-cells. The same was true of 2 lung cancer patients who subsequently received immune checkpoint (324). However, the disadvantage of targeting DEC-205 endocytic receptor, is its high expression on other immune cells, which may reduce antigen load reaching DC or worse still, promote tumour tolerance through targeting an immunosuppressive monocyte in the TME (325). There has been increasing interest in the cDC1 human subset following the emergence of their importance in mouse models of immune checkpoint blockade. However, difficulties with isolation of this rare subset has limited pre-clinical research. One group, however, have developed a chimeric monoclonal antibody, targeting CLEC9A c-type-lectin receptor allowing targeting of the cDC1 subset in-vivo (325). CLEC9A recognizes F-actin exposed on the surface of dead cells and delivers associated antigens to early endosomes for antigen processing, presentation and cross-presentation, a characteristic of cDC1 in mice. The expression of CLEC9A is more highly expressed on the cDC1 subset only, however, reports have documented low levels of expression on $CD14^{+}CD16^{-}$ monocytes (180). This group used a humanised mouse model NSG-A2, reconstituted with human CD34+ cord blood cells, which develops functional human T- and B-cells, monocytes,

pDCs, and cDC to directly compare anti-DEC205 and anti-CLEC9A humanized chimeric antibodies (326). Using fluorescent labelling they found anti-CLEC9A was localized to the cDC1 population, however, anti-DEC-205 stained a range of immune cells. Both the anti-DEC-205 and anti-CLEC9A were then fused with pp65 protein containing HLA-A*0201–restricted epitope NLV and delivered intravenously to the mice. The splenic DC were then isolated and co-cultured with NLV-specific $CD8^+$ T-cells and IFN-γ measured by ELISA. The anti-CLEC9A induced significant cross presentation in the cDC1 DC subset only as expected, while anti-DEC205 increased cross presentation in both cDC subsets. The anti-CLEC9A gave a significant increase in IFN-γ compared to isotype control, although anti-DEC205 showed a trend to increased survival in 5 mice (325). Overall a proof of principle that cDC1 subset could be successfully targeted in-situ was demonstrated.

A specific endocytic receptor had previously not been found for the cDC2 subset, until earlier this year when CLEC10A was proposed as a candidate (327). This group used transcriptomic data and flow cytometry to prove this C-type lectin is expressed highly on the cDC2 subset and although transcriptomic data suggested mRNA expression on intermediate monocytes ($CD14^{++}CD16^+$), only very low protein expression could be detected in these cells (328). Furthermore, monoclonal anti-CLEC10A-PE rapidly labelled cDC2 in co-culture and MUC-1 peptide attached to ligand of CLEC10A was able to increase cytokine secretion, when combined with TLR 7/8 (327). Hence, this is could be a novel target for future cDC2 targeting therapies. One limitation of all the endocytic receptors is the partial downregulation on maturation, however maturation was essential for T-cell responses in all these trials. Therefore, optimal sequencing of combination TLR and peptide delivery may be key to translation.

Another interesting approach to targeting DC in-situ is the use of nanoparticles. Kranz et al used novel RNA-lipoplexes nanoparticle, which allowed the lipid carriers net charge to target lymphoid areas (329). The

lipoplexes protect the RNA material from breakdown and allow subsequent antigen uptake by DC. Nanoparticles were labelled with RNA encoding a fluorescent protein and showed distribution of the RNA-lipoplexes was charge dependent. Fluorescence was observed in antigen-presenting dendritic cells and in macrophages in splenic and lymphoid tissue in mice and was not present in $CD11c^+$ depleted mice. They showed that although pDC were not fluorescently labelled (likely due to low $CD11c^+$ expression), still were activated producing a pulse of IFN-α 2-3 hours post infusion. This promoted maturation of surrounding DC and subsequent T-cell directed immunity. This group has started a phase I trial using GMP-produced RNA-LPX vaccines encoding four tumour antigens NY-ESO-1, MAGE-A3, tyrosinase and TPTE and have reported on the first three patients recruited. All three patients had a dose-dependent increase in IFN-α and CXCL10 and had measurable de-novo T-cell responses against at least one of the antigens (329). Hence, this seems a promising platform given any number of RNA antigens can be used.

Concluding remarks

In this piece of work we have summarised the favourable characteristics of using a p38i co-cultured with cDC2 prior to maturation. This is the first study to look at using circulating DC in the next generation of DC vaccines to treat GBM patients. This PhD also includes novel data using a small molecular inhibitor to manipulate the intracellular signalling to alter DC functional properties such as co-stimulatory molecules and cytokine release profile in GBM patients. We have also shown favourable characteristics of combining cDC2 therapy with immune checkpoint blockade. We are currently in the process of writing a phase I protocol for which we have funding for a Midlands wide collaboration. The University of Birmingham has a GMP Cell Therapy suite experienced at delivering MoDC vaccines. We will also proceed with our collaborators at Radboud University, Netherlands, who have expertise delivering cDC2 vaccines in melanoma. The initial study would be a first in man trial aiming to recruit relapsed GBM patients, on ≤4mg of Dex. The planned antigens include a collection of 6 epitopes (AIM-2, TRP-2, HER2, IL-13Rα2, gp100 and MAGE-1) used in Phase I/II ICT-107 trial, where all 6 antigens were shown to be overexpressed in 75% of GBM patients, while all patients express at least 3 antigens. In this trial measurable peptide specific responses were seen in a third of patients (282). An alternative antigen sources includes patient-derived autologous tumour lysate as recently used in the phase III DC-Vax-L vaccine trial (197). The maturation factors of choice would combine FSME, a strong danger signal which would historically localize infection to the brain with Imiquimod cream, a TLR-7 agonist shown to promote maturation in clinical GBM trials (164, 194, 330). Preferably, in a relapse trial, a second operation post DC vaccination would allow tumour infiltrate, particularly TILs populations to be measured in combination with PBMC peptide-specific/tumour lysate stimulated immuno-monitoring. A vaccine regime matching the DC-Vax-L protocol would be feasible with circulating cDC2 leukopheresis yields consisting vaccination Day 0, 10, 20 then

2-monthly. In the absence of data supporting a more effective means of administration intradermal route would be reasonable as performed in the phase III DC-Vax trial and phase I cDC2 melanoma trial (147, 197). If a responder is seen in the first 20 patients treated a proposed expansion cohort with multiple immune checkpoint blockade would be our next trial. Ideally this trial would include CTLA-4, PD-1 and TIM-3 blockade in combination to expand sufficient T-cell and remove the severely exhausted T-cell phenotype seen in GBM patients. A hypothetical vaccine programme for a phase I study is summarized in Figure 1. In a cost limitless setting this multimodal immune therapy approach will, in this author opinion, be necessary to induce clinically relevant anti-tumour responses in the GBM patient populations.

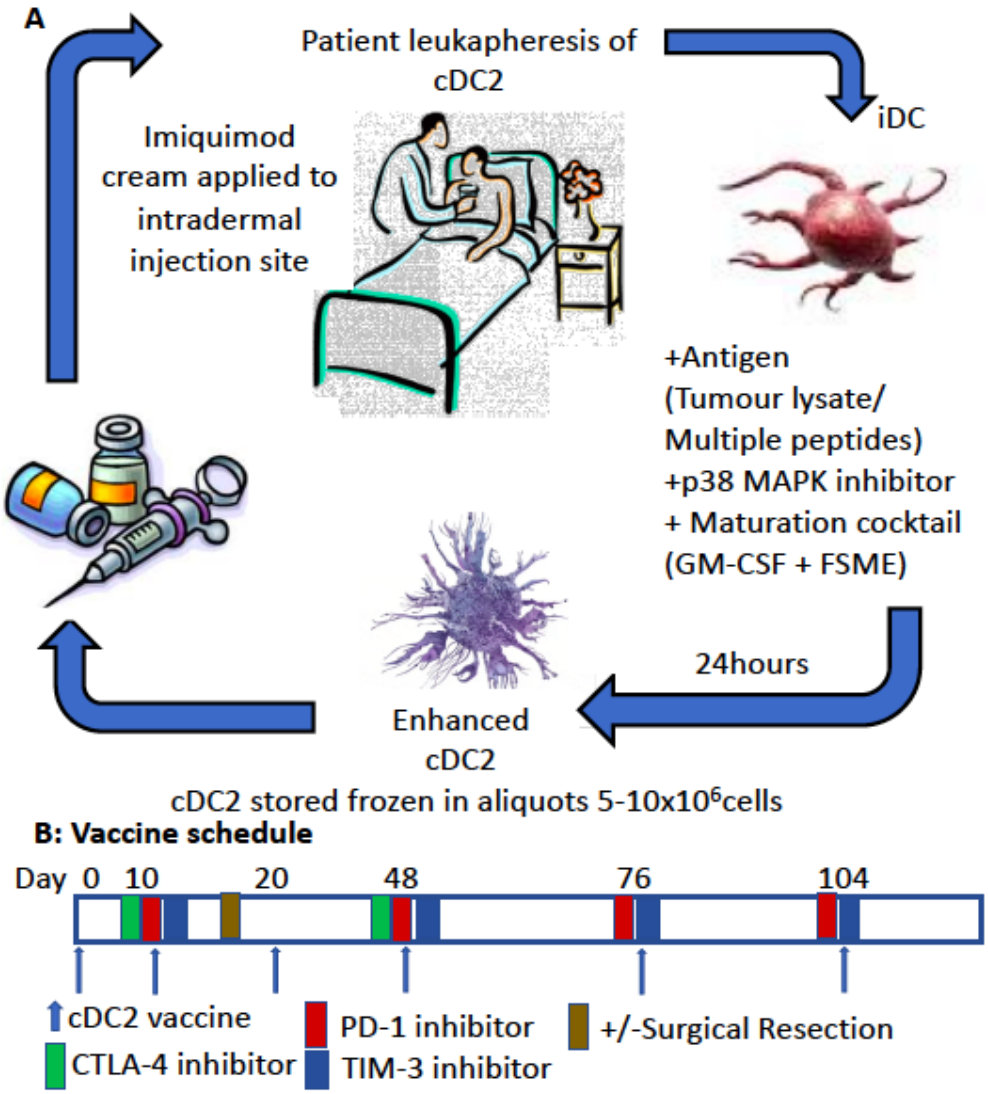


Figure 1: A hypothetical manufacturing process and trial schedule for the next generation of enhanced p38i cDC2 vaccines.
(A) Patients will receive leukopheresis and immediate culture of cDC2 with antigens, p38 MAPK inhibitor and maturation cocktail for 24 hours. DC are harvested for vaccine at Day 0 and the rest frozen for subsequent scheduled vaccines. (B) A treatment schedule combining vaccine and checkpoint blockade could be administrated 2 weeks after DC vaccine to facilitate expansion of T-cells (CTLA-4) and function (PD-1, TIM-3). A surgical resection would identify TIL populations and provide transcriptomic or IHC signatures of immune checkpoints, IFN-γ and potential biomarkers for response. Subsequent DC vaccination could initially be recommenced with combination checkpoint initially and then stop the CTLA-4 inhibitor to reduce toxicity. The PD-1 TIM-3 and DC vaccine combination could then be repeated monthly.

References

1. Wen PY, Kesari S. Malignant gliomas in adults. N Engl J Med. 2008;359(5):492-507.
2. Brodbelt A, Greenberg D, Winters T, Williams M, Vernon S, Collins VP, et al. Glioblastoma in England: 2007-2011. Eur J Cancer. 2015;51(4):533-42.
3. Brain Tumour Research UK. Report on National Rearch Funding - Addressing the historic underfunding of brain tumour research. Brain Tumour Research UK wwwbraintumourresearchorg. 2016.
4. Louis DN, Ohgaki H, Wiestler OD, Cavenee WK, Burger PC, Jouvet A, et al. The 2007 WHO classification of tumours of the central nervous system. Acta neuropathologica. 2007;114(2):97-109.
5. Bailey P, Cushing H. A classification of the tumours of the glioma group on a histogenetic basis, with a correlated study of prognosis. BJS. 1927;14(55):554-5.
6. Watanabe K, Tachibana O, Sata K, Yonekawa Y, Kleihues P, Ohgaki H. Overexpression of the EGF receptor and p53 mutations are mutually exclusive in the evolution of primary and secondary glioblastomas. Brain Pathol. 1996;6(3):217-23; discussion 23-4.
7. Ohgaki H, Kleihues P. Genetic pathways to primary and secondary glioblastoma. The American journal of pathology. 2007;170(5):1445-53.
8. Verhaak RG, Hoadley KA, Purdom E, Wang V, Qi Y, Wilkerson MD, et al. Integrated genomic analysis identifies clinically relevant subtypes of glioblastoma characterized by abnormalities in PDGFRA, IDH1, EGFR, and NF1. Cancer Cell. 2010;17(1):98-110.
9. Brennan CW, Verhaak RGW, McKenna A, Campos B, Noushmehr H, Salama SR, et al. The somatic genomic landscape of glioblastoma. Cell. 2013;155(2):462-77.
10. Prins RM, Soto H, Konkankit V, Odesa SK, Eskin A, Yong WH, et al. Gene expression profile correlates with T-cell infiltration and relative survival in glioblastoma patients vaccinated with dendritic cell immunotherapy. Clin Cancer Res. 2011;17(6):1603-15.
11. Hegi ME, Diserens AC, Gorlia T, Hamou MF, de Tribolet N, Weller M, et al. MGMT gene silencing and benefit from temozolomide in glioblastoma. N Engl J Med. 2005;352(10):997-1003.
12. Rivera AL, Pelloski CE, Gilbert MR, Colman H, De La Cruz C, Sulman EP, et al. MGMT promoter methylation is predictive of response to radiotherapy and prognostic in the absence of adjuvant alkylating chemotherapy for glioblastoma. Neuro Oncol. 2010;12(2):116-21.
13. Stupp R, Mason WP, van den Bent MJ, Weller M, Fisher B, Taphoorn MJ, et al. Radiotherapy plus concomitant and adjuvant temozolomide for glioblastoma. N Engl J Med. 2005;352(10):987-96.

14. deSouza RM, Shaweis H, Han C, Sivasubramiam V, Brazil L, Beaney R, et al. Has the survival of patients with glioblastoma changed over the years? Br J Cancer. 2016;114(2):146-50.
15. Kohler BA, Ward E, McCarthy BJ, Schymura MJ, Ries LA, Eheman C, et al. Annual report to the nation on the status of cancer, 1975-2007, featuring tumors of the brain and other nervous system. J Natl Cancer Inst. 2011;103(9):714-36.
16. Malmstrom A, Gronberg BH, Marosi C, Stupp R, Frappaz D, Schultz H, et al. Temozolomide versus standard 6-week radiotherapy versus hypofractionated radiotherapy in patients older than 60 years with glioblastoma: the Nordic randomised, phase 3 trial. The Lancet Oncology. 2012;13(9):916-26.
17. Maemondo M, Inoue A, Kobayashi K, Sugawara S, Oizumi S, Isobe H, et al. Gefitinib or chemotherapy for non-small-cell lung cancer with mutated EGFR. N Engl J Med. 2010;362(25):2380-8.
18. Rosell R, Carcereny E, Gervais R, Vergnenegre A, Massuti B, Felip E, et al. Erlotinib versus standard chemotherapy as first-line treatment for European patients with advanced EGFR mutation-positive non-small-cell lung cancer (EURTAC): a multicentre, open-label, randomised phase 3 trial. The Lancet Oncology. 2012;13(3):239-46.
19. Chapman PB, Hauschild A, Robert C, Haanen JB, Ascierto P, Larkin J, et al. Improved survival with vemurafenib in melanoma with BRAF V600E mutation. N Engl J Med. 2011;364(26):2507-16.
20. Motzer RJ, Hutson TE, Tomczak P, Michaelson MD, Bukowski RM, Rixe O, et al. Sunitinib versus interferon alfa in metastatic renal-cell carcinoma. N Engl J Med. 2007;356(2):115-24.
21. Sternberg CN, Davis ID, Mardiak J, Szczylik C, Lee E, Wagstaff J, et al. Pazopanib in locally advanced or metastatic renal cell carcinoma: results of a randomized phase III trial. J Clin Oncol. 2010;28(6):1061-8.
22. De Witt Hamer PC. Small molecule kinase inhibitors in glioblastoma: a systematic review of clinical studies. Neuro Oncol. 2010;12(3):304-16.
23. O'Brien SG, Guilhot F, Larson RA, Gathmann I, Baccarani M, Cervantes F, et al. Imatinib compared with interferon and low-dose cytarabine for newly diagnosed chronic-phase chronic myeloid leukemia. N Engl J Med. 2003;348(11):994-1004.
24. Plate KH, Breier G, Weich HA, Risau W. Vascular endothelial growth factor is a potential tumour angiogenesis factor in human gliomas in vivo. Nature. 1992;359(6398):845-8.
25. Jain RK, di Tomaso E, Duda DG, Loeffler JS, Sorensen AG, Batchelor TT. Angiogenesis in brain tumours. Nature reviews Neuroscience. 2007;8(8):610-22.
26. Ferrara N, Hillan KJ, Novotny W. Bevacizumab (Avastin), a humanized anti-VEGF monoclonal antibody for cancer therapy. Biochem Biophys Res Commun. 2005;333(2):328-35.
27. Friedman HS, Prados MD, Wen PY, Mikkelsen T, Schiff D, Abrey LE, et al. Bevacizumab alone and in combination with irinotecan in recurrent glioblastoma. J Clin Oncol. 2009;27(28):4733-40.

28. Kreisl TN, Kim L, Moore K, Duic P, Royce C, Stroud I, et al. Phase II trial of single-agent bevacizumab followed by bevacizumab plus irinotecan at tumor progression in recurrent glioblastoma. J Clin Oncol. 2009;27(5):740-5.
29. Chinot OL, Wick W, Mason W, Henriksson R, Saran F, Nishikawa R, et al. Bevacizumab plus radiotherapy-temozolomide for newly diagnosed glioblastoma. N Engl J Med. 2014;370(8):709-22.
30. Gilbert MR, Dignam JJ, Armstrong TS, Wefel JS, Blumenthal DT, Vogelbaum MA, et al. A randomized trial of bevacizumab for newly diagnosed glioblastoma. N Engl J Med. 2014;370(8):699-708.
31. Hodi FS, Lawrence D, Lezcano C, Wu X, Zhou J, Sasada T, et al. Bevacizumab plus ipilimumab in patients with metastatic melanoma. Cancer Immunol Res. 2014;2(7):632-42.
32. Elamin YY, Rafee S, Toomey S, Hennessy BT. Immune effects of bevacizumab: killing two birds with one stone. Cancer Microenviron. 2015;8(1):15-21.
33. Stupp R, Taillibert S, Kanner AA, Kesari S, Steinberg DM, Toms SA, et al. Maintenance Therapy With Tumor-Treating Fields Plus Temozolomide vs Temozolomide Alone for Glioblastoma: A Randomized Clinical Trial. JAMA. 2015;314(23):2535-43.
34. Kirson EDVTFVJea. Alternating electric fields arrest cell proliferation in animal tumour models and human brain tumours. PNAS. 2007;104(24):5.
35. NICE. Carmustine implants and temozolomide for the treatment of newly diagnosed high-grade glioma. NICE guidance TA121 2007.
36. Brem H, Piantadosi S, Burger PC, Walker M, Selker R, Vick NA, et al. Placebo-controlled trial of safety and efficacy of intraoperative controlled delivery by biodegradable polymers of chemotherapy for recurrent gliomas. The Polymer-brain Tumor Treatment Group. Lancet. 1995;345(8956):1008-12.
37. Westphal M, Hilt DC, Bortey E, Delavault P, Olivares R, Warnke PC, et al. A phase 3 trial of local chemotherapy with biodegradable carmustine (BCNU) wafers (Gliadel wafers) in patients with primary malignant glioma. Neuro Oncol. 2003;5(2):79-88.
38. Kappelle AC, Postma TJ, Taphoorn MJ, Groeneveld GJ, van den Bent MJ, van Groeningen CJ, et al. PCV chemotherapy for recurrent glioblastoma multiforme. Neurology. 2001;56(1):118-20.
39. Schmidt F, Fischer J, Herrlinger U, Dietz K, Dichgans J, Weller M. PCV chemotherapy for recurrent glioblastoma. Neurology. 2006;66(4):587-9.
40. Jackson CM, Lim M, Drake CG. Immunotherapy for brain cancer: recent progress and future promise. Clin Cancer Res. 2014;20(14):3651-9.
41. Wei SC, Duffy CR, Allison JP. Fundamental Mechanisms of Immune Checkpoint Blockade Therapy. Cancer Discov. 2018;8(9):1069-86.
42. Reardon DA, Omuro A, Brandes AA, Rieger J, Wick A, Sepulveda J, et al. OS10.3 Randomized Phase 3 Study Evaluating the Efficacy and Safety of Nivolumab vs Bevacizumab in Patients With Recurrent Glioblastoma: CheckMate 143. Neuro-Oncology. 2017;19(suppl_3):iii21-iii.
43. Van Meir EG, Hadjipanayis CG, Norden AD, Shu HK, Wen PY, Olson JJ. Exciting new advances in neuro-oncology: the avenue to a cure for malignant glioma. CA Cancer J Clin. 2010;60(3):166-93.

44. Perng P, Lim M. Immunosuppressive Mechanisms of Malignant Gliomas: Parallels at Non-CNS Sites. Front Oncol. 2015;5:153.
45. Jarry U, Jeannin P, Pineau L, Donnou S, Delneste Y, Couez D. Efficiently stimulated adult microglia cross-prime naive CD8+ T cells injected in the brain. European journal of immunology. 2013;43(5):1173-84.
46. Hambardzumyan D, Gutmann DH, Kettenmann H. The role of microglia and macrophages in glioma maintenance and progression. Nat Neurosci. 2016;19(1):20-7.
47. Ransohoff RM, Engelhardt B. The anatomical and cellular basis of immune surveillance in the central nervous system. Nat Rev Immunol. 2012;12(9):623-35.
48. Saijo K, Glass CK. Microglial cell origin and phenotypes in health and disease. Nat Rev Immunol. 2011;11(11):775-87.
49. Mantovani A, Sica A, Sozzani S, Allavena P, Vecchi A, Locati M. The chemokine system in diverse forms of macrophage activation and polarization. Trends Immunol. 2004;25(12):677-86.
50. Wei J, Gabrusiewicz K, Heimberger A. The controversial role of microglia in malignant gliomas. Clin Dev Immunol. 2013;2013:285246.
51. Wu A, Wei J, Kong L-Y, Wang Y, Priebe W, Qiao W, et al. Glioma cancer stem cells induce immunosuppressive macrophages/microglia. Neuro-oncology. 2010;12(11):1113-25.
52. Zou JP, Morford LA, Chougnet C, Dix AR, Brooks AG, Torres N, et al. Human glioma-induced immunosuppression involves soluble factor(s) that alters monocyte cytokine profile and surface markers. J Immunol. 1999;162(8):4882-92.
53. Yang I, Han SJ, Kaur G, Crane C, Parsa AT. The role of microglia in central nervous system immunity and glioma immunology. J Clin Neurosci. 2010;17(1):6-10.
54. Glass R, Synowitz M. CNS macrophages and peripheral myeloid cells in brain tumours. Acta Neuropathol. 2014;128(3):347-62.
55. Markovic DS, Vinnakota K, Chirasani S, Synowitz M, Raguet H, Stock K, et al. Gliomas induce and exploit microglial MT1-MMP expression for tumor expansion. Proc Natl Acad Sci U S A. 2009;106(30):12530-5.
56. Korn T, Kallies A. T cell responses in the central nervous system. Nat Rev Immunol. 2017;17(3):179-94.
57. Aspelund A, Antila S, Proulx ST, Karlsen TV, Karaman S, Detmar M, et al. A dural lymphatic vascular system that drains brain interstitial fluid and macromolecules. J Exp Med. 2015;212(7):991-9.
58. Louveau A, Smirnov I, Keyes TJ, Eccles JD, Rouhani SJ, Peske JD, et al. Structural and functional features of central nervous system lymphatic vessels. Nature. 2015;523(7560):337-41.
59. Postow MA, Callahan MK, Barker CA, Yamada Y, Yuan J, Kitano S, et al. Immunologic correlates of the abscopal effect in a patient with melanoma. N Engl J Med. 2012;366(10):925-31.
60. Grimaldi AM, Simeone E, Giannarelli D, Muto P, Falivene S, Borzillo V, et al. Abscopal effects of radiotherapy on advanced melanoma patients who

progressed after ipilimumab immunotherapy. Oncoimmunology. 2014;3:e28780.
61. Weller RO, Engelhardt B, Phillips MJ. Lymphocyte targeting of the central nervous system: a review of afferent and efferent CNS-immune pathways. Brain Pathol. 1996;6(3):275-88.
62. Laman JD, Weller RO. Drainage of cells and soluble antigen from the CNS to regional lymph nodes. J Neuroimmune Pharmacol. 2013;8(4):840-56.
63. Calzascia T, Masson F, Di Berardino-Besson W, Contassot E, Wilmotte R, Aurrand-Lions M, et al. Homing phenotypes of tumor-specific CD8 T cells are predetermined at the tumor site by crosspresenting APCs. Immunity. 2005;22(2):175-84.
64. Kivisakk P, Mahad DJ, Callahan MK, Trebst C, Tucky B, Wei T, et al. Human cerebrospinal fluid central memory CD4+ T cells: evidence for trafficking through choroid plexus and meninges via P-selectin. Proc Natl Acad Sci U S A. 2003;100(14):8389-94.
65. Ifergan I, Kebir H, Alvarez JI, Marceau G, Bernard M, Bourbonniere L, et al. Central nervous system recruitment of effector memory CD8+ T lymphocytes during neuroinflammation is dependent on alpha4 integrin. Brain. 2011;134(Pt 12):3560-77.
66. Abbott NJ, Ronnback L, Hansson E. Astrocyte-endothelial interactions at the blood-brain barrier. Nature reviews Neuroscience. 2006;7(1):41-53.
67. Abbott NJ, Patabendige AA, Dolman DE, Yusof SR, Begley DJ. Structure and function of the blood-brain barrier. Neurobiol Dis. 2010;37(1):13-25.
68. Engelhardt B, Ransohoff RM. Capture, crawl, cross: the T cell code to breach the blood-brain barriers. Trends Immunol. 2012;33(12):579-89.
69. Giunti D, Borsellino G, Benelli R, Marchese M, Capello E, Valle MT, et al. Phenotypic and functional analysis of T cells homing into the CSF of subjects with inflammatory diseases of the CNS. Journal of leukocyte biology. 2003;73(5):584-90.
70. Lossinsky AS, Shivers RR. Structural pathways for macromolecular and cellular transport across the blood-brain barrier during inflammatory conditions. Review. Histology and histopathology. 2004;19(2):535-64.
71. Konnecke H, Bechmann I. The Role of Microglia and Matrix Metalloproteinases Involvement in Neuroinflammation and Gliomas %J Clinical and Developmental Immunology2013. 15 p.
72. Greenwood J, Wang Y, Calder VL. Lymphocyte adhesion and transendothelial migration in the central nervous system: the role of LFA-1, ICAM-1, VLA-4 and VCAM-1. off. Immunology. 1995;86(3):408-15.
73. Cayrol R, Wosik K, Berard JL, Dodelet-Devillers A, Ifergan I, Kebir H, et al. Activated leukocyte cell adhesion molecule promotes leukocyte trafficking into the central nervous system. Nat Immunol. 2008;9(2):137-45.
74. Schlachetzki F, Zhu C, Pardridge WM. Expression of the neonatal Fc receptor (FcRn) at the blood-brain barrier. J Neurochem. 2002;81(1):203-6.
75. Roopenian DC, Akilesh S. FcRn: the neonatal Fc receptor comes of age. Nat Rev Immunol. 2007;7(9):715-25.
76. Ohtsuki S, Terasaki T. Contribution of carrier-mediated transport systems to the blood-brain barrier as a supporting and protecting interface for

the brain; importance for CNS drug discovery and development. Pharm Res. 2007;24(9):1745-58.
77. Goldberg SB, Gettinger SN, Mahajan A, Chiang AC, Herbst RS, Sznol M, et al. Pembrolizumab for patients with melanoma or non-small-cell lung cancer and untreated brain metastases: early analysis of a non-randomised, open-label, phase 2 trial. The Lancet Oncology. 2016;17(7):976-83.
78. Bouffet E, Larouche V, Campbell BB, Merico D, de Borja R, Aronson M, et al. Immune Checkpoint Inhibition for Hypermutant Glioblastoma Multiforme Resulting From Germline Biallelic Mismatch Repair Deficiency. J Clin Oncol. 2016;34(19):2206-11.
79. Amayiri N, Tabori U, Campbell B, Bakry D, Aronson M, Durno C, et al. High frequency of mismatch repair deficiency among pediatric high grade gliomas in Jordan. Int J Cancer. 2016;138(2):380-5.
80. Roszman TL, Brooks WH. Immunobiology of primary intracranial tumours. III. Demonstration of a qualitative lymphocyte abnormality in patients with primary brain tumours. Clinical and experimental immunology. 1980;39(2):395-402.
81. Brooks WH, Netsky MG, Normansell DE, Horwitz DA. Depressed Cell-meidated Immunity in patients with Primary Intracranial Tumours. The Journal of Experimental Medicine. 1972;136:1631-47.
82. Zou W. Regulatory T cells, tumour immunity and immunotherapy. Nat Rev Immunol. 2006;6(4):295-307.
83. Colombo MP, Piconese S. Regulatory-T-cell inhibition versus depletion: the right choice in cancer immunotherapy. Nat Rev Cancer. 2007;7(11):880-7.
84. Fecci PE, Mitchell DA, Whitesides JF, Xie W, Friedman AH, Archer GE, et al. Increased regulatory T-cell fraction amidst a diminished CD4 compartment explains cellular immune defects in patients with malignant glioma. Cancer Res. 2006;66(6):3294-302.
85. Yue Q, Zhang X, Ye HX, Wang Y, Du ZG, Yao Y, et al. The prognostic value of Foxp3+ tumor-infiltrating lymphocytes in patients with glioblastoma. J Neurooncol. 2014;116(2):251-9.
86. Wang L, Zhang B, Xu X, Zhang S, Yan X, Kong F, et al. Clinical significance of FOXP3 expression in human gliomas. Clin Transl Oncol. 2014;16(1):36-43.
87. Wainwright DA, Sengupta S, Han Y, Lesniak MS. Thymus-derived rather than tumor-induced regulatory T cells predominate in brain tumors. Neuro Oncol. 2011;13(12):1308-23.
88. Vasco C, Canazza A, Rizzo A, Mossa A, Corsini E, Silvani A, et al. Circulating T regulatory cells migration and phenotype in glioblastoma patients: an in vitro study. J Neurooncol. 2013;115(3):353-63.
89. Chongsathidkiet P, Jackson C, Koyama S, Loebel F, Cui X, Farber SH, et al. Sequestration of T cells in bone marrow in the setting of glioblastoma and other intracranial tumors. Nature Medicine. 2018;24(9):1459-68.
90. Patel SP, Kurzrock R. PD-L1 Expression as a Predictive Biomarker in Cancer Immunotherapy. Mol Cancer Ther. 2015;14(4):847-56.
91. Wintterle S, Schreiner B, Mitsdoerffer M, Schneider D, Chen L, Meyermann R, et al. Expression of the B7-related molecule B7-H1 by glioma

cells: a potential mechanism of immune paralysis. Cancer Res. 2003;63(21):7462-7.
92. Berghoff AS, Kiesel B, Widhalm G, Rajky O, Ricken G, Wohrer A, et al. Programmed death ligand 1 expression and tumor-infiltrating lymphocytes in glioblastoma. Neuro Oncol. 2015;17(8):1064-75.
93. Nduom EK, Wei J, Yaghi NK, Huang N, Kong LY, Gabrusiewicz K, et al. PD-L1 expression and prognostic impact in glioblastoma. Neuro Oncol. 2016;18(2):195-205.
94. Woroniecka K, Chongsathidkiet P, Rhodin K, Kemeny H, Dechant C, Farber SH, et al. T-Cell Exhaustion Signatures Vary with Tumor Type and Are Severe in Glioblastoma. Clin Cancer Res. 2018;24(17):4175-86.
95. Mohme M, Schliffke S, Maire CL, Runger A, Glau L, Mende KC, et al. Immunophenotyping of Newly Diagnosed and Recurrent Glioblastoma Defines Distinct Immune Exhaustion Profiles in Peripheral and Tumor-infiltrating Lymphocytes. Clin Cancer Res. 2018;24(17):4187-200.
96. Paley MA, Kroy DC, Odorizzi PM, Johnnidis JB, Dolfi DV, Barnett BE, et al. Progenitor and terminal subsets of CD8+ T cells cooperate to contain chronic viral infection. Science. 2012;338(6111):1220-5.
97. Mohme M, Schliffke S, Maire CL, Rünger A, Glau L, Mende KC, et al. Immunophenotyping of Newly Diagnosed and Recurrent Glioblastoma Defines Distinct Immune Exhaustion Profiles in Peripheral and Tumor-infiltrating Lymphocytes. Clinical Cancer Research. 2018;24:4187-200.
98. Fontana A, Hengartner H, de Tribolet N, Weber E. Glioblastoma cells release interleukin 1 and factors inhibiting interleukin 2-mediated effects. J Immunol. 1984;132(4):1837-44.
99. Siepl C, Bodmer S, Frei K, MacDonald HR, De Martin R, Hofer E, et al. The glioblastoma-derived T cell suppressor factor/transforming growth factor-beta 2 inhibits T cell growth without affecting the interaction of interleukin 2 with its receptor. European journal of immunology. 1988;18(4):593-600.
100. Friese MA, Wischhusen J, Wick W, Weiler M, Eisele G, Steinle A, et al. RNA interference targeting transforming growth factor-beta enhances NKG2D-mediated antiglioma immune response, inhibits glioma cell migration and invasiveness, and abrogates tumorigenicity in vivo. Cancer Res. 2004;64(20):7596-603.
101. Zagzag D, Salnikow K, Chiriboga L, Yee H, Lan L, Ali MA, et al. Downregulation of major histocompatibility complex antigens in invading glioma cells: stealth invasion of the brain. Lab Invest. 2005;85(3):328-41.
102. Schneider T, Sailer M, Ansorge S, Firsching R, Reinhold D. Increased concentrations of transforming growth factor beta1 and beta2 in the plasma of patients with glioblastoma. J Neurooncol. 2006;79(1):61-5.
103. Moore KW, de Waal Malefyt R, Coffman RL, O'Garra A. Interleukin-10 and the interleukin-10 receptor. Annu Rev Immunol. 2001;19:683-765.
104. Murai M, Turovskaya O, Kim G, Madan R, Karp CL, Cheroutre H, et al. Interleukin 10 acts on regulatory T cells to maintain expression of the transcription factor Foxp3 and suppressive function in mice with colitis. Nat Immunol. 2009;10(11):1178-84.

105. Huettner C, Paulus W, Roggendorf W. Messenger RNA expression of the immunosuppressive cytokine IL-10 in human gliomas. American Journal of Pathology. 1995;146(2):317–22.
106. Wagner S, Czub S, Greif M, Vince GH, Suss N, Kerkau S, et al. Microglial/macrophage expression of interleukin 10 in human glioblastomas. Int J Cancer. 1999;82(1):12-6.
107. Carlin JM, Borden EC, Sondel PM, Byrne GI. Biologic-response-modifier-induced indoleamine 2,3-dioxygenase activity in human peripheral blood mononuclear cell cultures. J Immunol. 1987;139(7):2414-8.
108. Wainwright DA, Balyasnikova IV, Chang AL, Ahmed AU, Moon KS, Auffinger B, et al. IDO expression in brain tumors increases the recruitment of regulatory T cells and negatively impacts survival. Clin Cancer Res. 2012;18(22):6110-21.
109. Hwu P, Du MX, Lapointe R, Do M, Taylor MW, Young HA. Indoleamine 2,3-dioxygenase production by human dendritic cells results in the inhibition of T cell proliferation. J Immunol. 2000;164(7):3596-9.
110. Wainwright DA, Chang AL, Dey M, Balyasnikova IV, Kim CK, Tobias A, et al. Durable therapeutic efficacy utilizing combinatorial blockade against IDO, CTLA-4, and PD-L1 in mice with brain tumors. Clin Cancer Res. 2014;20(20):5290-301.
111. Kotsarini C, Griffiths PD, Wilkinson ID, Hoggard N. A systematic review of the literature on the effects of dexamethasone on the brain from in vivo human-based studies: implications for physiological brain imaging of patients with intracranial tumors. Neurosurgery. 2010;67(6):1799-815; discussion 815.
112. Heiss JD, Papavassiliou E, Merrill MJ, Nieman L, Knightly JJ, Walbridge S, et al. Mechanism of dexamethasone suppression of brain tumor-associated vascular permeability in rats. Involvement of the glucocorticoid receptor and vascular permeability factor. J Clin Invest. 1996;98(6):1400-8.
113. Grossman SA, Ye X, Lesser G, Sloan A, Carraway H, Desideri S, et al. Immunosuppression in patients with high-grade gliomas treated with radiation and temozolomide. Clin Cancer Res. 2011;17(16):5473-80.
114. Papadopoulos MC, Saadoun S, Binder DK, Manley GT, Krishna S, Verkman AS. Molecular mechanisms of brain tumor edema. Neuroscience. 2004;129(4):1011-20.
115. Bourke E, Moynagh PN. Antiinflammatory Effects of Glucocorticoids in Brain Cells, Independent of NF-κB. The Journal of Immunology. 1999;163(4):2113.
116. Auphan N, DiDonato JA, Rosette C, Helmberg A, Karin M. Immunosuppression by Glucocorticoids: Inhibition of NF-κB Activity Through Induction of IκB Synthesis. Science. 1995;270(5234):286.
117. Hughes MA, Parisi M, Grossman S, Kleinberg L. Primary brain tumors treated with steroids and radiotherapy: low CD4 counts and risk of infection. Int J Radiat Oncol Biol Phys. 2005;62(5):1423-6.
118. Wong ET, Lok E, Gautam S, Swanson KD. Dexamethasone exerts profound immunologic interference on treatment efficacy for recurrent glioblastoma. Br J Cancer. 2015;113(2):232-41.

119. Pitter KL, Tamagno I, Alikhanyan K, Hosni-Ahmed A, Pattwell SS, Donnola S, et al. Corticosteroids compromise survival in glioblastoma. Brain. 2016;139(Pt 5):1458-71.
120. Herold MJ, McPherson KG, Reichardt HM. Glucocorticoids in T cell apoptosis and function. Cell Mol Life Sci. 2006;63(1):60-72.
121. Dietrich J, Rao K, Pastorino S, Kesari S. Corticosteroids in brain cancer patients: benefits and pitfalls. Expert Rev Clin Pharmacol. 2011;4(2):233-42.
122. Pufall MA. Glucocorticoids and Cancer. Adv Exp Med Biol. 2015;872:315-33.
123. Steinman RM, Cohn ZA. Identification of a novel cell type in peripheral lymphoid organs of mice. I. Morphology, quantitation, tissue distribution. J Exp Med. 1973;137(5):1142-62.
124. Steinman RM, Cohn ZA. Identification of a novel cell type in peripheral lymphoid organs of mice. II. Functional properties in vitro. J Exp Med. 1974;139(2):380-97.
125. Banchereau J, Steinman RM. Dendritic cells and the control of immunity. Nature. 1998;392(6673):245-52.
126. Peters JH, Ruppert J, Gieseler RK, Najar HM, Xu H. Differentiation of human monocytes into CD14 negative accessory cells: do dendritic cells derive from the monocytic lineage? Pathobiology. 1991;59(3):122-6.
127. Romani N, Gruner S, Brang D, Kampgen E, Lenz A, Trockenbacher B, et al. Proliferating dendritic cell progenitors in human blood. J Exp Med. 1994;180(1):83-93.
128. Sallusto F, Lanzavecchia A. Efficient presentation of soluble antigen by cultured human dendritic cells is maintained by granulocyte/macrophage colony-stimulating factor plus interleukin 4 and downregulated by tumor necrosis factor alpha. J Exp Med. 1994;179(4):1109-18.
129. Randolph GJ, Inaba K, Robbiani DF, Steinman RM, Muller WA. Differentiation of phagocytic monocytes into lymph node dendritic cells in vivo. Immunity. 1999;11(6):753-61.
130. MacDonald KP, Munster DJ, Clark GJ, Dzionek A, Schmitz J, Hart DN. Characterization of human blood dendritic cell subsets. Blood. 2002;100(13):4512-20.
131. Collin M, McGovern N, Haniffa M. Human dendritic cell subsets. Immunology. 2013;140(1):22-30.
132. Collin M, Bigley V. Human dendritic cell subsets: an update. Immunology. 2018;154(1):3-20.
133. Merad M, Sathe P, Helft J, Miller J, Mortha A. The dendritic cell lineage: ontogeny and function of dendritic cells and their subsets in the steady state and the inflamed setting. Annu Rev Immunol. 2013;31:563-604.
134. Dzionek A, Fuchs A, Schmidt P, Cremer S, Zysk M, Miltenyi S, et al. BDCA-2, BDCA-3, and BDCA-4: Three Markers for Distinct Subsets of Dendritic Cells in Human Peripheral Blood. The Journal of Immunology. 2000;165(11):6037-46.
135. Villani A-C, Satija R, Reynolds G, Sarkizova S, Shekhar K, Fletcher J, et al. Single-cell RNA-seq reveals new types of human blood dendritic cells, monocytes, and progenitors. Science. 2017;356(6335).

136. Alcantara-Hernandez M, Leylek R, Wagar LE, Engleman EG, Keler T, Marinkovich MP, et al. High-Dimensional Phenotypic Mapping of Human Dendritic Cells Reveals Interindividual Variation and Tissue Specialization. Immunity. 2017;47(6):1037-50 e6.
137. Hemont C, Neel A, Heslan M, Braudeau C, Josien R. Human blood mDC subsets exhibit distinct TLR repertoire and responsiveness. Journal of leukocyte biology. 2013;93(4):599-609.
138. Mittag D, Proietto AI, Loudovaris T, Mannering SI, Vremec D, Shortman K, et al. Human dendritic cell subsets from spleen and blood are similar in phenotype and function but modified by donor health status. J Immunol. 2011;186(11):6207-17.
139. Franks HA, Wang Q, Lax SJ, Collins MK, Escors D, Patel PM, et al. Novel function for the p38-MK2 signaling pathway in circulating CD1c+ (BDCA-1+) myeloid dendritic cells from healthy donors and advanced cancer patients; inhibition of p38 enhances IL-12 whilst suppressing IL-10. Int J Cancer. 2014;134(3):575-86.
140. Piccioli D, Tavarini S, Borgogni E, Steri V, Nuti S, Sammicheli C, et al. Functional specialization of human circulating CD16 and CD1c myeloid dendritic-cell subsets. Blood. 2007;109(12):5371-9.
141. Nizzoli G, Krietsch J, Weick A, Steinfelder S, Facciotti F, Gruarin P, et al. Human CD1c+ dendritic cells secrete high levels of IL-12 and potently prime cytotoxic T-cell responses. Blood. 2013;122(6):932-42.
142. Jefford M, Schnurr M, Toy T, Masterman KA, Shin A, Beecroft T, et al. Functional comparison of DCs generated in vivo with Flt3 ligand or in vitro from blood monocytes: differential regulation of function by specific classes of physiologic stimuli. Blood. 2003;102(5):1753-63.
143. Cravens PD, Hayashida K, Davis LS, Nanki T, Lipsky PE. Human peripheral blood dendritic cells and monocyte subsets display similar chemokine receptor expression profiles with differential migratory responses. Scand J Immunol. 2007;65(6):514-24.
144. Bar-On L, Jung S. Defining dendritic cells by conditional and constitutive cell ablation. Immunol Rev. 2010;234(1):76-89.
145. Schlitzer A, Ginhoux F. Organization of the mouse and human DC network. Curr Opin Immunol. 2014;26:90-9.
146. Gardner A, Ruffell B. Dendritic Cells and Cancer Immunity. Trends Immunol. 2016;37(12):855-65.
147. Schreibelt G, Bol KF, Westdorp H, Wimmers F, Aarntzen EH, Duiveman-de Boer T, et al. Effective Clinical Responses in Metastatic Melanoma Patients after Vaccination with Primary Myeloid Dendritic Cells. Clin Cancer Res. 2016;22(9):2155-66.
148. Prue RL, Vari F, Radford KJ, Tong H, Hardy MY, D'Rozario R, et al. A phase I clinical trial of CD1c (BDCA-1)+ dendritic cells pulsed with HLA-A*0201 peptides for immunotherapy of metastatic hormone refractory prostate cancer. J Immunother. 2015;38(2):71-6.
149. Jongbloed SL, Kassianos AJ, McDonald KJ, Clark GJ, Ju X, Angel CE, et al. Human CD141+ (BDCA-3)+ dendritic cells (DCs) represent a unique myeloid DC

subset that cross-presents necrotic cell antigens. J Exp Med. 2010;207(6):1247-60.
150. Wang JC, Kobie JJ, Zhang L, Cochran M, Mosmann TR, Ritchlin CT, et al. An 11-color flow cytometric assay for identifying, phenotyping, and assessing endocytic ability of peripheral blood dendritic cell subsets in a single platform. J Immunol Methods. 2009;341(1-2):106-16.
151. Poulin LF, Salio M, Griessinger E, Anjos-Afonso F, Craciun L, Chen JL, et al. Characterization of human DNGR-1+ BDCA3+ leukocytes as putative equivalents of mouse CD8alpha+ dendritic cells. J Exp Med. 2010;207(6):1261-71.
152. Haniffa M, Shin A, Bigley V, McGovern N, Teo P, See P, et al. Human tissues contain CD141hi cross-presenting dendritic cells with functional homology to mouse CD103+ nonlymphoid dendritic cells. Immunity. 2012;37(1):60-73.
153. Mildner A, Jung S. Development and function of dendritic cell subsets. Immunity. 2014;40(5):642-56.
154. Guilliams M, Dutertre C-A, Scott Charlotte L, McGovern N, Sichien D, Chakarov S, et al. Unsupervised High-Dimensional Analysis Aligns Dendritic Cells across Tissues and Species. Immunity. 2016;45(3):669-84.
155. Dorner BG, Dorner MB, Zhou X, Opitz C, Mora A, Guttler S, et al. Selective expression of the chemokine receptor XCR1 on cross-presenting dendritic cells determines cooperation with CD8+ T cells. Immunity. 2009;31(5):823-33.
156. Tel J, Schreibelt G, Sittig SP, Mathan TSM, Buschow SI, Cruz LJ, et al. Human plasmacytoid dendritic cells efficiently cross-present exogenous Ags to CD8+ T cells despite lower Ag uptake than myeloid dendritic cell subsets. Blood. 2013;121(3):459.
157. Sanchez-Paulete AR, Cueto FJ, Martinez-Lopez M, Labiano S, Morales-Kastresana A, Rodriguez-Ruiz ME, et al. Cancer Immunotherapy with Immunomodulatory Anti-CD137 and Anti-PD-1 Monoclonal Antibodies Requires BATF3-Dependent Dendritic Cells. Cancer Discov. 2016;6(1):71-9.
158. Salmon H, Idoyaga J, Rahman A, Leboeuf M, Remark R, Jordan S, et al. Expansion and Activation of CD103(+) Dendritic Cell Progenitors at the Tumor Site Enhances Tumor Responses to Therapeutic PD-L1 and BRAF Inhibition. Immunity. 2016;44(4):924-38.
159. Wimmers F, Schreibelt G, Skold AE, Figdor CG, De Vries IJ. Paradigm Shift in Dendritic Cell-Based Immunotherapy: From in vitro Generated Monocyte-Derived DCs to Naturally Circulating DC Subsets. Front Immunol. 2014;5:165.
160. Reizis B, Bunin A, Ghosh HS, Lewis KL, Sisirak V. Plasmacytoid dendritic cells: recent progress and open questions. Annu Rev Immunol. 2011;29:163-83.
161. Cox K, North M, Burke M, Singhal H, Renton S, Aqel N, et al. Plasmacytoid dendritic cells (PDC) are the major DC subset innately producing cytokines in human lymph nodes. Journal of leukocyte biology. 2005;78(5):1142-52.

162. Cervantes-Barragan L, Lewis KL, Firner S, Thiel V, Hugues S, Reith W, et al. Plasmacytoid dendritic cells control T-cell response to chronic viral infection. Proc Natl Acad Sci U S A. 2012;109(8):3012-7.
163. Kadowaki N, Antonenko S, Lau JY, Liu YJ. Natural interferon alpha/beta-producing cells link innate and adaptive immunity. The Journal of experimental medicine. 2000;192(2):219-26.
164. Tel J, Smits EL, Anguille S, Joshi RN, Figdor CG, de Vries IJ. Human plasmacytoid dendritic cells are equipped with antigen-presenting and tumoricidal capacities. Blood. 2012;120(19):3936-44.
165. Fonteneau JF, Gilliet M, Larsson M, Dasilva I, Munz C, Liu YJ, et al. Activation of influenza virus-specific CD4+ and CD8+ T cells: a new role for plasmacytoid dendritic cells in adaptive immunity. Blood. 2003;101(9):3520-6.
166. Tel J, Aarntzen EH, Baba T, Schreibelt G, Schulte BM, Benitez-Ribas D, et al. Natural human plasmacytoid dendritic cells induce antigen-specific T-cell responses in melanoma patients. Cancer Res. 2013;73(3):1063-75.
167. Lou Y, Liu C, Kim GJ, Liu YJ, Hwu P, Wang G. Plasmacytoid dendritic cells synergize with myeloid dendritic cells in the induction of antigen-specific antitumor immune responses. J Immunol. 2007;178(3):1534-41.
168. Skold AE, Mathan TSM, van Beek JJP, Florez-Grau G, van den Beukel MD, Sittig SP, et al. Naturally produced type I IFNs enhance human myeloid dendritic cell maturation and IL-12p70 production and mediate elevated effector functions in innate and adaptive immune cells. Cancer Immunol Immunother. 2018;67(9):1425-36.
169. Dey M, Chang AL, Miska J, Wainwright DA, Ahmed AU, Balyasnikova IV, et al. Dendritic Cell-Based Vaccines that Utilize Myeloid Rather than Plasmacytoid Cells Offer a Superior Survival Advantage in Malignant Glioma. J Immunol. 2015;195(1):367-76.
170. Schakel K, Mayer E Fau - Federle C, Federle C Fau - Schmitz M, Schmitz M Fau - Riethmuller G, Riethmuller G Fau - Rieber EP, Rieber EP. A novel dendritic cell population in human blood: one-step immunomagnetic isolation by a specific mAb (M-DC8) and in vitro priming of cytotoxic T lymphocytes. Eur, J Immunol. 1998;28(12):4084-93.
171. Schakel K, Kannagi R Fau - Kniep B, Kniep B Fau - Goto Y, Goto Y Fau - Mitsuoka C, Mitsuoka C Fau - Zwirner J, Zwirner J Fau - Soruri A, et al. 6-Sulfo LacNAc, a novel carbohydrate modification of PSGL-1, defines an inflammatory type of human dendritic cells. Immunity. 2002;17(3):289-301.
172. Hansel A, Gunther C, Ingwersen J, Starke J, Schmitz M, Bachmann M, et al. Human slan (6-sulfo LacNAc) dendritic cells are inflammatory dermal dendritic cells in psoriasis and drive strong TH17/TH1 T-cell responses. J Allergy Clin Immunol. 2011;127(3):787-94 e1-9.
173. Schakel K, von Kietzell M, Hansel A, Ebling A, Schulze L, Haase M, et al. Human 6-sulfo LacNAc-expressing dendritic cells are principal producers of early interleukin-12 and are controlled by erythrocytes. Immunity. 2006;24(6):767-77.
174. Hänsel A, Günther C, Baran W, Bidier M, Lorenz H-M, Schmitz M, et al. Human 6-sulfo LacNAc (slan) dendritic cells have molecular and functional

features of an important pro-inflammatory cell type in lupus erythematosus. J Autoimmun. 2013;40:1-8.
175. Schmitz M, Zhao S, Deuse Y, Schakel K, Wehner R, Wohner H, et al. Tumoricidal Potential of Native Blood Dendritic Cells: Direct Tumor Cell Killing and Activation of NK Cell-Mediated Cytotoxicity. The Journal of Immunology. 2005;174(7):4127-34.
176. Jackson CM, Lim M. Immunotherapy for Glioblastoma: Playing Chess, Not Checkers. Clin Cancer Res. 2018;24(17):4059-61.
177. Hegde PS, Karanikas V, Evers S. The Where, the When, and the How of Immune Monitoring for Cancer Immunotherapies in the Era of Checkpoint Inhibition. Clin Cancer Res. 2016;22(8):1865-74.
178. Joffre OP, Segura E, Savina A, Amigorena S. Cross-presentation by dendritic cells. Nat Rev Immunol. 2012;12(8):557-69.
179. Sancho D, Joffre OP, Keller AM, Rogers NC, Martinez D, Hernanz-Falcon P, et al. Identification of a dendritic cell receptor that couples sensing of necrosis to immunity. Nature. 2009;458(7240):899-903.
180. Huysamen C, Willment JA, Dennehy KM, Brown GD. CLEC9A is a novel activation C-type lectin-like receptor expressed on BDCA3+ dendritic cells and a subset of monocytes. J Biol Chem. 2008;283(24):16693-701.
181. Yerkovich ST, Roponen M, Smith ME, McKenna K, Bosco A, Subrata LS, et al. Allergen-enhanced thrombomodulin (blood dendritic cell antigen 3, CD141) expression on dendritic cells is associated with a TH2-skewed immune response. J Allergy Clin Immunol. 2009;123(1):209-16 e4.
182. Radford KJ, Tullett KM, Lahoud MH. Dendritic cells and cancer immunotherapy. Curr Opin Immunol. 2014;27:26-32.
183. Gornati L, Zanoni I, Granucci F. Dendritic Cells in the Cross Hair for the Generation of Tailored Vaccines. Front Immunol. 2018;9:1484.
184. Lin Z, Chiang NY, Chai N, Seshasayee D, Lee WP, Balazs M, et al. In vivo antigen-driven plasmablast enrichment in combination with antigen-specific cell sorting to facilitate the isolation of rare monoclonal antibodies from human B cells. Nat Protoc. 2014;9(7):1563-77.
185. Allen M, Bjerke M, Edlund H, Nelander S, Westermark B. Origin of the U87MG glioma cell line: Good news and bad news. Sci Transl Med. 2016;8(354):354re3.
186. Tacken PJ, Joosten B, Reddy A, Wu D, Eek A, Laverman P, et al. No Advantage of Cell-Penetrating Peptides over Receptor-Specific Antibodies in Targeting Antigen to Human Dendritic Cells for Cross-Presentation. The Journal of Immunology. 2008;180(11):7687-96.
187. Schaft N, Lankiewicz B, Gratama JW, Bolhuis RL, Debets R. Flexible and sensitive method to functionally validate tumor-specific receptors via activation of NFAT. J Immunol Methods. 2003;280(1-2):13-24.
188. Napolitani G, Rinaldi A, Bertoni F, Sallusto F, Lanzavecchia A. Selected Toll-like receptor agonist combinations synergistically trigger a T helper type 1-polarizing program in dendritic cells. Nat Immunol. 2005;6(8):769-76.
189. Yin X, Yu H, Jin X, Li J, Guo H, Shi Q, et al. Human Blood CD1c+ Dendritic Cells Encompass CD5high and CD5low Subsets That Differ

Significantly in Phenotype, Gene Expression, and Functions. J Immunol. 2017;198(4):1553-64.
190. Yanagimoto H, Takai S, Satoi S, Toyokawa H, Takahashi K, Terakawa N, et al. Impaired function of circulating dendritic cells in patients with pancreatic cancer. Clin Immunol. 2005;114(1):52-60.
191. Pinzon-Charry A, Ho CSK, Laherty R, Maxwell T, Walker D, Gardiner RA, et al. A Population of HLA-DR+ Immature Cells Accumulates in the Blood Dendritic Cell Compartment of Patients with Different Types of Cancer. Neoplasia. 2005;7(12):1112-22.
192. Gousias K, von Ruecker A, Voulgari P, Simon M. Phenotypical analysis, relation to malignancy and prognostic relevance of ICOS+T regulatory and dendritic cells in patients with gliomas. J Neuroimmunol. 2013;264(1-2):84-90.
193. O'Doherty U, Peng M, Gezelter S, Swiggard WJ, Betjes M, Bhardwaj N, et al. Human blood contains two subsets of dendritic cells, one immunologically mature and the other immature. Immunology. 1994;82(3):487-93.
194. Van Gool S, Maes W, Ardon H, Verschuere T, Van Cauter S, De Vleeschouwer S. Dendritic cell therapy of high-grade gliomas. Brain Pathol. 2009;19(4):694-712.
195. Schaller TH, Sampson JH. Advances and challenges: dendritic cell vaccination strategies for glioblastoma. Expert review of vaccines. 2017;16(1):27-36.
196. Anguille S, Smits EL, Lion E, van Tendeloo VF, Berneman ZN. Clinical use of dendritic cells for cancer therapy. The Lancet Oncology. 2014;15(7):e257-67.
197. Liau LM, Ashkan K, Tran DD, Campian JL, Trusheim JE, Cobbs CS, et al. First results on survival from a large Phase 3 clinical trial of an autologous dendritic cell vaccine in newly diagnosed glioblastoma. J Transl Med. 2018;16(1):142.
198. Kapsenberg ML. Dendritic-cell control of pathogen-driven T-cell polarization. Nat Rev Immunol. 2003;3(12):984-93.
199. Dubrow R, Darefsky AS. Demographic variation in incidence of adult glioma by subtype, United States, 1992-2007. BMC Cancer. 2011;11:325.
200. Olar A, Aldape KD. Using the molecular classification of glioblastoma to inform personalized treatment. J Pathol. 2014;232(2):165-77.
201. Kalinski P, Hilkens CM, Wierenga EA, Kapsenberg ML. T-cell priming by type-1 and type-2 polarized dendritic cells: the concept of a third signal. Immunol Today. 1999;20(12):561-7.
202. Pinzon-Charry A, Maxwell T, Lopez JA. Dendritic cell dysfunction in cancer: a mechanism for immunosuppression. Immunol Cell Biol. 2005;83(5):451-61.
203. Knutson KL, Disis ML. Tumor antigen-specific T helper cells in cancer immunity and immunotherapy. Cancer Immunol Immunother. 2005;54(8):721-8.
204. Guermonprez P, Valladeau J, Zitvogel L, Thery C, Amigorena S. Antigen presentation and T cell stimulation by dendritic cells. Annu Rev Immunol. 2002;20:621-67.

205. O'Garra A, Murphy KM. From IL-10 to IL-12: how pathogens and their products stimulate APCs to induce T(H)1 development. Nat Immunol. 2009;10(9):929-32.
206. Schoenberger SP, Toes REM, van der Voort EIH, Offringa R, Melief CJM. T-cell help for cytotoxic T lymphocytes is mediated by CD40–CD40L interactions. Nature. 1998;393:480.
207. Ridge JP, Di Rosa F, Matzinger P. A conditioned dendritic cell can be a temporal bridge between a CD4+ T-helper and a T-killer cell. Nature. 1998;393(6684):474-8.
208. Bennett SR, Carbone FR, Karamalis F, Miller JF, Heath WR. Induction of a CD8+ cytotoxic T lymphocyte response by cross-priming requires cognate CD4+ T cell help. The Journal of experimental medicine. 1997;186(1):65-70.
209. Bennett SR, Carbone FR, Karamalis F, Flavell RA, Miller JF, Heath WR. Help for cytotoxic-T-cell responses is mediated by CD40 signalling. Nature. 1998;393(6684):478-80.
210. Smith CM, Wilson NS, Waithman J, Villadangos JA, Carbone FR, Heath WR, et al. Cognate CD4+ T cell licensing of dendritic cells in CD8+ T cell immunity. Nature Immunology. 2004;5:1143.
211. Sun JC, Bevan MJ. Defective CD8 T cell memory following acute infection without CD4 T cell help. Science. 2003;300(5617):339-42.
212. Sun JC, Williams MA, Bevan MJ. CD4+ T cells are required for the maintenance, not programming, of memory CD8+ T cells after acute infection. Nat Immunol. 2004;5(9):927-33.
213. Shedlock DJ, Shen H. Requirement for CD4 T cell help in generating functional CD8 T cell memory. Science. 2003;300(5617):337-9.
214. Janssen EM, Lemmens EE, Wolfe T, Christen U, von Herrath MG, Schoenberger SP. CD4+ T cells are required for secondary expansion and memory in CD8+ T lymphocytes. Nature. 2003;421(6925):852-6.
215. Stupp R, Hegi ME, Mason WP, van den Bent MJ, Taphoorn MJB, Janzer RC, et al. Effects of radiotherapy with concomitant and adjuvant temozolomide versus radiotherapy alone on survival in glioblastoma in a randomised phase III study: 5-year analysis of the EORTC-NCIC trial. The Lancet Oncology. 2009;10(5):459-66.
216. Rozkova D, Horvath R, Bartunkova J, Spisek R. Glucocorticoids severely impair differentiation and antigen presenting function of dendritic cells despite upregulation of Toll-like receptors. Clin Immunol. 2006;120(3):260-71.
217. Mohty M, Jarrossay D, Lafage-Pochitaloff M, Zandotti C, Briere F, de Lamballeri XN, et al. Circulating blood dendritic cells from myeloid leukemia patients display quantitative and cytogenetic abnormalities as well as functional impairment. Blood. 2001;98(13):3750-6.
218. Mami NB, Mohty M, Aurran-Schleinitz T, Olive D, Gaugler B. Blood dendritic cells in patients with chronic lymphocytic leukaemia. Immunobiology. 2008;213(6):493-8.
219. Della Bella S, Nicola S, Brambilla L, Riva A, Ferrucci S, Presicce P, et al. Quantitative and functional defects of dendritic cells in classic Kaposi's sarcoma. Clin Immunol. 2006;119(3):317-29.

220. Almand B, Resser JR, Lindman B, Nadaf S, Clark JI, Kwon ED, et al. Clinical Significance of Defective Dendritic Cell Differentiation in Cancer. Clinical Cancer Research. 2000;6(5):1755-66.
221. van Cruijsen H, van der Veldt AA, Vroling L, Oosterhoff D, Broxterman HJ, Scheper RJ, et al. Sunitinib-induced myeloid lineage redistribution in renal cell cancer patients: CD1c+ dendritic cell frequency predicts progression-free survival. Clin Cancer Res. 2008;14(18):5884-92.
222. Bakdash G, Buschow SI, Gorris MA, Halilovic A, Hato SV, Skold AE, et al. Expansion of a BDCA1+CD14+ Myeloid Cell Population in Melanoma Patients May Attenuate the Efficacy of Dendritic Cell Vaccines. Cancer Res. 2016;76(15):4332-46.
223. Garcia A, Keinonen S, Sanchez AM, Ferrari G, Denny TN, Moody MA. Leukopak PBMC sample processing for preparing quality control material to support proficiency testing programs. J Immunol Methods. 2014;409:99-106.
224. Lemos NE, Farias MG, Kubaski F, Scotti L, Onsten TGH, Brondani LA, et al. Quantification of peripheral blood CD34(+) cells prior to stem cell harvesting by leukapheresis: a single center experience. Hematol Transfus Cell Ther. 2018;40(3):213-8.
225. Gasova Z, Marinov I, Vodvarkova S, Bohmova M, Bhuyian-Ludvikova Z. PBPC collection techniques: standard versus large volume leukapheresis (LVL) in donors and in patients. Transfus Apher Sci. 2005;32(2):167-76.
226. Gabrilovich D. Mechanisms and functional significance of tumour-induced dendritic-cell defects. Nat Rev Immunol. 2004;4(12):941-52.
227. Serre K, Giraudo L, Siret C, Leserman L, Machy P. CD4 T cell help is required for primary CD8 T cell responses to vesicular antigen delivered to dendritic cellsin vivo. European journal of immunology. 2006;36(6):1386-97.
228. Fiorentino DF, Bond MW, Mosmann TR. Two types of mouse T helper cell. IV. Th2 clones secrete a factor that inhibits cytokine production by Th1 clones. J Exp Med. 1989;170(6):2081-95.
229. Fiorentino DF, Zlotnik A, Vieira P, Mosmann TR, Howard M, Moore KW, et al. IL-10 acts on the antigen-presenting cell to inhibit cytokine production by Th1 cells. J Immunol. 1991;146(10):3444-51.
230. Steinbrink K, Wolfl M, Jonuleit H, Knop J, Enk AH. Induction of tolerance by IL-10-treated dendritic cells. J Immunol. 1997;159(10):4772-80.
231. Bosma BM, Metselaar HJ, Nagtzaam NM, de Haan R, Mancham S, van der Laan LJ, et al. Dexamethasone transforms lipopolysaccharide-stimulated human blood myeloid dendritic cells into myeloid dendritic cells that prime interleukin-10 production in T cells. Immunology. 2008;125(1):91-100.
232. (eMC) EMC. Dexamethasone 4mg tablets - Summaries of Product Characteristics (SPC). EMC - https://wwwmedicinesorguk/emc/product/7395/smpc.
233. Piemonti L, Monti P, Allavena P, Sironi M, Soldini L, Leone BE, et al. Glucocorticoids Affect Human Dendritic Cell Differentiation and Maturation. The Journal of Immunology. 1999;162(11):6473.
234. Jackson AM, Mulcahy LA, Zhu XW, O'Donnell D, Patel PM. Tumour-mediated disruption of dendritic cell function: inhibiting the MEK1/2-p44/42

axis restores IL-12 production and Th1-generation. Int J Cancer. 2008;123(3):623-32.
235. Rötzschke O, Falk K, Faath S, Rammensee HG. On the nature of peptides involved in T cell alloreactivity. The Journal of Experimental Medicine. 1991;174(5):1059.
236. Felix NJ, Allen PM. Specificity of T-cell alloreactivity. Nature Reviews Immunology. 2007;7:942.
237. Groux H, Bigler M, de Vries JE, Roncarolo MG. Interleukin-10 induces a long-term antigen-specific anergic state in human CD4+ T cells. J Exp Med. 1996;184(1):19-29.
238. Xu LW, Chow KK, Lim M, Li G. Current vaccine trials in glioblastoma: a review. J Immunol Res. 2014;2014:796856.
239. Win SJ, McMillan DG, Errington-Mais F, Ward VK, Young SL, Baird MA, et al. Enhancing the immunogenicity of tumour lysate-loaded dendritic cell vaccines by conjugation to virus-like particles. Br J Cancer. 2012;106(1):92-8.
240. Jackson AM, Mulcahy LA, Porte J, Franks HA, El Refaee M, Wang Q, et al. Role of mitogen-activated protein kinase and PI3K pathways in the regulation of IL-12-family cytokines in dendritic cells and the generation of T H-responses. Eur Cytokine Netw. 2010;21(4):319-28.
241. Gustafson MP, Lin Y, New KC, Bulur PA, O'Neill BP, Gastineau DA, et al. Systemic immune suppression in glioblastoma: the interplay between CD14+HLA-DRlo/neg monocytes, tumor factors, and dexamethasone. Neuro Oncol. 2010;12(7):631-44.
242. Li Q, Harden JL, Anderson CD, Egilmez NK. Tolerogenic Phenotype of IFN-gamma-Induced IDO+ Dendritic Cells Is Maintained via an Autocrine IDO-Kynurenine/AhR-IDO Loop. J Immunol. 2016;197(3):962-70.
243. Palucka K, Banchereau J. Dendritic-cell-based therapeutic cancer vaccines. Immunity. 2013;39(1):38-48.
244. Lee JC, Laydon JT, McDonnell PC, Gallagher TF, Kumar S, Green D, et al. A protein kinase involved in the regulation of inflammatory cytokine biosynthesis. Nature. 1994;372(6508):739-46.
245. Cuenda A, Rousseau S. p38 MAP-kinases pathway regulation, function and role in human diseases. Biochim Biophys Acta. 2007;1773(8):1358-75.
246. Arthur JS, Ley SC. Mitogen-activated protein kinases in innate immunity. Nat Rev Immunol. 2013;13(9):679-92.
247. Pargellis C, Tong L, Churchill L, Cirillo PF, Gilmore T, Graham AG, et al. Inhibition of p38 MAP kinase by utilizing a novel allosteric binding site. Nat Struct Biol. 2002;9(4):268-72.
248. Sweeney SE, Firestein GS. Mitogen activated protein kinase inhibitors: where are we now and where are we going? Ann Rheum Dis. 2006;65 Suppl 3:iii83-8.
249. Langosch S, Wehner R, Malecka A, Franks HA, Schakel K, Bachmann M, et al. Impact of p38 mitogen-activated protein kinase inhibition on immunostimulatory properties of human 6-sulfo LacNAc dendritic cells. Immunobiology. 2016;221(2):166-74.
250. Dieu M-C, Vanbervliet B, Vicari A, Bridon J-M, Oldham E, Aït-Yahia S, et al. Selective Recruitment of Immature and Mature Dendritic Cells by Distinct

Chemokines Expressed in Different Anatomic Sites. The Journal of Experimental Medicine. 1998;188(2):373-86.
251. Weber M, Hauschild R, Schwarz J, Moussion C, de Vries I, Legler DF, et al. Interstitial dendritic cell guidance by haptotactic chemokine gradients. Science. 2013;339(6117):328-32.
252. Worbs T, Hammerschmidt SI, Forster R. Dendritic cell migration in health and disease. Nat Rev Immunol. 2017;17(1):30-48.
253. Forster R, Schubel A, Breitfeld D, Kremmer E, Renner-Muller I, Wolf E, et al. CCR7 coordinates the primary immune response by establishing functional microenvironments in secondary lymphoid organs. Cell. 1999;99(1):23-33.
254. Britschgi MR, Favre S, Luther SA. CCL21 is sufficient to mediate DC migration, maturation and function in the absence of CCL19. European journal of immunology. 2010;40(5):1266-71.
255. Hosken NA, Bevan MJ. Defective presentation of endogenous antigen by a cell line expressing class I molecules. Science. 1990;248(4953):367.
256. Schuster J, Lai RK, Recht LD, Reardon DA, Paleologos NA, Groves MD, et al. A phase II, multicenter trial of rindopepimut (CDX-110) in newly diagnosed glioblastoma: the ACT III study. Neuro Oncol. 2015;17(6):854-61.
257. Yarchoan M, Johnson BA, 3rd, Lutz ER, Laheru DA, Jaffee EM. Targeting neoantigens to augment antitumour immunity. Nat Rev Cancer. 2017;17(4):209-22.
258. Wu AH, Xiao J, Anker L, Hall WA, Gregerson DS, Cavenee WK, et al. Identification of EGFRvIII-derived CTL epitopes restricted by HLA A0201 for dendritic cell based immunotherapy of gliomas. J Neurooncol. 2006;76(1):23-30.
259. Dunn GP, Dunn IF, Curry WT. Focus on TILs: Prognostic significance of tumor infiltrating lymphocytes in human glioma. Cancer Immun. 2007;7:12.
260. Krummel MF, Allison JP. CD28 and CTLA-4 have opposing effects on the response of T cells to stimulation. J Exp Med. 1995;182(2):459-65.
261. Hui E, Cheung J, Zhu J, Su X, Taylor MJ, Wallweber HA, et al. T cell costimulatory receptor CD28 is a primary target for PD-1-mediated inhibition. Science. 2017;355(6332):1428-33.
262. Rudd CE, Taylor A, Schneider H. CD28 and CTLA-4 coreceptor expression and signal transduction. Immunol Rev. 2009;229(1):12-26.
263. Chen L, Flies DB. Molecular mechanisms of T cell co-stimulation and co-inhibition. Nat Rev Immunol. 2013;13(4):227-42.
264. Inaba K, Witmer-Pack M, Inaba M, Hathcock KS, Sakuta H, Azuma M, et al. The tissue distribution of the B7-2 costimulator in mice: abundant expression on dendritic cells in situ and during maturation in vitro. J Exp Med. 1994;180(5):1849-60.
265. Elgueta R, Benson MJ, de Vries VC, Wasiuk A, Guo Y, Noelle RJ. Molecular mechanism and function of CD40/CD40L engagement in the immune system. Immunol Rev. 2009;229(1):152-72.
266. Abdi K, Singh NJ, Matzinger P. Lipopolysaccharide-activated dendritic cells: "exhausted" or alert and waiting? J Immunol. 2012;188(12):5981-9.

267. Abdi K, Laky K, Padhan K, Petrovas C, Skinner J, Kabat J, et al. Cutting Edge: Quantitative Determination of CD40L Threshold for IL-12 and IL-23 Production from Dendritic Cells. The Journal of Immunology. 2018.
268. De Vries IJ, Krooshoop DJ, Scharenborg NM, Lesterhuis WJ, Diepstra JH, Van Muijen GN, et al. Effective migration of antigen-pulsed dendritic cells to lymph nodes in melanoma patients is determined by their maturation state. Cancer Res. 2003;63(1):12-7.
269. Byrne KT, Vonderheide RH. CD40 Stimulation Obviates Innate Sensors and Drives T Cell Immunity in Cancer. Cell Rep. 2016;15(12):2719-32.
270. Engering A, Geijtenbeek TBH, van Vliet SJ, Wijers M, van Liempt E, Demaurex N, et al. The Dendritic Cell-Specific Adhesion Receptor DC-SIGN Internalizes Antigen for Presentation to T Cells. The Journal of Immunology. 2002;168(5):2118-26.
271. Lin H, Wei S, Hurt EM, Green MD, Zhao L, Vatan L, et al. Host expression of PD-L1 determines efficacy of PD-L1 pathway blockade-mediated tumor regression. J Clin Invest. 2018;128(2):805-15.
272. Brown JA, Dorfman DM, Ma F-R, Sullivan EL, Munoz O, Wood CR, et al. Blockade of Programmed Death-1 Ligands on Dendritic Cells Enhances T Cell Activation and Cytokine Production. The Journal of Immunology. 2003;170(3):1257.
273. Ju X, Silveira PA, Hsu WH, Elgundi Z, Alingcastre R, Verma ND, et al. The Analysis of CD83 Expression on Human Immune Cells Identifies a Unique CD83+-Activated T Cell Population. J Immunol. 2016;197(12):4613-25.
274. Lechmann M, Berchtold S, Hauber J, Steinkasserer A. CD83 on dendritic cells: more than just a marker for maturation. Trends Immunol. 2002;23(6):273-5.
275. Parlato S, Santini SM, Lapenta C, Di Pucchio T, Logozzi M, Spada M, et al. Expression of CCR-7, MIP-3β, and Th-1 chemokines in type I IFN-induced monocyte-derived dendritic cells: importance for the rapid acquisition of potent migratory and functional activities. Blood. 2001;98:3022-9.
276. Verdijk P, Aarntzen EH, Lesterhuis WJ, Boullart AC, Kok E, van Rossum MM, et al. Limited amounts of dendritic cells migrate into the T-cell area of lymph nodes but have high immune activating potential in melanoma patients. Clin Cancer Res. 2009;15(7):2531-40.
277. Bregy A, Wong TM, Shah AH, Goldberg JM, Komotar RJ. Active immunotherapy using dendritic cells in the treatment of glioblastoma multiforme. Cancer Treat Rev. 2013;39(8):891-907.
278. van Rijn A, Paulis L, te Riet J, Vasaturo A, Reinieren-Beeren I, van der Schaaf A, et al. Semaphorin 7A Promotes Chemokine-Driven Dendritic Cell Migration. J Immunol. 2016;196(1):459-68.
279. Randolph GJ, Angeli V, Swartz MA. Dendritic-cell trafficking to lymph nodes through lymphatic vessels. Nat Rev Immunol. 2005;5(8):617-28.
280. Bretou M, Saez PJ, Sanseau D, Maurin M, Lankar D, Chabaud M, et al. Lysosome signaling controls the migration of dendritic cells. Sci Immunol. 2017;2(16).
281. Weller M, Butowski N, Tran DD, Recht LD, Lim M, Hirte H, et al. Rindopepimut with temozolomide for patients with newly diagnosed,

EGFRvIII-expressing glioblastoma (ACT IV): a randomised, double-blind, international phase 3 trial. The Lancet Oncology. 2017;18(10):1373-85.
282. Phuphanich S, Wheeler CJ, Rudnick JD, Mazer M, Wang H, Nuno MA, et al. Phase I trial of a multi-epitope-pulsed dendritic cell vaccine for patients with newly diagnosed glioblastoma. Cancer Immunol Immunother. 2013;62(1):125-35.
283. Zhang JG, Eguchi J, Kruse CA, Gomez GG, Fakhrai H, Schroter S, et al. Antigenic profiling of glioma cells to generate allogeneic vaccines or dendritic cell-based therapeutics. Clin Cancer Res. 2007;13(2 Pt 1):566-75.
284. Xu Q, Liu G, Yuan X, Xu M, Wang H, Ji J, et al. Antigen-specific T-cell response from dendritic cell vaccination using cancer stem-like cell-associated antigens. Stem Cells. 2009;27(8):1734-40.
285. Mullen AC, High FA, Hutchins AS, Lee HW, Villarino AV, Livingston DM, et al. Role of T-bet in Commitment of Th1 Cells before IL-12-Dependent Selection. Science. 2001;292:1907-10.
286. Afkarian M, Sedy JR, Yang J, Jacobson NG, Cereb N, Yang SY, et al. T-bet is a STAT1-induced regulator of IL-12R expression in naive CD4+ T cells. Nat Immunol. 2002;3(6):549-57.
287. Ouyang W, Ranganath SH, Weindel K, Bhattacharya D, Murphy TL, Sha WC, et al. Inhibition of Th1 development mediated by GATA-3 through an IL-4-independent mechanism. Immunity. 1998;9(5):745-55.
288. Au-Yeung BB, Zikherman J, Mueller JL, Ashouri JF, Matloubian M, Cheng DA, et al. A sharp T-cell antigen receptor signaling threshold for T-cell proliferation. Proc Natl Acad Sci U S A. 2014;111(35):E3679-88.
289. Viola A, Lanzavecchia A. T cell activation determined by T cell receptor number and tunable thresholds. Science. 1996;273(5271):104-6.
290. Huang J, Brameshuber M, Zeng X, Xie J, Li QJ, Chien YH, et al. A single peptide-major histocompatibility complex ligand triggers digital cytokine secretion in CD4(+) T cells. Immunity. 2013;39(5):846-57.
291. Richer MJ, Nolz JC, Harty JT. Pathogen-specific inflammatory milieux tune the antigen sensitivity of CD8(+) T cells by enhancing T cell receptor signaling. Immunity. 2013;38(1):140-52.
292. Kim C, Jay DC, Williams MA. Dynamic functional modulation of CD4+ T cell recall responses is dependent on the inflammatory environment of the secondary stimulus. PLoS Pathog. 2014;10(5):e1004137.
293. Agarwal P, Raghavan A, Nandiwada SL, Curtsinger JM, Bohjanen PR, Mueller DL, et al. Gene regulation and chromatin remodeling by IL-12 and type I IFN in programming for CD8 T cell effector function and memory. J Immunol. 2009;183(3):1695-704.
294. Bluestone JA, Mackay CR, O'Shea JJ, Stockinger B. The functional plasticity of T cell subsets. Nat Rev Immunol. 2009;9(11):811-6.
295. Liu HP, Cao AT, Feng T, Li Q, Zhang W, Yao S, et al. TGF-beta converts Th1 cells into Th17 cells through stimulation of Runx1 expression. European journal of immunology. 2015;45(4):1010-8.
296. Hodi FS, Chiarion-Sileni V, Gonzalez R, Grob J-J, Rutkowski P, Cowey CL, et al. Nivolumab plus ipilimumab or nivolumab alone versus ipilimumab alone

in advanced melanoma (CheckMate 067): 4-year outcomes of a multicentre, randomised, phase 3 trial. The Lancet Oncology. 2018;19(11):1480-92.
297. Reck M, Rodriguez-Abreu D, Robinson AG, Hui R, Csoszi T, Fulop A, et al. Pembrolizumab versus Chemotherapy for PD-L1-Positive Non-Small-Cell Lung Cancer. N Engl J Med. 2016;375(19):1823-33.
298. Omuro A, Vlahovic G, Lim M, Sahebjam S, Baehring J, Cloughesy T, et al. Nivolumab with or without ipilimumab in patients with recurrent glioblastoma: results from exploratory phase I cohorts of CheckMate 143. Neuro Oncol. 2018;20(5):674-86.
299. Chen DS, Mellman I. Oncology meets immunology: the cancer-immunity cycle. Immunity. 2013;39(1):1-10.
300. Joyce JA FD. T cell exclusion, immune privilege, and the tumor microenvironment. Science. 2015;348(6230):74-80.
301. Simpson TR, Li F, Montalvo-Ortiz W, Sepulveda MA, Bergerhoff K, Arce F, et al. Fc-dependent depletion of tumor-infiltrating regulatory T cells co-defines the efficacy of anti–CTLA-4 therapy against melanoma. The Journal of Experimental Medicine. 2013;210(9):1695-710.
302. Kuipers H, Muskens F, Willart M, Hijdra D, van Assema FB, Coyle AJ, et al. Contribution of the PD-1 ligands/PD-1 signaling pathway to dendritic cell-mediated CD4+ T cell activation. European journal of immunology. 2006;36(9):2472-82.
303. Baumeister SH, Freeman GJ, Dranoff G, Sharpe AH. Coinhibitory Pathways in Immunotherapy for Cancer. Annu Rev Immunol. 2016;34:539-73.
304. Carbognin L, Pilotto S, Milella M, Vaccaro V, Brunelli M, Calio A, et al. Differential Activity of Nivolumab, Pembrolizumab and MPDL3280A according to the Tumor Expression of Programmed Death-Ligand-1 (PD-L1): Sensitivity Analysis of Trials in Melanoma, Lung and Genitourinary Cancers. PLoS One. 2015;10(6):e0130142.
305. Tumeh PC, Harview CL, Yearley JH, Shintaku IP, Taylor EJ, Robert L, et al. PD-1 blockade induces responses by inhibiting adaptive immune resistance. Nature. 2014;515(7528):568-71.
306. Reardon DA. Safety and activity of nivolumab (nivo) monotherapy and nivo in combination with ipilimumab (ipi) in recurrent glioblastoma (GBM): Updated results from checkmate 143. Journal of Clinical Oncology. 2016;34 (suppl; abstr 2014).
307. Wang C, Thudium KB, Han M, Wang XT, Huang H, Feingersh D, et al. In vitro characterization of the anti-PD-1 antibody nivolumab, BMS-936558, and in vivo toxicology in non-human primates. Cancer Immunol Res. 2014;2(9):846-56.
308. Sanmamed MF, Chester C, Melero I, Kohrt H. Defining the optimal murine models to investigate immune checkpoint blockers and their combination with other immunotherapies. Ann Oncol. 2016;27(7):1190-8.
309. Coffelt SB, de Visser KE. Revving Up Dendritic Cells while Braking PD-L1 to Jump-Start the Cancer-Immunity Cycle Motor. Immunity. 2016;44(4):722-4.
310. Smyth MJ, Teng MW. 2018 Nobel Prize in physiology or medicine. Clinical & translational immunology. 2018;7(10):e1041-e.

311. Schumacher TN, Schreiber RD. Neoantigens in cancer immunotherapy. Science. 2015;348(6230):69.
312. McGranahan N, Furness AJ, Rosenthal R, Ramskov S, Lyngaa R, Saini SK, et al. Clonal neoantigens elicit T cell immunoreactivity and sensitivity to immune checkpoint blockade. Science. 2016;351(6280):1463-9.
313. Garg AD, Coulie PG, Van den Eynde BJ, Agostinis P. Integrating Next-Generation Dendritic Cell Vaccines into the Current Cancer Immunotherapy Landscape. Trends Immunol. 2017;38(8):577-93.
314. Wolfl M, Schwinn S, Yoo YE, Ress ML, Braun M, Chopra M, et al. Src-kinase inhibitors sensitize human cells of myeloid origin to Toll-like-receptor-induced interleukin 12 synthesis. Blood. 2013;122(7):1203-13.
315. Ott PA, Hu Z, Keskin DB, Shukla SA, Sun J, Bozym DJ, et al. An immunogenic personal neoantigen vaccine for patients with melanoma. Nature. 2017;547(7662):217-21.
316. Kalaora S, Wolf Y, Feferman T, Barnea E, Greenstein E, Reshef D, et al. Combined Analysis of Antigen Presentation and T-cell Recognition Reveals Restricted Immune Responses in Melanoma. Cancer Discov. 2018;8(11):1366-75.
317. Anagnostou V, Smith KN, Forde PM, Niknafs N, Bhattacharya R, White J, et al. Evolution of Neoantigen Landscape during Immune Checkpoint Blockade in Non-Small Cell Lung Cancer. Cancer Discov. 2017;7(3):264-76.
318. Van Gool SW. Brain Tumor Immunotherapy: What have We Learned so Far? Front Oncol. 2015;5:98.
319. Lesterhuis WJ, de Vries IJ, Schreibelt G, Lambeck AJ, Aarntzen EH, Jacobs JF, et al. Route of administration modulates the induction of dendritic cell vaccine-induced antigen-specific T cells in advanced melanoma patients. Clin Cancer Res. 2011;17(17):5725-35.
320. Karachi A, Dastmalchi F, Mitchell DA, Rahman M. Temozolomide for immunomodulation in the treatment of glioblastoma. Neuro Oncol. 2018;20(12):1566-72.
321. Moller HG, Rasmussen AP, Andersen HH, Johnsen KB, Henriksen M, Duroux M. A systematic review of microRNA in glioblastoma multiforme: micro-modulators in the mesenchymal mode of migration and invasion. Mol Neurobiol. 2013;47(1):131-44.
322. Sana J, Busek P, Fadrus P, Besse A, Radova L, Vecera M, et al. Identification of microRNAs differentially expressed in glioblastoma stem-like cells and their association with patient survival. Sci Rep. 2018;8(1):2836.
323. Duffy JP, Harrington EM, Salituro FG, Cochran JE, Green J, Gao H, et al. The Discovery of VX-745: A Novel and Selective p38alpha Kinase Inhibitor. ACS Med Chem Lett. 2011;2(10):758-63.
324. Dhodapkar MV, Sznol M, Zhao B, Wang D, Carvajal RD, Keohan ML, et al. Induction of antigen-specific immunity with a vaccine targeting NY-ESO-1 to the dendritic cell receptor DEC-205. Sci Transl Med. 2014;6(232):232ra51.
325. Tullett KM, Leal Rojas IM, Minoda Y, Tan PS, Zhang JG, Smith C, et al. Targeting CLEC9A delivers antigen to human CD141(+) DC for CD4(+) and CD8(+)T cell recognition. JCI Insight. 2016;1(7):e87102.

326. Ding Y, Wilkinson A, Idris A, Fancke B, O'Keeffe M, Khalil D, et al. FLT3-Ligand Treatment of Humanized Mice Results in the Generation of Large Numbers of CD141+ and CD1c+ Dendritic Cells In Vivo. The Journal of Immunology. 2014;192:1982-9.
327. Heger L, Balk S, Luhr JJ, Heidkamp GF, Lehmann CHK, Hatscher L, et al. CLEC10A Is a Specific Marker for Human CD1c(+) Dendritic Cells and Enhances Their Toll-Like Receptor 7/8-Induced Cytokine Secretion. Front Immunol. 2018;9:744.
328. Wong KL, Tai JJ, Wong WC, Han H, Sem X, Yeap WH, et al. Gene expression profiling reveals the defining features of the classical, intermediate, and nonclassical human monocyte subsets. Blood. 2011;118(5):e16-31.
329. Kranz LM, Diken M, Haas H, Kreiter S, Loquai C, Reuter KC, et al. Systemic RNA delivery to dendritic cells exploits antiviral defence for cancer immunotherapy. Nature. 2016;534(7607):396-401.
330. Prins RM, Craft N, Bruhn KW, Khan-Farooqi H, Koya RC, Stripecke R, et al. The TLR-7 agonist, imiquimod, enhances dendritic cell survival and promotes tumor antigen-specific T cell priming: relation to central nervous system antitumor immunity. J Immunol. 2006;176(1):157-64.